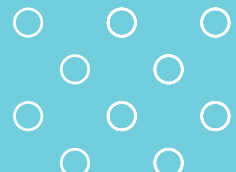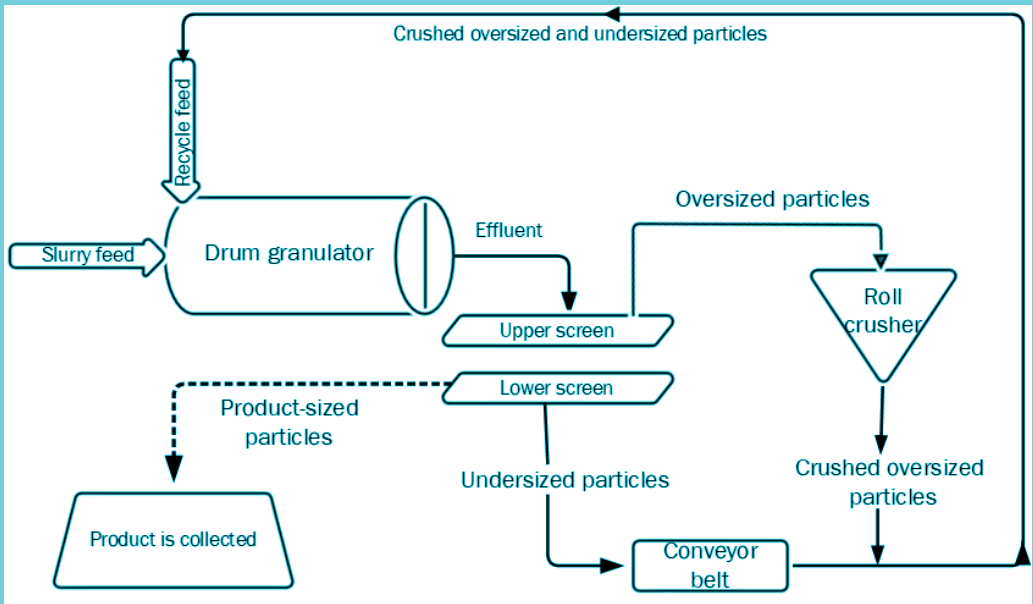Ludmila Vesjolaja

Dynamics and Control for Efficient Fertilizer Processes

USN

Ludmila Vesjolaja

Dynamics and Control for Efficient Fertilizer Processes

A PhD dissertation in
Process, Energy and Automation Engineering

Preface

This thesis is written to fulfill the graduation requirements of the degree of Doctor of Philosophy in PhD programme Process, Energy and Automation Engineering at the University of South–Eastern Norway (USN). The work has been conducted as a part of the project 'Exploiting multi-scale simulation and control in developing next generation high efficiency fertilizer technologies' (HEFTY) at Yara Technology and Projects and the Research Council through project no. 269507/O20. The PhD project work has been conducted under the supervision of Professor Bernt Lie, with co-supervision by Professor Finn Aakre Haugen.

The dissertation contains a study on modelling and control of granulation loop processes with particle recycle. The thesis consists of seven scientific papers, three conference papers and four journal papers. It is divided into two main parts. The first part gives an overview of the research topic and its goals, followed by an extended literature review. Further, the summary of the methods used, and the summary of the scientific papers together with conclusions are given. The second part contains the main contributions as a compendium of scientific publications.

Porsgrunn, 30th August 2021

Ludmila Vesjolaja

Acknowledgment

Abstract

Granulation processes have been a subject of research for more than 60 years. During these years of research, there has been a significant improvement in qualitative and quantitative knowledge of the granulation processes, their behaviour and dependence on various process variables and properties. However, in spite of extensive research in the granulation field, industrial granulation plants still suffer from oscillatory behaviour in the product quality and quantity. Typically, the oscillatory behaviour is observed in continuous granulation loop plants where off-spec particles are recycled back into the granulator. The observed oscillatory behaviour leads to a reduction in profit, overloading of the process equipment, increased operational risks, and unforeseen plant shut-downs. Consequently, the elimination of the oscillatory behaviour in the continuous granulation loop plants is of great importance. Towards this goal, mathematical modelling with control of the granulation loop process is an important task. Thus, the thesis focuses on modelling and control of the continuous drum granulation processes with particle recycle.

The development of an efficient mathematical model that can be used for further control purposes, is studied in this research. One of the most important units in the granulation loop required for the overall model development is the granulator. In the granulator particle growth and particle collision occurs. In the thesis, macro-scale modelling of the granulation process is used. Different granulation mechanisms are investigated for developing the granulator model. Several discretization schemes (for the internal and the external coordinate discretization) are applied and used for finding the numerical solution of the resulting model. This model of the granulation loop process includes models of the granulator, screens, and a crusher.

Further, the developed granulation loop model is used for control studies. Several possibilities are investigated in order to eliminate the oscillatory behaviour seen in granulation loop plants. The thesis suggests the manipulation of either the crusher gap spacing or the fraction of the recycled product-sized particles to eliminate the oscillatory behaviour seen in the product quality. In the thesis, both classical control (PI controller or P+PI controllers) and advanced control (model predictive control) have been applied to control the produced particle size in the granulation process.

Keywords: granulation loop, particle agglomeration, particle layering, dynamic population balance model, PI control, non-linear model predictive control

Contents

Contents

Nomenclature

Acronyms	Explanation
CFD	Computational Fluid Dynamics
CS	Control Strategy
DEM	Discrete Element Methods
DLC	Double-Loop Control
MPC	Model Predictive Control
NMPC	Non-linear Model Predictive Control
NPK	Nitrogen-Phosphorus-Potassium
ODE	Ordinary Differential Equation
PB	Population Balance
PBE	Population Balance Equation
PDE	Partially Differential Equation
PID	Proportional Integral Derivative
PSD	Particle Size Distribution

Roman symbols	Explanation
B	birth rate due to particle agglomeration
D	death rate due to particle agglomeration
d	particle diameter
d_{50}	particle median diameter
G	growth rate due to particle layering
H	Heaviside step function
K_c	proportional gain of the controller
K_{eff}	separation efficiency of the screen
K_p	process gain
m	mass density function
$\dot{m}$	mass flow rate
$P(s)$	transfer function
T_i	integral time constant
t	time
u	control input
v	velocity
y	controlled output

Contents

Greek symbols	Explanation
α	valve opening
β	agglomeration rate (kernel)
γ	particle size distribution function
ζ	damping factor
λ	dimensionless term
ρ	particle density
σ	standard deviation
τ	time delay
Υ	probability function of the screen
ω	natural frequency

Subscripts	Explanation
c	controller
crush	crusher
e	effluent from the granulator
i	influent to the granulator
i	size class
k	discrete time step
low	lower screen
o	over-sized particles
p	product-sized particles
sl	slurry
u	under-sized particles
upp	upper screen
z	compartment of the granulator

Part I: Overview

1 Introduction

1.1 Background

Granulation is considered as one of the most powerful techniques in the fertilizer industry to manufacture products of the desired quality. Granulation is well-known for its ability to yield products of the desired size, improve shelf-life of the products, and to reduce their propensity to form cakes or lumps. However, operation of granulation plants on an industrial scale can be challenging. There are several operational challenges that arise in granulation loop plants. One of the challenges is the observed oscillatory behaviour in the product quality (e.g., particle size) and product quantity (e.g., mass flow rates). The oscillatory behaviour makes it difficult to maintain the desired product quality in terms of uniformity in granule size. Moreover, the oscillatory behaviour in the production rates can lead not only to decreased profits, but also to overloading of process equipment, which results in increased operational risks and unforeseen plant shut-downs. Consequently, elimination of the oscillatory behavior that would make granulation loops steadier to operate is a key research interest in the fertilizer industry.

1.2 Process description

This thesis is focused on the last part of Nitrogen-Phosphorus-Potassium (NPK) fertilizer production. The NPK fertilizer is a high value fertilizer that contains the three main elements essential for crop nutrition. The NPK production plants use a continuous wet granulation process to produce different grades of fertilizers that contain N,P and K, in various ratios. A typical schematic of a granulation process with recycle, called the granulation loop, is shown in Figure 1.1.

When a slurry (fertilizer melt) is sprayed into an agitated powder (recycled particles) in a granulator, particle enlargement (granulation) occurs. The granulation process results in the formation of composite granules. The produced granules have several advantages over their non-granulated form, such as improved product flow properties, homogeneity, ease in handling, packaging, and storage of the product.
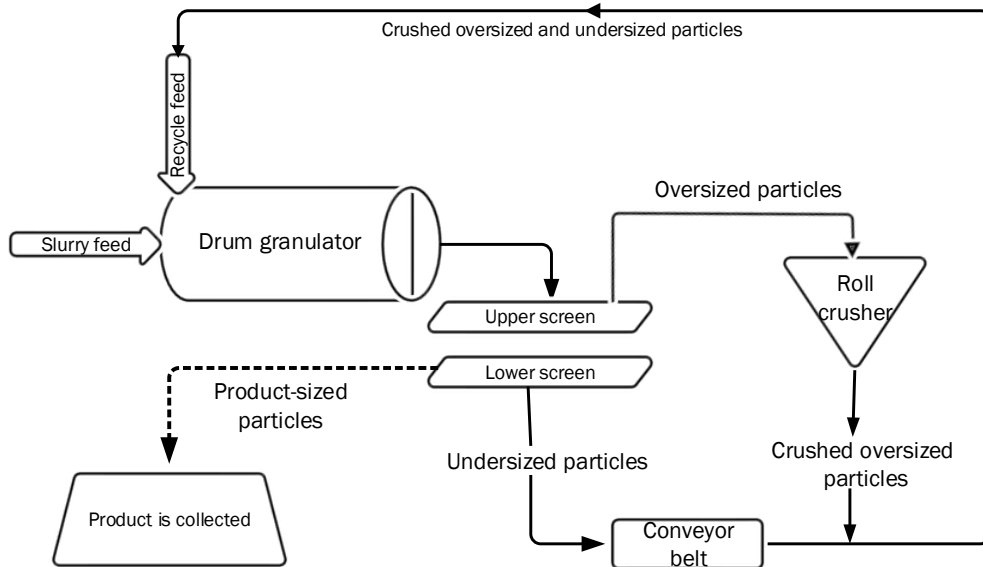
Figure 1.1: A schematic diagram of the granulation loop process with particle recycle studied in the thesis
[1].

The granulators can be of different types, e.g., fluidized bed, pan granulators, spherodizers, rotary drum granulators, and others. This thesis is focused on tumbling granulators, e.g., spherodizers and rotary drums. A spherodizer is shown in Figure 1.2. The granulator bed in the spherodizer is equipped with blades and the spherodizer is equipped to perform simultaneous granule drying. Such granulator configuration is used to facilitate so-called 'onion skin' formation on the particle, i.e., coating/layering of the fertilizer melt on the particles, and to reduce collision between particles. Drum granulators, as opposed to spherodizers, are neither fitted with the blades nor equipped for drying of the granules which is performed in the separate unit, i.e., in a drying drum. In the drum granulators, the fertilizer melt is introduced in the granulator bed using spraying nozzles that are situated at various places in the granulator.

As granules leave the granulator, they are sent to a double-deck screen. The screens are used to separate the granules in the effluent from the granulator into fractions of three sizes: under-sized particle fraction, product-sized particle fraction, and over-sized particle fraction. Particles that are small enough and can pass through both of the screens (the upper and the lower screen in Figure 1.1) are the under-sized particles. The under-sized particles are then recycled to the granulator. The over-sized particle fraction, i.e., particles that are too large to pass through the upper screen, and, therefore, remain lying on the upper screen are sent to the crusher. The over-sized particle crushing is performed using a double-roll crusher. The crushed over-sized particles are combined with the under-sized particles, forming a recycle stream (off-spec particles). The off-spec
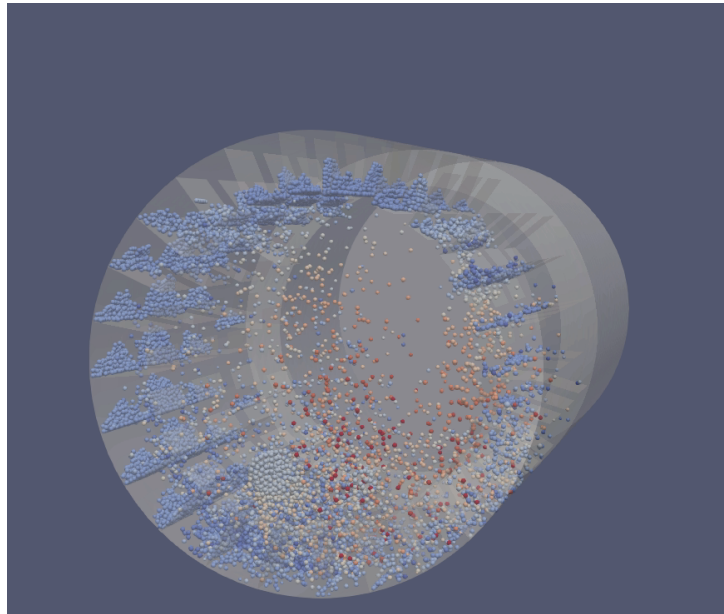
Figure 1.2: A spherodizer in operation. The colours of the particles indicate the particles' various velocities (blue colour – the lowest particle velocity, red colour - the highest particle velocity). The illustration is made for HEFTY project, drawn by SINTEF Materials and Chemistry, Flow Technology Group.

particles are recycled back to the granulator where they act as nuclei for formation of the new granules. Thus, the off-spec particles are needed to seed the granulator. Another reason of the off-spec particle recycling is a wide particle size distribution (PSD) of the granules at the granulator discharge. A relative small fraction of the granules that leave the granulator are in a required size range. Typically, the recycle ratio, i.e., ratio between the off-spec particles and the product-sized particles in the granulation loop plants is 4:1. Thus, recycling of the particles is also necessary from an economic point of view. Not least, the off-spec particles cannot be considered as waste material and discarded from an environmental point of view and, therefore, should be recycled [1].

1.3 Importance and necessity of research

Operation of the granulation loop process described in Section 1.2 faces operational challenges. From a process control point of view, there are several operational challenges to be overcome in the industrial-scale granulation loop plants. Some of these are:

- Operation below the designed capacity
- Wide PSD of the produced particles compared to the desired product PSD
- Large recycle ratios

- Oscillatory behaviour associated with the operation of the granulation loops

A fundamental industrial challenge for operation of the granulation loop processes is the elimination of the oscillatory behaviour. A typical oscillatory behaviour observed in an NPK plant is shown in Figure 1.3. Figure 1.3 shows the oscillatory behaviour in the product quality, i.e., in the median diameter of the produced particles d_{50}. Similar oscillatory behaviour is also observed in the product quantity, including in the production rates. The oscillatory behavior is linked to the entire granulation loop since the granulator receives a fluctuating recycled input stream.
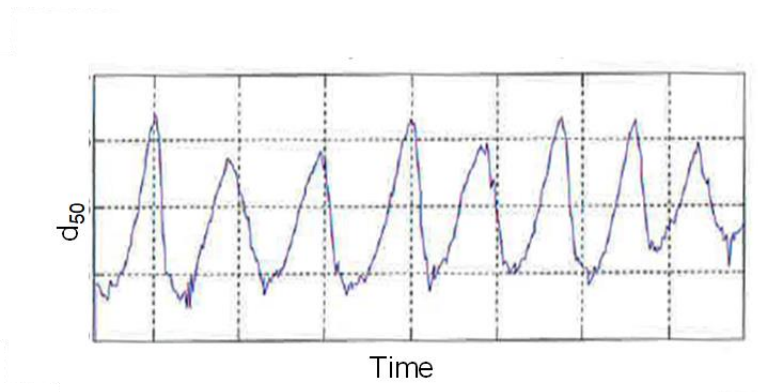
Figure 1.3: An illustration of the oscillatory behaviour in the produced particle size (median diameter, d_{50}) in the industrial-scale granulation loop plant [2].

The oscillatory behaviour observed in the product quality and the product quantity is extremely detrimental because it causes cost-ineffective production, especially in the granulation plants where expensive raw materials and/or hazardous materials are used. In addition, the oscillatory behavior may lead not only to reduced profits, but even to overloading of the process equipment. Typically, the equipment used in the granulation loop processes has limitations, e.g., maximum capacity of transport belts, crusher capacity, etc. Overloading of such processing equipment results in increased operational risks and unforeseen plant shut-downs. Furthermore, the design and operation of granulation loops are often achieved by trial and error, and are frequently based on previous experience. Thus, thorough studies, aided by the advances in numerical techniques and process control, are required to address the problem. It is critical to eliminate the oscillatory behaviour and make granulation loop processes more steady in operation.
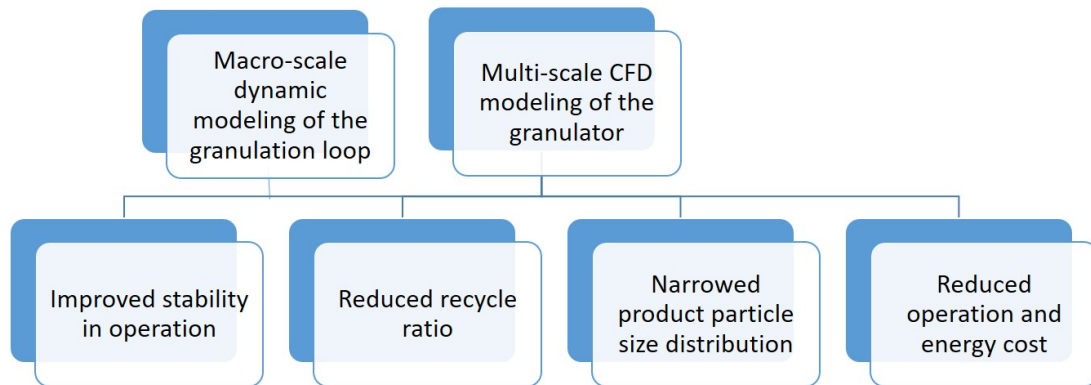
Figure 1.4: A schematic representation of the main goals of the HEFTY project: Two modeling scales to solve the innovation challenges.

1.4 Objectives and scope

This project is conducted in collaboration with Yara Technology and Projects and is a part of a project named 'Exploiting multi-scale simulation and control in developing next generation high efficiency fertilizer technologies' (HEFTY), Research Council project no. 269507/O20. The project leader is Yara Technology and Projects, while University of South-Eastern Norway and SINTEF Materials and Chemistry, Flow Technology Group are project partners. The main goal of the HEFTY project is to enable cost effective production and deliver granulated fertilizers of consistent quality, Figure 1.4. For this, two modelling approaches to the granulation process are considered, namely, multi-scale CFD modeling of the granulator itself (SINTEF), and macro-scale dynamic modelling of the granulation loop process (this PhD research project). The dynamic granulation loop model, developed within this PhD research project, will be used to develop new control strategies for the operation of the granulation loops. The developed control strategies should contribute to an improved operation of the fertilizer production and eliminate the oscillatory behaviour in the product quality (particle size). With this regard, the following research questions/hypothesis are formulated:

1. A proper population balance model can reproduce oscillations observed on granulation loop plants.

2. Control algorithm based on the model can improve operation of granulation loops (with respect to eliminating the observed oscillations).

The main objectives of this PhD study are divided into three areas as follows:

Objective / Paper	1a	1b	2	3
A			▭	
B	▭			
C	▭		▭	
D		▭		
E				▭
F				▭
G				▭

Figure 1.5: An overview of the papers shows how the papers (A-G) are distributed over the objectives listed in Section 1.4. Colours are used to separate the different areas of the defined objectives (similar colours are used in Figure 1.6 to distinguish between different objectives).

1. Develop a mathematical model of the granulation loop shown in Figure 1.1. The developed mathematical model should be simple enough yet sufficient to capture the necessary (important) dynamics of the granulation loop process.

   a) Develop a dynamic model of a granulator and to apply appropriate granulation mechanism(s) that particles are subjected to during granulation, such as particle growth due to particle layering and/or particle agglomeration.

   b) Develop a control relevant model of the whole granulation loop with particle recycle. The developed model should include a granulator, screens, a crusher, and the particle recycle.

      - Screens. The effluent from the granulator should be divided into three size fractions: product-sized particles, under-sized particles, and over-sized particles.

      - Crusher. The over-sized particles should be sent to the crusher where the sizes of the particles are reduced using a roll crusher.

      - Recycle feed. The recycle feed should contain crushed over-sized particle flow and the under-sized particle flow feeds.

2. Find and apply a numerical scheme (schemes for the internal and the external co-ordinate discretization) to solve the developed model of the granulation loop process. It is important that the developed model can be solved sufficiently fast so that it can be used for real-time implementation. Thus, a good balance between the model complexity (accuracy) and the model solution time should be considered.

3. Apply the developed granulation loop model in control studies. Here, the main objective is to find/suggest control strategies that would suppress or eliminate the oscillatory behaviour seen in the sizes of the produced particles (d_{50}) and, thus making the granulation loops more steady in operation.

1.5 Contributions
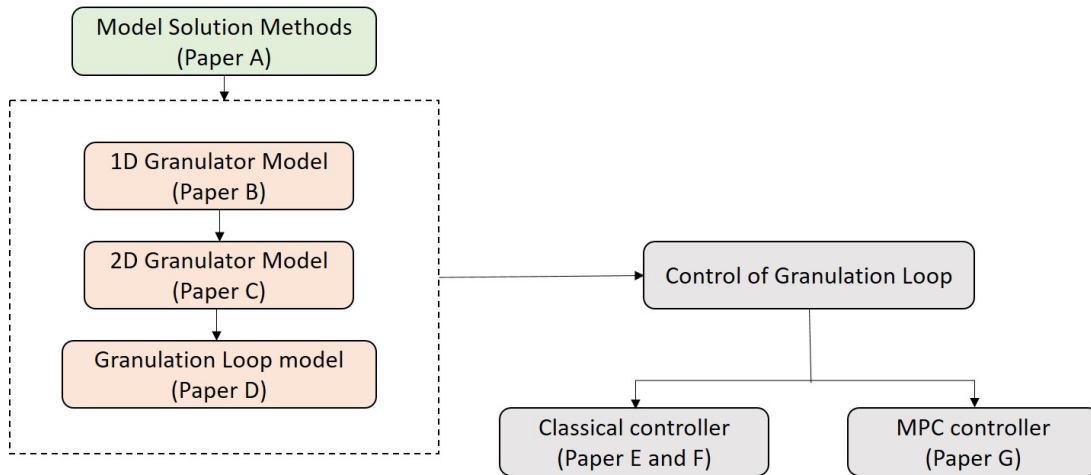
Figure 1.6: An schematic representation of the interconnections of the main contributions. Colours are used to separate the different areas of the defined objectives in Section 1.4 (similar colours are used in Figure 1.5 to distinguish between different objectives).

The work done to achieve the stated objectives in Section 1.4 is listed here. The contributions of this work are distributed over seven scientific papers, labelled A to G. The papers and the objectives they cover are shown in Figure 1.5, while Figure 1.6 illustrates interconnections between the contributions and papers listed below.

Each of the main contributions is presented as one or more articles as follows:

1. Development of a mathematical model of the granulation loop shown in Figure 1.1. The developed mathematical model can capture the necessary dynamics of the granulation loop process.

   a) Development of a 1-dimensional (1D) dynamic model of the granulator using the population balance principles. Paper B.

   The model can capture particle growth that occurs inside the granulator due to both particle layering and particle agglomeration. The resulting population balance equation (PBE) is a partial differential equation (PDE) that is transformed into a set of ordinary differential equations (ODEs) with respect to the particle size (1D model).

    b) Development of a 2-dimensional (2D) dynamic model of the granulator using the population balance principles. Paper C.

       Like the 1D model, the developed 2D model can capture particle growth due to particle layering and particle agglomeration. Here, the resulting PDE is transformed into set of ODEs with respect to the particle size and the axial position in the granulator.

    c) Development of a control-relevant model of the continuous drum granulation loop process with particle recycle. Paper D.

       The developed model includes mathematical models of a granulator, screens, and a crusher. The recycled particles are fed back into the granulator. The developed model can reproduce the oscillatory behaviour seen in granulation loop plants.

2. Application of the various discretization schemes to the PBE over the granulator: particle layering and particle agglomeration. Papers A, C and D.

   The two growth mechanisms require different types of discretization schemes. For the particle layering term discretization, three finite volume schemes were applied, while for the particle agglomeration term discretization, three sectional schemes and a finite volume scheme were used. For the simplified granulation process, the comparison between the numerical solutions and the analytical solutions are given in Paper A. In Papers C and D, the developed models are solved based on the results obtained in Paper A. The developed models can be solved sufficiently fast to be used in real-time implementation.

3. Control of granulation loop process with particle recycle: elimination of the oscillatory behaviour in the produced particle median size. Papers E, F and G.

    a) A design of two control strategies (CS) that would eliminate the oscillatory behaviour in the produced particle d_{50}: In CS1, the particle d_{50} is controlled by manipulating the crusher gap spacing, while in CS2, some fraction of the product-sized particles are sent back to the granulator to control the particles d_{50}. Papers E, F and G.

    b) Elimination of the oscillatory behaviour in the produced particles d_{50} using a classical control (PI or P+PI controllers). In paper E, the double loop control structure is applied with the CS1 and CS2 strategies. Comparison between the double-loop control structure and the classical PI controller for controlling the particle size in granulation loop processes is reported in Paper F.

    c) Application of the advanced control to control the granulation loop process. The model-based predictive controller (MPC) is applied to control the produced particle d_{50} using the suggested control strategies. Comparison of the

simulation results of the MPC controller and the double-loop control structure is reported in Paper G.

Novelty of the research work is as follows:

1. A thorough evaluation of the numerical discretization schemes applicable for finding the numerical solution of the population balance equation.

2. Proposal of a new control strategy (CS2) for eliminating the observed oscillations.

3. A through evaluation of a new control strategy (CS2) with the competing control strategy (CS1).

4. Application of the double-loop control structure to granulation loop process.

5. Application of the advanced non-linear model predictive control to granulation loop process.

1.6 Outline of thesis

The thesis is presented as a compendium of scientific publications and consists of two main parts. The first part is the synopsis of the research work in five chapters. Chapter 1 presents an overview of the research work, importance of the research, objectives and contributions. Chapter 2 presents an extensive literature review. Chapter 3 summarizes methods and approaches used to fulfill the research objectives, while summary of the scientific publications with discussions is given in Chapter 4. The conclusions drawn from this research, and recommendations for the future work, are presented in Chapter 5.

The second part is the main part of the thesis. It is a collection of scientific publications that have either been published already (Paper A - Paper E) or are currently under review (Paper F and Paper G).

2 Literature review

'Granulation is a process of agglomerating particles together into larger, semi-permanent aggregates (granules) in which the original particles can still be distinguished' [3]. Typically, granulation processes are divided into two types: dry granulation and wet granulation processes. In dry granulation processes, no liquid is used to facilitate the granulation process. In wet granulation processes, unlike the dry granulation processes, a slurry (liquid binder or melt) is used to ensure the granulation process. The slurry is sprayed or poured onto the particles (fine powders) or onto the moving surface as they are agitated in a granulator. The wet granulation processes are usually performed via tumbling and rotation of the material [3–6]. This review focuses on the wet granulation processes.

The granules produced during the wet granulation process have several advantageous over their non-granule form, such as: (i) improved product flow properties and homogeneity, (ii) ease of handling, storage, and packaging of the product, (iii) dust reduction, and (iv) reduced co-mixing of materials, which reduces the risk of product segregation. The produced granules have a higher proportion of surface area compared to their non-granule form which is highly useful in the processes where fast dissolution rates are required. In addition, granulation processes permit the reuse of waste material to manufacture marketable products [3, 4, 7, 8].

Granulation is a particle design technique that uses the process design and the formulation design to control the desired particle properties. Some of the process design choices are: type of the granulation process (e.g., batch or continuous, internal or external drying of the particles), type of the granulator (e.g., pan granulator, fluidized bed, spherodizer, rotary drum), and operating conditions. In the formulation design, the choice between the powder properties and the liquid properties is made. As to the desired particle properties, some of the most frequently used desired particle properties are the particle size, the porosity and the moisture content [3, 4, 7–9].

A word about linguistics in the thesis:

- Depending on the industry, a variety terms are used to describe industrial size enlargement processes, such as *granulation, agglomeration, balling, pelletization*. In this work, *granulation* is used to describe the size enlargement processes. A wet granulation process is considered if another process is not stated.

- Particle *layering* is also denoted *coating, snow-balling, onion-skinning.* In this work, *layering* is used to describe coating of a slurry onto the particle.

- Particle *agglomeration* is also denoted particle *coalescence.* In this work, *agglomeration* is used to describe collision and sticking together of particles.

2.1 Granulation mechanisms

Granule formation has traditionally been described in terms of a number of different mechanisms. In modern formulation, for ease of quantitative representation, the granule formation can be viewed as a combination of three sets of rate processes: (i) particle nucleation and wetting, (ii) particle growth and consolidation, and (iii) particle attrition and breakage [3, 6–8, 10].

2.1.1 Wetting and nucleation

Wetting and nucleation is the first step in the granulation process (Figure 2.1). In the spraying zone, the liquid spray droplets interacts with the powder. The effort is to distribute the liquid evenly throughout the powder. As the result of this step the initial aggregates are formed. Wetting and nucleation plays a significant role in granule formation. However, due to poor knowledge of the factors that control the wetting and nucleation processes, this mechanism is rarely identified and separated from the other two granulation mechanisms [3, 8, 10].
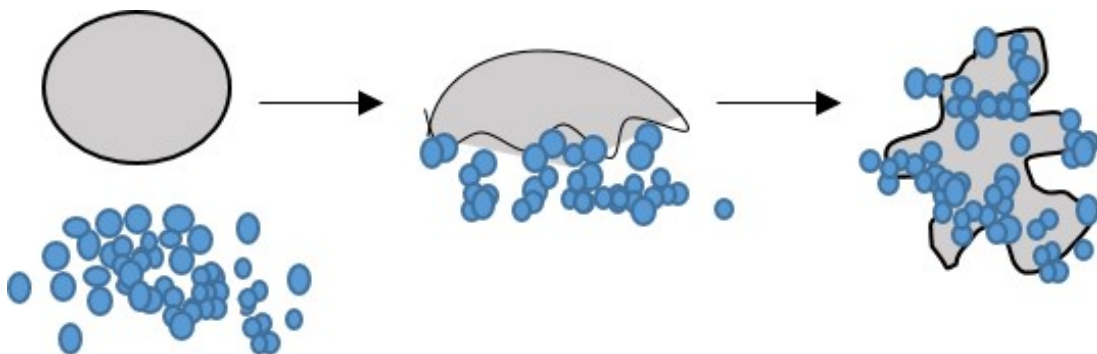
Figure 2.1: The first granulation mechanism: wetting and nucleation. Colour explanation: blue–liquid, grey–powder.

2.1.2 Growth and consolidation

The growth of particles typically occurs through two mechanisms: particle layering and particle agglomeration (Figure 2.2). Particle layering refers to a mechanism of continuous particle growth that occurs due to successive coating of a liquid phase onto the particle surface. The liquid phase in the form of a melt, solution, or a slurry, solidifies and forms an 'onion skin' on the surface of the particle. As a result, the particle increases in volume and mass. However, the number of particles in the system does not change. As a result of this mechanism, compact and hard granules are produced [3, 8].
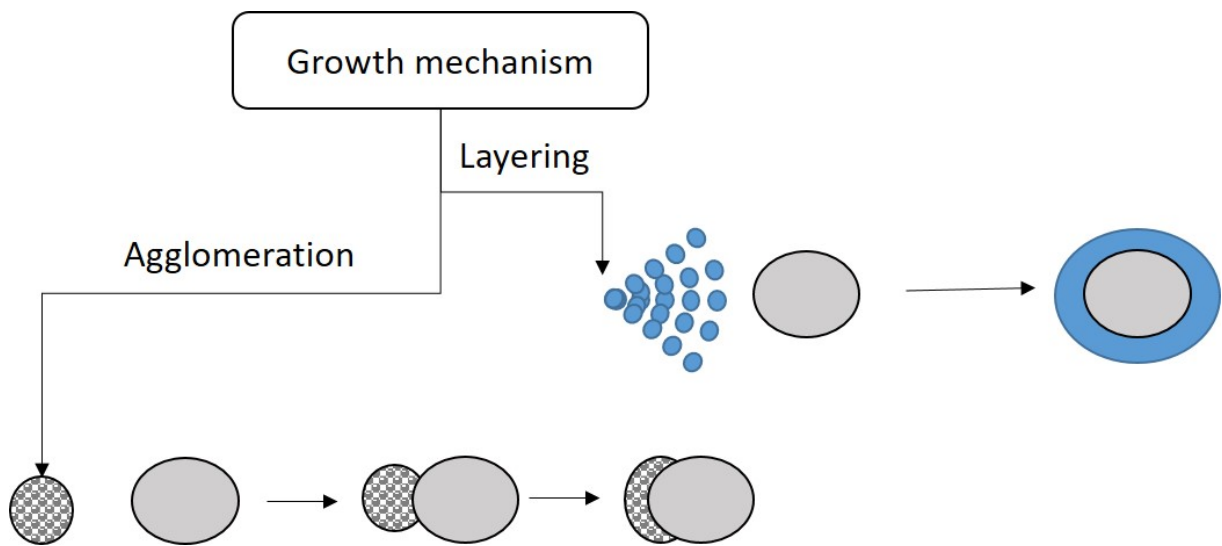
Figure 2.2: A representation of the second granulation mechanism: growth of particles due to a particle layering and a binary particle agglomeration.

Particle agglomeration refers to a discrete particle growth mechanism. Such particle growth behaviour is caused by the collisions among particles and the collided particles sticking to each other. Binary particle agglomeration occurs due to successful collision (permanent agglomeration) of two particles, resulting in the formation of a larger, composite particle (Figure 2.2). Particle agglomeration can take place as soon as the granulation process has been initiated (simultaneously with the particle wetting and nucleation), and also in the later granulation stage when the liquid is already added to the granulator. Whether the collision of the particles is successful or not depends on various aspects, such as mechanical properties of the particles (granule strength), and availability of the liquid binder near the particle surface. Binary agglomeration results in a reduction of the total number of particles: two particles *die*, and a new particle is *born* [3, 7].

Particle consolidation: particle consolidation is opposite to the particle growth mechanism, and leads to a reduction in the particle size and porosity: the air and the liquid

entrapped in the particle are squeezed out of the particle surface. This results in the reduction of the particle strength. Consolidation occurs due to the particles colliding with each other and with the equipment walls [3].

2.1.3 Attrition and breakage

Wet particle breakage by fragmentation is a discrete event, that changes the number of particles in the system (Figure 2.3). Breakage effects are important in high shear devices, especially in high intensity mixer granulation. Particle breakage phenomena in tumbling granulators (e.g., rotary drums) on the other hand has a significantly lower effect on the particle size compared to the growth mechanism. Therefore, there are few studies dedicated to the particle breakage in tumbling drums.
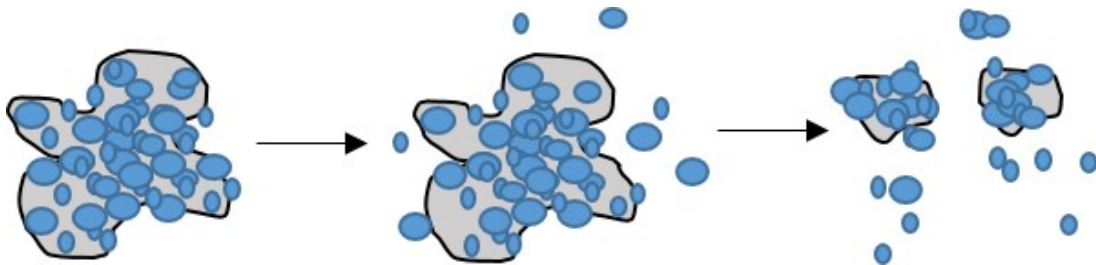
Figure 2.3: An illustration shows the third granulation mechanism: particle attrition and breakage.

Particle attrition refers to the fracture of dried particles. The attrition rate is a negative rate, and it leads to an effect that is opposite of the particle layering mechanism. The particle attrition rate is proportional to the bed conditions, and is highly dependent on the particle velocities inside the granulator. In general, particle attrition leads to dust formation which is a highly undesirable effect in the granulation processes. However, this mechanism is important in granulators where high granule velocities are used. Examples of such systems are fluidized- and spouted-bed granulators [3, 7, 8].

2.2 Modelling of granulation processes

2.2.1 Overview

Effective operation of granulation processes requires mathematical models of the process. Mathematical models are used for online control and monitoring, as well as for offline optimization. The choice among the modelling approaches for granulation processes depends on the objectives of the research. Typically, modelling of the granulation process

can be divided into 4 types: (i) particle scale, (ii) volume of powder scale, (iii) granulator scale, and (iv) granulation loop scale, as shown in Table 2.1 [7, 11].

Table 2.1: Different scales for modeling granulation processes [7, 11].

Scale	Area of analysis	Modeling method
Particle	Physico-chemical interactions	Models of liquid bridge dynamics [3]
		DEM models [12]
Volume of powder	Granulation mechanisms Rate equations	Agglomeration models [3, 4, 7, 13]
		DEM models [12]
		Monte-Carlo methods [4]
Granulator	Mixing patterns	PB modeling [14]
	Operation	CFD-DEM [15, 16]
Granulation loop	Process design Process optimization	PB modeling [17]
		Data driven-DEM modeling [18]
		CFD-DEM-PB modeling [19]

In *particle scale*, two situations are considered: (i) single particle-particle interactions, and a deformation of the particle embedded in a granule, and (ii) particle-binder physico-chemical interactions, including collision of a particle with a drop of a binder. In *volume of powder scale*, granulation rate processes, such as nucleation, growth, and breakage, are considered. Balance equations, describing evolution of the particle property distributions (size, porosity, etc) are considered in the *granulator scale*. In the *granulation loop scale*, all the unit operations and their interactions are considered, e.g., particle classification, particle crushing, and particle recycling [7, 11]. The thesis is focused on the *granulation loop scale* modelling.

The most recent studies are concerned with modelling of fluidized bed granulators [16, 19–27], while only a few are on modelling twin screw granulators [17, 28, 29] and rotary drum granulators [15, 18, 30]. Population balance modeling still remains the most used approach for modeling granulation processes, e.g., in [17, 20–23, 25, 26, 28] the authors have developed mechanistic models based on the PB to study granulation processes. Several studies are focused on micro-scale modelling (particle-particle interactions) of granulation processes using CFD (computational fluid dynamics) modelling [16, 30] or coupled CFD-DEM (computational fluid dynamics coupled with discrete element method) modelling

[15, 31], as well as CFD-DEM-PB modelling (computational fluid dynamics coupled with discrete element method and population balance model) [19, 32–34]. Many of these studies are focused on understanding and modelling of particle growth due to agglomeration [23, 24, 26, 31, 35], model validation [17, 19–22, 25], and influence of process variables on granule formation [15, 28–30]. In the most recent study, Cronin et al. [26] have proposed a new time-dependent rate constant of the agglomeration kernel for the modelling of fluidized bed granulation. The developed agglomeration rate model [26] is conceptually simple and employs only one empirically fitting parameter. Vzivzek et al. [23] proposed that in TiO_2 granulation process, the agglomeration rate is significantly higher than the breakage rate. The authors in [23] also have suggested using a reduced-order approach, with granule size as the only internal coordinate for efficient tracking of the PSDs of TiO_2 in the fluidized bed. Bellinghausen et al. [36] focused their research on particle nucleation rather than particle agglomeration. In [36], the authors have developed two new nuclei size distribution models: (i) empirical model that assumes a log-normal distribution, and (ii) semi-mechanistic model that is based on a method suggested in [37], which applies the Poisson distribution function.

2.2.2 Population balance

Ramkrishna in [38] has defined a population balance equation (PBE) as 'an equation in the number density'. In other words, 'PBE represents the number balance of particles of a particular state' [38]. PBE can also be viewed as the rate equation that describes the evolution of particle property distribution in the granulator [7]. The concept of the PBE can be written as [4],

$$
\underbrace{\text{the rate of change of the density function}}_{\text{inclass, location, time}} = \underbrace{\text{flow in}}_{\text{through boundary}} - \underbrace{\text{flow out}}_{\text{through boundary}}
$$
$$
+ \underbrace{\text{grow in}}_{\text{from lower classes}} - \underbrace{\text{grow out}}_{\text{from current class}} + \underbrace{\text{agglomeration in}}_{\text{to current class}} - \underbrace{\text{agglomeration out}}_{\text{from current class}}
$$
$$
+ \underbrace{\text{break-up in}}_{\text{from upper classes}} - \underbrace{\text{break-up out}}_{\text{from current class}} . \quad (2.1)
$$

The first two terms on the rhs. of Equation 2.1 describe the convective flow of particles in and out of the granulator (boundary). The other terms on the rhs. of Equation 2.1 cover the granulation mechanisms described in Section 2.1: the third and the fourth terms on the rhs represent the particle layering and particle consolidation mechanisms, respectively; particle agglomeration is represented by the fifth and the sixth terms on the rhs., while particle breakage mechanism is represented by the last two terms on the rhs of Equation 2.1.

PBEs are frequently used for: (i) process design to predict particle properties, e.g., predicting the produced particle PSDs, (ii) process control and optimization, and (iii) sensitivity analysis to study possible perturbations in product quality due to a change in operating conditions [7]. However, poor understanding of the rate processes (quantitative representations of granulation mechanisms), and challenging solution methods resulting from the PBEs, especially for agglomeration problems, limit the use of PBEs in granulation processes [7].

In the PBEs, particle properties are denoted as an internal coordinate, while particle location (spatial position) is denoted as an external coordinate. Some of the particle properties (internal) of a special interest are: size, shape, density, moisture content, gas content, porosity, composition, age, etc. [4, 7, 38, 39]. Mathematical representation of the number-based PBE with one internal (particle diameter), and one external (spatial position in the granulator) coordinate is given by Equation 2.2:

$$\frac{\partial n(d,z,t)}{\partial t} = -\frac{\partial}{\partial d}\left[Gn(d,z,t)\right] + B_{\mathrm{a}}(d,z,t) - D_{\mathrm{a}}(d,z,t) + B_{\mathrm{b}}(d,z,t) - D_{\mathrm{b}}(d,z,t)$$
$$-\frac{\partial}{\partial z}\left[vn(d,z,t)\right], \quad (2.2)$$

where $n(d,z,t)$ is the number density function, d is the particle diameter, z is the spatial position, and t is the time. The first term on the rhs. represents the particle growth due to layering at a growth rate G ; the second and the third terms on the rhs. stand, respectively, for particle birth (B_{a}) and death (D_{a}) due to agglomeration. The particle birth (B_{b}) and death (D_{b}) rates due to breakage are represented by the fourth and the fifth terms on the rhs. respectively. The final term on the rhs. represents a continuous process and gives the flow of particles with the velocity v through the granulator. As to the first granulation mechanism, i.e., nucleation and wetting, it is not included in the PBE because it is rarely separated from the particle growth mechanism, and rarely identified at the granulator scale and granulation loop scale modelling of the granulation processes. Nucleation is relatively significant when the feed (continuous phase) PSD is much smaller than the smallest product (produced granule) PSD. However, the less is the differences between the feed PSD and the produced granule PSD, the less is the effect of nucleation on the change in PSD during the granulation. During granulation loop processes in fertilizer industry, the produced granules are post-treated, i.e., dried before they are recycled back into the granulator. In this case, the recycled feed has a broad PSD. Thus, the feed PSD overlaps the produced granules' PSD, making the nucleation mechanism insignificant in granulation loop scale modelling.

The following is a representation of the *layering term, G* as described in Section 2.1. Layering is a continuous process (differential growth) that is initiated by the formation of a coating of the slurry on the particle. Frequently, in PB modelling, a particle size-independent linear growth rate is assumed [40, 41]. Particle size-independent growth rate

assumes that each particle has the same exposure to a new slurry feed, while a linear growth rate assumes that the growth rate is proportional to a projected particle surface area, as shown in Figure 2.4. These simplifications do not imply segregation of particles by size [7].
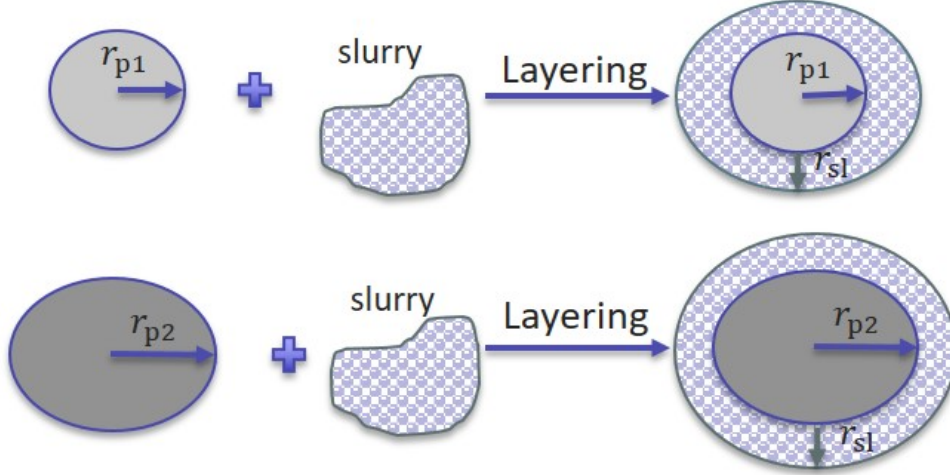
Figure 2.4: A diagrammatic representation showing that the linear growth rate of particles is independent of the original particle-size.

Representation of the *agglomeration terms*, B_a and D_a: particle agglomeration is a discrete event that results in reduced particle number in the system. Quantitative representation of the agglomeration process is very challenging. One of the most widely used agglomeration process models for granulator-scale modelling was introduced by Hulburt and Katz in [42]. Formulation of the agglomeration process [42] assumes a binary particle agglomeration process, i.e., two particles colliding with each other. During binary particle agglomeration, two particles *die*, and one particle is *born* [3, 7]. The birth of particles due to binary agglomeration is represented by the equation:

$$B_a = \frac{1}{2} \int_0^v \beta\left(t, v-w, w\right) n\left(t, v-w\right) n\left(t, w\right) dw. \tag{2.3}$$

The above equation 2.3 shows the *birth* of particles of volume v as a result of agglomeration of particles of volumes $v-w$ and w [7]. Merging of particles of volume v with any other particle, i.e., the *death* of particles is represented by the equation,

$$D_a = -n\left(t, v\right) \int_0^\infty \beta\left(t, v, w\right) n\left(t, w\right) dw. \tag{2.4}$$

In Equations 2.3 and 2.4, β is the agglomeration rate, also called the agglomeration kernel. The agglomeration kernel defines the collision frequency of the two colliding

particles. Collision frequency depends on various particle properties, as well as on the granulator properties (process system properties). Some of the most important properties are: particle size, moisture content, particle flow patterns, energy consumption, particle deform-ability, granulator configuration, and operating conditions. Another factor that affects the agglomeration kernel is the *success* of the agglomeration or rebounding after particle collision. It has been found in [43] that successful agglomeration depends greatly on the viscous-fluid layer (moisture content), elastic-plastic properties, as well as on the head of the collision [8]. Some particle collisions do not lead to particle deformation (Type I agglomeration). However, those particle collisions that lead to deformations of the particles (Type II agglomeration) are challenging to model and only a few qualitative formulations have been developed [7, 8, 43, 44]. Thus, the agglomeration kernel is a key parameter that defines the agglomeration process – both the overall rate of agglomeration and the particle distribution are affected by the agglomeration kernel. Modelling of the agglomeration process is challenging, and, so far, only empirical or semi-empirical agglomeration kernels have been developed [4, 35, 44–50].

Representation of the *breakage terms*, $B_{\rm b}$ and $D_{\rm b}$: particle breakage in tumbling granulators is not significant [3, 7], therefore, only a few studies regarding wet breakage in tumbling granulators have been published [51–53]. On the other hand, breakage effects in high-shear mixers have been intensively studied [51, 54–56]. In [51] it was shown that the bigger particles are more susceptible to breakage than the smaller particles. As in the agglomeration process, particle breakage is also a discrete event. Formulations for the breakage effects in PBEs are as follows:

$$B_{\rm b}(v) = \int_v^\infty b(v,w)\,k_{\rm b}(w)\,n(w)\,dw, \tag{2.5}$$

and

$$D_{\rm b}(v) = k_{\rm b}(v)n(v). \tag{2.6}$$

Particle breakage is dependent on two key parameters: (i) breakage rate constant $k_{\rm b}(w)$, and (ii) breakage function $b(v,w)$. The formulation of the particle breakage (Equation 2.5 and 2.5) is similar to the formulation of the particle binary agglomeration (Equation 2.3 and 2.4). However, in contrast with to binary agglomeration, the particle breakage process can have more than two fragment particles [7]. Quantitative representation of the breakage effects is challenging and complex. Some of the empirical models representing particle breakage by fragmentation are given in [53, 57, 58].

2.3 Solution of population balance equation

The PBE representing the granulation process (Equation 2.2) is a partial integro-differential equation that is challenging to solve. The integral function appears in the agglomeration

terms: the particle birth (B_a) and the particle death (D_a) terms in the Equations 2.3 and 2.4 respectively. Analytic solutions of such partial integro-differential equations are available only for ideal and simplified cases. Some of the analytic solutions for different initial conditions (e.g., exponential) and different agglomeration kernels (e.g., constant, sum, and product kernels) are given in [59]. Thus, approximation methods must be applied to solve real PBEs. PBEs are typically solved using discretization methods. First, the dimensionality of the PDE is reduced with respect to the internal coordinate, e.g., particle size. For this, a continuous size distribution is divided (discretized) into a finite number of size sections (cells) using a geometric or a linear type grid. The PDE (in the form of the PBE) is transformed into a set of ODEs using an appropriate discretization scheme. Secondly, the set of ODEs (semi-discrete formulations of the PBEs) are solved using an appropriate time integrator.

The two growth mechanisms in Equation 2.2 require different types of discretization schemes – layering is a continuous process that does not change the number of particles in the system, while agglomeration is a discrete process that changes the number of particles in the system. Consequently, for agglomeration, it is important that the discretization scheme should assign the *newly born* and the *dead* particles accurately.

Approximation of the layering term: The particle growth term due to layering in Equation 2.2 represents a hyperbolic system, and the solution to PBE, the particle property distribution, can be very sharp [60]. Various numerical methods can be applied to approximate the PBE, including discretization methods and the Monte Carlo method [60]. The most widely used method to approximate the layering term is a discretization method. Different discretization schemes can be applied to the layering term discretization, from finite element schemes [61–63] to finite volume schemes and sectional schemes. As to finite volume schemes, these are widely used in process engineering applications, including process control and process optimization [60, 64, 65]. Some of the simplest and widely used finite volume schemes are: a first order upwind scheme, a central difference scheme, and various high resolution schemes. The high resolution schemes, e.g., Koren methods [60, 66], Kurganov and Tadmor [67, 68] method, and Hundsdorfer and Verwer methods [69], use a higher order flux in the smooth regions, and a lower order flux near discontinuities. Thus, these schemes are prone to produce smooth solutions near discontinuities while attaining higher solution accuracy than the first order upwind scheme [64]. Originally, the high resolution schemes were developed for studying gas dynamics. Lately, these have been used also to find the numerical solutions of PBEs, e.g., in [60, 70–73]. For practical applications of PBEs, it is important to lower the computational cost. One of the approaches to lower the computational cost is to use the discretization scheme on non-homogeneous grids. The previously mentioned finite volume schemes are applied on linear grids. However, their application on non-homogeneous grids is challenging. Various studies are focused on the development of such discretization schemes. Some of these are the Hounslow et al. [74] sectional scheme, the improved Hounslow scheme developed by Park and Rogak [75], moving sectional schemes (Langrangian type schemes) reported in

[76, 77], as well as hybrid grid methods [78, 79].

Approximation of the agglomeration term: Agglomeration results in reduction of the number of particles in the system. Thus, it is important that the numerical scheme conserves the total number and mass of particles in the system while accurately distributing the *newborn* and the *dead* particles into the cells. Development of such schemes is challenging. The main challenge in development of these scheme is the assigning the *newborn* and the *dead* particles accurately while conserving the selected property distributions (e.g., mass, number).

Frequently used methods for solving PBEs for agglomeration process are: wavelet-based adaptive methods [80–82], Monte Carlo simulation methods [8, 65, 83, 84], methods of moments [85–88], sectional methods [4, 39, 74, 89–95], and modified finite volume methods [65, 96–101]. In practical process engineering applications, the sectional methods are widely used to find the numerical solution of the agglomeration models. The sectional methods are famous for their relatively simple implementation, accurate prediction of the selected property distributions, and low computational time. These characteristics enable the use of PBEs for real time model based process control and optimization.

2.3.1 Discretization schemes on geometric type grids

Discretization of the continuous size domain using the geometric type grids is frequently employed in process engineering applications due to its less computational cost compared to the discretization schemes that uses linear type grids. One of the earliest sectional schemes that used geometric type grids are reported in [74, 76, 102–104]. Some of these schemes, e.g., [102], have been found to accurately predict the total particle volume. However, these schemes fail to predict the change in the total number of particles. Others, e.g., [76], accurately predicted the change in the total number of particles but fail to conserve the total particle volume [64, 98].

The first sectional scheme that could accurately predict the change in the number of particles while conserving the total particle volume is Hounslow's discretization scheme [74]. Hounslow's scheme [74] is valid only on the geometric type grids with a factor of two in size, i.e., $v_{i+1} = 2v_i$. According to Hounslow's scheme, the change in the number of particles in the ith cell is caused by four binary interaction mechanisms. Two of these four mechanisms represent the particle *birth* in the ith cell, while the other two mechanism represent the particle *death* in the ith cell. Hounslow's scheme assumes the particle *birth* in the ith cell to be due to particles' interaction: (i) between the $(i-1)$-th cell with the particles in the first to the $(i-2)$-th cells, and (ii) between the two particles in the $(i-1)$-th cell. The particle *death* in $(i-1)$-th cell can occur due to particles' interaction (i) between two particles in the (i)-th cell, and (ii) between the particle in the (i)-th cell with the larger particle from the higher cell [64, 74]. The main advantage of the

Hounslow's scheme is its low computational cost. Discretization on the geometric grid leads to a smaller number of cells, and that, in turn, lowers the computational cost. The main disadvantages of Hounslow's scheme is a relatively less accurate solution in terms of property distribution and restrictions on specified grids. Discretization on the geometric grid leads to a decrease (compared to linear grid) in the number of cells, which reduces the accuracy of the solution. In addition, Hounslow's scheme can be applied only on geometric type grids with a factor of two in size. In [105], the authors have generalized Hounslow scheme to other geometric type grids. Thereafter, limitations of the generalized Hounslow scheme presented in [105] have been solved, and the adjusted Hounslow scheme that can be used on various geometric grids (with different factors) is reported in [106]. In [89, 91], the authors have improved the generalized Hounslow's scheme reported in [106] by reducing the computation time. The schemes developed in [89, 91, 106] overcome the main disadvantage of Hounslow's scheme but are relatively complex in implementation which limits their use.

2.3.2 Discretization schemes on linear type grids

The use of discretization schemes that can be applied on linear grids is advantageous. Discretization on the linear grids is typically characterized by greater accuracy. This advantage is more important in the granulation processes where agglomeration is modelled since each particle needs to find a new position in the size interval. However, the computational costs of the sectional schemes that are applied on the linear grids are higher compared to those applied on geometric grids [64].

In [107], the authors have developed a sectional scheme called a fixed pivot scheme that can be used on linear type grids. The fixed pivot scheme is based on Hounslow's scheme [74] and eliminates the disadvantage of the use of Hounslow's scheme being limited only to geometric grids. The fixed pivot scheme can be used on both the geometric grids and linear grids. It was found that the fixed pivot scheme produces accurate results for the selected moments, while overestimates the whole particle property distribution, i.e., over-predicts the number density in the large size range when applied on coarse grids [64]. In order to overcome the disadvantage (overestimation of the results) of the fixed pivot scheme, a moving pivot scheme was introduced in [90]. Discretization of the PBE using the moving pivot scheme results in a system of stiff differential equations, and practical application of the scheme is limited by its complexity [64].

Another frequently used sectional scheme for solving agglomeration models is the cell average scheme [64, 92]. Like the fixed pivot scheme, the cell average scheme can be applied both on the geometric and the linear type grids. There are two main differences between the cell average scheme and the fixed pivot scheme: (i) volume averaging, and (ii) domain of particles which contributes to birth at a node. In the fixed pivot scheme, each *birth* that takes place in a cell is directly assigned to the appropriate node. In the cell average

scheme, on the other hand, first the average volume of all *born* particles is calculated, and then only the particles are assigned to the appropriate nodes. As was shown in [64], averaging of the volume increases the accuracy of the scheme. Volume averaging performed in the cell average scheme also results in a broader, particle domain compared to the fixed pivot scheme, which may contribute with a *birth* at the node (Figure 2.5). In the fixed pivot scheme the particle domain covers two adjacent cells partly, while in the cell average scheme the adjacent cells are covered completely. Thus, the cell average scheme keeps more information about the cell, while the fixed pivot scheme has more numerical dissipation [64]. The finite volume schemes are also used for approximation of
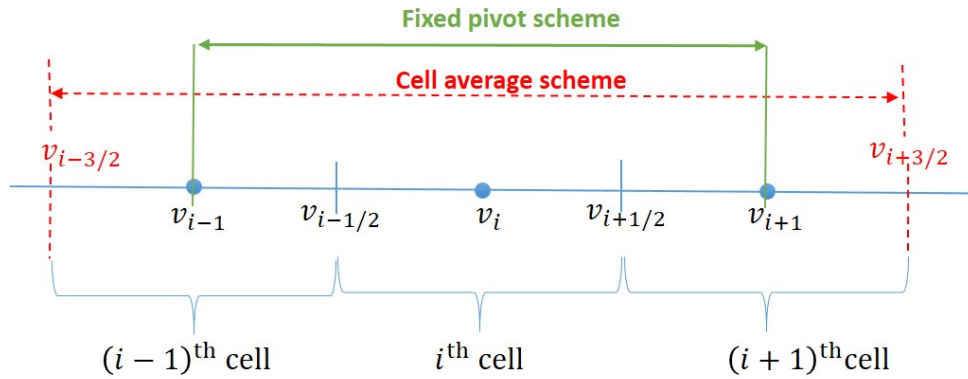
Figure 2.5: Differences in the particle domain which may contribute a *birth* at the node v_i using the cell average scheme and the fixed pivot scheme [64].

the agglomeration models [65, 96–101]. In the finite schemes, the PBE is transformed into a conservation law of mass. One of the first finite volume schemes developed for the agglomeration processes was formulated by Filbet and Laurencot [96]. Since then, various formulations of the modified finite volume schemes were developed. These include, Forestier and Mancini formulation [97]. One of the latest schemes formulated is by Kumar et al. [108], and another is the weighted finite volume scheme formulated by Kaur et al. [101].

2.4 Control of granulation processes

The operation of granulation loops is not trivial and often presents operational challenges. Various studies on granulation loops have addressed the following challenges: (i) operation of granulation loops below their nominal design capacity, (ii) high recycle ratios (ratio between off-spec particles and product-sized particles), and (iii) observed oscillatory behaviour in the product quality (e.g., in particle median size) and the product quantity (e.g., in mass flow rates). These challenges may cause overloading of process equipment and unforeseen plant shut-downs that make the plant operations uneconomical and pose

greater safety hazards [4, 8, 45, 94, 109–114]. Even though it is evident that in-depth process control and optimization studies are required to address the above-mentioned challenges, the development of general control strategies and methods continues to be a challenging task [94, 109, 112, 114–122]. These challenges have several aspects: (i) complex granulation loop interactions (Figure 2.6) summarized in the Wang et al. review paper [4], (ii) distributed nature of the resulting PBEs, (iii) model uncertainties, (iv) nonlinear and multi-variable input–output behavior, (v) deficiency of sensors for in-line monitoring of the particle properties, and (vi) insufficiency of the manipulated variables [4, 94, 112, 115, 123, 124].
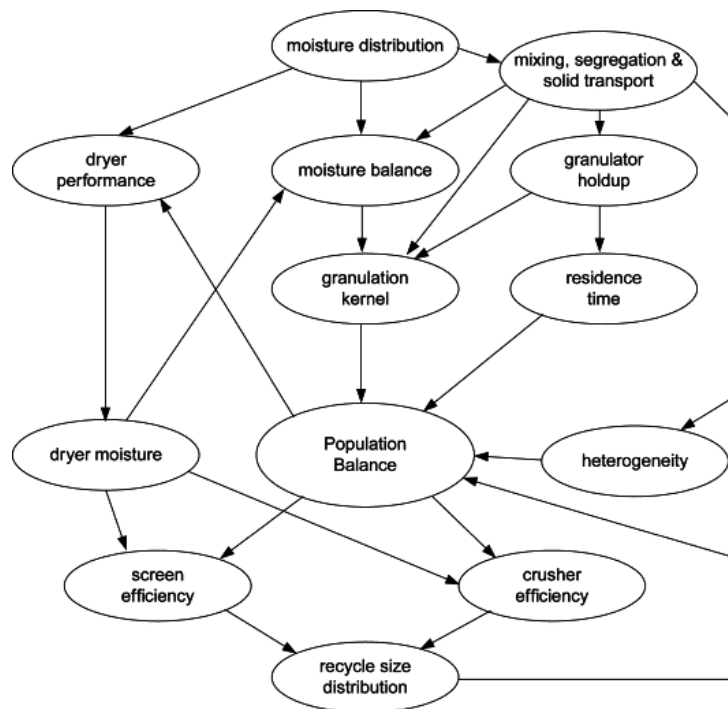
Figure 2.6: Granulation loop interactions [4].

Various control methods have been applied to the granulation processes to address the operation challenges, ranging from classical control [94, 95, 109, 125–128] to advanced control methods, such as non-linear control [114, 116, 129–135] and model predictive control (MPC) [110, 136–140].

2.4.1 Classical control

The proportional-integral-derivative (PID) controller is still the most used control algorithm in the industry due to its simple structure and ease of operation [141]. In [126], the authors have proposed a strategy to control fertilizer granulation loops using classical

control, i.e., using a PI controller. Zhang et al. [126] considered the PSD in the recycle feed (defined as the mass fraction of under-sized and over-sized particles in the recycle feed) as the controlled variable, while the water addition rate to the slurry feed as manipulatable variable. Closed loop simulations were performed using the PI controller. This simulation study showed that the proposed control structure could track the set point. However, this control structure showed a long response time to reach the new steady state. Thus, eliminating the long dynamic transition time still remained a challenging task. Zhang et al. [126] have also pointed out that it might be useful to use feedforward control to address this challenge. Thereafter, in [125], the authors have used feedforward compensation to control the granulation process. The authors focused on control of particle properties in a continuous binder-agglomeration process. Mort et al. [125] have proposed a simple control strategy that utilizes feedback control with feed-forward compensation to control the produced particle size and/or bulk density. Optimal control for drum granulation processes were studied by Wang et al. [39, 45]. These studies indicated the necessity of developing agglomeration kernels that would show the dependency of the particle agglomeration on process parameters.

In recent years, several studies on dynamics of granulation processes have been published. Most of these studies are focused on the control of fluidized bed granulators [23, 94, 95, 109, 118, 119, 129–131, 142, 143], and a few on twin screw wet granulation processes typically used in pharmaceutical industry [117, 144–147]. Open-loop dynamics of fluidized beds are studied in [148–151], while closed loop dynamics in [94, 95, 109, 137]. The goal of these studies is to find a method to make granulation processes more steady in operation. Neugebauer et al. [95] are possibly the first to show experimentally that the process dynamics in fluidized beds can be improved significantly by using even relatively simple control strategies. In [95], the authors implemented a cascade controller for a continuous fluidized bed layering granulation process to enhance the dynamics of the process and to eliminate oscillatory behaviour in the PSDs. In the developed control strategy, the granulator bed mass in the inner loop is controlled using a PI-controller by manipulating the rejection rate of the produced particles. In the outer loop, the particle Sauter mean diameter in the bed is controlled by manipulating the crusher power. The results showed that it is possible to eliminate the oscillatory behaviour seen in the PSD using only manipulation of the inner loop or a cascade control (inner loop and outer loop) as the control strategy. They observed that the convergence rate towards the operating point is significantly higher when the cascade control strategy is used, 5 h vs 40 h, respectively [95]. Later, Neugebauer et al. [94] suggested a new concept for the control of fluidized-bed layering granulation with external particle classification and crushing. The authors in [94] proposed to use three loops to control fluidized bed process. The first loop (the basic loop) is used to control the bed mass by manipulating the particle rejection rate from the granulator. For this, a standard PI controller is used. The second loop is used to control the particle Sauter diameter by manipulating the crusher gap. The third loop is used to control (indirectly) the porosity by manipulating the thermal conditions. The

Table 2.2: A brief overview of the control structures used in the granulation process studies.

Control method	Manipulatable variable	Controlled variable	Reference
Classical PI	produced particle rejection rate	bed mass	[95]
Cascade	1. produced particle rejection rate 2. crusher power	1. bed mass 2. Sauter diameter	[95]
Classical PID	1. aggregation rate 2. feed particle size distribution	1. produced particle median size 2. produced particle distribution width	[127]
PI, decentralized approach	1.produced particle rejection rate 2.porosity 3. mill grade	1.bed mass 2.gas inlet temperature 3.Sauter diameter	[94]
H_∞ loop shaping control	mill grade	second moment of particle size distribution	[132]
Discrepancy based control	suspension injection rate	third moment of particle size distribution	[114]
Linear MPC	1. aggregation rate 2.feed nuclei size distribution	1. produced particle median size 2.produced particle distribution width	[127]
Linear MPC	1.binder spray rate 2.solid feed fresh feed rate	1. produced particle median size 2.produced particle rejection rate	[110]
Linear MPC	median diameter of milled and re-cycled particles	bed mass	[137]

oscillatory behaviour in the resultant particle PSD was eliminated using the decentralized PI control. Control of fluidized bed granulators with external particle classification and crushing is also extensively studied by Palis [118, 129–131]. In these simulation studies an adaptive discrepancy based control is used to study the fluidized bed granulation process. The most recent study by Palis [118] is focused on control induced oscillatory behaviour in fluidized bed spray granulation. In [118], Palis suggests that the oscillatory behaviour in the produced particle PSDs is caused by the mass controller that is typically used in fluidized bed granulators. Palis also suggests that the mass-controller-induced oscillatory behaviour is not due to specific control strategies but rather occurs on the all fluidized bed granulators where bed mass controllers are used [118]. A brief overview of the control structures used in granulation processes is given in Table 2.2

2.4.2 Model predictive control

One of the first studies regarding possible application of a model predictive control for particulate processes is given in [152]. In [152], non-linear MPC using a physically based model was applied to the crystallization process. Later, in [140, 153, 154], the authors extended the work of Miller and Rawlings [152], and applied non-linear MPC to a semi-batch polymerization process. Gatzke and Doyle III [140] have also proposed applying a linear MPC, having a quadratic objective function, to control the particle density in the polymerization process. Further, Crowley et al. [153] and Immanuel and Doyle III

[154], suggested that just as MPC was used in the polymerization process, it can be applied also to the granulation process [8]. Thereafter, Pottmann et al. [139] applied MPC to a simulated granulation process. In [139], the bulk density was controlled by tracking the set point, while the 5th and the 90th percentiles of the particle sizes were constrained between limits. Here the authors used a linear MPC strategy – a physically based granulation model was linearized, which transformed the MPC problem into a quadratic programming problem.

In the last 10 years, few attempts have been made to control granulation loop processes using MPC design. In a simulation study by Glaser et al. [110], the authors applied MPC to a drum granulation loop process. A non-linear drum granulation loop model (based on a 1D PB granulator model) was linearized using step response data, and the linear models was then used as the prediction model for linear MPC. The non-linear granulation loop model was used as a simulator, representing the real plant. In [110], the authors developed a multiple-input-multiple-output (MIMO) system to control the granulation loop. In the MIMO system, the binder spray rate and an additional solid feed rate were considered as manipulatable variables, while the median particle size in the recycle feed and the mass in the granulator were considered as controlled variables. The simulation results in [110] showed that it is possible to eliminate the oscillatory behaviour in the recycle flow using the proposed MIMO structure. Later, Ramachandran and Chaudhury [136] have continued the work of Glaser et al. [110]. In [136], a validated 3D PB model of the granulator (validated using a batch granulation pilot plant) was used for control studies. However, the study was focused only on the drum granulator, not on the entire granulation loop including the particle recycle. Ramachandran and Chaudhury [136] have pointed out that PSD width could not be controlled using their model. They suggested that more thorough studies should be made to achieve control over PSD width.

A few works on the application of MPC on fluidized bed granulation processes are also available in literature [137, 138]. In [137], linear MPC was applied to a simulated fluidized spray granulation process with an external product classification. Particle growth due to layering was assumed to be the only granulation mechanism that contributed to the particle growth in the fluidized bed. Later, in [138], the authors extended their previous work reported in [137] by applying the model on a different fluidized bed configurations. Thus, in [138], linear MPC was applied to a fluidized spray granulation process with an internal product classification to control the produced particle size.

3 Methods and Approaches

3.1 Mathematical models (Objective 1)

In this section, only the main granulation loop model formulations will be mentioned. Details regarding modeling of the granulation process are given in Papers B, C, and D.

3.1.1 Granulator model (Objective 1a)

Mathematical model of the multi-compartment granulator was developed using the PB principles. The resulting PBE for solid phase is given by Equation 3.1,

$$\frac{\partial m(d,z,t)}{\partial t} = -d^3 \frac{\partial}{\partial d}\left[G\frac{m(d,z,t)}{d^3}\right] + B(d,z,t) - D(d,z,t) - \frac{\partial}{\partial z}[v \cdot m(d,z,t)], \qquad (3.1)$$

where $m(d,z,t)$ is the mass density function, d is the particle diameter, z is the particle position in the granulator, t is time, G is the particle linear growth rate, B is the particle *birth* due to agglomeration, D is the particle *death* due to agglomeration, and v is the velocity of the particles through the granulator.

The following considerations and assumptions were made while developing the granulator model (Equation 3.1):

- Type of PBE: In an industrial application, it is relatively easier to work with mass-based PBEs instead of number-based PBEs. Therefore, a mass-based PBE was used.

- Choice of internal coordinate: The main goal of developing the model was to further use it in control studies, i.e., to eliminate the oscillatory behaviour in the particle size. Thus, the natural choice for internal coordinate was the particle size. In the PBE, the particle size is represented by its diameter.

- Choice of external coordinate: The external coordinate is the particle position in the granulator. Here, the length of the granulator is divided into three compartments of equal size, and a concept of output equivalent (*perfect mixing*) inside each of the compartments is assumed (details are given in Paper C).

- Choice of the granulation mechanisms: Change in the particle size was assumed to be due to particle growth mechanisms: particle layering and particle agglomeration. The roles of other granulation mechanisms were assumed to be negligible compared to the particle growth mechanisms. Particle nucleation is hardly distinguishable when a granulation process with particle recycle is used (see Section 2.1.1 for more details), thus particle nucleation was not modelled. Particle attrition and breakage effects were not included in the model since drum granulators operate at relatively low velocities and low shear (see Section 2.1.3 for more details).

- Particles are assumed as ideal spheres of consistent particle density.

Particle growth due to layering (G in Equation 3.1): In the NPK granulation process, a fresh fertilizer melt (slurry) is added to the granulator to ensure particle growth. In the thesis, it was assumed that the each particle has the same exposure to slurry material, and the growth rate is the same for all the particles. Thus, a size-independent linear growth rate was used to model the particle layering process. Details are given in Papers B, C and D.

Particle agglomeration (B and D in Equation 3.1): In the thesis, it is assumed that two particles are colliding with each other, i.e., binary particle agglomeration is modelled. The particle *birth* (B) and particle *death* (D) due to binary agglomeration are modeled using the Hulburt and Katz formulation [42]. In the agglomeration model, the agglomeration kernel defines the collision frequency between two particles. Both the particle size-independent and the particle size-dependent agglomeration kernels were applied in the granulator model in Paper B and Paper C. Further, in the study on the granulation loop model, the particle size-dependent Kapur agglomeration kernel [49] is used.

3.1.2 Granulation loop model (Objective 1b)

The overall flow scheme used for modelling the continuous granulation loop process is given in Figure 3.1. The granulator is modelled using the PBE given in Section 3.1 and described in detail in Paper D.

Particle classification: The effluent from the granulator is separated into three size classes of flows: over-sized, product-sized, and under-sized particle flows. In the real plant, the particle flow separation into different size classes is performed using a double-deck screen. In the thesis, the double-deck screen is modelled using the probability functions P defined in [155, 156].

If P defines the probability with which particles remain lying on the screen, then the mass flow rate of the over-sized particle flow that remains lying on the upper screen is calculated as,

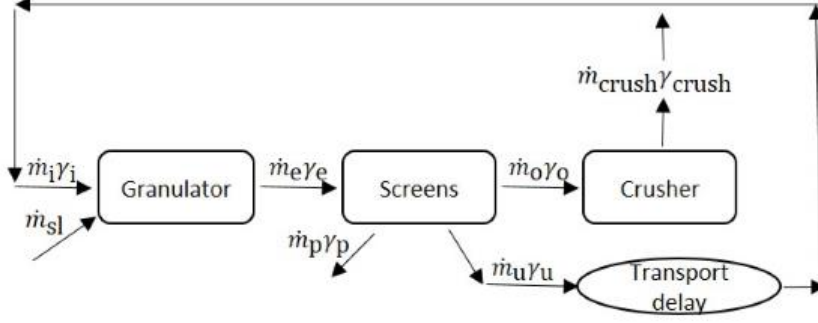$$\dot{m}_o \gamma_o = P_{upp} \dot{m}_e \gamma_e. \tag{3.2}$$

Figure 3.1: A simplified diagram of a granulation loop process flow. Here, $\dot{m}_{\text{sl}}$ is the slurry flow rate, $\dot{m}_{\text{i}}$, $\dot{m}_{\text{e}}$, $\dot{m}_{\text{o}}$, $\dot{m}_{\text{u}}$, $\dot{m}_{\text{p}}$, $\dot{m}_{\text{crush}}$ are the mass flow rates of influent, effluent, over-sized, under-sized, product-sized and crushed particles respectively. The corresponding distribution functions of the influent, effluent, over-sized, under-sized, product-sized and crushed particles particles are denoted with γ_{i}, γ_{e}, γ_{o}, γ_{u}, and γ_{p}, γ_{crush}, respectively [1].

If $(1-P)$ is the probability with which particles pass through the screen, then the product-sized mass flow rate that passes through the upper screen, but remains lying on the lower screen, is calculated as

$$\dot{m}_{\text{p}}\gamma_{\text{p}} = (1 - P_{\text{upp}})\,P_{\text{low}}\dot{m}_{\text{e}}\gamma_{\text{e}}. \tag{3.3}$$

The mass flow rate of the under-sized particles that pass through the upper and lower screens is defined as,

$$\dot{m}_{\text{u}}\gamma_{\text{u}} = (1 - P_{\text{upp}})\,(1 - P_{\text{low}})\,\dot{m}_{\text{e}}\gamma_{\text{e}}. \tag{3.4}$$

In Equations 3.2- 3.4, $\dot{m}_{\text{o}}$, $\dot{m}_{\text{u}}$, $\dot{m}_{\text{p}}$ are the mass flow rates of over-sized, under-sized, and product-sized particles, respectively. The corresponding distribution functions of the over-sized, under-sized, and product-sized particles are denoted with γ_{o}, γ_{u}, and γ_{p}, respectively. The functions P_{upp} and P_{low} are the upper and the lower screen probabilities, respectively. Detailed formulations of the probability functions are given in Paper D.

Particle transport: The elevator that is used to transfer under-sized particles together with the crushed over-sized particles to the recycle belt is modeled as a transport delay.

Particle crushing: Prior to recycle, the over-sized particle flow is sent to a double-roll crusher. In the crusher, the particles are reduced in size, resulting in a particle flow having a new PSD. The main parameter of the roll crusher that affects the size of the crushed particles is the crusher gap spacing, d_{crush}. In this study, the Gaussian distribution function is used to model the particle crushing. The Gaussian distribution function is used

to re-distribute the total over-sized mass flow with the new distribution function, γ_{crush}. Detailed formulations of the crusher model are given in Paper D. The total over-sized particle flow rate at the crusher discharge is defined as,

$$\dot{m}_{crush}\gamma_{crush} = \left(\sum \dot{m}_o\gamma_o\right) \cdot \gamma_{crush}, \tag{3.5}$$

and the total mass flow rate that is recycled back to the granulator is,

$$\dot{m}_i\gamma_i = \dot{m}_{crush}\gamma_{crush} + \dot{m}_u\gamma_u. \tag{3.6}$$

3.2 Numerical methods (Objective 2)

The PBE over the granulator is, in fact, a PDE. In the thesis, the PDE was solved numerically using discretization methods. In order to find the numerical solution of the PDE, first, the PDE was transformed into a semi-discrete form. Second, an appropriate time integrator was used to find the numerical solution of the resulting semi-discrete PDE.

Methods used for obtaining semi-discrete form of the PBE (Equation 3.1): Discretization of the PBE is 2-dimensional, namely, the internal coordinate (particle size), and the external coordinate (particle position in the granulator). The internal coordinate was discretized into 80 particle sizes using a linear grid. Depending on the growth mechanism, different discretization algorithms were used for internal coordinate discretization. First, to compare numerical solutions with the analytic solution, simplified tests were performed using various discretization schemes. The tested schemes and the modelled granulation processes on which they were tested are listed in Figure 3.2.

The solutions to the agglomeration process were obtained using Kumar et al.'s new finite volume scheme [108], and three sectional schemes, i.e, Hounslow's scheme, fixed pivot scheme, and the cell average scheme. For the layering process discretization, three finite volume schemes were applied, i.e., first order upwind scheme, second order central difference scheme, and a high resolution scheme extended with the Koren flux limiter function. Details of this study are given in Paper A and they were used to choose the appropriate discretization methods for the granulation loop model. Figure 3.3 shows discretization methods that were used in the thesis for finding numerical solution of PBE in the granulation loop model.

A solution method for the semi-discrete PBE: The semi-discrete process model representing the granulation loop process were solved using a built-in ODE integrator in Simulink. In this study, a 4-th order Runge-Kutta (RK-4) integrator with fixed time step (20 s) was used.
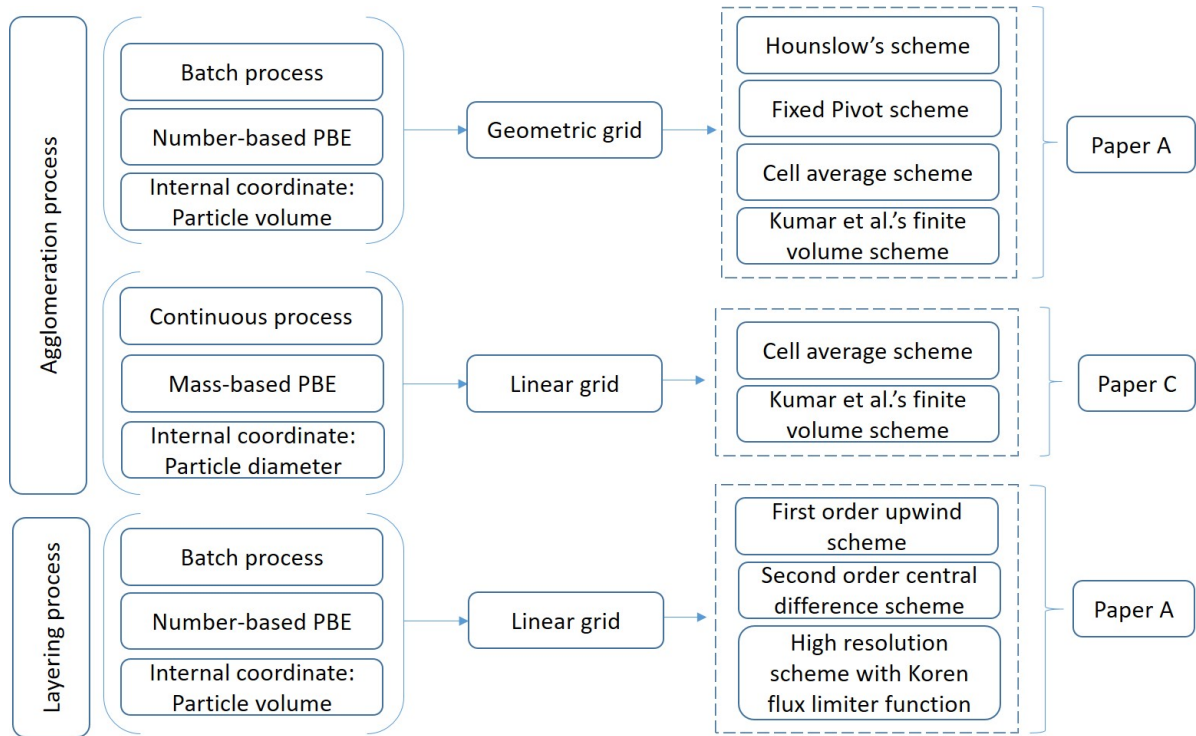
Figure 3.2: Discretization schemes that were applied to simplified granulation processes. For numerical assessment of the schemes , the resulting numerical solutions were compared with the analytic solution given in Paper A.
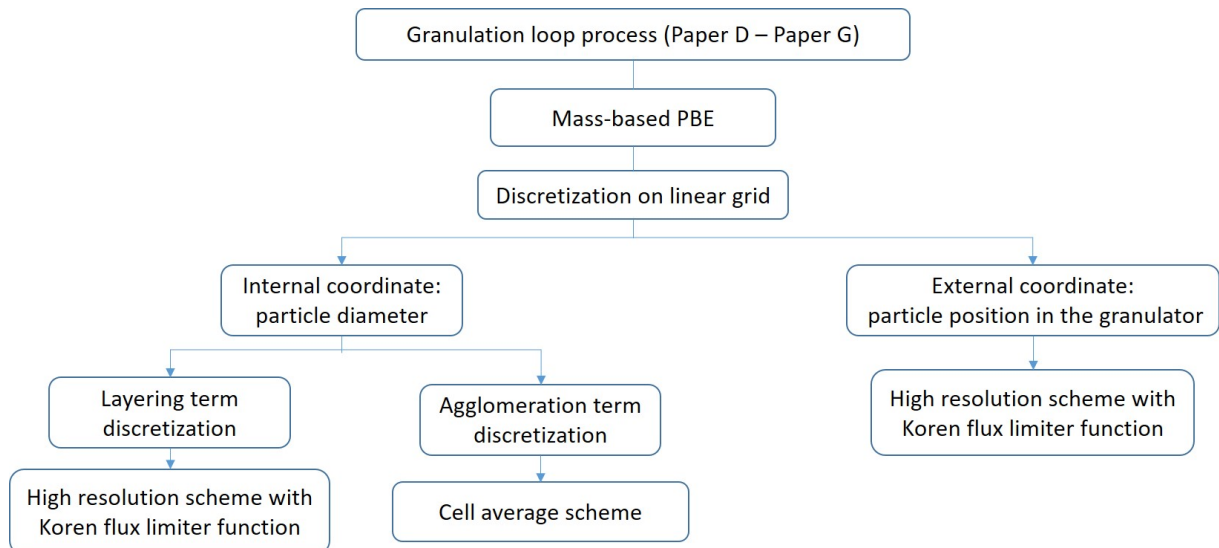

Figure 3.3: Discretization schemes for PBE over the granulator that were used in the overall granulation loop model.

All the simulations used in this thesis were performed with Simulink and MATLAB [157].

3.3 Control of granulation loop process (Objective 3)

In the thesis, the main purpose of controlling the granulation loop plant is to eliminate the oscillatory behaviour observed in the product quality, i.e., in the produced particle median size d_{50}. For this purpose, two control strategies (CS) were designed. The developed CSs were implemented using the classical controllers (PI or P+PI) and model predictive controllers. The methods used are described below and summarized in Figure 3.4.
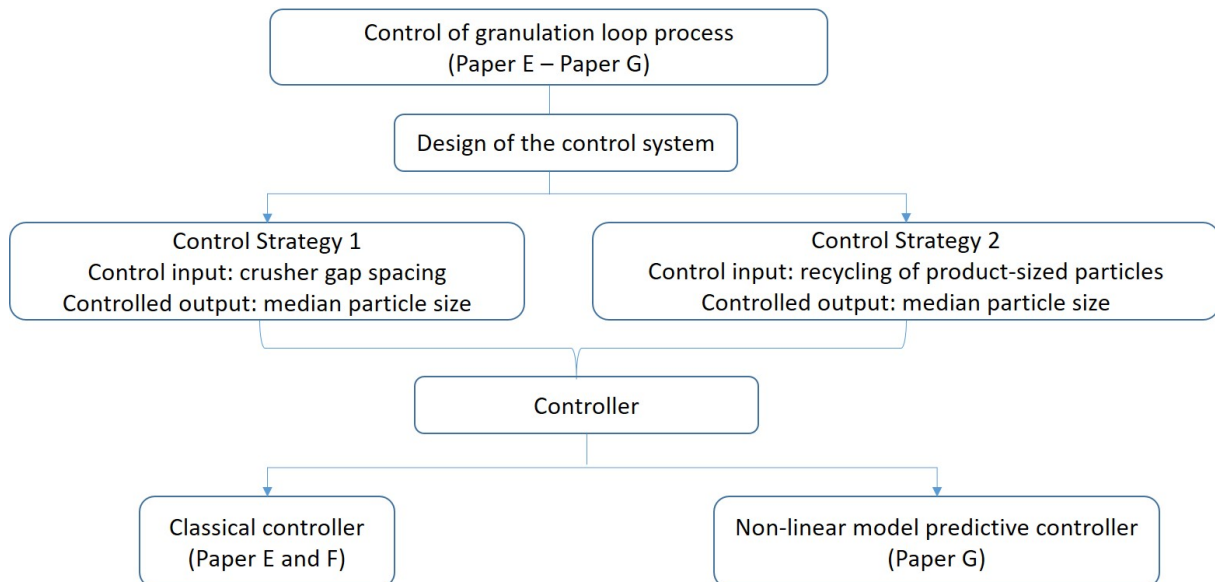
Figure 3.4: A summary of methods that were used to eliminate the oscillatory behaviour in the particle median size: two control strategies were designed, and used with both classical control and advanced control to control the granulation process.

3.3.1 Design of the control system

Control Strategy 1: Based on the process control objective, the natural choice for the controlled output is the produced particle median diameter d_{50} at the granulator discharge before particle flow is separated into different size fractions. The particle d_{50} is the particle diameter that corresponds to the intercept for 50% of cumulative mass. In CS1, the produced particle d_{50} is controlled by manipulating the the crusher gap spacing, d_{crush}. This strategy was developed based on the previously studies (Paper D), which showed

that the oscillatory behaviour in the particle d_{50} is strongly dependent on the size of the crushed particles that are recycled back to the granulator. The open loop simulations using the model developed in this thesis, showed that it is possible to control the particle d_{50}, and to eliminate the oscillatory behaviour in the particle d_{50} by manipulating the crusher gap spacing, d_{crush}. The CS1 strategy (details given in Paper E) assumes that the granulation plant configuration allows operators to easily manipulate the crusher gap spacing from the control room. Such crushers are not typically seen in the granulation loop plants. Typically, the crusher gap spacing in the plant needs to be changed manually and directly by the plant operators. As alternative to CS1, a second control strategy (CS2) was developed.

Control Strategy 2: In the CS2 strategy, as in CS1, the controlled output is the granule PSD distribution, as measured by d_{50}, at the granulator discharge before the particles are separated into different size fractions. However, unlike in CS1, the produced particles d_{50} are controlled by sending some of the product-sized particles back to the granulator. Thus, the control input is a three-way valve opening α that can be used to regulate the amount of product-sized particles to be recycled. When the valve is closed ($\alpha = 0$), none of the product-sized particles are recycled; when the valve is open ($0 < \alpha \leq 1$) – some fraction of the product-sized particles flow rate is added to the off-spec particle flow on the recycle belt. The CS2 strategy of recycling a small part of product sized particles can be economically advantageous as it reduces the oscillatory behaviour in product quality and product quantity, and thus, reduces the operating cost and energy consumption, as well as lower the risks of the unforeseen plant shut-downs. Details of the CS2 strategy are given in Paper E.

3.3.2 Controllers

Control of the produced particle d_{50} in the granulation loop process was performed using: (i) a classical PI controller, and (ii) a double loop control structure using P+PI controllers to control the granulation process with particle recycle. The details of the application of these control structures are given in Paper E and Paper F.

Classical PI controller: For finding the classical PI controller parameters, first, the granulation loop process was approximated using a transfer function of the oscillatory process. The process parameters used in the transfer function were obtained using a simulated step response data. Then, the controller parameters were identified. The PI controller was tuned using Skogestad's tuning rules for oscillatory processes [158]. The controller was then fine-tuned. Details regarding application of the classical PI controller are given in Paper F. Application of the above control strategy in the granulation process eliminated the oscillatory behaviour in the produced particle size. However, the convergence rate towards the operating point was relatively low. Thereafter, the double-loop control

structure was implemented in the granulation process to achieve a higher convergence rate.

Double loop control structure: This structure for oscillatory systems [141] was applied to eliminate the oscillatory behaviour and to achieve higher convergence rate towards the operating point. In the double-loop control structure, two controllers are used: (i) a damping controller (inner controller) which converts an underdamped system into an overdamped system, and (ii) a main controller (outer controller) which is tuned to achieve a specified performance. Here, a P controller was chosen as the inner controller, and the PI controller as the outer controller. Details of the design and application of this control structure are given in Paper E. A comparison based on simulation results between the classical PI controller and the double loop structure is given in Paper F.

Model predictive control (MPC): The MPC was also used to eliminate the oscillatory behaviour in the produced particle d_{50} that occurs in granulation loop plants. In this thesis, the non-linear granulation loop process model was directly utilized to formulate the nonlinear optimization problem. Thus, a non-linear MPC was used. In the optimization problem, the prediction horizon was the same as the control horizon, and the control inputs were split into four groups of unequal length. The constrained non-linear optimization problem was solved using the *fmincon* solver in MATLAB [157], with the Sequential Quadratic Programming optimization algorithm. Details of design and application of the NMPC in the granulation process are given in Paper G.

4 Summary and Discussion of papers

4.1 Paper A - Solving the population balance equation for granulation processes: particle layering and agglomeration

Summary: Paper A compares different numerical schemes for solving PBEs by comparing the numerical solutions with the analytic tractable solutions. The PBEs used in this study represent batch granulation processes with the particle volume as the internal coordinate.

Still nowadays the upwind scheme is frequently used for solving PBEs that incorporate only the layering process. In most recent studies, e.g. in [115] and [95] the PBE representing the layering process in a fluidized bed is discretized using the first order upwind scheme. As to particle agglomeration, the Hounslow's discretization scheme seems to be most frequently used to find numerical solutions to the agglomeration procesess [39, 110]. Comparison of the cell average scheme with the finite volume scheme developed by Filbet and Laurencot [96] is reported in [98]. Authors in [98] applied the mentioned two schemes for agglomeration and breakage processes. In Paper A, the work of [98] was extended by comparing a recent finite volume scheme [108] with the cell average and other two sectional methods.

Paper A considers two granulation processes. In the first case, the PBE represents the granulation process that uses a particle layering mechanism. In the second case, the PBE represents the granulation process due to a binary particle agglomeration mechanism. The mentioned granulation mechanism requires different type of discretization schemes. In the first case, when the particle layering process is assumed, a semi-discrete form of the PDE is found using three finite volume schemes: first order upwind scheme, second order central difference scheme, and a high resolution scheme extended with the Koren flux limiter function. In the second case, when the agglomeration process is assumed, a semi-discrete form of PDE is found using the finite volume scheme of Kumar et al [108], and three sectional schemes: Hounslow's scheme, fixed pivot scheme, and cell average scheme. Assessment of accuracy of the numerical schemes is based by comparing the numerical solutions with analytically tractable solutions, i.e., by comparing the number density function and separate moments of the function.

Novelty of this paper is a thorough comparison of the discretization schemes that can be applied for solving PDEs that occur during modeling of the granulation process using the PBE. In addition, a recent finite volume scheme [108] is applied to solve the agglomeration process. The performance of the scheme is also compared with other 3 sectional schemes. Results of this study are contributing in the field of granulation modeling, specially for the models that are build for further model based control studies.

Discussion: The research presented in Paper A has a key significance in developing the model of the granulation process. In this study, only simplified batch processes are simulated since analytical solutions are available only for simplified granulation processes. However, the results of this paper are further used to develop a dynamic model of a drum granulator that is a part of an overall model of the granulation loop process (objective 1). The choice of the tested solution schemes in Paper A are based on the further use of the model. The overall model of the granulation loop process, including the particle recycle, is further used in the control studies (objective 3) with the goal of eliminating the observed oscillatory behaviour in the produced PSDs. Consequently, the numerical schemes should produce accurate enough model solutions to capture the dominant dynamics of the granulation process. Such a model should also reproduce the oscillatory behaviour observed in granulation loop plants. The choice of the tested solutions is also based on the length of computational time: the tested schemes must produce numerical solutions sufficiently fast (low computational time) for the model to be useful for real-time model predictive control. Only semi-discrete discretization methods are considered in this study because the control theories are typically based on the applications of the ODEs rather than discrete model formulations.

The results of this paper are further used to develop the granulation model in Paper B and Paper C. Based on the comparative study, it was decided to use the high resolution scheme for finding a semi-discrete form of the PDE that represented the layering process. The high resolution scheme showed the highest numerical solution accuracy among the tested schemes. The first order upwind scheme showed low accuracy, while the central difference scheme produced oscillations when the solution changed abruptly. As to the choice of the agglomeration term discretization, a decision was made to use the cell average scheme which not only attained higher accuracy in shorter computational time but also was conceptually simple.

4.2 Paper B - Population balance modelling for fertilizer granulation process

Summary: Paper B focuses on developing the model of the granulator. PBEs used in this study. The model represents a continuous granulation process with the particle diameter

as the internal coordinate. A granulator is assumed 'perfectly mixed', i.e., there is no change in the particle properties throughout the process of granulation.

PBEs representing granulation processes typically include or particle layering mechanism or incorporates both particle layering together with the particle agglomeration mechanism. In recent studies [95, 115, 132], the granulation process in fluidized bed granulators is modelled by assuming only the particle layering mechanism. The particle layering in [95, 115, 132] is modelled using a particle-size independent linear growth rate, while the discretization is performed using the first order upwind scheme. Combined processes, i.e., PBE incorporating particle layering together with the particle agglomeration is studied by Glaser et al. [110]. Glaser et al. [110], similarly to [95, 115, 132] have modelled the layering term using the size-independent linear growth rate. The agglomeration process is modelled using the Hulburt and Katz formulation [42] with the empirical formulation of the agglomeration kernel. In [110], discretization of the particle layering and the particle agglomeration is performed using the Hounslow scheme. Paper B analyzes various granulation mechanisms. For this, three cases are considered: (i) particle growth due to layering, (ii) particle growth due to agglomeration, and (iii) particle growth due to both the particle layering and agglomeration. Thus, three types of processes are modelled. In the first case, similarly to [95, 110, 115, 132], the change in particle size is modelled using the size-independent linear growth rate. In the second case, similarly to [110], the particle *birth* and *death* due the to binary particle agglomeration is modelled using the Hulburt and Katz formulation [42]. In the third case, the change in the particle size is assumed to occur both due to the particle layering and agglomeration. In addition, two types of the agglomeration kernels are considered: (i) particle size independent, and (ii) particle size dependent agglomeration kernels. Unlike [95, 110, 115, 132], the semi discrete form of the resulting PBEs is obtained using two discretization methods; the layering term is discretized using the high resolution scheme, while the agglomeration term is discretized using the cell average scheme. The results of this study contribute to a deeper understanding of the effect of granulation mechanisms on the grow of particles.

Novelty of Paper B includes, (i) formulation of the cell average scheme for the mass-based PBE with the diameter as the internal coordinate, (ii) analysis of different agglomeration kernel effect on the grow of particles, (iii) application of the high resolution scheme to the granulation process incorporating the particle layering mechanism.

Discussion: Paper B partly covers granulator model development (objective 1a). Here development of a 1D model is presented. The number-based PBEs in Paper A are converted into a mass-based formulations assuming that the particles are ideal spheres of consistent density. The particle layering model assumes that all the particles are equally exposed to the slurry material, and particles in the granulator grow at the same rate irrespective of the original particle size. Even though these assumptions might not be a realistic basis for the model, such models are frequently used in macro scale modelling of granulation processes.

Quantitative representation of the particle agglomeration is challenging. The agglomeration process is typically modeled using the Hulburt and Katz formulation [42]. In Hulburt and Katz formulation [42], the collision frequency is defined by the agglomeration kernel. However, only empirical or semi-empirical formulations of the agglomeration kernels of the granulation processes are available. Thus, further experimental studies are needed to define the agglomeration kernel accurately. Here, various agglomeration models (size-dependent and size-independent agglomeration kernels) are tested. The developed granulator model utilizes one of the most frequently used agglomeration kernels, i. e., Kapur agglomeration kernel which is a particle-size dependent agglomeration kernel.

Similar to Paper A, the developed model solution is found by discretizing the resulting PBEs. Here, the results in Paper A are used to choose the appropriate discretization schemes. Thus, the layering term is discretized using the high resolution scheme extended with the Koren flux limiter, while the agglomeration term is discretized using the cell average scheme. In Paper A, discretization is performed for the particle size, while the granulator is assumed to be perfectly mixed. Further extension of the granulator model is presented in Paper C.

4.3 Paper C - Application of population balance equation for continuous granulation process in spherodizers and rotary drums

Summary: Paper C presents the extended model of the granulator. The developed model is 2D with respect to the internal coordinate (particle diameter) and to the external coordinate (particle location in the granulator). Extension of the model is achieved by developing a multi-compartment granulator. The granulator is divided into equal-sized compartments. In each of the compartment the concept of output equivalent (*perfect mixing*) is assumed. Solution schemes for the internal coordinate are similar to those used in Paper B. The external coordinate is discretized using the high resolution scheme extended by Koren flux limiter function. This differs from [39], where the external coordinate is discretized using the orthogonal collocation method. In [39] and Paper C, similar drum granulation models are used. However, models of the agglomeration kernel in Paper C and [39] are different. Wang et al [39] utilizes the model of the empirical agglomeration kernel that was obtained in the drum granulation pilot plant in University of Queensland. While in Paper C, the Kapur agglomeration kernel is used.

In paper C, various cases of simulation are used to gain deeper understanding of the developed granulation models. In these simulations, the number of compartments in the granulator is varied, ranging from *perfectly mixed* granulator to a 100-compartment granulator. Thus, the novelty of Paper C is comparison of different number multi-compartment

granulators and their influence on numerical results and model execution time. Analysis of simulation results is based on comparing both the changes in the particle size distributions and the particle median sizes. In addition, the simulations with different agglomeration kernels (the particle size dependent and the particle size independent) are also performed.

Discussion: Paper C shows the development of the granulator model (objective 1a). The developed 1D granulator model in Paper B is extended to a 2D model. The developed multi-compartment granulator model accounts for property inhomogeneity in the granulator, and introduces a transport delay from the inlet of the granulator to its outlet. The computational time involved in the developed 2D model is more than in the case of 1D model. However, such model extension is necessary in this thesis since the developed model is further used for control studies where knowledge of transport delays is important (e.g., for obtaining correct transfer functions).

Paper C also compares solution accuracy and computational time of the models that are obtained using two discretization schemes, i.e., the cell average scheme and the new finite volume scheme by Kumar et al. [108]. The above mentioned schemes showed the best accuracy among the tested schemes for agglomeration term discretization in Paper A. Here, a comparison was made to find out whether one scheme has any advantages over another when applied to the developed granulator model. However, no significant differences between the two schemes were observed. Since the cell average scheme is conceptually simple, the scheme is further used for discretizing the agglomeration term in the overall granulation loop model with particle recycle. Thus, the results obtained in paper C contribute to further development of the entire granulation loop process with particle recycle (objective 1b).

4.4 Paper D - Dynamic model for simulating transient behaviour of rotary drum granulation loop

Summary: Paper D is concerned with the modelling of the continuous granulation loop process with particle recycle. In Paper D, a multi-compartment granulator model is used. The PBE is mass-based with the particle diameter as the internal coordinate, and particle position in the granulator as the external coordinate. In the developed model, the change in the particle size occurs due to the layering mechanism, and due to the agglomeration mechanism. The effluent from the granulator is separated into three size-based fractions: over-sized, under-sized, and product-sized particle flows. The flow is classified using the probability functions. The over-sized particle flow is sent through the crusher that is modelled using the Gaussian distribution function. The crushed over-sized and the under-sized particle flows are combined and sent back to the granulator.

Granulation loop model in Paper D is similar to the model presented by Radichkov et al. [111]. In [111], the model of the fluidized bed spray granulation with external product classification is developed. Similarly to Paper D, the granulator model includes the particle layering mechanism that assumes particle-size independent linear growth rate. Unlike Paper D where the particle agglomeration also contributes to the particle size change, in [111], the particle attrition mechanism is included in the model. The first order upwind scheme is used to discretize the internal coordinate, and the numerical bifurcation analysis is performed in paper [111].

The novelty of this paper is the development of the multi-compartment granulation loop model that incorporates both the particle layering mechanism and the particle agglomeration mechanism with the Kapur agglomeration kernel. The solution of the granulation model (discretization of the internal and the external coordinates) is obtained using relatively accurate and fast (model execution time) discretization schemes: the finite volume scheme extended with the flux limiter function and the cell average scheme. In addition, different simulation scenarios were created to analyze the process dynamics and understand the probable reason for the occurrence of the oscillatory behaviour. Both the effect of the crusher gap spacing and the slurry feed on process dynamics are studied in the paper D.

Discussion: Paper D shows the developed model of the granulation loop process with particle recycle (objective 1b). The granulator model is based on the model developed in Paper C. The granulator model is the 2D model that assumes both particle growth mechanisms. The model uses simple formulations for particle classification and particle crushing. However, even using these models, the resulting granulation loop model could reproduce the oscillatory behaviour seen in the real granulation loop plants. Consequently, the developed granulation loop model can be further used for control studies with the objective of eliminating the oscillatory behaviour (objective 3). As Paper D suggests, the occurrence of the oscillatory behaviour depends on the PSD in the recycle feed, i.e., on the crushed particle PSD. This dynamic behaviour is further used to design control strategies in Papers E to G.

4.5 Paper E - Double-loop Control Structure for Rotary Drum Granulation Loop

Summary: Paper E is concerned with control of the granulation loop process with particle recycle. Here, the main objective of the granulation process control is to eliminate the oscillatory behaviour observed in the produced particle size. A simulation study is performed using the developed in Paper D model of the granulation loop process.

Table 4.1: Result summary of Paper E (m.v. — manipulatable variable; c.v.—controlled variable).

Control strategy	Convergence rate towards the reference point	
	Controller turned on at minimum point in the cycle	Controller turned on at maximum point in the cycle
CS1 m.v.: crusher gap spacing c.v.: produced particle median diameter	6 h	6 h
CS2 m.v.: valve opening that defines how much of the product-sized particles is recycled c.v.: produced particle median diameter	7 h	6 h

In Paper E, two control strategies are suggested with the aim of eliminating the oscillatory behaviour in the particle size. In one of the control strategies (CS1), the control over the median size of the produced particles is achieved by manipulating the crusher gap spacing. In addition, a novel control strategy (CS2) is developed in Paper E. CS2 suggests to recycle some of the product-sized particles back to the granulator to control the median size of the produced particles. The results in Paper E show that it is possible to eliminate the oscillatory behaviour in the median size of produced particles by using the above control strategies. The main numerical results of Paper E are summarized in Table 4.1 (results for DLC structure).

In addition to a development of the novel control strategy, Paper E applies a double-loop control structure to eliminate the oscillatory behaviour. The double-loop control structure was not used before for controlling the granulation processes. Paper E first suggests the use of a P controller to transform the oscillatory system (granulation loop process) into an overdamped system. Then to follow it by using a PI controller to achieve the specified performance, i.e., to track the reference point. The proposed double-loop control structure is applied in both the control strategies.

To compare with, in [95], the authors implemented the feedback control to eliminate the oscillatory behaviour in fluidized-bed granulator. Unlike Paper E, the feedback control strategy based on a simple PI controller and a cascade controller is used to dampen the oscillatory behaviour, thus two control strategies are developed. In the first control strategy, unlike Paper D, the bed mass is controlled by manipulating the rejection rate of the produced particles using the PI controller. In the second control strategy to improve

the process dynamics, a cascade control with two loops is used. In the inner loop, the bed mass is controlled by manipulating the rejection rate of the produced particles, while in the outer loop, the particle Sauter mean diameter is controlled by manipulating the crusher power.

Discussion: Paper E utilizes the simulation results presented in Paper D, that the occurrence of oscillatory behaviour depends on the particle size distribution in the recycle feed. Thus, a 'direct control' of the produced particle median size by manipulating the crusher gap spacing is proposed in the CS1. The CS1 assumes that the crusher gap spacing can be manipulated easily by the plant operators. However, such crushers are not typically seen in granulation plants. Thus, a novel control strategy is proposed in Paper E. As alternative to CS1, CS2 suggests that a fraction of the product size particles can be recycled back to the granulator (together with the crushed over-sized and under-sized particles) to control the produced particle size and, thus, to eliminate the oscillatory behaviour.

The proposed control strategies differ from those previously reported in open literature. In the previously published works, a different drum configuration is assumed, e.g., in [110, 136] the authors assumes additional input (fine powder) to the drum as the manipulatable variable, or by manipulating the moisture/solid feed rates. The moisture effect is not discussed in this thesis. In real applications, the moisture effect on particle growth is dependent on the physical-chemical properties of the product, particle-binder interactions, granulator configurations and operating conditions. Wang et al. [45] have proposed a model that includes the moisture effect on particle growth. However, the model presented in [45] is empirical model having more than 10 fitting parameters and applicable to a specific pilot plant configuration where moisture content is measured. The effect of the use of accurate moisture content (e.g., moisture/solid ratio) on process dynamics requires experimental data that are not available in this research.

The control strategies proposed in Paper E can eliminate the oscillatory behaviour in the produced particle size. Thereafter, in Paper F and Paper G, the research is focused on application of different controllers for obtaining a higher convergence rate towards the operating point.

4.6 Paper F - Comparison of feedback control structures for operation of granulation loops

Summary: Paper F, like Paper E, deals with the control of granulation loops using classical control. Paper F compares two feedback control structures to control the granulation loop processes. In one of the control structures, a classical PI controller is used to control the produced particle size. In the another control structure, two loops are used to control the the produced particle size. In both the control structures, the controlled output is the

Table 4.2: Result summary of Paper F (DLC—double-loop control structure).

Point in the cycle at which controller was turned on	Convergence rate towards the reference point	
	classical PI	DLC
Minimum	50 h	7 h
Maximum	50 h	6 h

production of particles of median size, while the input is controlled through a three-way valve that decides the quantity of product-sized particles to be recycled back into the granulator. A brief result summary of Paper F is given in Table 4.2.

Paper F shows that it is possible to eliminate the oscillatory behaviour in the particle size by using a classical PI controller. However, the convergence rate towards the operating point is higher when the double-loop control structure is used. An analysis of the controller's ability to compensate for disturbance is also made in the paper. For this analysis, the adjustment of crusher gap spacing is considered as the disturbance.

The novelty of Paper F is the thorough comparison of two feedback control structures. Paper F shows advantages of double-loop control structure over the classical PI control structure by comparing the convergence rate towards the reference point. In addition, Paper F presents ability of the double-loop control structure to compensate for disturbances.

Discussion: The study presented in Paper F compares the convergence rates towards the operating point that are obtained using various control structures. The double-loop control structure is previously applied to the granulation loop process in Paper E. However, the study in Paper F emphasizes the advantages of using the double-loop control strategy over the structure based on the classical PI controller. The use of damping controller contributes to a significantly higher convergence rate towards the reference point. Additional use of P controller, instead of simple PI controller, does not complicates the implementation of the control strategy in real plants. Therefore, it is highly recommended. Also, Paper F fills in the gap in Paper E by including the information regarding the controller's ability to compensate for disturbances that might affect the process. In Paper E, ability to compensate for disturbances is shown for the control strategy where the particle d_{50} is controlled by recycling some of the product-sized particles to the granulator. The controller's ability to compensate for disturbances for the control strategy where the crusher gap spacing is used the control input is given in Figure 4.1. In Figure 4.1, a slurry mass flow rate is assumed as a process disturbance. Disturbances are applied when the controller is turned on ($0 < t < 75$ h), and when the controller is turned off ($t \geq 75$ h). In the manual

control, i.e., when the controller is turned off, the value of the crusher gap spacing is the same as the last obtained value when the controller was turned on ($u_{\text{manual}} = u_{\text{automatic}}$). Figure 4.1 shows that the controller is able to compensate for the applied disturbances.
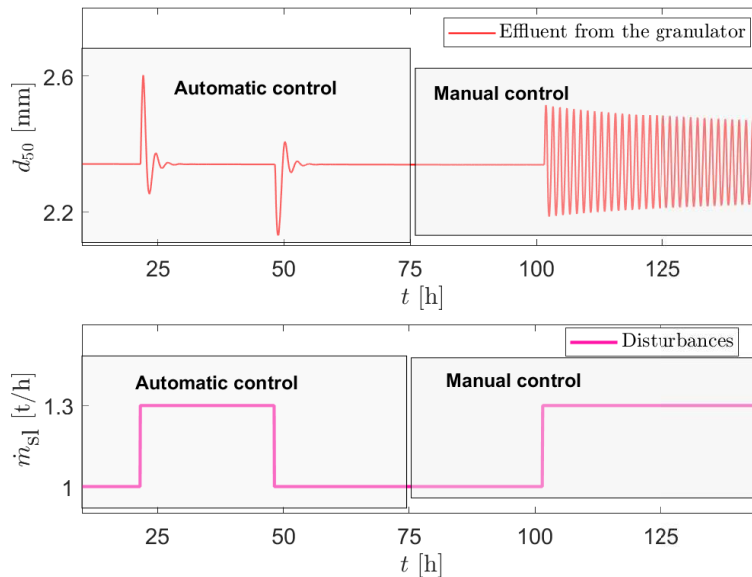

Figure 4.1: Disturbance rejection using the double-loop control structure: Disturbance is the slurry mass flow rate, and the controller is turned off at $t = 75$ h with $u_{\text{manual}} = u_{\text{automatic}}$.

4.7 Paper G - Non-linear model predictive control for drum granulation loop process

Summary: Paper G focuses on the use of advanced control in granulation loops. In this paper, a model predictive controller is used to control the granulation loop process. The granulation process is controlled through two control strategies: in one, the produced particle median size is controlled by manipulating the crusher gap spacing, while in the other, it is controlled by manipulating the valve opening to decide how much of the product-sized particles are recycled back into the granulator. The choice of the manipulatable/controlled variable differs with the research published in [110]. In [110], linear MPC is applied to drum granulation process to study the ability of the controller to compensate for disturbances. The produced particle rejection rate from the granulator is controlled by the additional fresh solid feed, while the particle median diameter is controlled by manipulating the controlled by the binder spray rate[110]. The linear MPC is also applied in fluidized bed granulator [137]. Unlike Paper B, the study in [137] focuses on controlling the bed mass by manipulating the median diameter of the milled and recycled particles.

Table 4.3: Result summary of Paper G. Abbreviations in the table: m.v. — manipulatable variable; c.v.—controlled variable.

Control strategy	Convergence rate towards the reference point
CS1 m.v.: crusher gap spacing c.v.: produced particle median diameter	4.4 h
CS2 m.v.: valve opening that defines how much of the product-sized particles is recycled c.v.: produced particle median diameter	3.5 h

The main novelty of Paper B is the application of the non-linear MPC to eliminate the oscillatory behaviour in the particle size. The MPC design consists of the process block, Kalman filter, and the prediction model block. The process and the prediction model is a non-linear model of the granulation loop process described in paper D. Paper G also shows that it is possible to eliminate the oscillatory behaviour by solving a minimization (optimization) problem used in the MPC design.

The another contribution of this paper is the comparison between the classical control and the advanced control. Results obtained with the double-loop control structure (paper E) are compared with results obtained using the non-linear MPC. The analysis is based on comparison of the convergence rate towards the reference point. Paper G suggests that the higher convergence rate towards the operating point is obtained when the non-linear MPC is used to control the produced particle median size by manipulating the crusher gap spacing. A brief summary of numerical results are given in Table 4.3.

Discussion: The study covered in Paper G is performed to eliminate the oscillatory behaviour in the produced particle size using the advanced control and to examine the convergence rate towards the operating point. According to the simulation results in Paper G, it seems that the MPC might be a good choice for controlling the granulation loop process. Paper G also supports the simulation results obtained in Paper E. The use of the control strategy in which the produced particle size is controlled by manipulating the crusher gap is preferable due to higher convergence rate towards the operating point. Thus, it might be economically advantageous for fertilizer industry to acquire a crusher with crusher gap spacing that is remotely and easily adjustable from the control room.

5 Conclusions and Recommendations

5.1 Conclusions

The main research objective of this thesis is to develop a mathematical model of the granulation loop process that includes particle recycle. This topic is discussed in four papers, with particular focus on population balance modeling and granulation mechanisms that are important for modelling granulation processes. The mathematical model of the granulator is developed using the population balance principles. The developed granulator model is capable of tracking changes in the particle size distribution resulting from two particle growth mechanisms, namely, through layering and agglomeration. The overall mathematical model of the granulation loop process includes particle enlargement process in the granulator; particle classification step, in which particles are divided into three fractions according to their sizes; particle crushing; and particles being recycled back into the granulator.

The developed granulation loop model can reproduce the oscillatory behaviour seen in the produced particle size and particle mass flow rates. The analysis of the system dynamics suggests that the occurrence of the oscillatory behaviour is connected to the particle recycle. More precisely, the occurance of the oscillatory behaviour is connected with a certain particle size distribution in the recycle feed or when the crusher gap spacing is below a certain width.

The second research objective is to use the developed mathematical model of the granulation loop in control studies. This topic is discussed in three papers with particular focus on suggesting control strategies to eliminate the oscillatory behaviour and using various controllers for the suggested control strategies. In this thesis, two control strategies are proposed to eliminate the oscillatory behaviour and to make the process more steady in operation. In one of the control strategies, the produced particle median size is controlled by manipulating the crusher gap spacing (CS1). In another, the produced particle median size is achieved by manipulating the return fraction to define how much of the product-sized particles are recycled back to the granulator (CS2). The former control strategy has an advantage over the latter in terms of convergence rate: a higher convergence rate towards the operating point was achieved by manipulating the crusher gap spacing. Similar results were obtained with both of the controllers, the classical control and the advanced controller (MPC). With a double loop control structure (DLC) utilizing P controller to

convert the oscillatory system to an overdamped system, a significantly higher convergence rate towards the operating point was achieved. However, even better performance can be achieved with the non-linear model predictive controller (NMPC).

Novelty of the research work includes:

1. A thorough evaluation of the numerical discretization schemes applicable for finding the numerical solution of the population balance equation. Both the particle layering process and the particle agglomeration process are studied in this research. Several discretization schemes are applied for these processes and their numerical results are compared with exact solutions.

2. Proposal of a novel control strategy (CS2) for eliminating the observed oscillatory behavior. The novel control strategy suggests to use product-sized particles to eliminate the oscillatory behavior in the produced particle median size.

3. A through evaluation of a new control strategy (CS2) with the competing control strategy (CS1). Both of the control strategies are applied with DLC and the NMPC. The performance of the both control strategies is compared based on the convergence rate towards the reference point.

4. Application of the DLC structure to the granulation loop process. The DLC structure uses P+PI controller that is ready available in control systems. Performance of the DLC was also analysed by turning on the controller in different places in the oscillation cycle.

5. Application of the advanced non-linear model predictive control to the granulation loop process.

The research results give the following answers to the research questions:

1. Yes, the population balance model can reproduce oscillatory behaviour observed on granulation loop plants. The population balance model is able to track the dynamics in the granulator, in particular changes in the particle PSDs. Simulations of the population balance model shows that oscillatory behavior occurs due to the recycle feed.

2. Yes, the control algorithm based on the model can improve operation of granulation loops (with respect to eliminating the observed oscillations). A comparison of the simulation results between the NMPC and the DLC shows that it is possible to achieve higher convergence rate in the produced particle median diameter when the non-linear MPC is used. Higher convergence rate is obtained for both control strategies. In the case of CS1 strategy, the oscillatory behaviour is eliminated after 6.5 h vs 3.5 h for the DLC and NMPC, respectively. In the case of CS2, the oscillatory behaviour is eliminated after 7 h vs 4.4 h for the DLC and NMPC, respectively.

5.2 Recommendations

The mathematical model of the granulation process considers only the solid phase. Therefore, the model can be extended by including the liquid phase. Inclusion of the liquid phase would probably contribute in designing new control structures for controlling the granulation process. For modelling the liquid phase, experimental data is required. The effect of liquid content on the particle growth is highly dependent on the particles' physicochemical properties and operating conditions. Thus, further research is necessary to determine the effect of liquid content on particle growth, i.e., a product-specific empirical formulation should be obtained.

Another interesting possibility in considering additional flow inputs to the granulator, i.e., fine powder stream that is sometimes added to maintain the granulation process. Extending the mathematical model of the granulation loop process by adding one more input is trivial. However, the specific plant configurations would limit the use of the process input. The additional process input would contribute in designing new control structures.

Extension of the model by adding additional flow inputs together with the liquid content would perhaps enable the use of multiple-input-multiple-output non-linear MPC. This would lead to greater understanding of the granulation loop dynamics and perhaps would lead a faster elimination of the oscillatory behavior.

Further research in numerical approximation of the population balance. The further research could focus on finding and applying discretization schemes for combined granulation process, i.e., numerical schemes that could be applied both on the layering term discretization, as well as on the agglomeration term discretization. This would potentially decrease the model solution time that is important in the model based control. In the case of multi-dimensional population balance (e.g., tracking liquid content together with the particle size) it is crucial to find discretization scheme that can fast enough solve the model. Addition of another coordinate will lead to a larger number of states that will decrease the model solution computational time significantly.

Simulation studies included in this thesis show the advantages of the use of NMPC controller over classical controllers in eliminating the oscillatory behaviour in the produced particle size. However, implementation of the NMPC in a real plant requires an accurate process model. Thus, it is recommended that model validation be carried out before its implementation.

The developed mathematical model of the granulation loop process can also be used to design linear MPC. For this, the developed non linear model should be first linearized and then used as the prediction model.

5 Conclusions and Recommendations

Also, further studies can include the combined use of classical controller and and MPC controller. One of the possibilities is to first use the P controller to convert the oscillatory process to an overdamped system. This would enable the use of MPC controllers based on step response models.

Bibliography

[1] L. Vesjolaja, B. Glemmestad, B. Lie, Dynamic model for simulating transient behaviour of rotary drum granulation loop, Modeling, Identification and Control (2020).

[2] L. Vesjolaja, B. Glemmestad, B. Lie, Double-loop control structure for rotary drum granulation loop, Processes 8 (2020) 1423.

[3] S. Iveson, J. Litster, K. Hapgood, B. Ennis, Nucleation, growth and breakage phenomena in agitated wet granulation processes: a review, Powder Technology 117 (2001) 3–39.

[4] F. Wang, I. Cameron, Review and future directions in the modelling and control of continuous drum granulation, Powder Technology 124 (2002) 238–253.

[5] P. A. L. Wauters, Modelling and mechanisms of granulation. (2003).

[6] S. A. de Koster, K. Pitt, J. D. Litster, R. M. Smith, High-shear granulation: An investigation into the granule consolidation and layering mechanism, Powder Technology 355 (2019) 514–525.

[7] J. Litster, B. Ennis, The science and engineering of granulation processes, volume 15, Springer Science & Business Media, 2004.

[8] I. Cameron, F. Wang, C. Immanuel, F. Stepanek, Process systems modelling and applications in granulation: A review, Chemical Engineering Science 60 (2005) 3723–3750.

[9] W. Meng, L. Kotamarthy, S. Panikar, M. Sen, S. Pradhan, M. Marc, J. D. Litster, F. J. Muzzio, R. Ramachandran, Statistical analysis and comparison of a continuous high shear granulator with a twin screw granulator: Effect of process parameters on critical granule attributes and granulation mechanisms, International Journal of Pharmaceutics 513 (2016) 357–375.

[10] P. Mort, G. Tardos, Scale-up of agglomeration processes using transformations, KONA Powder and Particle Journal 17 (1999) 64–75.

[11] G. D. Ingram, I. T. Cameron, Challenges in multiscale modelling and its application to granulation systems, Developments in Chemical Engineering and Mineral Processing 12 (2004) 293–308.

[12] G. Lian, C. Thornton, M. J. Adams, Discrete particle simulation of agglomerate impact coalescence, Chemical Engineering Science 53 (1998) 3381–3391.

[13] J. Ottino, D. Khakhar, Mixing and segregation of granular materials, Annual Review of Fluid Mechanics 32 (2000) 55–91.

[14] M. Vanni, Approximate population balance equations for aggregation–breakage processes, Journal of Colloid and Interface Science 221 (2000) 143–160.

[15] A. Patil, J. Morud, S. T. Johansen, A cfd-dem based model for wet granulation process in a rotary drum, in: 2019 AIChE Annual Meeting, AIChE, 2019.

[16] A. Tabeei, A. Samimi, D. Mohebbi-Kalhori, Cfd modeling of an industrial scale two-fluid nozzle fluidized bed granulator, Chemical Engineering Research and Design 159 (2020) 605–614.

[17] M. Askarishahi, M. Maus, D. Schröder, D. Slade, M. Martinetz, D. Jajcevic, Mechanistic modelling of fluid bed granulation, part i: Agglomeration in pilot scale process, International Journal of Pharmaceutics 573 (2020) 118837.

[18] Y. Li, J. Bao, A. Yu, R. Yang, A combined data-driven and discrete modelling approach to predict particle flow in rotating drums, Chemical Engineering Science 231 (2021) 116251.

[19] A. Tamrakar, R. Ramachandran, Cfd–dem–pbm coupled model development and validation of a 3d top-spray fluidized bed wet granulation process, Computers & Chemical Engineering 125 (2019) 249–270.

[20] D. R. Ochsenbein, M. Billups, B. Hong, E. Schäfer, A. J. Marchut, O. K. Lyngberg, Industrial application of heat-and mass balance model for fluid-bed granulation for technology transfer and design space exploration, International Journal of Pharmaceutics 1 (2019) 100028.

[21] I. C. Kemp, A. van Millingen, H. Khaled, Development and verification of a novel design space and improved scale-up procedure for fluid bed granulation using a mechanistic model, Powder Technology 361 (2020) 1021–1037.

[22] H. Y. Ismail, M. Singh, A. B. Albadarin, G. M. Walker, Complete two dimensional population balance modelling of wet granulation in twin screw, International Journal of Pharmaceutics 591 (2020) 120018.

[23] K. Žižek, M. Gojun, I. Grčić, Simulating the wet granulation of tio2 photocatalyst in fluidized bed: Population balance modelling and prediction of coalescence rate, Powder Technology 379 (2021) 1–11.

[24] E. Zhalehrajabi, K. K. Lau, K. KuShaari, W. H. Tay, T. Hagemeier, A. Idris, Modelling of urea aggregation efficiency via particle tracking velocimetry in fluidized bed granulation, Chemical Engineering Science 223 (2020) 115737.

[25] H. Nemati, S. Shekoohi, Particle number balance approach for simulation of a multi-chamber fluidized bed urea granulator; modeling and validation, Powder Technology 369 (2020) 96–105.

[26] K. Cronin, F. J. G. Ortiz, D. Ring, F. Zhang, A new time-dependent rate constant of the coalescence kernel for the modelling of fluidised bed granulation, Powder Technology 379 (2021) 321–334.

[27] C. Neugebauer, E. Diez, L. Mielke, S. Palis, A. Bück, E. Tsotsas, A. Kienle, S. Heinrich, Dynamics of spray granulation in continuously operated horizontal fluidized beds, in: Dynamic Flowsheet Simulation of Solids Processes, Springer, 2020, pp. 67–107.

[28] S. Shirazian, H. Y. Ismail, M. Singh, R. Shaikh, D. M. Croker, G. M. Walker, Multi-dimensional population balance modelling of pharmaceutical formulations for continuous twin-screw wet granulation: Determination of liquid distribution, International Journal of Pharmaceutics 566 (2019) 352–360.

[29] C. Portier, K. Pandelaere, U. Delaet, T. Vigh, A. Kumar, G. Di Pretoro, T. De Beer, C. Vervaet, V. Vanhoorne, Continuous twin screw granulation: influence of process and formulation variables on granule quality attributes of model formulations, International Journal of Pharmaceutics 576 (2020) 118981.

[30] W. Rong, Y. Feng, P. Schwarz, P. Witt, B. Li, T. Song, J. Zhou, Numerical study of the solid flow behavior in a rotating drum based on a multiphase cfd model accounting for solid frictional viscosity and wall friction, Powder Technology 361 (2020) 87–98.

[31] C. Kang, D. Chan, Numerical simulation of 2d granular flow entrainment using dem, Granular Matter 20 (2018) 1–17.

[32] S. V. Muddu, A. Tamrakar, P. Pandey, R. Ramachandran, Model development and validation of fluid bed wet granulation with dry binder addition using a population balance model methodology, Processes 6 (2018) 154.

[33] K. Hayashi, S. Watano, Novel population balance model for granule aggregation and breakage in fluidized bed granulation and drying, Powder Technology 342 (2019) 664–675.

[34] T. Baba, H. Nakamura, H. Takimoto, S. Ohsaki, S. Watano, K. Takehara, T. Higuchi, T. Hirosawa, T. Yamamoto, Dem–pbm coupling method for the layering granulation of iron ore, Powder Technology 378 (2021) 40–50.

[35] I. Golovin, G. Strenzke, R. Dürr, S. Palis, A. Bück, E. Tsotsas, A. Kienle, Parameter identification for continuous fluidized bed spray agglomeration, Processes 6 (2018) 246.

Bibliography

[36] S. Bellinghausen, E. Gavi, L. Jerke, P. K. Ghosh, A. D. Salman, J. D. Litster, Nuclei size distribution modelling in wet granulation, Chemical Engineering Science 4 (2019) 100038.

[37] K. P. Hapgood, M. X. Tan, D. W. Chow, A method to predict nuclei size distributions for use in models of wet granulation, Advanced Powder Technology 20 (2009) 293–297.

[38] D. Ramkrishna, Population balances: Theory and applications to particulate systems in engineering, Academic press, 2000.

[39] F. Wang, I. Cameron, A multi-form modelling approach to the dynamics and control of drum granulation processes, Powder Technology 179 (2007) 2–11.

[40] L. Mörl, Anwendungsmöglichkeiten und Berechnung von Wirbelschichtgranulationstrocknungsanlagen, Ph.D. thesis, Technische Hochschule Magdeburg, 1981.

[41] L. Mörl, M. Mittelstrab, J. Sachse, Zum kugelwachstum bei der wirbelschichttrocknung von suspensionen oder losungen, Chemical Technology 29 (1977) 540–541.

[42] H. Hulburt, S. Katz, Some problems in particle technology: A statistical mechanical formulation, Chemical Engineering Science 19 (1964) 555–574.

[43] L. Liu, J. Litster, S. Iveson, B. Ennis, Coalescence of deformable granules in wet granulation processes, AIChE Journal 46 (2000) 529–539.

[44] L. Liu, J. Litster, Population balance modelling of granulation with a physically based coalescence kernel, Chemical Engineering Science 57 (2002) 2183–2191.

[45] F. Wang, X. Ge, N. Balliu, I. Cameron, Optimal control and operation of drum granulation processes, Chemical Engineering Science 61 (2006) 257–267.

[46] P. Kapur, D. Fuerstenau, Coalescence model for granulation, Industrial & Engineering Chemistry Process Design and Development 8 (1969) 56–62.

[47] A. Adetayo, B. Ennis, Unifying approach to modeling granule coalescence mechanisms., AIChE Journal 43 (1997) 927–934.

[48] N. Ouchiyama, T. Tanaka, The probability of coalescence in granulation kinetics, Industrial & Engineering Chemistry Process Design and Development 14 (1975) 286–289.

[49] P. Kapur, Kinetics of granulation by non-random coalescence mechanism, Chemical Engineering Science 27 (1972) 1863–1869.

[50] A. Golovin, The solution of the coagulation equation for raindrops, taking condensation into account, Soviet Physics-Docklady 8 (1963) 191–193.

58

[51] P. Knight, A. Johansen, H. Kristensen, T. Schaefer, J. Seville, An investigation of the effects on agglomeration of changing the speed of a mechanical mixer, Powder Technology 110 (2000) 204–209.

[52] S. Watano, H. Takashima, K. Miyanami, Scale-up of agitation fluidized bed granulation. v. effect of moisture content on scale-up characteristics, Chemical and Pharmaceutical Bulletin 45 (1997) 710–714.

[53] A. Salman, J. Fu, D. Gorham, M. Hounslow, Impact breakage of fertiliser granules, Powder Technology 130 (2003) 359–366.

[54] P. Vonk, C. Guillaume, J. Ramaker, H. Vromans, N. Kossen, Growth mechanisms of high-shear pelletisation, International Journal of Pharmaceutics 157 (1997) 93–102.

[55] J. Ramaker, M. A. Jelgersma, P. Vonk, N. Kossen, Scale-down of a high-shear pelletisation process: flow profile and growth kinetics, International Journal of Pharmaceutics 166 (1998) 89–97.

[56] T. Schaefer, P. Holm, H. Kristensen, Melt granulation in a laboratory scale high shear mixer, Drug Development and Industrial Pharmacy 16 (1990) 1249–1277.

[57] M. Yekeler, A. Ozkan, Determination of the breakage and wetting parameters of calcite and their correlations, Particle & Particle Systems Characterization: Measurement and Description of Particle Properties and Behavior in Powders and Other Disperse Systems 19 (2002) 419–425.

[58] K. van den Dries, O. M. de Vegt, V. Girard, H. Vromans, Granule breakage phenomena in a high shear mixer; influence of process and formulation variables and consequences on granule homogeneity, Powder Technology 133 (2003) 228–236.

[59] W. T. Scott, Analytic studies of cloud droplet coalescence i, Journal of the Atmospheric Sciences 25 (1968) 54–65.

[60] S. Qamar, M. P. Elsner, I. A. Angelov, G. Warnecke, A. Seidel-Morgenstern, A comparative study of high resolution schemes for solving population balances in crystallization, Computers & Chemical Engineering 30 (2006) 1119–1131.

[61] M. Nicmanis, M. Hounslow, A finite element analysis of the steady state population balance equation for particulate systems: Aggregation and growth, Computers & Chemical Engineering 20 (1996) S261–S266.

[62] V. John, T. Mitkova, M. Roland, K. Sundmacher, L. Tobiska, A. Voigt, Simulations of population balance systems with one internal coordinate using finite element methods, Chemical Engineering Science 64 (2009) 733–741.

[63] N. V. Mantzaris, P. Daoutidis, F. Srienc, Numerical solution of multi-variable cell population balance models. iii. finite element methods, Computers & Chemical Engineering 25 (2001) 1463–1481.

[64] J. Kumar, Numerical approximations of population balance equations in particulate systems, Ph.D. thesis, Otto-von-Guericke-Universität Magdeburg, Universitätsbibliothek, 2006.

[65] S. Bhoi, D. Sarkar, Hybrid finite volume and monte carlo method for solving multidimensional population balance equations in crystallization processes, Chemical Engineering Science 217 (2020) 115511.

[66] B. Koren, A robust upwind discretization method for advection, diffusion and source terms, in: C. B. Vreugdenhil, B. Koren (Eds.), Numerical Methods for Advection-Diffusion Problems, Notes on Numerical Fluid Mechanics, 1993, pp. 117–138.

[67] A. Kurganov, E. Tadmor, New high-resolution central schemes for nonlinear conservation laws and convection–diffusion equations, Journal of Computational Physics 160 (2000) 241–282.

[68] J. Cheng, C. Yang, M. Jiang, Q. Li, Z.-S. Mao, Simulation of antisolvent crystallization in impinging jets with coupled multiphase flow-micromixing-pbe, Chemical Engineering Science 171 (2017) 500–512.

[69] W. Hundsdorfer, J. G. Verwer, Numerical solution of time-dependent advection-diffusion-reaction equations, volume 33, Springer Science & Business Media, 2013.

[70] R. Gunawan, I. Fusman, R. D. Braatz, High resolution algorithms for multidimensional population balance equations, AIChE Journal 50 (2004) 2738–2749.

[71] D. L. Ma, D. K. Tafti, R. D. Braatz, High-resolution simulation of multidimensional crystal growth, Industrial & Engineering Chemistry Research 41 (2002) 6217–6223.

[72] F. Puel, G. Févotte, J. Klein, Simulation and analysis of industrial crystallization processes through multidimensional population balance equations. part 1: a resolution algorithm based on the method of classes, Chemical Engineering Science 58 (2003) 3715–3727.

[73] R. D. Braatz, Advanced control of crystallization processes, Annual Reviews in Control 26 (2002) 87–99.

[74] M. Hounslow, R. Ryall, V. Marshall, A discretized population balance for nucleation, growth, and aggregation, AIChE Journal 34 (1988) 1821–1832.

[75] S. Park, S. Rogak, A novel fixed-sectional model for the formation and growth of aerosol agglomerates, Journal of Aerosol Science 35 (2004) 1385–1404.

[76] F. Gelbard, Y. Tambour, J. H. Seinfeld, Sectional representations for simulating aerosol dynamics, Journal of Colloid and Interface Science 76 (1980) 541–556.

[77] Y. P. Kim, J. H. Seinfeld, Simulation of multicomponent aerosol condensation by the moving sectional method, Journal of Colloid and Interface Science 135 (1990) 185–199.

[78] M. Z. Jacobson, R. P. Turco, Simulating condensational growth, evaporation, and coagulation of aerosols using a combined moving and stationary size grid, Aerosol science and technology 22 (1995) 73–92.

[79] M. Z. Jacobson, Development and application of a new air pollution modeling system—ii. aerosol module structure and design, Atmospheric Environment 31 (1997) 131–144.

[80] Y. Liu, I. Cameron, A new wavelet-based adaptive method for solving population balance equations, Powder Technology 130 (2003) 181–188.

[81] Y. Liu, I. Cameron, S. Bhatia, A wavelet-based adaptive technique for adsorption problems involving steep gradients, Computers & Chemical Engineering 25 (2001) 1611–1619.

[82] J. Utomo, T. Zhang, N. Balliu, M. O. Tadé, Numerical studies of wavelet-based method as an alternative solution for population balance problems in a batch crystalliser, IFAC Proceedings Volumes 42 (2009) 213–218.

[83] A. Das, J. Kumar, Population balance modeling of volume and time dependent spray fluidized bed aggregation kernel using monte carlo simulation results, Applied Mathematical Modelling 92 (2021) 748–769.

[84] H. Zhao, C. Zheng, A population balance-monte carlo method for particle coagulation in spatially inhomogeneous systems, Computers & Fluids 71 (2013) 196–207.

[85] A. Buffo, V. Alopaeus, Solution of bivariate population balance equations with high-order moment-conserving method of classes, Computers & Chemical Engineering 87 (2016) 111–124.

[86] L. Müller, A. Klar, F. Schneider, A numerical comparison of the method of moments for the population balance equation, Mathematics and Computers in Simulation 165 (2019) 26–55.

[87] M. Pigou, J. Morchain, P. Fede, M.-I. Penet, G. Laronze, New developments of the extended quadrature method of moments to solve population balance equations, Journal of Computational Physics 365 (2018) 243–268.

[88] S. Alzyod, M. Attarakih, H.-J. Bart, The sectional quadrature method of moments (sqmom): An extension to nonhomogeneous bivariate population balances, Chemical Engineering Research and Design 115 (2016) 195–203.

[89] E. Wynn, Simulating aggregation and reaction: New hounslow dpb and four-parameter summary, AIChE journal 50 (2004) 578–588.

[90] S. Kumar, D. Ramkrishna, On the solution of population balance equations by discretization - ii. a moving pivot technique, Chemical Engineering Science 51 (1996) 1333–1342.

[91] M. Peglow, J. Kumar, G. Warnecke, S. Heinrich, E. Tsotsas, L. Mörl, M. Hounslow, An improved discretized tracer mass distribution of hounslow et al., AIChE journal 52 (2006) 1326–1332.

[92] J. Kumar, M. Peglow, G. Warnecke, S. Heinrich, L. Mörl, Improved accuracy and convergence of discretized population balance for aggregation: The cell average technique, Chemical Engineering Science 61 (2006) 3327–3342.

[93] A. Bouaniche, L. Vervisch, P. Domingo, A hybrid stochastic/fixed-sectional method for solving the population balance equation, Chemical Engineering Science 209 (2019) 115198.

[94] C. Neugebauer, A. Bück, A. Kienle, Control of particle size and porosity in continuous fluidized-bed layering granulation processes, Chemical Engineering Technology 43 (2020) 813–818.

[95] C. Neugebauer, E. Diez, A. Bück, S. Palis, S. Heinrich, A. Kienle, On the dynamics and control of continuous fluidized bed layering granulation with screen-mill-cycle, Powder Technology 354 (2019) 765–778.

[96] F. Filbet, P. Laurençot, Numerical simulation of the smoluchowski coagulation equation, SIAM Journal on Scientific Computing 25 (2004) 2004–2028.

[97] L. Forestier-Coste, S. Mancini, A finite volume preserving scheme on nonuniform meshes and for multidimensional coalescence, SIAM Journal on Scientific Computing 34 (2012) B840–B860.

[98] J. Kumar, G. Warnecke, M. Peglow, S. Heinrich, Comparison of numerical methods for solving population balance equations incorporating aggregation and breakage, Powder Technology 189 (2009) 218–229.

[99] M. Singh, R. Singh, S. Singh, G. Walker, T. Matsoukas, Discrete finite volume approach for multidimensional agglomeration population balance equation on unstructured grid, Powder Technology 376 (2020) 229–240.

[100] M. Singh, J. Kumar, A. Bück, A volume conserving discrete formulation of aggregation population balance equations on non-uniform meshes, IFAC-PapersOnLine 48 (2015) 192–197.

[101] G. Kaur, J. Kumar, S. Heinrich, A weighted finite volume scheme for multivariate aggregation population balance equation, Computers & Chemical Engineering 101 (2017) 1–10.

[102] R. Batterham, J. Hall, G. Barton, Pelletizing kinetics and simulation of full scale balling circuits (1981).

[103] D. A. Gillette, A study of aging of lead aerosols—ii: a numerical model simulating coagulation and sedimentation of a leaded aerosol in the presence of an unleaded background aerosol, Atmospheric Environment (1967) 6 (1972) 451–462.

[104] P. Marchal, R. David, J. Klein, J. Villermaux, Crystallization and precipitation engineering—i. an efficient method for solving population balance in crystallization with agglomeration, Chemical Engineering Science 43 (1988) 59–67.

[105] J. Lister, D. Smit, M. Hounslow, Adjustable discretized population balance for growth and aggregation, AIChE Journal 41 (1995) 591–603.

[106] E. J. Wynn, Improved accuracy and convergence of discretized population balance of lister et al., AIChE journal 42 (1996) 2084–2086.

[107] S. Kumar, D. Ramkrishna, On the solution of population balance equations by discretization - i. a fixed pivot technique, Chemical Engineering Science 51 (1996) 1311–1332.

[108] J. Kumar, G. Kaur, E. Tsotsas, An accurate and efficient discrete formulation of aggregation population balance equation., Kinetic & Related Models 9 (2016).

[109] I. M. Cotabarren, D. E. Bertín, V. Bucalá, J. Piña, Feedback control strategies for a continuous industrial fluidized-bed granulation process, Powder Technology 283 (2015) 415–432.

[110] T. Glaser, C. Sanders, F. Wang, I. Cameron, J. Litster, J. M.-H. Poon, R. Ramachandran, C. Immanuel, F. Doyle III, Model predictive control of continuous drum granulation, Journal of Process Control 19 (2009) 615–622.

[111] R. Radichkov, T. Müller, A. Kienle, S. Heinrich, M. Peglow, L. Mörl, A numerical bifurcation analysis of continuous fluidized bed spray granulator with external product classification, Chemical Engineering and Processing 45 (2006) 826–837.

[112] C. Neugebauer, S. Palis, A. Bück, E. Tsotsas, S. Heinrich, A. Kienle, A dynamic two-zone model of continuous fluidized bed layering granulation with internal product classification, Particuology 31 (2017) 8–14.

[113] D. E. Bertin, I. Cotabarren, J. Piña, V. Bucalá, Granule size distribution for a multi-chamber fluidized-bed melt granulator: Modeling and validation using process measurement data, Chemical Engineering Science 104 (2013) 319–329.

[114] S. Palis, A. Kienle, Discrepancy based control of continuous fluidized bed spray granulation with internal product classification, IFAC Proceedings Volumes 45 (2012) 756–761.

Bibliography

[115] C. Dreyschultze, C. Neugebauer, S. Palis, A. Bück, E. Tsotsas, S. Heinrich, A. Kienle, Influence of zone formation on stability of continuous fluidized bed layering granulation with external product classification, Particuology 23 (2015) 1–7.

[116] S. Palis, A. Kienle, H∞ loop shaping control for continuous fluidized bed spray granulation with internal product classification, Industrial & Engineering Chemistry Research 52 (2013) 408–420.

[117] R. Mathe, T. Casian, I. Tomuţă, Multivariate feed forward process control and optimization of an industrial, granulation based tablet manufacturing line using historical data, International Journal of Pharmaceutics 591 (2020) 119988.

[118] S. Palis, Control induced instabilities in fluidized bed spray granulation, Journal of Process Control 93 (2020) 97–104.

[119] T. Shaqarin, A. Al-Rawajfeh, M. Hajaya, N. Alshabatat, B. R. Noack, Model-based robust h∞ control of a granulation process using smith predictor with reference updating, Journal of Process Control 77 (2019) 38–47.

[120] S. Palis, A. Kienle, Online parameter identification for continuous fluidized bed spray granulation with external sieve-mill cycle, in: 2017 22nd International Conference on Methods and Models in Automation and Robotics (MMAR), IEEE, 2017, pp. 594–598.

[121] S. Palis, C. Dreyschultze, A. Kienle, A methodology for experimental determination of stability boundaries with application to fluidized bed spray granulation, in: Computer Aided Chemical Engineering, volume 33, Elsevier, 2014, pp. 625–630.

[122] A. Bück, C. Neugebauer, K. Meyer, S. Palis, E. Diez, A. Kienle, S. Heinrich, E. Tsotsas, Influence of operation parameters on process stability in continuous fluidised bed layering with external product classification, Powder Technology 300 (2016) 37–45.

[123] M. D. Díez, B. E. Ydstie, M. Fjeld, B. Lie, Inventory control of particulate processes, Computers & Chemical Engineering 32 (2008) 46–67.

[124] F. Boukouvala, V. Niotis, R. Ramachandran, F. J. Muzzio, M. G. Ierapetritou, An integrated approach for dynamic flowsheet modeling and sensitivity analysis of a continuous tablet manufacturing process, Computers & Chemical Engineering 42 (2012) 30–47.

[125] P. R. Mort, S. W. Capeci, J. W. Holder, Control of agglomerate attributes in a continuous binder-agglomeration process, Powder Technology 117 (2001) 173–176.

64

[126] J. Zhang, J. Litster, F. Wang, I. Cameron, Evaluation of control strategies for fertiliser granulation circuits using dynamic simulation, Powder Technology 108 (2000) 122–129.

[127] C. F. Sanders, M. J. Hounslow, F. J. Doyle III, Identification of models for control of wet granulation, Powder Technology 188 (2009) 255–263.

[128] S. Palis, C. Dreyschultze, C. Neugebauer, A. Kienle, Auto-tuning control systems for improved operation of continuous fluidized bed spray granulation processes with external product classification, Procedia Engineering 102 (2015) 133–141.

[129] S. Palis, Adaptive discrepancy based control of continuous fluidized bed spray granulation with external sieve-mill cycle, IFAC-PapersOnLine 52 (2019) 218–222.

[130] S. Palis, Control of multi-chamber continuous fluidized bed spray granulation, IFAC-PapersOnLine 52 (2019) 406–411.

[131] S. Palis, Non-identifier-based adaptive control of continuous fluidized bed spray granulation, Journal of Process Control 71 (2018) 46–51.

[132] S. Palis, A. Kienle, Stabilization of continuous fluidized bed spray granulation with external product classification, Chemical Engineering Science 70 (2012) 200–209.

[133] S. Palis, A. Kienle, Stabilization of continuous fluidized bed spray granulation-a lyapunov approach, IFAC Proceedings Volumes 43 (2010) 1362–1367.

[134] S. Palis, A. Kienle, Discrepancy based control of particulate processes, Journal of Process Control 24 (2014) 33–46.

[135] A. Zuyev, A. Kienle, P. Benner, Construction of a lyapunov functional for a class of controlled population balance models, PAMM 17 (2017) 827–828.

[136] R. Ramachandran, A. Chaudhury, Model-based design and control of a continuous drum granulation process, Chemical Engineering Research and Design 90 (2012) 1063–1073.

[137] A. Bück, S. Palis, E. Tsotsas, Model-based control of particle properties in fluidised bed spray granulation, Powder Technology 270 (2015) 575–583.

[138] A. Bück, R. Dürr, M. Schmidt, E. Tsotsas, Model predictive control of continuous layering granulation in fluidised beds with internal product classification, Journal of Process Control 45 (2016) 65–75.

[139] M. Pottmann, B. A. Ogunnaike, A. A. Adetayo, B. J. Ennis, Model-based control of a granulation system, Powder Technology 108 (2000) 192–201.

[140] E. P. Gatzke, F. J. Doyle III, Model predictive control of a granulation system using soft output constraints and prioritized control objectives, Powder Technology 121 (2001) 149–158.

Bibliography

[141] J. H. Park, S. W. Sung, I.-B. Lee, An enhanced pid control strategy for unstable processes, Automatica 34 (1998) 751–756.

[142] G. Tian, Y. Wei, J. Zhao, W. Li, H. Qu, Application of pulsed spray and moisture content control strategies on quality consistency control in fluidized bed granulation: A comparative study, Powder Technology 363 (2020) 232–244.

[143] T. Reimers, J. Thies, P. Stöckel, S. Dietrich, M. Pein-Hackelbusch, J. Quodbach, Implementation of real-time and in-line feedback control for a fluid bed granulation process, International Journal of Pharmaceutics 567 (2019) 118452.

[144] N. Kittikunakorn, S. Paul, J. J. Koleng III, T. Liu, R. Cook, F. Yang, V. Bi, T. Durig, C. C. Sun, A. Kumar, et al., How does the dissimilarity of screw geometry impact twin-screw melt granulation, European Journal of Pharmaceutical Sciences 157 (2021) 105645.

[145] G. C. Pereira, S. V. Muddu, A. D. Román-Ospino, D. Clancy, B. Igne, C. Airiau, F. J. Muzzio, M. Ierapetritou, R. Ramachandran, R. Singh, Combined feedforward/feedback control of an integrated continuous granulation process, Journal of Pharmaceutical Innovation 14 (2019) 259–285.

[146] A. Megarry, A. Taylor, A. Gholami, H. Wikström, P. Tajarobi, Twin-screw granulation and high-shear granulation: The influence of mannitol grade on granule and tablet properties, International Journal of Pharmaceutics 590 (2020) 119890.

[147] G. Dahlgren, P. Tajarobi, E. Simone, B. Ricart, J. Melnick, V. Puri, C. Stanton, G. Bajwa, Continuous twin screw wet granulation and drying—control strategy for drug product manufacturing, Journal of Pharmaceutical Sciences 108 (2019) 3502–3514.

[148] C. Neugebauer, S. Palis, A. Bück, E. Diez, S. Heinrich, E. Tsotsas, A. Kienle, Influence of mill characteristics on stability of continuous layering granulation with external product classification 38 (2016) 1275–1280.

[149] M. Schmidt, A. Bück, E. Tsotsas, Experimental investigation of the influence of drying conditions on process stability of continuous spray fluidized bed layering granulation with external product separation, Powder Technology 320 (2017) 474–482.

[150] M. Schmidt, C. Rieck, A. Bück, E. Tsotsas, Experimental investigation of process stability of continuous spray fluidized bed layering with external product separation, Chemical Engineering Science 137 (2015) 466–475.

[151] S. Heinrich, M. Peglow, M. Ihlow, M. Henneberg, L. Mörl, Analysis of the start-up process in continuous fluidized bed spray granulation by population balance modelling, Chemical Engineering Science 57 (2002) 4369–4390.

[152] S. M. Miller, J. B. Rawlings, Model identification and control strategies for batch cooling crystallizers, AIChE Journal 40 (1994) 1312–1327.

[153] T. J. Crowley, E. S. Meadows, E. Kostoulas, F. J. Doyle Iii, Control of particle size distribution described by a population balance model of semibatch emulsion polymerization, Journal of Process Control 10 (2000) 419–432.

[154] C. D. Immanuel, F. J. Doyle III, Hierarchical multiobjective strategy for particle-size distribution control, AIChE Journal 49 (2003) 2383–2399.

[155] O. Molerus, H. Hoffmann, Darstellung von windsichtertrennkurven durch ein stochastisches modell, Chemie Ingenieur Technik 41 (1969) 340–344.

[156] S. Heinrich, M. Peglow, M. Ihlow, L. Mörl, Particle population modeling in fluidized bed-spray granulation—analysis of the steady state and unsteady behavior, Powder Technology 130 (2003) 154–161.

[157] MATLAB, The MathWorks, Inc., Natick, Massachusetts, United States., 2019b.

[158] H. Manum, Extensions of Skogestad's SIMC tuning rules to oscillatory and unstable processes, Technical Report, Technical report, 2005.

Part II: Scientific Publications

Paper A

Solving the population balance equation for granulation processes: particle layering and agglomeration

Authors L. Vesjolaja, B. Glemmestad, B. Lie

Solving the population balance equation for granulation processes: particle layering and agglomeration

Ludmila Vesjolaja[1]   Bjørn Glemmestad[2]   Bernt Lie[1]

[1]Department of Electrical Engineering, IT and Cybernetics, University of South-Eastern Norway,
`{ludmila.vesjolaja,bernt.lie}@usn.no`
[2]Process Modeling and Control Department, Yara Technology Center, Norway, `bjorn.glemmestad@yara.com`

Abstract

Granulation processes are frequently used in the fertilizer industry to produce different grades of mineral fertilizers. Large recycle ratios and poor product quality control are some of the problems faced by such industries. Thus, for real time model based process control and optimization, it is necessary to find an appropriate numerical scheme can find solution of the model sufficiently accurate and fast. In this study, population balance principles were used to model particle granulation processes. Different numerical schemes were tested to find simple yet sufficiently accurate solution schemes for population balance equation. Numerical schemes were applied to find the solution of both the *layering* term and the *agglomeration* term that appear in the population balance equation. The accuracies of the numerical schemes were assessed by comparing the numerical results with analytical, tractable solutions. Comparison of the accuracy of numerical schemes showed that a high resolution scheme with Koren flux limiter function might be a good choice for the *layering* term discretization, while a cell averaging technique and a new finite volume method of Kumar et al. (2016) produce a sufficiently accurate solution for the *agglomer-ation* term discretization.

Keywords: population balance, numerical scheme, layering, agglomeration

1   Introduction

Granulation is a particle enlargement process during which fine particles and/or atomizable liquids are converted into granules via a series of complex physical processes (Litster and Ennis, 2004). Here, the focus is on modeling a granulation process used for mineral fertilizer production. In the fertilizer industry, depending on desired product properties, different types of granulators are used, e.g., spherodizers and drum granulators.

Formation of the particles (granulation mechanisms) depends on the granulator type and operating conditions. Particle growth due to layering is predominant in spherodizers. Layering is a continuous process (differential growth) during which particle growth occurs due to a successive coating of a liquid phase onto a granule (Litster and Ennis, 2004). In drum granulators, on the other
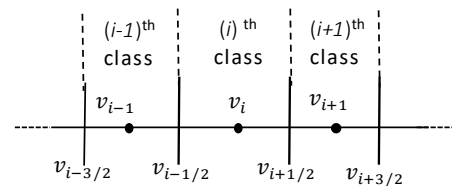
Figure 1. Size discretization into classes (cells) using linear grid.

hand, particle collision occurs, and thus particle agglomeration contributes significantly to particle size change. In this paper, binary particle agglomeration is assumed for population balance (PB) modeling. Binary agglomeration refers to a particle growth mechanism that occurs due to successful collision of two particles, resulting in the formation of a larger, composite particle. Thus, the agglomeration results in a reduction of the total number of particles, while the total mass remains conserved (Litster and Ennis, 2004).

The operation of granulation plants at an industrial scale can be challenging (Litster and Ennis, 2004; Radichkov et al., 2006; Heinrich et al., 2003). Periodic instability associated with the operation of the granulation circuit has been reported. This causes the particle size distribution (PSD) flowing out of the granulator to oscillate, thus making it difficult to maintain the desired product quality, e.g., particle size. Thus, to address and solve these challenges, it is essential to have a dynamic model of the granulator that can further be used to design optimal control structures. The model should be both simple and sufficiently accurate to reflect the underlying physical mechanisms that take place in the granulator. The resulting population balance equations (PBEs) are nonlinear in nature and are challenging to solve. Analytical solutions of these PBEs are available only for ideal and simplified cases, and thus for most of the cases, numerical methods are needed to solve such PBEs. For real time model based process control and optimization, it is necessary to find an appropriate numerical scheme that is sufficiently accurate and fast. Therefore, the main focus

of this paper has been (i) investigation of the accuracy of different numerical schemes that are suitable for discretizing PBEs by comparing the numerical results with analytically tractable solutions; (ii) application of various finite volume techniques (first order upwind, second order central difference, and a high resolution scheme) to the growth by a layering process; (iii) application of different sectional methods (Hounslow method, cell average technique, fixed pivot scheme), and a new finite volume method of Kumar et al. (2016) to the agglomeration process.

2 Population Balance Equation (PBE)

Population balance (PB) is frequently used to describe dynamics of particle property distributions, e.g., particle size distribution, moisture content in particles and porosity (Ramkrishna, 2000). The general form of a number based PBE with particle size (x) as the internal coordinate, spatial variation (z) as the external coordinate, and time t as time coordinate is represented as

$$\frac{\partial n(x,z,t)}{\partial t} = -\frac{\partial}{\partial x}\left[Gn(x,z,t)\right] + B(x,z,t) - D(x,z,t) \\ -\frac{\partial}{\partial z}\left[\frac{dz}{dt}n(x,z,t)\right], \quad (1)$$

where $n(x,z,t)$ is the number density function $\left[\frac{no}{mm^3 \cdot [internal\ coordinate]}\right]$. The first term on the right hand side represents the particle growth due to layering, the second and third terms stand for particle birth and death, respectively, due to agglomeration, while the last term represents a continuous process and gives the flow of particles through the granulator. G is the growth rate $\left[\frac{internal\ coordinate}{s}\right]$ (Ramkrishna, 2000). The birth B and death D terms usually include integrals that lead to partial integro-differential equations which make the solution of the PBEs complicated. Mathematical expressions for birth and death terms are shown in Section 4 when describing different numerical schemes for binary agglomeration. Further simplifications of the general PBE (Eq. 1) are possible and are dependent on the nature of the process taken into consideration.

At this point, it is convenient to define moments of particle size distributions that will be used later for discussion of the simulation results. The l-th moment of the PSD is defined as

$$\mu^l = \int_0^\infty x^l n(x) dx. \quad (2)$$

The first moments are of particular interest. Depending on the choice of internal coordinate (e.g., particle volume or particle length) the moments are related to the total number, length, area, and volume of particles.

3 Numerical schemes for *layering* term discretization

PBEs are non-linear in general and analytical solutions are available only for simplified processes. Thus, a simple 1-D batch process for which an analytical solution is available is modeled so that the accuracy of the numerical schemes can be reliably evaluated. In a batch granulation process there is no continuous particle flow through the granulator. If the particle size change in the granulator is mainly due to layering (e.g., in spherodizers), and the size of a particle is represented by its volume v, then Eq. 1 reduces to

$$\frac{\partial n(v,t)}{\partial t} = -\frac{\partial}{\partial v}\left[Gn(v,t)\right]. \quad (3)$$

In Eq. 3, the concept of *perfect mixing* inside the granulator is applied: particle property (e.g., size distribution) inside the granulator is the same at every point inside the granulator. In this paper, the solution to PBEs containing growth term G (Eq. 3) is found by transforming the partial differential equation (PDE) into a system of ordinary differential equations (ODEs), i.e., by reducing the dimensionality of the problem with respect to the particle size. The set of ODEs can then be solved using an appropriate time integrator. In this paper, a Runge-Kutta 4-th order (RK-4) time integration method is used for all simulations.

For particle size discretization, first the particles are classified into N_c particle classes which are numbered by $i \in \{1, 2, ...N_c\}$ classes (cells) using a *linear grid* as shown in Figure 1.

Here, i represents the i-th particle class, v_i is the volume of the particle of the i-th class, $v_{i\pm\frac{1}{2}}$ is the left and the right boundaries of the i-th class, and $\triangle v = v_{i+\frac{1}{2}} - v_{i-\frac{1}{2}}$ is the size of the classes. The dots in each class (Figure 1) represent the cell centers. Secondly, an appropriate numerical scheme is applied to convert Eq. 3 into set of ODEs. Integration of Eq. 3 over cell i from $v_{i-\frac{1}{2}}$ to $v_{i+\frac{1}{2}}$ gives

$$\frac{dN_i(t)}{dt} = G\left(v_{i-\frac{1}{2}}\right)n\left(v_{i-\frac{1}{2}},t\right) - G\left(v_{i+\frac{1}{2}}\right)n\left(v_{i+\frac{1}{2}},t\right). \quad (4)$$

In a simplified case, a solution of Eq. 4 can be found analytically: The particle growth due to layering in a batch process does not change the total number of particles in the batch, but only the particle volume is changed. If t denotes the time for particle growth, v_{initial} denotes the initial volume of the particles (for all classes), and G is the constant growth rate, then the new volume (v_{new}) of the particles after the growth due to layering is given as

$$v_{\text{new}} = v_{\text{initial}} + t \cdot G. \quad (5)$$

However, in real applications, analytical solutions are difficult to obtain, and, thus various numerical schemes are applied to approximate the right hand side of Eq. 4. The

PBE represented by Eq. 3 is a hyperbolic equation due to the layering term, and Eq. 3 can be approximated using a finite volume scheme that automatically incorporates conservation of number in a growth process.

In this paper, three finite volume schemes are compared for particle size discretization, namely a first order upwind scheme (FU) and a second order central difference scheme (SCD). The first order upwind (FU) scheme uses the approximation defined by Eq. 6 and 7:

$$n\left(v_{i-\frac{1}{2}},t\right) \approx \frac{1}{\Delta v}\left[N_{i-1}(t)\right], \qquad (6)$$

and

$$n\left(v_{i+\frac{1}{2}},t\right) \approx \frac{1}{\Delta v}\left[N_i(t)\right]. \qquad (7)$$

Thus, approximation of Eq. 4 using the FU scheme leads to

$$\frac{dN_i}{dt} \approx \frac{1}{\Delta v}\left[G\left(v_{i-\frac{1}{2}}\right)N_{i-1}(t) - G\left(v_{i+\frac{1}{2}}\right)N_i(t)\right]. \qquad (8)$$

Assuming constant growth rate in all cells, Eq. 8 simplifies to

$$\frac{dN_i^{\mathrm{FU}}}{dt} \approx \frac{G}{\Delta v}\left[N_{i-1}(t) - N_i(t)\right]. \qquad (9)$$

The second order central difference (SCD) scheme uses the approximation

$$n\left(v_{i-\frac{1}{2}},t\right) \approx \frac{1}{\Delta v}\frac{[N_{i-1}(t) + N_i(t)]}{2}, \qquad (10)$$

and

$$n\left(v_{i+\frac{1}{2}},t\right) \approx \frac{1}{\Delta v}\frac{[N_i(t) + N_{i+1}(t)]}{2}. \qquad (11)$$

Thus, discretization of Eq. 4 over a cell i using the SCD scheme results in

$$\frac{dN_i^{\mathrm{SCD}}}{dt} \approx \frac{G}{\Delta v}\frac{[N_{i-1}(t) - N_{i+1}(t)]}{2}, \qquad (12)$$

where particle growth G is assumed constant in all the cells.

A finite volume scheme that is extended by a flux limiter is also applied to Eq. 4 to reduce the dimensionality of the PBEs with respect to the particle size. In particular, the Koren flux limiter function (Koren, 1993) is used to achieve a robust upwind discretization scheme to Eq. 4. High resolution schemes are considered to attain higher accuracy than the first order upwind schemes. In addition, these methods avoid spurious oscillations by applying a high order flux in the smooth regions and a low order flux near discontinuities (Koren, 1993; Kumar, 2006). Assuming constant G in all cells, Eq. 4 can be discretized with the Koren scheme as

$$\frac{dN_i^{\mathrm{KFL}}}{dt} \approx G \cdot \left[n\left(v_{i-\frac{1}{2}}\right) - n\left(v_{i+\frac{1}{2}}\right)\right], \qquad (13)$$

where,

$$n\left(v_{i-\frac{1}{2}},t\right) \approx \frac{1}{\Delta v}\big[N_{i-1}(t)$$
$$\times \frac{1}{2}\phi\left(\widetilde{\theta}_{i-\frac{1}{2}}\right)\cdot(N_{i-1}(t) - N_{i-2}(t))\big], \quad (14)$$

and

$$n\left(v_{i+\frac{1}{2}},t\right) \approx \frac{1}{\Delta v}\left[N_i(t) + \frac{1}{2}\phi\left(\widetilde{\theta}_{i+\frac{1}{2}}\right)\cdot(N_i(t) - N_{i-1}(t))\right]. \qquad (15)$$

Here, ϕ is the limiter function defined as

$$\phi\left(\widetilde{\theta}\right) = \max\left[0, \min\left(2\widetilde{\theta}, \min\left(\frac{1}{3} + \frac{2\widetilde{\theta}}{3}, 2\right)\right)\right]. \qquad (16)$$

Parameter $\widetilde{\theta}$ is defined as,

$$\widetilde{\theta}_{i-\frac{1}{2}} = \frac{N_i - N_{i-1} + \chi}{N_{i-1} - N_{i-2} + \chi}, \quad \widetilde{\theta}_{i+\frac{1}{2}} = \frac{N_{i+1} - N_i + \chi}{N_i - N_{i-1} + \chi}, \qquad (17)$$

with a very small constant χ (e.g., 10^{-8}) to avoid division by zero.

4 Numerical schemes for *agglomeration* term discretization

PBE for a batch agglomeration process using the particle volume as internal coordinate is given by

$$\frac{\partial n(v,z,t)}{\partial t} = B(v,z,t) - D(v,z,t). \qquad (18)$$

Here, the particle birth (B) and death (D) due to binary agglomeration are modeled using the Hulburt and Katz formulation (Hulburt and Katz, 1964). For a pure agglomeration process, the Hulburt and Katz equation (Hulburt and Katz, 1964) is given as

$$\frac{\partial n(t,v)}{\partial t} = B - D =$$
$$\frac{1}{2}\int_0^v \beta(t,v-\varepsilon,\varepsilon)n(t,v-\varepsilon)n(t,\varepsilon)d\varepsilon$$
$$- n(t,v)\int_0^\infty \beta(t,v,\varepsilon)n(t,\varepsilon)d\varepsilon. \qquad (19)$$

Equation 19 represents a 1-D batch process assuming *perfect mixing* inside the granulator. In Eq. 19, β is the agglomeration rate (kernel) that defines the collision frequency of the two particles with volumes v and $v - \varepsilon$.

Agglomeration is a discrete event, and PB modeling of the agglomeration process results in partial integro-differential equations. The integral function appears in the birth (B) and death (D) terms in Eq. 19. Such systems are difficult to solve, and analytical solutions are available only for a limited number of simplified problems. Some of the analytical solutions for different initial conditions and different agglomeration kernels (e.g., constant,

sum and product kernels) are given in Scott (Scott, 1968). Here, for simplicity, the performance of different numerical schemes has been assessed using a constant agglomeration kernel with an exponential initial distribution:

$$n(v,0) = \frac{N_0}{v_0} \exp\left(\frac{-v}{v_0}\right), \qquad (20)$$

is given as

$$n(v,t) = \frac{4N_0}{v_0(\varpi+2)^2} \exp\left(\frac{-2\kappa}{(\varpi+2)}\right), \qquad (21)$$

In Equations 20 and 21, N_0 and v_0 represent the initial number of particles per unit volume and initial mean volume of the particles. The dimensionless volume unit κ, and the dimensionless time variable ϖ are given by Eq. 22:

$$\kappa = \frac{v}{v_0}, \quad \text{and} \quad \varpi = N_0 \beta_0 t. \qquad (22)$$

As a result of particle agglomeration, the total number of particles reduces while the total mass remains constant. The main challenge is to find/develop approximation techniques that would assign the newborn particles accurately while conserving the chosen moments. To achieve this, various numerical methods for expressing the agglomeration term in PBEs are developed, among others the method of moments, the method of successive approximations, the finite volume methods, and the sectional methods. A review of various numerical techniques is summarized in (Ramkrishna, 2000). This paper focuses on applying different sectional methods, as well as a newly developed finite volume technique by Kumar et al.'s (Kaur et al., 2017; Singh et al., 2015; Kumar et al., 2016).

Approximation of the continuous size distribution by a finite number of size sections (cells) has been made using a *geometric type grids*, i.e., the whole particle size interval is divided into a finite number of cells (classes) using geometric progression. This type of grid has been chosen because Hounslow's discretization method, one of the numerical schemes being compared, can be applied only to geometric type grids. The choice of numerical schemes has been made based on suitability for further application of the model for control purposes, i.e., the scheme should posses simplicity in implementation and be sufficiently fast (low computation time), while producing relatively accurate numerical results.

4.1 Hounslow's scheme

According to Hounslow's discretization scheme (Hounslow et al., 1988), the approximation of the continuous size distribution by a finite number of cells is performed using a geometric grid with a factor of two in size, i.e., $v_{i+1} = 2v_i$. Hounslow's discretization scheme (H) is based on four binary interaction mechanisms that can contribute to changes of particles number in the i-th cell. Two of these four mechanisms change the number of particles due

to particle births in the i-th cell, while the other two mechanisms contribute for particle deaths in the i-th cell. Application of the H scheme to the agglomeration process (Eq. 19) gives the total rate of change of particles in each i-th cell as

$$\frac{dN_i^{\text{H}}}{dt} = \sum_{j=1}^{i-2} 2^{j-i+1} \beta_{i-1,j} N_{i-1} N_j + \frac{1}{2} \beta_{i-1,i-1} N_{i-1}^2 -$$

$$N_i \sum_{j=1}^{i-1} 2^{j-i} \beta_{i,j} N_j - N_i \sum_{j=i}^{N_c} \beta_{i,j} N_j. \quad (23)$$

Here, the first term on the right hand side represents the births of particles that are formed due to collision of particles in the $(i-1)$-th cell with the particles from the first to the $(i-2)$-th cells. The second term on the right hand side stands for the births of particles that are born in cell i by the collision between two particles in the $(i-1)$-th cell. The last two terms in Eq. 23 accounts for the death of particles in the i-th cell.

4.2 Cell average scheme

The cell average (CA) scheme was introduced by Kumar (Kumar et al., 2006; Kumar, 2006). The CA scheme can be applied to both a geometric grid and a linear grid. Here, a geometric grid discretization has been chosen to be able to compare simulation results with the Hounslow's scheme. In the CA scheme, at first the total birth of particles in each cell denoted by B_i is computed:

$$B_i = \sum_{j=1}^{N_{c,i}} B_i^j = \sum_{j,k}^{j \geq k} \left(1 - \frac{1}{2}\delta_{jk}\right) \beta_{jk} N_j N_k, \qquad (24)$$

where the two aggregating particles with volumes v_j and v_k should fulfill the condition $v_{i-\frac{1}{2}} \leq v_j + v_k \leq v_{i+\frac{1}{2}}$; δ_{jk} is the delta Dirac function such that $\delta_{jk} = 1$ for $j = k$, otherwise $\delta_{jk} = 0$; β_{jk} is the agglomeration kernel for binary agglomeration of particles from the j-th and the k-th cells.

Then the average volume of the newly formed particles in each cell denoted by $\bar{v}_i$ is calculated. The average volume of the particle is then given as

$$\bar{v}_i = \frac{\sum_{j=1}^{N_{c,i}} v_i^j B_i^j}{B_i} = \left[\frac{\sum_{j,k}^{j \geq k} \left(1 - \frac{1}{2}\delta_{jk}\right) \beta_{jk} N_j N_k (v_j + v_k)}{\sum_{j,k}^{j \geq k} \left(1 - \frac{1}{2}\delta_{jk}\right) \beta_{jk} N_j N_k}\right]. \qquad (25)$$

The next step in the CA scheme is to assign the total birth of particles B_i appropriately to different cells depending on the position of the average volume of all newborn particles relative to the cell center volume v_i. In total, there are four birth contributions at node v_i: two coming from the i-th cell itself (when $\bar{v}_i < v_i$ and $\bar{v}_i > v_i$), and two from the neighboring $(i-1)$-th and $(i+1)$-th cells (when $\bar{v}_{i-1} > v_{i-1}$ and $\bar{v}_{i+1} < v_{i+1}$). To combine all the possible birth contributions, for convenience the dimensionless term $\lambda_i^{\pm}(v)$ is introduced:

$$\lambda_i^{\pm}(v) = \frac{v - v_{i\pm1}}{v_i - v_{i\pm1}}. \qquad (26)$$

The discretized PBE using the CA technique takes the form of

$$\frac{dN_i}{dt} = B_i^{\mathrm{CA}} - D_i^{\mathrm{CA}}, \tag{27}$$

where

$$
\begin{aligned}
B_i^{\mathrm{CA}} &= B_{i-1}\lambda_i^-(\bar{v}_{i-1})H(\bar{v}_{i-1}-v_{i-1}) \\
&\quad + B_i\lambda_i^-(\bar{v}_i)H(v_i-\bar{v}_i) + B_i\lambda_i^+(\bar{v}_i)H(\bar{v}_i-v_i) \\
&\quad + B_{i+1}\lambda_i^+(\bar{v}_{i+1})H(v_{i+1}-\bar{v}_{i+1}),
\end{aligned} \tag{28}
$$

and

$$D_i^{\mathrm{CA}} = N_i \sum_{k=1}^{N_c} \beta_{i,k} N_k. \tag{29}$$

Here, the Heaviside step function H is given as

$$
H(v) = \begin{cases} 1, & \text{if } v > 0 \\ \frac{1}{2}, & \text{if } v = 0 \\ 0, & \text{if } v < 0. \end{cases} \tag{30}
$$

4.3 Fixed pivot scheme

The fixed pivot (FP) technique was developed by Kumar and Ramkrishna (Kumar and Ramkrishna, 1996). The scheme is based on the Hounslow's method, however, the disadvantage of using only geometric grids with Hounslow's method is eliminated in the fixed pivot scheme. This scheme can be used with any type of grid including linear grids. Here, for comparison of numerical solutions, the same geometric grid as in the Hounslow and CA schemes has been chosen. The main difference between the FP and CA schemes is in assigning the new-born particles to the cells. In the FP scheme, each individual birth in a cell is directly assigned to the appropriate cells, unlike in the CA scheme where the average volume of all the newly born particles is first calculated, and then only the assignment of the particles is performed.

The discrete form of the PBE with the FP scheme is then written as (Kumar and Ramkrishna, 1996)

$$\frac{dN_i}{dt} = B_i^{\mathrm{FP}} - D_i^{\mathrm{FP}}, \tag{31}$$

where

$$B_i^{\mathrm{FP}} = \sum_{j,k}^{j \geqslant k} \left(1 - \frac{1}{2}\delta_{jk}\right) \eta(\tilde{v}) \beta_{jk} N_j N_k, \tag{32}$$

such that $v_{i-1} \leq v_j + v_k \leq v_{i+1}$ and

$$D_i^{\mathrm{FP}} = D_i^{\mathrm{CA}} = N_i \sum_{k=1}^{N_c} \beta_{i,k} N_k. \tag{33}$$

Here, $\tilde{v} = v_k + v_j$ and $\beta_{j,k} = \beta(t, v_j, v_k)$ is the agglomeration kernel. The expression $\eta(\tilde{v})$ for each particle birth assignment is given by Eq. 34,

$$
\eta(\tilde{v}) = \begin{cases} \frac{v_{i+1}-\tilde{v}}{v_{i+1}-v_i}, & v_i \leq \tilde{v} < v_{i+1} \\ \frac{\tilde{v}-v_{i-1}}{v_i-v_{i-1}}, & v_{i-1} \leq \tilde{v} < v_i. \end{cases} \tag{34}
$$
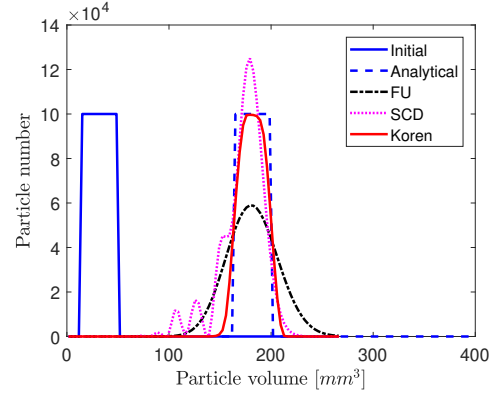
Figure 2. Comparison of PSDs with different numerical schemes for a layering batch process.

4.4 Kumar et al.'s new finite volume scheme

Recently, an accurate and efficient discretization method for agglomeration PBE was proposed in (Kumar et al., 2016) based on the finite volume approach. This scheme has an improvement over the finite volume scheme proposed by (Forestier and Mancini, 2012). The scheme provides better solution of several moments in addition to the mass conservation property compared to the scheme in (Forestier and Mancini, 2012). The Kumar et al.'s new finite volume (NFV) scheme assumes the number density function as the point masses concentrated on the cell representatives. The discrete PBE using Kumar et al.'s (Ku-

Table 1. Parameters used to solve PBE for particle layering process.

Parameter	Layering
Range of v [mm^3]	0-400
Number of cells	80
Grid type	linear
G [mm$^3 \cdot$ s^{-1}]	1
Time step for RK4 [s]	0.1

mar et al., 2016) scheme is then given as

$$\frac{dn_i^{\mathrm{NFV}}}{dt} = \frac{1}{2} \sum_{(j,k)\in Q^i} \beta_{j,k} n_j n_k \frac{\Delta v_j \Delta v_k}{\Delta v_i} S_{i,j,k} - \sum_{j=1}^{N_c} \beta_{i,j} n_i n_j \Delta v_j, \tag{35}$$
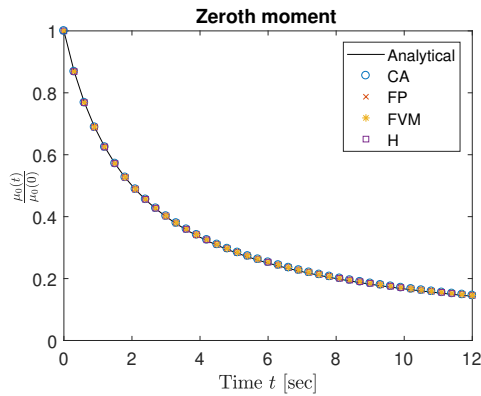
where factor $S_{i,j,k}$ accounts for mass conservation and is defined as

$$S_{i,j,k} = \frac{v_j + v_k}{v_i}. \tag{36}$$

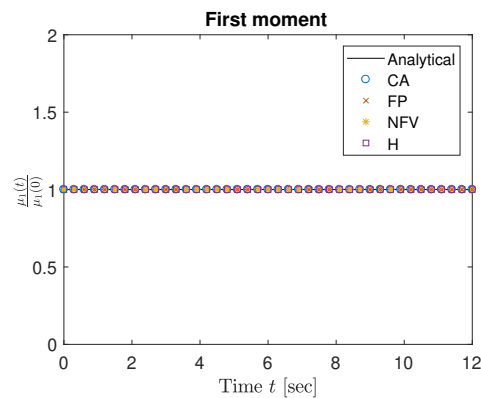The set Q^i be a set that contains the pair of cells j and k such that the sum of the cell's representatives, $v_j + v_k$, falls in the domain of cell i represented by cell node v_i:

$$Q^i = \{(j,k) \in N_c \times N_c : v_{i-\frac{1}{2}} < v_j + v_k \leq v_{i+\frac{1}{2}}\}. \tag{37}$$

In the NFV scheme, to ensure that no mass leaves the

Figure 3. Numerical results for zeroth moment using various numerical schemes for particle agglomeration.

Figure 4. Mass conservation with various numerical schemes.

upper boundary of the size domain (for mass conservation),

$$\beta(v_j, v_k) = \begin{cases} \beta(v_j, v_k), & (v_j + v_k) \le v_{\max} \\ 0, & \text{otherwise,} \end{cases} \quad (38)$$

where $v_{\max}$ is the maximum particle volume.

Table 2. Parameters used to solve PBE for binary particle agglomeration process.

Parameter	Agglomeration
Range of v [mm^3]	0-400
Number of cells	15
Grid type	geometric
β_0 [s^{-1}]	1
Time step for RK4 [s]	0.1
N_0	1
v_0 [mm^3]	1

5 Simulation Results and Discussion

5.1 Simulation Setup

The comparison of different numerical schemes is performed by applying corresponding discretization methods
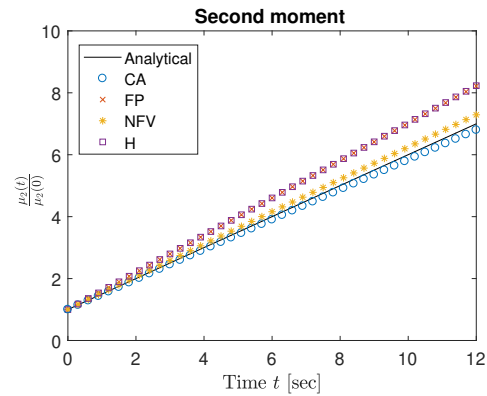
Figure 5. Numerical results for second moment using the various numerical schemes for pure agglomeration.

to batch processes as described in Section 3 and Section 4. Only batch processes with number based PBE with volume as the particle size, are used in these simulations. Such simplified processes are used in order to asses the performance of numerical schemes by comparing their numerical solutions with the analytically tractable solution.

The semi-discrete form (set of ODEs) of the PBEs obtained from particle class size are solved using a 4-th order Runge-Kutta method with fixed time step. Dynamic simulations are performed using MATLAB (MATLAB, 2017). Chosen simulation settings used to asses the accuracy of the numerical schemes for the particle layering process are given in Table 1 while for the particle agglomeration process in Table 2.

5.2 Comparison of numerical solutions for layering process

In order to compare the numerical schemes for particle growth due to layering, the number based PBE is utilized as discussed in Section 3. All the simulation cases for the granulation process due to layering are carried out using linear grid for particle size discretization. The entire particle size range is divided into 80 uniformly distributed cells (classes) and a constant growth rate is assumed (see Table 1). The initial PSD distribution is chosen as

$$N(v, 0) = \begin{cases} 10 \times 10^4 & 15 \le v \le 50, \\ 0 & \text{otherwise.} \end{cases} \quad (39)$$

Three finite volume schemes, i.e., first order upwind (FU), second order central difference (SCD), and Koren flux limiter (KFL) schemes are applied to simulate a pure layering batch process. In addition, simulations with an analytically tractable solution (Eq. 5) are carried out to reliably evaluate the accuracy of the numerical schemes. Simulation results (Figure 2) showed that the resulting particle number distribution obtained using the FU scheme has a diffusive behavior but the solution is stable and smooth. Since a significantly smeared solution is observed, the accuracy of the FU scheme is considered to be low. The numerical result obtained with the SCD scheme

(Figure 2) should have a higher accuracy compared to the FU scheme owing to its higher order. This, however, is true only for smooth solutions. The SCD scheme produces oscillations when the solution changes abruptly, i.e., in the presence of discontinuous analytical solutions. Fortunately, the oscillations that appear in the solution with the SCD scheme do not appear in the numerical solution when the KFL scheme was used. Thus, the highest accuracy among the three tested finite volume schemes is achieved using the finite volume scheme extended with the Koren flux limiter, Figure 2. Higher accuracy of the latter scheme is achieved since in the smooth solution regions, the Koren flux limiter function (in general a second order flux limiter) shows second order accuracy, while in the region where discontinuities appear, the flux limiter acts like a first order scheme, and thus produces a smooth solution. The drawback of the solution obtained with the KFL scheme is the increased computational time: the FU and SCD schemes can be solved relatively faster than the KFL scheme.

5.3 Comparison of numerical solutions for agglomeration process

Comparison of numerical schemes for the pure agglomeration process is carried out on a geometric grid with a factor of 2 in size ($v_{i+1} = 2v_i$) using 15 cells (Table 2).

The four different numerical schemes that are applied to the process for comparison are: Hounslow (H), fixed pivot (FP), cell average (CA), and a new Kumar et al.'s (2016) finite volume (NFV) scheme. The moments are calculated using discrete form of Eq. 2:

$$\mu^l = \sum_i^{Nc} x^l \Delta x_i n_i \qquad (40)$$

Assessment of the accuracy of the numerical schemes is performed by comparing the numerical solutions with an analytically tractable solution as mentioned in Section 4.

Simulation results showed that three tested numerical schemes produce solutions where conservation of the zeroth moment (total number conservation) and the first moment (mass conservation) are fulfilled (Figure 3 and Figure 4). No deviation is observed between the analytical solution and the numerical solutions for the first two moments for any of the numerical schemes.

However, the discrepancy between the numerical solutions and the analytical solution shows up for higher moments (second moment, as shown in Figure 5). The best accuracy for the second moment is observed for the numerical solution using the CA scheme.

The NFV scheme also predicts the second moment sufficiently accurate. The poorest solution accuracy for the second moment is produced when the H and the FP schemes are used. In addition, these two sectional schemes produce the same simulation results. This is due to the specific choice of the grid for particle size discretization: The FP scheme becomes equivalent to the H
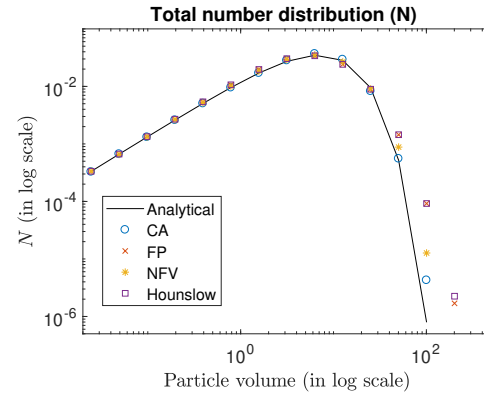
Figure 6. Simulation results for the total number distribution.

scheme when the geometric grid is used with a factor of 2 (Kumar, 2006). Thus, the FP and H schemes should produce the same results when such geometric discretization is used.

Another significant task is to evaluate the performance of the numerical schemes to predict the particle number distribution, usually visualized in log scale as shown in Figure 6. As the particles flow towards the higher size range in the agglomeration process, it is interesting to see how the numerical schemes perform at higher particle size range (thus log scale is used for improved visualization). Here, again, we can see the the discrepancy between the numerical and the analytical solutions. For lower particle size range, all the numerical schemes predicted accurately the particle number distribution. However, for higher particle size range, deviations from the analytical solution are observed. Among the tested numerical schemes, the FP and H schemes over-predict the actual results and thus show the poorest prediction of the particle number distribution. Similar to the moments prediction, the CA scheme and the NFV scheme show relatively better agreement with the analytical solution even for a coarse grid (15 cells).

6 Conclusions

Comparison of numerical schemes for solving population balance equations is presented in this paper, for pure layering and pure agglomeration problems. Discretization of the *layering* term is performed by applying various finite volume schemes. Among the three tested approximation schemes, the Koren flux limiter scheme exhibits relatively better performance in terms of accuracy. However, the Koren scheme also needs a higher computational time compared to the other tested numerical schemes. Numerical solutions for the agglomeration process were obtained by applying different sectional methods, as well as a recent finite volume scheme. The numerical performance of the cell average scheme and the new finite volume scheme in predicting the particle size distribution at higher particle size range is relatively better than Hounslow's scheme and the fixed pivot scheme. The former schemes produce a

PSD that is in good agreement with the analytical solution with coarser grid.

7 Acknowledgment

References

L. Forestier and S. Mancini. A finite volume preserving scheme on nonuniform meshes and for multidimensional coalescence. *SIAM Journal of Scientific Computing*, 34(6), 2012. doi:10.1137/110847998.

S. Heinrich, M. Peglow, M. Ihlow, and L. Mörl. Particle population modeling in fluidized bed-spary granulaiton - analysis of the steady state and unsteady behavior. *Powder Technology*, 130:154–161, 2003. doi:10.1016/S0032-5910(02)00259-0.

MJ Hounslow, RL Ryall, and VR Marshall. A discretized population balance for nucleation, growth, and aggregation. *AIChE Journal*, 34(11):1821–1832, 1988.

H.M. Hulburt and S. Katz. Some problems in particle technology: A statistical mechanical formulation. *Chemical Engineering Science*, 19(8):555–574, 1964.

G Kaur, J. Kumar, and S. Heinrich. A weighted finite volume scheme for multivariate aggregation population balance equation. *Computers & Chemical Engineering*, 101:1–10, 2017.

B. Koren. A robust upwind discretization method for advection, diffusion and source terms. In C. B. Vreugdenhil and B. Koren, editors, *Numerical Methods for Advection-Diffusion Problems, Notes on Numerical Fluid Mechanics*, pages 117–138. 1993.

J. Kumar. *Numerical approximations of population balance equations in particulate systems*. PhD thesis, Otto-von-Guericke-Universität Magdeburg, Universitätsbibliothek, 2006.

J. Kumar, M. Peglow, G. Warnecke, S. Heinrich, and L. Mörl. Improved accuracy and convergence of discretized population balance for aggregation: The cell average technique. *Chemical Engineering Science*, 61(10):3327–3342, 2006.

J. Kumar, G. Kaur, and E. Tsotsas. An accurate and efficient discrete formulation of aggregation population balance equation. *Kinetic & Related Models*, 9(2), 2016.

S. Kumar and D. Ramkrishna. On the solution of population balance equations by discretization - i. a fixed pivot technique. *Chemical Engineering Science*, 51(8):1311–1332, 1996.

J. Litster and B. Ennis. *The science and engineering of granulation processes*, volume 15. Springer Science & Business Media, 2004.

MATLAB. 2017a. The MathWorks, Inc., Natick, Massachusetts, United States., 2017.

R. Radichkov, T. Müller, A. Kienle, S. Heinrich, M. Peglow, and L. Mörl. A numerical bifurcation analysis of continuous fluidized bed spray granulator with external product classification. *Chemical Engineering and Processing*, 45:826–837, 2006. doi:10.1016/j.cep.2006.02.003.

D. Ramkrishna. *Population balances: Theory and applications to particulate systems in engineering*. Academic press, 2000.

WT Scott. Analytic studies of cloud droplet coalescence i. *Journal of the atmospheric sciences*, 25(1):54–65, 1968.

M. Singh, J. Kumar, and A. Bück. A volume conserving discrete formulation of aggregation population balance equations on non-uniform meshes. *IFAC-PapersOnLine*, 48(1):192–197, 2015.

Paper B

Population balance modelling for fertilizer granulation process

Authors L. Vesjolaja, B. Glemmestad, B. Lie

Population balance modelling for fertilizer granulation process

Ludmila Vesjolaja[1]   Bjørn Glemmestad[2]   Bernt Lie[1]

[1]Department of Electrical Engineering, IT and Cybernetics, University of South-Eastern Norway, Norway,
`{ludmila.vesjolaja,bernt.lie}@usn.no`
[2]Process Modeling and Control Department, Yara Technology Center, Norway, `bjorn.glemmestad@yara.com`

Abstract

Few granulation plants are operated optimally. It is common to operate granulation plants below their maximum design capacity, and in many cases, periodic instabilities may also occur. From a process control and optimization point of view, it is desirable to develop a dynamic model that can show the dominating dynamics of a granulation process and can be used for design of optimal operation of the granulation plant. In this paper, a dynamic model of a drum granulator is developed using population balance (PB). Different simulation scenarios are used to analyze various granulation mechanisms that are characteristic to drum granulators. Simulation results show that for the drum granulator, the particle agglomeration has a greater impact on the change in particle size distribution (PSD) compared to the particle growth due to layering. In addition, coarser particles are produced when a size-dependent agglomeration kernel is used in the granulator model. For combined processes, i.e., processes where the particle growth due to layering and agglomeration are considered simultaneously, coarser particles with a wider PSD are obtained with the size-dependent agglomeration kernel.

Keywords: granulation, population balance, agglomeration, layering

1 Introduction

Granulation is a particle enlargement process during which fine particles and/or atomizable liquids are converted into granules via a series of complex physical processes. In a typical granulation plant, the main operational goal is to produce granules with improved properties compared to their ungranulated form, and therefore, to meet product quality requirements (e.g., produce granules with the desired PSD, moisture content, porosity, etc.). Granulation processes are used in a wide range of industrial applications, such as in pharmaceuticals, chemicals, and fertilizer industries (Litster and Ennis, 2004). However, the operation of granulation plants in an industrial scale can be challenging. Many granulation plants have a high recycle-to-product ratio, and it is common to operate granulation plants below their maximum design capacity. In addition, periodic instability associated with the operation of the granulation circuit have been reported (Radichkov et al., 2006; Heinrich et al., 2003). This causes the PSD of

the particles flowing out of the granulator to oscillate, thus making it difficult to maintain the desired product quality. An increase in the production of off-spec particles (oversized and undersized) gives rise to a higher recycle-to-product ratio, and the plant does not operate in an optimal manner. One way to address these problems is to develop a mathematical model of the granulator that can be used to study and understand various dynamics occurring in the granulator. The model can further be used to design optimal control structures to increase the efficiency of the plant.

The most widely used approaches for modeling granulation processes include Discrete Element Modeling, as well as PB modeling. In this study, since the focus is on the development of a dynamic model suitable for control purposes, PB modeling has been used to develop a mathematical model of a drum granulator. A rich literature related to PB modeling of a granulation process is available (Randolph and Larson, 1962; Wang et al., 2006; Wang and Cameron, 2007). In these works, (i) the effect of different granulation mechanisms to the PSD of the granulator outflow is neglected, (ii) the numerical scheme (Hounslow discretization method) used for solving the population balance equation (PBE) is relatively inaccurate (shows overprediction as also mentioned in (Kumar, 2006; Kumar et al., 2006)) , and (iii) many of the processes are only batch processes. In this paper, a dynamic model of a continuous drum granulator using the PB framework is developed. The resulting integro-differential PBEs are discretized using an accurate numerical scheme, namely the cell average technique (Kumar, 2006) and the flux limitation scheme (Koren, 1993). The developed model is simulated to understand and analyze how different granulation mechanisms affect the PSD of the granules formed in the granulator.

2 Granulation Mechanisms

According to (Iveson et al., 2001), the granulation process is divided into three basic mechanisms: (i) nucleation and wetting, (ii) growth and consolidation, and (iii) breakage and attrition. Different granulation mechanisms are predominant depending on the type of the granulator being used. For continuous drum granulation with recycling, effects of nucleation, breakage, and attrition mechanisms are believed to be negligible compared to particle growth due to layering and agglomeration (Fig. 1). Particle nu-

https://doi.org/10.3384/ecp1815395

95

Proceedings of The 59th Conference on Simulation
and Modelling (SIMS 59), 26-28 September 2018,
Oslo Metropolitan University, Norway
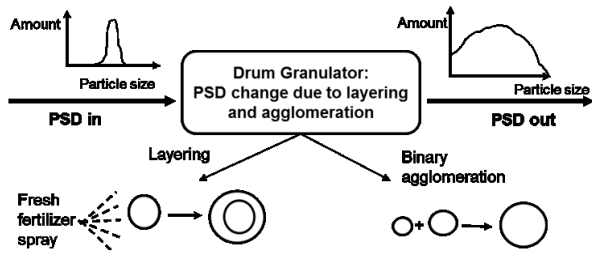
Figure 1. Main granulation mechanisms characteristic to drum granulators.

cleation is insignificant for this particular process as it is a continuous process in which the recycle feed acts as seeds for the granulator. Particle breakage is mainly important in a high shear granulators, e.g., granulation mechanism due to breakage can be significant in pharmaceutical industries where high shear granulators are typically used. As to the attrition, this granulation mechanism might give significant changes in PSD only when high velocities (e.g., fluidized bed spray) granulators are used (Litster and Ennis, 2004). Layering occurs due to a successive coating of a liquid phase onto a granule. As a result, the granule grows in its mass, and the volume increases, but the number of granules in the system remains unchanged. No collision between granules is assumed during this particle growth (Litster and Ennis, 2004). Layering is a continuous process (differential growth), and an assumption of size-independent linear growth rate is common in the PB modeling of granulation processes. This simplification implies that each granule has the same exposure to a new fertilizer spray feed material, and a volumetric growth rate is proportional to a projected granule surface area (Litster and Ennis, 2004). Binary agglomeration refers to a particle growth mechanism that occurs due to successful collision of two particles, resulting in the formation of a larger composite particle. Agglomeration is a discrete (sudden) process that changes the total number of particles: two particles *die*, and a new particle is *born* as a result of collision of two particles. Thus, the agglomeration results in a reduction in the total number of particles, while the total mass remains conserved (Litster and Ennis, 2004).

3 Model Development

3.1 Population Balance Principles

Balance laws such as mass and energy balances are often used in process modeling to describe dynamics of different physical and chemical processes. With particulate processes, PB is frequently used to describe dynamics of particle property distribution. A detailed derivation and explanation of the PBE can be found in Ramkrishna (Ramkrishna, 2000). The general form of a PBE with particle diameter (L) as the internal coordinate is represented as,

$$\frac{\partial n(L,t)}{\partial t} = -\frac{\partial}{\partial L}\left[Gn(L,t)\right] + B(L,t) - D(L,t)$$
$$-\frac{\partial}{\partial z}\left[\frac{dz}{dt}n(L,z,t)\right], \quad (1)$$

where $n(L,t)$ is the number density function. The first term on the right hand side represents the particle growth due to layering, the second and the third terms stand for particle birth and death respectively, and the last term represents a continuous process and gives the flow of particles through the granulator. G is the growth rate and z represents the distance along the axial direction of the drum granulator. The birth and the death terms usually include integrals which make the solution of the population balance equation complicated. In this paper, a plug flow along the axial direction of the drum granulator has been assumed. For simplifying the model complexity, a concept of *output equivalent* (perfect mixing) inside the granulator can be assumed. Thus, Eq. (1) can be simplified to

$$\frac{\partial n(L,t)}{\partial t} = -\frac{\partial}{\partial L}\left[Gn(L,t)\right] + B(L,t) - D(L,t)$$
$$+ \dot{n}_i\gamma_i - \dot{n}_e\gamma_e. \quad (2)$$

Here, $\dot{n}_i$ is the number flowrate of particles entering the granulator (influent), $\dot{n}_e$ is the number flowrate of particles leaving the granulator (effluent), γ_i is the size distribution function of the inlet flow of the particles (influent), γ_e is the size distribution function of the outlet flow of the particles (effluent).

In addition, for the PBE of Eq. (2), the following assumptions are made:

- The concept of *perfect mixing* inside the granulator is applied: particle property (size) inside the granulator is the same as at the outlet of the granulator.

- Particle breakage in neglected since the drum granulator is operating at low shear forces. Thus, the birth (B) and death (D) rates are only due to binary agglomeration.

- Particle size reduction due to attrition is neglected since the granulation drum does not operate at high velocities.

3.2 Growth Rate for Layering

The formulation of the particle growth rate for layering (G) is based on combination of the work of (Mörl, 1981) and (Mörl et al., 1977), as summarized in (Drechsler et al., 2005). This model assumes linear size-independent growth rate, meaning that a small particle gets less slurry per unit time than a larger particle, but the growth rate (the change of particle diameter over time) is constant for all particle sizes. Thus, the growth rate due to layering depends on a slurry rate (fresh fertilizer spray rate, $\dot{m}_{sl}$),

96

moisture fraction in the slurry ($X_{\text{sl,i}}$), and the total surface area of the particles ($A_{\text{p,tot}}$) as given by Eqs. (3) and (4).

$$G = \frac{\partial L}{\partial t} = \frac{2\dot{m}_{\text{sl}}(1 - X_{\text{sl,i}})}{\rho A_{\text{p,tot}}}, \qquad (3)$$

$$A_{\text{p,tot}} = \pi n \int_{L=0}^{L=\infty} L^2 dL. \qquad (4)$$

3.3 Particle Agglomeration

Particle agglomeration is a discrete event, which is challenging to model. One of the most widely used formulations of the agglomeration process was introduced by (Kapur and Fuerstenau, 1969). The general form of a length-based agglomeration is represented by Eqs. (5) and (6),

$$B(L,t) = \frac{L^2}{2}$$
$$\times \int_0^L \frac{\beta\left[\left(L^3 - \lambda^3\right)^{\frac{1}{3}}, \lambda\right] n\left[\left(L^3 - \lambda^3\right)^{\frac{1}{3}}, t\right] n(\lambda, t)}{\left(L^3 - \lambda^3\right)^{\frac{2}{3}}} d\lambda, \qquad (5)$$

$$D(L,t) = n(L,t) \int_0^\infty \beta(L,\lambda) n(\lambda,t) d\lambda. \qquad (6)$$

Here, β is the agglomeration (coalescence) kernel. The agglomeration kernel is a key parameter that controls the overall rate of agglomeration. Despite more than 50 years of research, only empirical and semi-empirical agglomeration kernels are available. Thus, these should be fitted to experimental data. Some of the most frequently used agglomeration kernels for two colliding particles with volumes v and w in granulation processes are summarized in Table 1. Here, β_0 is the part of the agglomeration kernel which usually depends on the operating conditions of the granulator such as the drum speed, bed depth and the moisture content in the particles. In this paper, the value of β_0 has been taken to be a constant (however tunable) for simplifying the model development. For a more detailed analysis, β_0 should be expressed as a function of process parameters and fitted with the experimental data. This has been left as a potential future work.

Table 1. Overview of agglomeration kernels.

Agglomeration kernel	References
$\beta = \beta_0$	Random kernel
$\beta = \beta_0 \times (v + w)$	Golovin (Golovin, 1963)
$\beta = \beta_0 \times \left(\frac{(v+w)^a}{(vw)^b}\right)$	Kapur (Kapur, 1972)
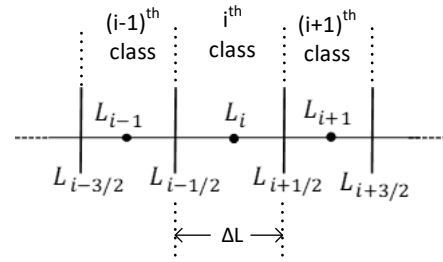
Figure 2. Size discretization into classes (cells).

4 Numerical Solution

Various discretization techniques/schemes can be used to discretize the continuous PBE of Eq. (2) into a set of ordinary differential equations (ODEs) which can then be solved with an appropriate ODE solver. In this work, the particle size is represented by the diameter of the particle. To obtain the particle size distribution, the particles are classified into $i \in 1, 2, ... N_c$ classes or cells as shown in Figure 2. Here, i represents the ith particle class, L_i is the diameter of the particle of the ith class, $L_{i\pm\frac{1}{2}}$ is the left and the right boundary of the ith class and $\triangle L = L_{i-\frac{1}{2}} - L_{i-\frac{1}{2}}$ is the size of the classes. The dots in each class represent the cell center. As was discussed in Section 2, the particle size change inside the drum granulator can be considered to be due to

- pure layering (agglomeration mechanism ignored),

- pure agglomeration (layering mechanism ignored),

- combined process (both layering and agglomeration considered).

In this paper, all the three cases of granulation mechanisms are considered separately and described in detail in the subsequent subsections.

4.1 Pure Layering

If the growth of particles is considered to be only due to layering, Eq. (2) reduces to,

$$\frac{\partial n(L,t)}{\partial t} = -\frac{\partial}{\partial L}[Gn(L,t)] + \dot{n}_i \gamma_i - \dot{n}_e \gamma_e. \qquad (7)$$

The PDE represented by Eq. (7) can be discretized into a system of ODEs using a finite volume scheme. In this paper, a high resolution scheme, based on the flux limiting approach, is chosen as the numerical scheme for particle size discretization. Particularly, the Koren flux limiting method (Koren, 1993) is used in this paper. The high resolution flux limiting methods attain higher accuracy than the first order upwind scheme. In addition, these methods also avoid spurious oscillations by applying a high order flux in the smooth regions and a low order flux near

discontinuities. Equation (7) can be discretized with the Koren scheme as

$$\frac{dN_i}{dt} = Gn\left(t, L_{i-\frac{1}{2}}\right) - Gn\left(t, L_{i+\frac{1}{2}}\right) + \dot{N}_i \gamma_i - \dot{N}_e \gamma_e, \quad (8)$$

where,

$$n\left(t, L_{i-\frac{1}{2}}\right) \approx \frac{1}{\Delta L} \left[N_{i-1} + \frac{1}{2}\phi\left(\widetilde{\theta}_{i-\frac{1}{2}}\right)(N_{i-1} - N_{i-2}) \right], \quad (9)$$

$$n\left(t, L_{i+\frac{1}{2}}\right) \approx \frac{1}{\Delta L} \left[N_i + \frac{1}{2}\phi\left(\widetilde{\theta}_{i+\frac{1}{2}}\right)(N_i - N_{i-1}) \right]. \quad (10)$$

Here, ϕ is the limiter function defined as

$$\phi\left(\widetilde{\theta}\right) = \max\left[0, \min\left(2\widetilde{\theta}, \min\left(\frac{1}{3} + \frac{2\widetilde{\theta}}{3}, 2\right)\right)\right]. \quad (11)$$

Parameter $\widetilde{\theta}$ is defined as

$$\widetilde{\theta}_{i-\frac{1}{2}} = \frac{N_i - N_{i-1} + \varepsilon}{N_{i-1} - N_{i-2} + \varepsilon}, \quad \widetilde{\theta}_{i+\frac{1}{2}} = \frac{N_{i+1} - N_i + \varepsilon}{N_i - N_{i-1} + \varepsilon}, \quad (12)$$

with a very small constant ε to avoid division by zero.

In an industrial application, it is relatively easier to work with mass-based population balance equations (PBEs) instead of number-based PBEs due to: (i) PSD in a real plant is typically measured by sieving and weighting, and (ii) mass-based PBE is more convenient to use from a numerical point of view (huge number of particles compared to their masses). To convert the number-based formulation given by Eqs. (8)-(12) to a mass-based formulation, Eq. (13) is applied,

$$N_i = \frac{6M_i}{\pi \rho L_i^3}. \quad (13)$$

Equation (13) was derived assuming that all particles are ideal spheres with constant density. After rearranging, the growth due to layering in a mass-based PBE can be represented as

$$\frac{dM_i}{dt} = L_i^3 \left[Gm\left(t, L_{i-\frac{1}{2}}\right) - Gm\left(t, L_{i+\frac{1}{2}}\right) \right] + \dot{M}_i \gamma_i - \dot{M}_e \gamma_e, \quad (14)$$

where,

$$m\left(t, L_{i-\frac{1}{2}}\right) \approx \frac{1}{\Delta L}\left\{ \frac{M_{i-1}}{L_{i-1}} + \frac{1}{2}\phi\left(\theta_{i-\frac{1}{2}}\right) \times \left(\frac{M_{i-1}}{L_{i-1}^3} - \frac{M_{i-2}}{L_{i-2}^3}\right) \right\}, \quad (15)$$

$$m\left(t, L_{i+\frac{1}{2}}\right) \approx \frac{1}{\Delta L}\left\{ \frac{M_i}{L_i} + \frac{1}{2}\phi\left(\theta_{i+\frac{1}{2}}\right) \times \left(\frac{M_i}{L_i^3} - \frac{M_{i-1}}{L_{i-1}^3}\right) \right\}, \quad (16)$$

with

$$\theta_{i-\frac{1}{2}} = \frac{\frac{M_i}{L_i^3} - \frac{M_{i-1}}{L_{i-1}^3} + \varepsilon}{\frac{M_{i-1}}{L_{i-1}^3} - \frac{M_{i-2}}{L_{i-2}^3} + \varepsilon}, \quad \theta_{i+\frac{1}{2}} = \frac{\frac{M_{i+1}}{L_{i+1}^3} - \frac{M_i}{L_i^3} + \varepsilon}{\frac{M_i}{L_i^3} - \frac{M_{i-1}}{L_{i-1}^3} + \varepsilon}. \quad (17)$$

Here M_i is the total mass of the particle in the ith class. The growth rate G is considered to be size-independent as described in more detail in Section 3.2. The growth rate due to layering is modeled using Eqs. (3) and (4). In addition, if T_R is the retention time, then, $\dot{M}_e \gamma_e = \frac{M_i}{T_R}$.

4.2 Pure agglomeration

If the change in the particle size is considered to be due to agglomeration only, Eq. (2) reduces to

$$\frac{\partial n(L,t)}{\partial t} = B(L,t) - D(L,t) + \dot{n}_i \gamma_i - \dot{n}_e \gamma_e. \quad (18)$$

Analytical solutions of the pure agglomeration problems can be found in some simplified cases. Thus, numerical techniques are needed to solve the resulted PBEs. However, the discretization of agglomeration terms (B, D) is more challenging compared to the growth due to layering. Agglomeration is a discrete event and the birth and death of particles can be considered to be source and sink terms, respectively. A suitable numerical scheme that is simple to implement and produce exact numerical results of some selected moments is the cell averaging technique (Kumar, 2006; Kumar et al., 2006). The cell average scheme is referred to as a sectional method, and assigns all the new-born particles within a cell more precisely compared to other sectional methods. Using the cell average scheme, Eq. (18) can be discretized with respect to the particle size as

$$\frac{dN_i}{dt} = B_{i-1}\lambda_i^-\left(\bar{L}_{i-1}\right)H\left(\bar{L}_{i-1} - L_{i-1}\right) + B_i\lambda_i^-\left(\bar{L}_i\right)H\left(L_i - \bar{L}_i\right) + B_i\lambda_i^+\left(\bar{L}_i\right)H\left(\bar{L}_i - L_i\right) + B_{i+1}\lambda_i^+\left(\bar{L}_{i+1}\right)H\left(L_{i+1} - \bar{L}_{i+1}\right) - N_i\sum_{k=1}^{N_c}\beta_{ik}N_k + \dot{N}_i\gamma_i - \dot{N}_e\gamma_e. \quad (19)$$

Here, N_c is the total number of particle size classes or cells. B_i is the birth of particles in the ith cell due to binary agglomeration of two particles from the jth and k^{th} cell respectively, and can be expressed as

$$B_i = \frac{1}{2}\sum_{j=1}^{i}\sum_{k=1}^{i}\beta_{jk}N_jN_k, \quad (20)$$

where condition $L_{i-\frac{1}{2}} \leq \left(L_j^3 + L_k^3\right)^{\frac{1}{3}} \leq L_{i+\frac{1}{2}}$ should be fulfilled. β_{jk} is the agglomeration kernel for binary agglomeration of particles from the jth and the kth cells. $\bar{L}_i$ is the

https://doi.org/10.3384/ecp1815395

98

Proceedings of The 59th Conference on Simulation and Modelling (SIMS 59), 26-28 September 2018, Oslo Metropolitan University, Norway

average diameter of all the new-born particles in the ith cell, and is given as

$$\bar{L}_i = \left[\frac{\sum_{j=1}^{i} \sum_{k=1}^{i} \beta_{jk} N_j N_k \left(L_j^3 + L_k^3 \right)}{\sum_{j=1}^{i} \sum_{k=1}^{i} \beta_{jk} N_j N_k} \right]^{\frac{1}{3}}, \qquad (21)$$

with dimensionless term $\lambda_i^{\pm}(L)$ given as

$$\lambda_i^{\pm}(L) = \frac{L^3 - L_{i\pm1}^3}{L_i^3 - L_{i\pm1}^3} \qquad (22)$$

The Heaviside step function H is defined as

$$H\left(\widetilde{L}\right) = \begin{cases} 1, & \text{if } \widetilde{L} > 0 \\ \frac{1}{2}, & \text{if } \widetilde{L} = 0 \\ 0, & \text{if } \widetilde{L} < 0. \end{cases} \qquad (23)$$

The cell average technique can be used to preserve any two moments. Here, we have chosen to preserve the zeroth moment (total number of particles conserved) and the third moment (total mass conserved) taking the diameter-based formulation. Using Eq. (13), the mass based form of the PBE can be written as

$$\begin{aligned} \frac{dM_i}{dt} = L_i^3 [& B_{i-1} \lambda_i^-(\bar{L}_{i-1}) H(\bar{L}_{i-1} - L_{i-1}) \\ & + B_i \lambda_i^-(\bar{L}_i) H(L_i - \bar{L}_i) + B_i \lambda_i^+(\bar{L}_i) H(\bar{L}_i - L_i) \\ & + B_{i+1} \lambda_i^+(\bar{L}_{i+1}) H(L_{i+1} - \bar{L}_{i+1})] - M_i \sum_{k=1}^{N_c} \beta_{ik} \frac{M_k}{L_k^3} \\ & + \dot{M}_i \gamma_i - \dot{M}_e \gamma_e, \quad (24) \end{aligned}$$

where the birth of the particles B_i are given as

$$B_i = \frac{1}{2} \sum_{j=1}^{i} \sum_{k=1}^{i} \beta_{jk} \frac{M_j}{L_j^3} \frac{M_k}{L_k^3}, \qquad (25)$$

and the average diameter of all the new-born particles in the ith class is

$$\bar{L}_i = \left[\frac{\sum_{j=1}^{i} \sum_{k=1}^{i} \beta_{jk} \frac{M_j}{L_j^3} \frac{M_k}{L_k^3} \left(L_j^3 + L_k^3 \right)}{\sum_{j=1}^{i} \sum_{k=1}^{i} \beta_{jk} \frac{M_j}{L_j^3} \frac{M_k}{L_k^3}} \right]^{\frac{1}{3}}. \qquad (26)$$

With T_R being the retention time, $\dot{M}_e \gamma_e = \frac{M_i}{T_R}$.

In this paper, agglomeration kernels (β_{jk} and β_{ik}) are defined using the Kapur model (Kapur, 1972) with $a = \frac{1}{3}$ and $b = 0$; this is one of the most widely used kernels for drum granulation. With the diameter-based formulation, the agglomeration kernels are given as

$$\beta_{xy} = \left(\frac{6}{\pi}\right)^{\frac{2}{3}} \frac{1}{\rho} \beta_0 K_{xy} = \left(\frac{6}{\pi}\right)^{\frac{2}{3}} \frac{1}{\rho} \beta_0 \left(L_x^3 + L_y^3 \right)^{\frac{1}{3}}. \quad (27)$$

The term $\left(\frac{6}{\pi}\right)^{\frac{2}{3}} \frac{1}{\rho}$ arises during the conversion from the number-based formulation to the mass-based formulation of PBEs. Subscript xy means either jk or ik. β_0 is the particle size independent part of the agglomeration kernel. K_{jk} and K_{ik} are the parts of the agglomeration kernel which are particle size dependent as shown in Eq. (27).

4.3 Combined Process

In the case of the combined process, a change in the particle size is a result of both particle growth due to layering, and particle binary agglomeration. The number-based PBE for the combined process is represented by (2). For conversion to the mass-based PBE, (13) is used. Size discretization for the growth term (G) is performed using the Koren flux limiting scheme as discussed in Section 4.1. Particle birth (B) and death (D) terms are size discretized using the cell averaging technique as was discussed in detail in Section 4.2. The resulting size discretized mass-based PBE for the combined process is written as

$$\begin{aligned} \frac{dM_i}{dt} = L^3 & \left[Gm\left(t, L_{i-\frac{1}{2}}\right) - Gm\left(t, L_{i+\frac{1}{2}}\right) \right] \\ + L_i^3 [& B_{i-1} \lambda_i^-(\bar{L}_{i-1}) H(\bar{L}_{i-1} - L_{i-1}) + B_i \lambda_i^-(\bar{L}_i) H(L_i - \bar{L}_i) \\ & + B_i \lambda_i^+(\bar{L}_i) H(\bar{L}_i - L_i) + B_{i+1} \lambda_i^+(\bar{L}_{i+1}) H(L_{i+1} - \bar{L}_{i+1})] \\ & - M_i \sum_{k=1}^{N_c} \beta_{ik} \frac{M_k}{L_k^3} + \dot{M}_i \gamma_i - \dot{M}_e \gamma_e, \quad (28) \end{aligned}$$

where all symbols in (28) are described in previous Sections 4.1 and 4.2.

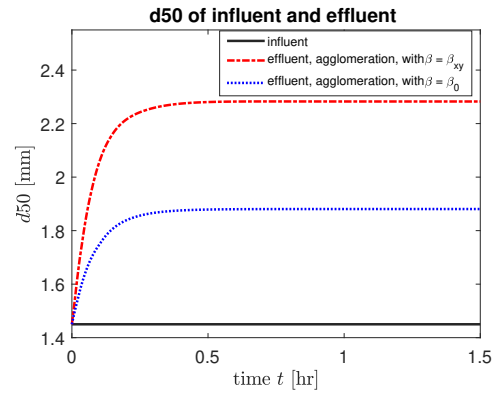## 5 Simulation Results and Discussion

5.1 Simulation Setup

The discretized PBEs for a continuous drum granulation process described by Eqs. (14), (24), and (28) are solved using a 4th order Runge-Kutta method with fixed time step. Dynamic simulations are performed using MATLAB (MATLAB, 2017). Simulations for continuous drum granulation are performed using parameters summarized in Table 2.
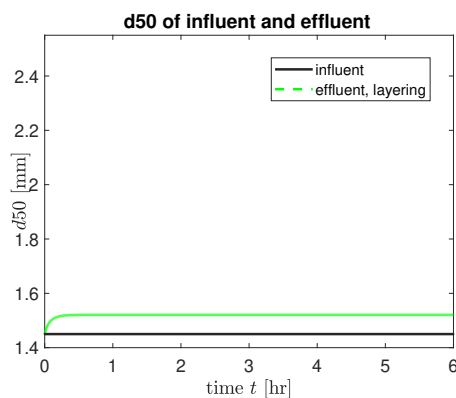
Table 2. Simulation setup parameters.

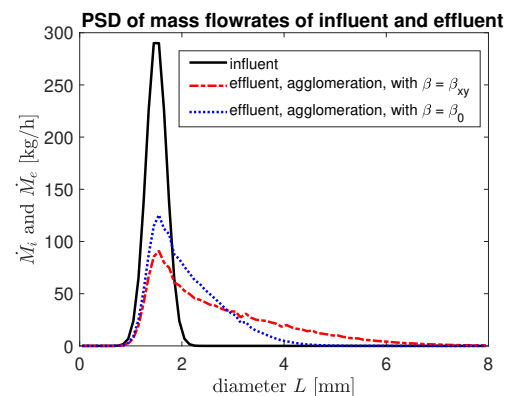| Parameter	Value
Range of L [mm]	0-8
Number of classes	80
ρ [$kg \cdot m^{-3}$]	1300
β_0 [s^{-1}]	$8.5 \cdot 10^{-11}$
T_R [s]	360
$\dot{m}_{sl,i}$ [$kg \cdot s^{-1}$]	250
$X_{sl,i}$	0.1
Time step for RK4 [s]	10
Simulation time [h]	2.5
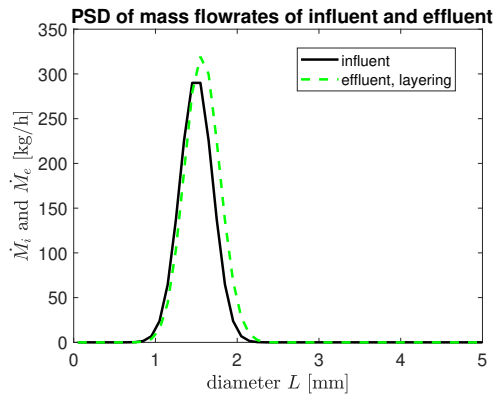
Figure 3. Influent and effluent PSD of the drum granulator for pure layering.

Figure 4. Change of the average particle size for pure layering.

Figure 5. Change of the average particle size for pure agglomeration.

Figure 6. Influent and effluent PSD of the drum granulator for pure agglomeration.

5.2 Simulation Results for Pure Layering and Pure Agglomeration

In this paper, simulations results are compared by analyzing the PSD at the inlet (Gaussian distribution) and the outlet of the drum granulator. In addition, the evolution of the average size of the particles represented by their d_{50} diameter (median diameter that corresponds to intercept for 50% of cumulative mass) are also studied. Figure 3 compares the PSD of the inlet flow and the outlet flow from the granulator after the system has reached the steady state. The only granulation mechanisms affecting the PSD is layering. Clearly, the PSD at the outlet of the drum granulator has changed and has become slightly wider compared to the inlet distribution. The fraction of coarser particles increases due to layering, and, thus more of large particles are produced. Figure 4 shows that the average size of the particles has increased from 1.45 mm to 1.52 mm when only the layering is the driving mechanism for particle size change. Thus, in average, particles have grown by $\sim 5\%$ using the model parameters summarized in Table 2.

However, when agglomeration was chosen as a granulation mechanism, the average particle size has grown by $\sim 30\%$ compared to its initial value (Figure 5). This increase in particle size (d_{50} to 1.85 mm) was observed

when agglomeration was modeled using a constant (size-independent) agglomeration kernel. The inclusion of particle size-dependency on the agglomeration rate has increased the average particle size even more (Figure 5). The d_{50} has grown from 1.45 mm (at the inlet) to 2.28 mm at the outlet of the granulator (with size-dependent agglomeration kernel). This gives $\sim 58\%$ increase in the average particle size. As expected, the same trend is observed in PSDs of the inlet and outlet mass flow rates (Figure 6).

Granulation produces larger particles when the agglomeration rate is assumed to be dependent on particle size compared to size-independent agglomeration rate. As shown in Figure 6, agglomeration with the size-dependent kernel has produced particles whose size are as large as 5 mm, while no particles with this size are produced with the size-independent kernel.

5.3 Simulations Results for Combined Process

To simulate the combined process, simultaneous particle binary agglomeration and particle growth due to layering is considered to be taking place in the drum granulator. In Figure 7, a comparison of the PSDs between pure agglomeration (with constant agglomeration kernel) and combined process is shown.
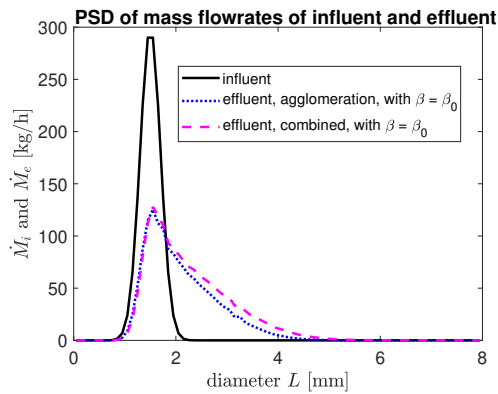
Figure 7. PSDs for pure agglomeration and combined process with size-independent kernel.
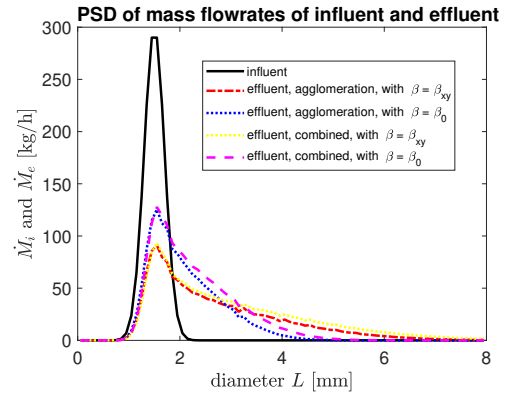
Figure 9. Comparison of PSD for pure agglomeration and combined process.
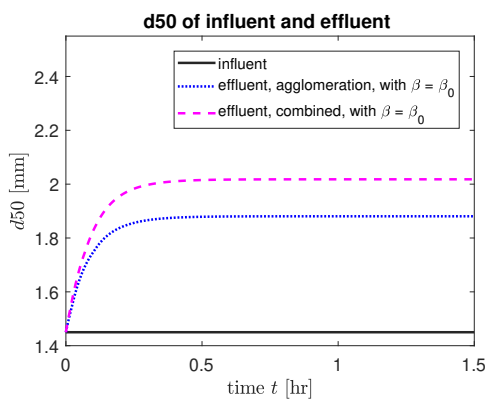
Figure 8. Change in d_{50} for pure agglomeration and combined process with size-independent kernel.
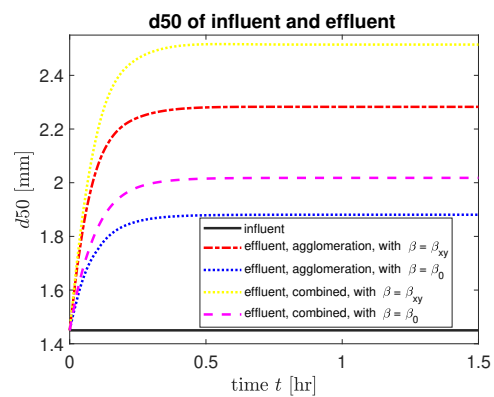
Figure 10. Comparison of d_{50} for pure agglomeration and combined process.

For the combined process, the PSD at the outlet is wider compared to the pure agglomeration granulation process. The mass fractions of coarser particles (>2 mm) become larger, and hence, larger particles are produced with the combined process. The comparison of these two granulation processes with the d_{50} plot (Figure 8) confirms the PSD shown in Figure 7. With the combined process, a higher value of d_{50} is obtained as compared to the pure agglomeration.

The d_{50} of the particles has increased by $\sim 7\%$ (with a constant agglomeration kernel) for the combined process compared to the pure agglomeration process. A similar trend of the particle size change is observed for processes when a size-dependent agglomeration kernel is used in the simulations (Figures 9 and 10). The PSD is wider, and larger particles are produced when the combined process is simulated (Figure 9). The latter is also reflected in the d_{50} plots (Figure 10). Interestingly, the value of d_{50} has grown from 2.28 mm for the pure agglomeration process to 2.52 mm for the combined process (Figure 10). This gives $\sim 10\%$ difference in average particle size for the pure and the combined process compared with the size-dependent kernel. This difference is $\sim 7\%$ when simulations are performed with the constant agglomeration kernel. Thus, particle enlargement and hence the total change

in PSD for the combined process is more intensive if particle agglomeration is driven by a size-dependent agglomeration kernel.

The plots of PSDs (Figure 9) reveal the same pattern (larger particles are produced with the combined processes compared to pure agglomeration). The PSDs of different processes start to deviate from each other when particle size fractions are larger than 1.2 mm. Granulation processes that are simulated with the constant agglomeration kernel produce more particles that are in the range of [1.2, 3.2] mm of size, compared to those processes that are simulated with the size-dependent agglomeration kernel. In contrast, the processes that are simulated by assuming size-dependent agglomeration kernels, result in a larger amount of coarse particles (≥ 3.2 mm), e.g., simulations with the size-dependent kernel produces particles with sizes as high as 6 mm, while no particles with such size is produced when the size-independent kernel is used (true for both pure agglomeration and combined process).

Based on the simulation results discussed above, the particle growth in drum granulators due to layering seems to play a minor role compared to the granulation mechanism for the particle binary agglomeration. This trend was indicated in others works (Wang et al., 2006; Wang and Cameron, 2007).

The agglomeration kernel is indeed an important parameter for modeling drum granulation processes. Not only the proper formulation of the size-independent part is needed, but also the dependency of agglomeration rate to particle size should be analyzed in order to obtain a proper model of the real plant.

6 Conclusions

In this paper, a comparative study on various model forms for representing a drum granulation process is given. Different granulation mechanisms are compared based on simulation results represented by particle size distributions and the d_{50} diameter (to reflect the average size of particles) at the influent and the effluent of the drum granulator. For the drum granulator under consideration, the simulation results lead to the following conclusions:

- Particle growth due layering has very small effect on the change of the particle sizes compared to particle binary agglomeration.

- Inclusion of the particle size dependency on the agglomeration kernel affects the mass distribution function, i.e., particles with a wider PSD and larger particles are produced compared to simulations with a constant agglomeration kernel.

- The combined process increases the growth of particles by $\sim 7\%$ (with size-independent kernel) and by $\sim 10\%$ (with size-dependent kernel) compared to a pure agglomeration process.

The choice of the agglomeration kernel directly affects the PSD of the particles. The size-independent part of the kernel should be calculated by taking into account the operational parameters of the actual drum granulator.

7 Acknowledgment

References

J. Drechsler, M. Peglow, S. Heinrich, M. Ihlow, and L. Mörl. Investigating the dynamic behaviour of fluidized bed spray granulation processes applying numerical simulation tools. *Chemical Engineering Science*, 60(14):3817–3833, 2005.

A.M. Golovin. The solution of the coagulation equation for raindrops, taking condensation into account. *Soviet Physics-Docklady*, 8(2):191–193, 1963.

S. Heinrich, M. Peglow, M. Ihlow, and L. Mörl. Particle population modeling in fluidized bed-spary granulaiton - analysis of the steady state and unsteady behavior. *Powder Technology*, 130:154–161, 2003. doi:10.1016/S0032-5910(02)00259-0.

S.M. Iveson, J.D. Litster, K. Hapgood, and B.J. Ennis. Nucleation, growth and breakage phenomena in agitated wet granulation processes: a review. *Powder technology*, 117(1-2): 3–39, 2001.

PC Kapur. Kinetics of granulation by non-random coalescence mechanism. *Chemical Engineering Science*, 27(10):1863–1869, 1972.

P.C. Kapur and D.W. Fuerstenau. Coalescence model for granulation. *Industrial & Engineering Chemistry Process Design and Development*, 8(1):56–62, 1969.

B. Koren. A robust upwind discretization method for advection, diffusion and source terms. In C. B. Vreugdenhil and B. Koren, editors, *Numerical Methods for Advection-Diffusion Problems, Notes on Numerical Fluid Mechanics*, pages 117–138. 1993.

J. Kumar. *Numerical approximations of population balance equations in particulate systems*. PhD thesis, Otto-von-Guericke-Universität Magdeburg, Universitätsbibliothek, 2006.

J. Kumar, M. Peglow, G. Warnecke, S. Heinrich, and L. Mörl. Improved accuracy and convergence of discretized population balance for aggregation: The cell average technique. *Chemical Engineering Science*, 61(10):3327–3342, 2006.

J. Litster and B. Ennis. *The science and engineering of granulation processes*, volume 15. Springer Science & Business Media, 2004.

MATLAB. 2017a. The MathWorks, Inc., Natick, Massachusetts, United States., 2017.

L. Mörl. *Anwendungsmöglichkeiten und Berechnung von Wirbelschichtgranulationstrocknungsanlagen*. PhD thesis, Technische Hochschule Magdeburg, 1981.

L. Mörl, M. Mittelstrab, and J. Sachse. Zum kugelwachstum bei der wirbelschichtrocknung von suspensionen oder losungen. *Chemical Technology*, 29(10):540–541, 1977.

R. Radichkov, T. Müller, A. Kienle, S. Heinrich, M. Peglow, and L. Mörl. A numerical bifurcation analysis of continuous fluidized bed spray granulator with external product classification. *Chemical Engineering and Processing*, 45:826–837, 2006. doi:10.1016/j.cep.2006.02.003.

D. Ramkrishna. *Population balances: Theory and applications to particulate systems in engineering*. Academic press, 2000.

A.D. Randolph and M.A. Larson. Transient and steady state size distributions in continuous mixed suspension crystallizers. *AIChE Journal*, 8(5):639–645, 1962.

F.Y. Wang and I.T. Cameron. A multi-form modelling approach to the dynamics and control of drum granulation processes. *Powder Technology*, 179(1-2):2–11, 2007.

F.Y. Wang, X.Y. Ge, N. Balliu, and I.T. Cameron. Optimal control and operation of drum granulation processes. *Chemical Engineering Science*, 61(1):257–267, 2006.

Paper C

Application of population balance equation for continuous granulation process in spherodizers and rotary drums

Authors L. Vesjolaja, B. Glemmestad, B. Lie

Application of population balance equation for continuous granulation process in spherodizers and rotary drums

Ludmila Vesjolaja[1]   Bjørn Glemmestad[2]   Bernt Lie[1]

[1]Department of Electrical Engineering, IT and Cybernetics, University of South-Eastern Norway,
`{ludmila.vesjolaja,bernt.lie}@usn.no`
[2]Process Modeling and Control Department, Yara Technology Center, Norway, `bjorn.glemmestad@yara.com`

Abstract

In this paper, a dynamic model for a granulation process is developed. A population balance is used to capture dynamic particle size distribution in the spherodizer model and in the rotary drum granulator model. Particle growth due to layering is assumed in the spherodizer simulation model, while particle binary agglomeration is taken as the main granulation mechanism in the rotary drum simulation model. The developed models are 2-dimensional(2D) models that are discretized in terms of its internal coordinate (particle diameter), external coordinate (axial length of the granulators). Simulations using the developed models provide valuable data on dynamic fluctuations in the outlet particle size distribution for the granulators. In addition, the simulations results give a valuable information for the control studies of the granulation process. The simulation results showed that the extension of the model from 1D model to 2D model using the discretization of the external coordinate in the model, introduces a transport delay that is important in control studies.

Keywords: spherodizer, rotary drum, population balance, dynamic model, time delay

1 Introduction

Granulation processes are used in a wide range of industrial applications, including fertilizer industries. Fertilizer manufacturing using the granulation process has received considerable research interest during the last few decades, due to (i) the increasing requirements for efficient production of high quality fertilizers for increased food production in a growing global population, and (ii) difficult process control and operation, e.g., among others (Herce et al., 2017; Ramachandran et al., 2009; Valiulis and Simutis, 2009; Wang et al., 2006) and (Cameron et al., 2005) have focused their research on granulation processes. This paper is focused on the last part of the mineral fertilizer production, i.e. on the granulation loop. The granulation loop is used to produce different grades of fertilizers. A typical schematic of a granulation process with the recycle loop is shown in Figure 1. The granulation loop consists of a granulator, granule classifier (screener), and a crusher. The granulator receives the fines from the external particle feed, as well as from the

recycled styream. These particle feeds are sprayed with a fertilizer liquid melt (slurry), and granules are formed. Different granulation mechanisms depending on the granulator type and conditions are responsible for these granule formation.

Process control of granulation loops is challenging. Typically, the PSD of the granules leaving the granulator is wider compared to the required PSD of the final product. A typical recycle ratio between the off-spec particles (80 %) and the required product-sized particles (20 %). Thus, it is important to develop a dynamic model that could further be used in control relevant studies. This paper is focused on developing dynamic models of two types of granulators, namely spherodizers and rotary drums. Depending on the granulator type and operating conditions, different granulation mechanisms (granule formation mechanism) are predominant. In spherodizers, the main granulation mechanism is particle growth due to layering. Layering is a continuous process during which particle growth occurs due to a successive coating of a liquid phase onto a granule. In rotary drum granulators, on the other hand, particle collision occurs, and thus particle agglomeration contributes significantly to particle size change. In this paper, binary particle agglomeration is assumed for population balance (PB) modeling. Binary agglomeration refers to a granule formation mechanism that occurs due to successful collision of two particles, resulting in the formation of a larger, composite particle (Litster and Ennis, 2004; Vesjolaja et al., 2018).

This paper is an extension of our previous study that is summarized in (Vesjolaja et al., 2018). Here, the dynamic model of the granulator is improved by increasing the dimensionality of the model, i.e., a 2D model instead of a 1D model is developed. The improved dynamic model provides valuable data on dynamic fluctuations in the outlet particle size distribution for the granulators. Thus, the contributions of this paper are: (i) the 1D model is extended to the 2D model (ii) developed 2D models are applied for two types of granulators, spherodizers and rotary drums, and (iii) two different numerical schemes, a finite volume scheme and a sectional scheme, are applied to the developed 2D dynamic models.
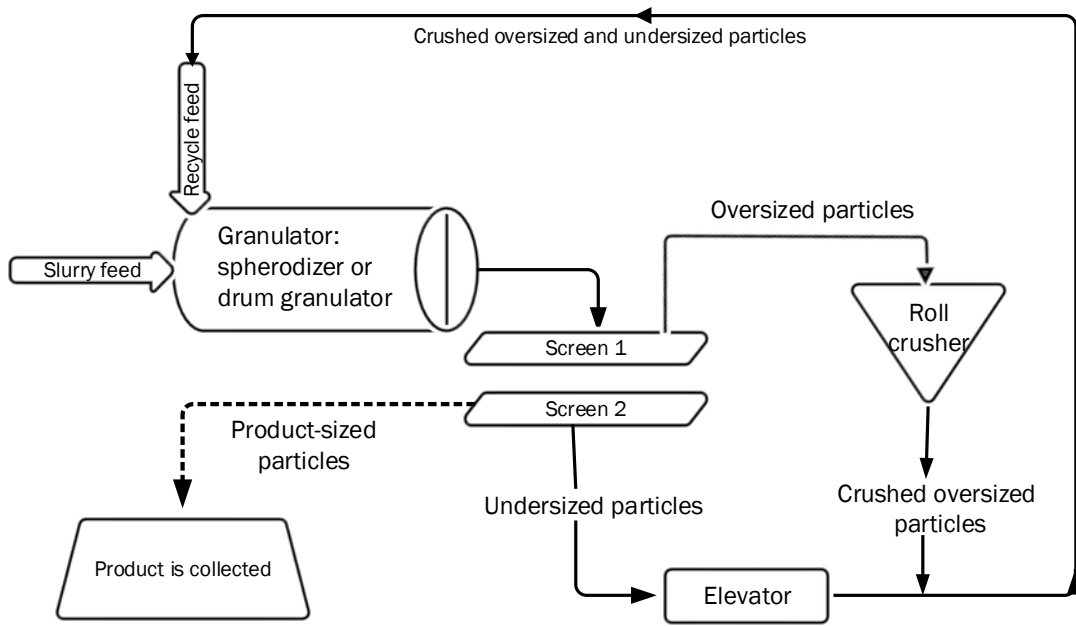
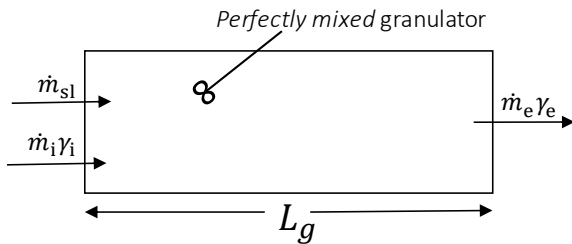**Figure 1.** Schematic diagram of granulation loop.

Figure 2. Graphical representation of the *perfectly mixed* granulator.
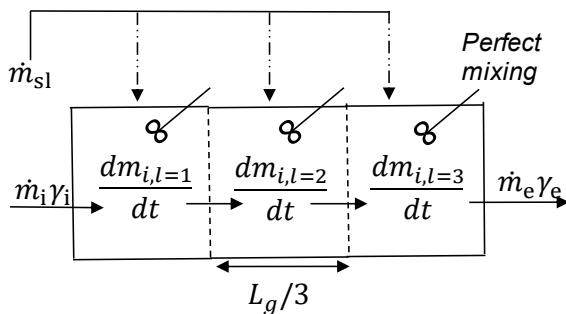

Figure 3. Graphical representation of the multi-compartment granulator. Abreviations: N_z is the number of the compartments in the granulator; L_g is the length of the granulator.

2 Application of PBE to granulation process in spherodizers

In the fertilizer production plant under consideration, a continuous granulation process is used. In an industrial application, it is relatively easier to work with mass based population balance equations (PBEs) instead of number based PBEs due to (i) the PSD in a real plant is typically measured by sieving and weighting, and (ii) mass based PBE is more convenient to use from a numerical point of view due to a huge number of particles compared to their mass. In addition, the size of the particles is represented in terms of their diameters (L) since measuring of PSDs in the plant are based on sieve diameter. A number based PBE with particle volume as internal coordinate is described in (Ramkrishna, 2000). Thus, it is essential to convert PBEs from their volume based formulations to length based formulations. In addition, number based PBEs should be converted into mass based PBEs. The mass based PBE for the spherodizer (continuous layering process) taking particle diameter as the internal coordinate, is formulated as

$$\frac{\partial m(L,z,t)}{\partial t} = -L^3 \frac{\partial}{\partial L}\left[G\frac{m(L,z,t)}{L^3}\right] - \frac{\partial}{\partial z}\left[\frac{dz}{dt}m(L,z,t)\right].$$
(1)

where m is the mass density function $\left[\frac{kg}{mm^3 \cdot [mm]}\right]$. The first term on the right hand side represents the particle growth due to layering, while the last term represents a continuous process and gives the flow of particles through the granulator. G is the growth rate $\left[\frac{mm}{s}\right]$. Equation 1 is derived by assuming that all particles are ideal spheres
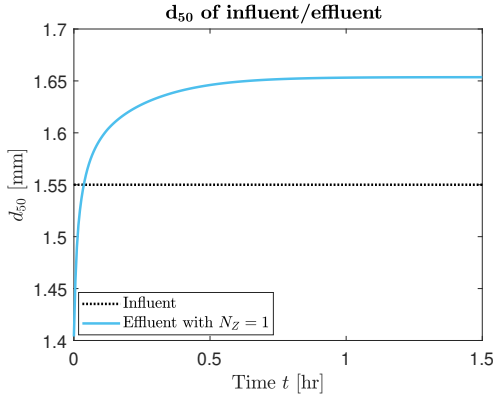
Figure 4. d_{50} for influent and effluent.

with a constant solid density ρ.

Here, the particle growth rate for layering (G) is modeled assuming a linear size-independent growth rate. Mathematical expressions for a linear size-independent growth rate are given in Equation 2.

$$G = \frac{2\dot{m}_{sl}(1 - X_{sl,i})}{\rho A_{p,tot}},$$
$$A_{p,tot} = \pi n \int_{L=0}^{L=\infty} L^2 dL, \qquad (2)$$

where $\dot{m}_{sl}$ is the fresh fertilizer spray rate, $X_{sl,i}$ is the moisture fraction in the slurry and total $A_{p,tot}$ is the surface area of the particles.

2.1 Internal coordinate

Integration of Eq. 1 for i-th size class gives

$$\frac{dM_i}{dt} = L_i^3 G \cdot \left[m\left(t, L_{i-\frac{1}{2}}\right) - m\left(t, L_{i+\frac{1}{2}}\right) \right]. \qquad (3)$$

For simplicity, in Equation 3, the particle flux term is neglected as it is dependent on the external coordinate (the discretization of the external coordinate is described in Section 2.2).

Discretization of the internal coordinate, i.e., discretization of the growth term for particle diameter, has been performed using a finite volume scheme extended by a flux limiter function. High resolution schemes are considered to attain higher accuracy than the first order upwind schemes. In addition, these methods avoid spurious oscillations by applying a high order flux in the smooth regions and a low order flux near discontinuities (Koren, 1993; Kumar, 2006). In this paper, a Koren flux limiter function (KFL) is used to achieve a robust upwind discretization scheme to Eq. 3. Discretization of the internal coordinate is performed on a linear grid using the KFL scheme. KFL scheme for the mass based PBE with the particle diameter (not volume) as internal coordinate is given in (Vesjolaja et al., 2018).

2.2 External coordinate

For a continuous granulation process, a plug flow along the axial direction is assumed. Here, the external coordi-nate (particle fluxes in and out of the granulator), given by the term $\frac{\partial}{\partial z}\left[\frac{dz}{dt} m(L,z,t)\right]$ is treated in two different ways as described below as Case I and Case II, respectively.

Case I: In this simplified case, a concept of *output equivalent* inside the granulator is used (Figure 2). This means that the entire granulator is treated as *perfectly mixed* throughout its length (L_g). The whole granulator is treated as a single compartment with $N_z = 1$ where N_z denotes the number of compartments. Thus, the particle flux term reduces to

$$\frac{\partial}{\partial z}\left[\frac{dz}{dt} m(L,z,t)\right] = \dot{m}_i \gamma_i - \dot{m}_e \gamma_e, \qquad (4)$$

where the particle flux out from the granulator is defined as

$$\dot{m}_e \gamma_e = \frac{m_i}{\tau} \gamma_e. \qquad (5)$$

Here, $\dot{m}_i$ is the mass flow rate of particles entering the granulator (influent), $\dot{m}_e$ is the mass flow rate of particles leaving the granulator (effluent), γ_i is the size distribution function of the influent, γ_e is the size distribution function of the effluent, m_i is the mass of the i-th particle size class, and τ is the retention (residence) time.

Case II: In this case, the granulator is divided into N_z equally sized compartments, Figure 3. The influent to the granulator enters the 1-st compartment and the effluent leaves the granulator from the N_z-th or the last compartment. The particle flux term is discretized by using one of the finite volume schemes. In this paper, a high resolution scheme with Koren flux limiter function (KFL) is used to discretize the spatial domain. For this, the granulator is divided into N_z uniformly spaced compartments, and each compartment is assumed to be *perfectly mixed*. Integration of the particle flux term for N_z compartments gives

$$\frac{\partial}{\partial z}\left(\frac{dz}{dt} m_{i,z}\right) = w\frac{\partial}{\partial z}(m_{i,z}) = w\left[m_{i,z-\frac{1}{2}} - m_{i,z+\frac{1}{2}} \right], \qquad (6)$$

where $\frac{dz}{dt} = w$ is the particle velocity along the granulator and is assumed to be constant inside the granulator. The approximation of the terms $m_{i,z\pm\frac{1}{2}}$ is then performed using a KFL scheme (Koren, 1993). The approximation of the terms $m_{i,z\pm\frac{1}{2}}$ using the KFL scheme is given by Eq. 7 and Eq. 8.

$$m_{i,z-\frac{1}{2}} \approx \frac{1}{\Delta z}\left\{ \frac{M_{i,z-1}}{L_i} + \frac{1}{2}\phi\left(\theta_{i-\frac{1}{2}}\right) \times \left(\frac{M_{i,z-1}}{L_i^3} - \frac{M_{i,z-2}}{L_i^3} \right) \right\}, \qquad (7)$$

$$m_{i,z+\frac{1}{2}} \approx \frac{1}{\Delta z}\left\{ \frac{M_{i,z}}{L_i} + \frac{1}{2}\phi\left(\theta_{i-\frac{1}{2}}\right) \times \left(\frac{M_{i,z}}{L_i^3} - \frac{M_{i,z-1}}{L_i^3} \right) \right\}, \qquad (8)$$
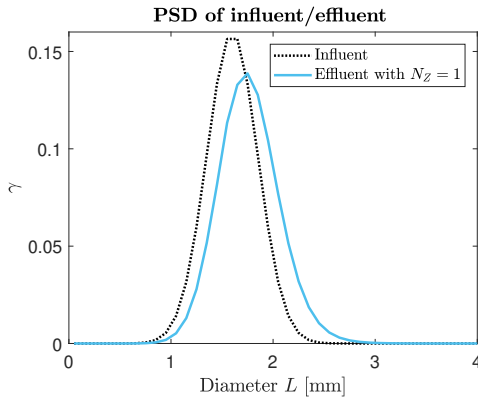
Figure 5. PSD of influent and effluent.

where, M_i is the total mass of the particle in the ith class and $\Delta z = \frac{L_g}{N_z}$ is the length of the each section in the granulator (Figure 3). The limiter function ϕ in Eq. 7 and Eq. 8 is defined as

$$\phi(\theta) = \max\left[0, \min\left(2\theta, \min\left(\frac{1}{3} + \frac{2\theta}{3}, 2\right)\right)\right], \quad (9)$$

and parameter θ is defined as

$$\theta_{i-\frac{1}{2}} = \frac{\frac{M_{i,z}}{L_i^3} - \frac{M_{i,z-1}}{L_i^3} + \varepsilon}{\frac{M_{i,z-1}}{L_i^3} - \frac{M_{i,z-2}}{L_i^3} + \varepsilon}, \quad \theta_{i+\frac{1}{2}} = \frac{\frac{M_{i,z+1}}{L_i^3} - \frac{M_{i,z}}{L_i^3} + \varepsilon}{\frac{M_{i,z}}{L_i^3} - \frac{M_{i,z-1}}{L_i^3} + \varepsilon}.$$
$$(10)$$

The constant ε is a very small number to avoid division by zero, e.g. $\varepsilon = 10^{-8}$.

3 Application of PBE to granulation process in rotary drums

The model for the rotary drum granulator (continuous agglomeration process) includes binary agglomeration of the particles and is given as

$$\frac{\partial m(L,z,t)}{\partial t} = B(L,z,t) - D(L,z,t) - \frac{\partial}{\partial z}\left[\frac{dz}{dt}m(L,z,t)\right]. \quad (11)$$

To solve the model, the entire particle size range is divided into uniformly distributed classes. The particle flux term (the last term on the right hand side of Eq. 11) is treated in two different ways as described in detail in Section 2.2. The agglomeration terms (the first two terms on the right hand side of Eq. 11) are discretized using the cell average scheme (Kumar et al., 2006; Kumar, 2006) as well as Kumar et al.'s new finite volume scheme (Kumar et al., 2016).

The cell average (CA) scheme was introduced by Kumar (Kumar et al., 2006; Kumar, 2006) and it belongs to the sectional methods of discretization. In the CA scheme, at first the total birth of particles in each cell denoted is computed. Then the average volume of the newly formed

particles in each cell is calculated. The next step in the CA scheme is to assign the total birth of particles appropriately to different cells depending on the position of the average volume of all newborn particles relative to the cell center volume. However, the CA scheme discussed in (Kumar et al., 2006; Kumar, 2006) is valid when the particle volume represents the internal coordinate. Thus, the volume based formulation of the CA scheme should be transformed into the diameter based formulation of the CA scheme. For this, the zeroth moment (total number of particles), and the third moment (total mass of particles) has been chosen to be conserved (compared to zeroth and first moments for volume based definition). Mathematical expressions of diameter based formulation for the CA scheme are given in (Vesjolaja et al., 2018).

Kumar et al.'s new finite volume scheme (Kumar et al., 2016) is based on the finite volume approach proposed by (Forestier and Mancini, 2012). Recently, new approach of solving PBE was proposed in (Kumar et al., 2016). This scheme is an accurate and efficient discretization method for agglomeration tern discretization. It has an improvement over the finite volume scheme proposed by (Forestier and Mancini, 2012) since it provides better solution of several moments in addition to the mass conservation property. Mathematical formulations are given in (Kumar et al., 2016).

Table 1. Parameters used for simulating granulation in spherodizers

Parameter	Spherodizer
Range of L [mm]	0-8
Number of cells	80
Grid type	linear
ρ [kg·m^{-3}]	1300
Length of granulator [m]	10
τ [min]	10
$\dot{m}_{\text{sl,i}}$ [kg·h^{-1}]	100
$X_{\text{sl,i}}$	0.05
Time step for RK4 [s]	20

In this paper, the agglomeration kernel (β) is defined using the Kapur agglomeration kernel model (Kapur, 1972) by taking $a = 2$ and $b = 1$. Using the diameter based formulation, the agglomeration kernel takes the form

$$\beta_{ik} = \left(\frac{6}{\pi}\right)^{\frac{2}{3}} \frac{1}{\rho} \beta_0 K_{ik}, \quad (12)$$

where the term $\left(\frac{6}{\pi}\right)^{\frac{2}{3}} \frac{1}{\rho}$ arises during the conversion from a number-based formulation to the mass-based formulation of PBEs, β_0 is the particle size independent part of the agglomeration kernel, and K_{ik} is the particle size dependent part of the agglomeration kernel as shown in Eq.13.

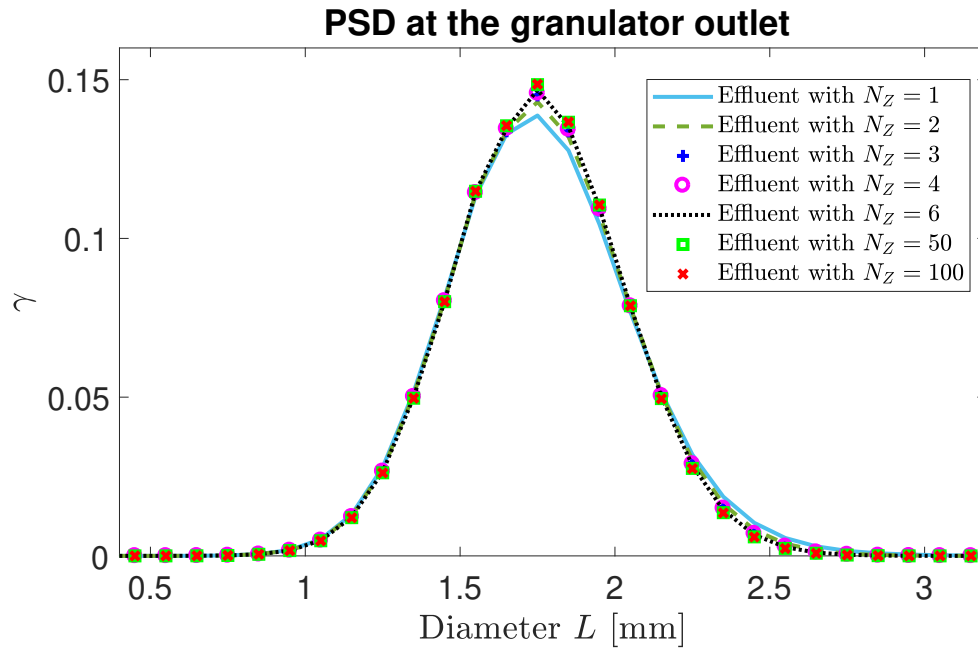$$K_{ik} = \frac{(L_i + L_k)^2}{L_i L_k}, \quad (13)$$

PSD at the granulator outlet

Figure 6. PSDs at the outlet of the spherodizer for different number of compartments.

4 Simulation Results and Discussion

4.1 Simulation Setup

The semi-discrete form (set of ODEs) of the PBEs obtained from particle class size and spatial discretizations are solved using a 4-th order Runge-Kutta method with fixed time step. Dynamic simulations are performed using MATLAB (MATLAB, 2017). The parameters used to simulate the application of PBE to the fertilizer granulation process in spherodizers and rotary drums are given in Table 1 and Table 2 respectively .

Table 2. Parameters used for simulating granulation in rotary drums.

Parameter	Rotary drum
Range of L [mm]	0-8
Number of cells	80
Grid type	linear
ρ [kg· m^{-3}]	1300
β_0 [s^{-1}]	$1.0 \cdot 10^{-11}$
Length of granulator [m]	6
τ [min]	6
$\dot{m}_{sl,i}$ [kg· h^{-1}]	100
$X_{sl,i}$	0.05
Time step for RK4 [s]	20

4.2 Simulation results for granulation in spherodizers

The granulation process in spherodizers is simulated for two simulation cases: Case I where the entire granulator

Table 3. Comparison of the computational time (in seconds) with different numerical schemes for rotary drum simulations.

Numerical scheme	$\beta = \beta_0$	$\beta = \beta_{ik}$
CA with $N_z = 1$	3.3	6.0
CA with $N_z = 3$	9.0	17.0
NFV with $N_z = 1$	3.6	6.2
NFV with $N_z = 3$	9.1	17.3

is assumed 'perfectly mixed', and Case II where the entire granulator length is divided into uniformly sized compartments as described in Section 2.2.

The mass based formulation of the PBE with diameter representing the particle size, is used, and the spherodizer is a continuous process with influent and effluent. Table 1 lists the simulation settings and parameters values. Simulation results are presented by particle size distribution (PSD) plots in terms of particle diameter, as well as by particle median diameter d_{50}. The values of d_{50} are obtained from the cumulative mass distribution. Linear interpolation is used to extract d_{50} values that correspond to intercept for 50 % of cumulative mass.

Simulation results obtained for the application of the PBEs in spherodizers is depicted in Figure 4, Figure 5 and Figure 6. Figure 4 and Figure 5 shows the change in particle sizes that occurs during a continuous granulation process in the *perfectly mixed* spherodizer (solution of the PBE is found using KFL scheme). Clearly, the particles grow in size inside the granulator. As a result, d_{50} of the effluent is larger than d_{50} of the influent, Figure 4, and more of coarse-sized particles is produced,
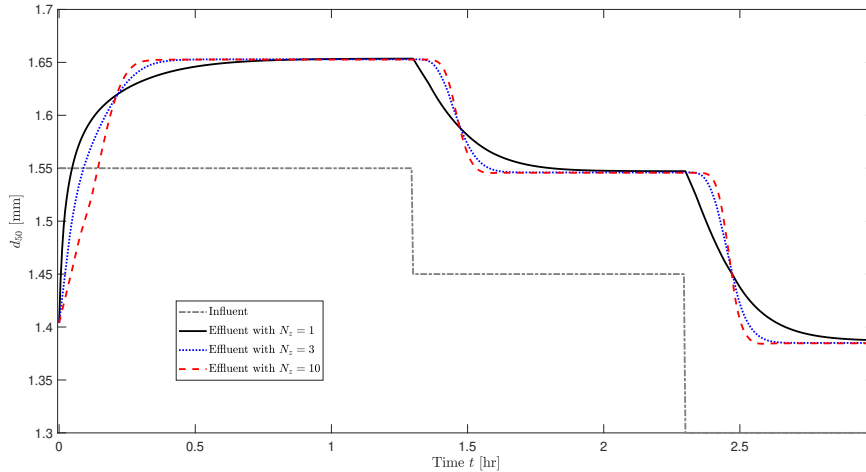
Figure 7. d_{50} at the outlet of the spherodizer for different number of compartments.
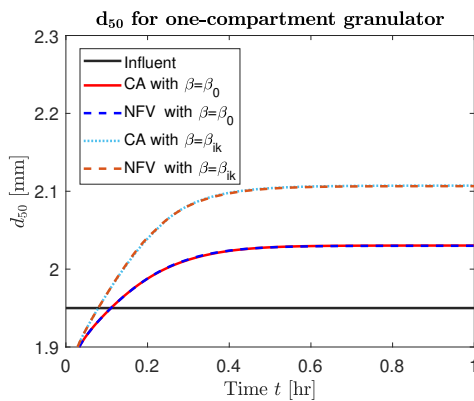
Figure 8. Simulation results for d_{50} with size-dependent and size-independent agglomeration kernels assuming *perfectly mixed* drum granulator.

Figure 5. Simulation results with the inclusion of spatial discretization of the granulator are depicted in Figure 6 and Figure 7. In Figure 6, PSDs of the effluent at the outlet of the granulator with different number of compartments (N_z) are compared. The PSD plot with $N_z = 50$ can be considered as a reference plot since no change in PSD is observed when increasing the number of compartments in the granulator (PSD plot with $N_z = 100$). Differences in PSDs appear mainly for the coarser particle fractions (with $L > 1.5$ mm), while for the finer particles (with $L < 1.5$ mm), the *perfectly mixed* granulator gives accurate enough results. Figure 7 shows d_{50} of the effluent as a step change in the influent is given. In a multi-compartment granulator a time delay is introduced as a step change of d_{50} in influent is given. Thus, inclusion of the spatial discretization could be important for development of a control-relevant dynamic model of the graulator. Based on Figure 6 and Figure 7, it can be concluded that diving the whole granulator space in 3 compartments could be sufficient to achieve a sufficiently accurate model

compared to the *perfectly mixed* granulator ($N_z = 1$). The only disadvantage of discretizing the granulator in space is the increased computational time. As the value of N_z increases, i.e., as the number of compartments in the granulator increases, the computational time also increases. In particular, with a standard PC used for the simulation (i5 with 4 cores, 8 GB RAM and 2.1 GHz CPU), the computational time for one-compartment granulator was 0.5 s, and for the three-compartment granulator was 0.9 s (about 2 times more).

4.3 Simulation results for granulation in rotary drums

The granulation process in drum granulators is simulated using the CA scheme, as well as the NFV scheme. Similar to the spherodizers, the simulations have been performed for a multi-compartment drum granulator model and also with the *perfectly mixed* assumption. The mass based formulation of the PBE with particle diameter representing the size, is used to assess the PSD. The simulation results are also compared for a size-independent ($\beta = \beta_0$) and a size-dependent ($\beta = \beta_{ik}$) agglomeration kernel.

With the *perfectly mixed* assumption, i.e., for $N_z = 1$, the simulation results are depicted in Figure 8. As expected, the CA scheme and the NFV scheme produce similar results (d_{50} of the effluent) for both the size-independent and the size-dependent agglomeration kernels. Due to binary agglomeration, the particles grow in size. However, with the size-dependent agglomeration kernel, the d_{50} of the effluent is higher than with the size-independent constant kernel.

Simulation results for the multi-compartment drum granulator model are shown in Figure 9. Figure 9 compares the PSD of the influent, as well as PSDs of the effluents that correspond to each of the compartments of the granulator. Clearly, particles in the first compartment are smaller in size compared to the second and third compartments of the granulator. Particles increase in their sizes
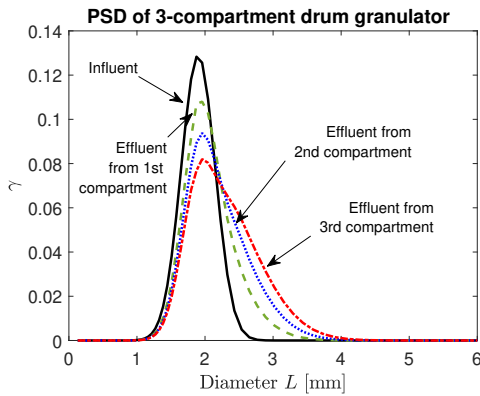
Figure 9. PSD for influent/effluent in 3-compartment drum granulator with the CA scheme.

as they are transported along the granulator, and as a result, the coarser fractions of the particles increase while their finer fractions decrease. The computational time is also compared for different choices of N_z as listed in Table 3. As expected, the computational time needed for solving the model increases with increasing the number of compartments in the drum granulator. This observation is valid with both the CA and the NFV schemes used to solve the model, and for both types of agglomeration kernels. However, inclusion of the size-dependent agglomeration kernel increase the computational time significantly: it takes almost twice the time to obtain the solution with size-dependent agglomeration kernel ($\beta = \beta_{ik}$) compared to the size-independent kernel $\beta = \beta_0$.

5 Conclusions

In this paper, the population balance equations for the spherodizer and the rotary drum granulator were developed. To account for property inhomogeneity in the granulators, multi-compartment models of the granulators were also developed. The simulation results showed that the discretization of the external coordinate (axial length of the granulator) in the model, introduces a transport (time) delay from the inlet of the granulator to its outlet. Inclusion of the correct transport delay is important for control studies. However, the ability of the model to capture transport delay inside the granulator comes with the cost of increased computational time. Two different discretization schemes, namely Kumar's new finite volume scheme and the cell average scheme showed similar simulation results in terms of the model solution accuracy and computational time. Model solution was obtained relatively fast for both simulation scenarios: with the constant agglomeration kernel and with the size-dependent agglomeration kernel. Thus, the developed models and model solution techniques can be used for further control-relevant studies.

6 Acknowledgment

References

I.T. Cameron, F.Y. Wang, C.D. Immanuel, and F. Stepanek. Process systems modelling and applications in granulation: A review. *Chemical Engineering Science*, 60(14):3723–3750, 2005.

L. Forestier and S. Mancini. A finite volume preserving scheme on nonuniform meshes and for multidimensional coalescence. *SIAM Journal of Scientific Computing*, 34(6), 2012. doi:10.1137/110847998.

C. Herce, A. Gil, M. Gil, and C. Cortés. A cape-taguchi combined method to optimize a npk fertilizer plant including population balance modeling of granulation-drying rotary drum reactor. In *Computer Aided Chemical Engineering*, volume 40, pages 49–54. Elsevier, 2017.

PC Kapur. Kinetics of granulation by non-random coalescence mechanism. *Chemical Engineering Science*, 27(10):1863–1869, 1972.

B. Koren. A robust upwind discretization method for advection, diffusion and source terms. In C. B. Vreugdenhil and B. Koren, editors, *Numerical Methods for Advection-Diffusion Problems, Notes on Numerical Fluid Mechanics*, pages 117–138. 1993.

J. Kumar. *Numerical approximations of population balance equations in particulate systems*. PhD thesis, Otto-von-Guericke-Universität Magdeburg, Universitätsbibliothek, 2006.

J. Kumar, M. Peglow, G. Warnecke, S. Heinrich, and L. Mörl. Improved accuracy and convergence of discretized population balance for aggregation: The cell average technique. *Chemical Engineering Science*, 61(10):3327–3342, 2006.

J. Kumar, G. Kaur, and E. Tsotsas. An accurate and efficient discrete formulation of aggregation population balance equation. *Kinetic & Related Models*, 9(2), 2016.

J. Litster and B. Ennis. *The science and engineering of granulation processes*, volume 15. Springer Science & Business Media, 2004.

MATLAB. 2017a. The MathWorks, Inc., Natick, Massachusetts, United States., 2017.

R. Ramachandran, C.D. Immanuel, F. Stepanek, J.D. Litster, and F.J. Doyle III. A mechanistic model for breakage in population balances of granulation: Theoretical kernel development and experimental validation. *Chemical Engineering Research and Design*, 87(4):598–614, 2009.

D. Ramkrishna. *Population balances: Theory and applications to particulate systems in engineering*. Academic press, 2000.

G. Valiulis and R. Simutis. Particle growth modelling and simulation in drum granulator-dryer. *Information Technology and Control*, 38(2), 2009.

L. Vesjolaja, B. Glemmestad, and B. Lie. Population balance modelling for fertilizer granulation process. *Proceedings of The 59th Conference on Simulation and Modelling (SIMS 59), 26-28 September 2018, Oslo Metropolitan University, Norway*, 2018.

F.Y. Wang, X.Y. Ge, N. Balliu, and I.T. Cameron. Optimal control and operation of drum granulation processes. *Chemical Engineering Science*, 61(1):257–267, 2006.

Paper D

Dynamic model for simulating transient behaviour of rotary drum granulation loop

Dynamic model for simulating transient behaviour of rotary drum granulation loop

L. Vesjolaja[1]   B. Glemmestad[2]   B. Lie[1]

[1]*Department of Electrical Engineering, IT and Cybernetics, University of South-Eastern Norway.
E-mail:* {*ludmila.vesjolaja, bernt.lie*}*@usn.no*

[2]*Process Modeling and Control Department, Yara Technology Center, Norway. E-mail:bjorn.glemmestad@yara.com*

Abstract

In this paper, a dynamic model for a rotary drum granulation loop with external product separator is developed. A population balance is used to capture dynamic particle size distribution in the 3-compartment rotary drum granulator model. Particle agglomeration along with particle growth due to layering are assumed as granulation mechanisms in the rotary drum. The model of the granulation loop includes models of the drum, screens and a crusher. Simulations using the developed model provide valuable data on dynamic fluctuations in the inlet and the outlet particle size distribution for the rotary drum. Simulation results showed that at smaller crusher gap spacings, the instabilities of the drum granulation loop occur, and damped oscillations are observed. Above the critical crusher gap spacing, sustained periodic oscillations are observed. The reason for oscillations is the off-spec particle flow that is recycled back to the granulator.

Keywords: granulation loop; population balance; layering; agglomeration

1 Introduction

Granulation processes are used in a wide range of industrial applications, such as those in pharmaceutical and fertilizer industries (Litster and Ennis, 2004). This paper is focused on the last part of NPK (Nitrogen, Phosphorus, Potassium) fertilizer production. A granulation loop is used to produce different grades, i.e., various N:P:K ratios, of fertilizers. The NPK fertilizer is a high value type of fertilizer containing the three main elements essential for crop nutrition. Various NPK grades are specially developed for different crops growing in different climates and soils. Fertilizer manufacturing using the granulation process has received considerable research interest during the last few decades, due to (i) the increasing requirements for efficient production of high quality fertilizers for increased food production in a growing global population, (ii) difficult process control and operation, e.g.,

among others Bück et al. (2016); Ramachandran and Chaudhury (2012); Herce et al. (2017); Ramachandran et al. (2009); Valiulis and Simutis (2009); Wang et al. (2006) and Cameron et al. (2005) have focused their research on granulation processes. The granulation loop studied in this paper consists of a rotary drum granulator, a granule classifier (screens), and a roll crusher. A typical schematic of a granulation process with a recycle loop is shown in Figure 1. Rotary drums as granulation units are frequently used in fertilizer industries due to the ability of rotary drums to handle large amount of material.

During the granulation process, a slurry of liquid ammonium nitrate and partly dissolved minerals is solidified to form granules. Granules that are too small (under-sized particles) are recycled to the granulation unit and granules that are too large (over-sized particles) are first crushed and then recycled back to the granulator. The recycle feed is an integral part of the
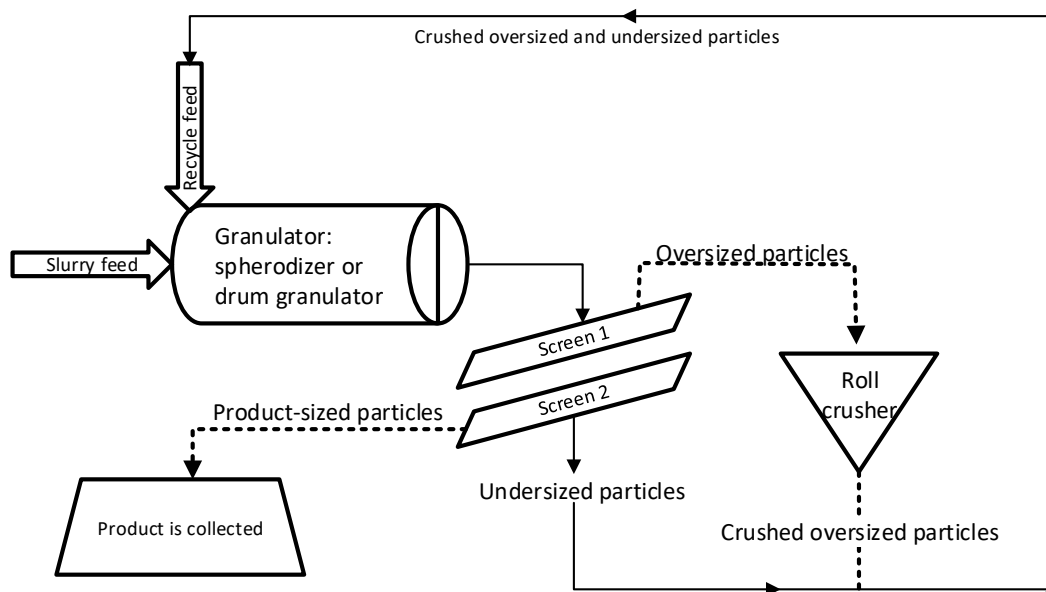
Figure 1: Schematic diagram of granulation loop.

granulation process. The recycle feed flow rate as well as its particle size distribution (PSD) are important for proper process operation. The recycle of off-spec (under-sized and over-sized) particles is needed to seed the granulator. Another reason to recycle the feed is a wide PSD of the granules at the granulator discharge. Typically, the PSD of the granules leaving the granulator is wider compared to the required PSD of the final product. In addition, the off-spec granules cannot be considered as a waste material, and must be recycled from an economic and environmental point of view. Unfortunately, for some granulation technologies, the amount of the recycled material is large. A typical recycle ratio in granulation plants is 4:1. This implies a high ratio between the off-spec particles ($\sim 80\%$) and the required product size particles ($\sim 20\%$).

Process control of granulation loops is challenging. Granulation loops may show oscillatory behavior for certain operating points. Instability is linked to the entire granulation loop, since the granulator receives as input a fluctuating recycled stream. Similar oscillations in granulation loop are reported in Drechsler et al. (2005) and Radichkov et al. (2006); the authors have analyzed granulation loop dynamics for fluidized bed granulators. Particle size change in fluidized beds has been assumed to be caused by particle layering and attrition mechanisms. Particle agglomeration is neglected in Drechsler et al. (2005) and Radichkov et al. (2006).

The contributions of this paper are (i) proposing a control relevant model of the granulation loop with a rotary drum granulator, (ii) including both particle agglomeration and particle growth by layering in the rotary drum model by using a population balance equation, (iii) developing a 3-compartment rotary drum model for simulations of granulation loop, and (iv) analyzing and suggesting possible improvements for stability of the drum granulation loop.

The paper is organized as follows: In Section 2, a mathematical model of a granulation loop, including models of a rotary drum, screens, and a crusher, is given. In Section 3, the numerical solution methods for the developed model are provided. Simulation setup, results, and discussions are given in Section 4, while conclusions are drawn in Section 5.

2 Model development

2.1 Model for granulator

In this study, population balance principles have been used to develop a mathematical model of a granulator suitable for control purposes. Population balance (PB) is frequently used to describe dynamics of particle property distributions. In the granulator model, a mass based population balance equation (PBE) with particle diameter as the internal coordinate is used. This choice of PBE is made because the PSD in a real
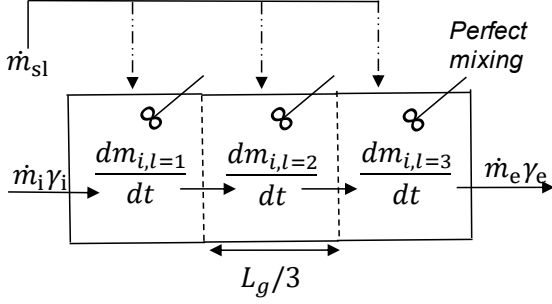
Figure 2: Multi-compartment rotary drum model.

plant is typically measured by sieving and weighting. The general form of a mass based PBE with particle diameter (L) as the internal coordinate, spatial variation (z) as the external coordinate, and time coordinate (t) is represented as

$$\frac{\partial m(L,z,t)}{\partial t} = -L^3 \frac{\partial}{\partial L}\left[G\frac{m(L,z,t)}{L^3}\right] + B(L,z,t)$$
$$- D(L,z,t) - \frac{\partial}{\partial z}\left[\frac{dz}{dt}m(L,z,t)\right], \quad (1)$$

where $m(L,z,t)$ is the mass density function, L is the particle diameter, G is the particle growth rate, B is the particle birth rate, and D is the particle death rate (Ramkrishna, 2000). The first term on the right hand side represents the particle growth due to layering, the second and third terms stand for particle birth and death, respectively, due to agglomeration, and the last term represents a continuous process and gives the flow of particles through the granulator. Equation 1 is derived by assuming that all particles are ideal spheres with a constant solid density.

Particle growth due to layering (G) is a continuous process during which particle growth occurs by successive coating of a liquid phase onto a granule (Litster and Ennis, 2004; Iveson et al., 2001). In a given case, a fresh fertilizer melt (slurry) is added to the rotary drum to ensure particle growth. As a result, the particle mass grows, and the volume increases, but the number of particles in the system remains unchanged. Assuming a size-independent linear growth (Mörl, 1981; Mörl et al., 1977), i.e., assuming that each granule has the same exposure to a slurry material, the layering term is modeled as

$$G = \frac{2\dot{m}_{sl}(1 - X_{sl,i})}{\rho A_{p,tot}}, \quad (2)$$

$$A_{p,tot} = \pi m \int_{L=0}^{L=\infty} L^2 dL. \quad (3)$$

Here, m is the mass of the particles, $\dot{m}_{sl}$ is the slurry flow rate, $X_{sl,i}$ is the moisture fraction in the slurry, and $A_{p,tot}$ is the total surface area of the particles as given by Equation 3.

In rotary drum granulators, particle collision cannot be avoided, and thus should be included in the model. In this paper, for simplicity, binary particle agglomeration is assumed. Binary agglomeration refers to a granulation mechanism that occurs due to successful collision of two particles, resulting in the formation of a larger, composite particle. Agglomeration is a discrete (sudden) process event that changes the total number of particles: two particles *die*, and a new particle is *born* as a result of collision of two particles. Thus, the agglomeration results in a reduction of the total number of particles, while the total mass remains conserved (Litster and Ennis, 2004; Iveson et al., 2001). Here, the particle birth (B) and death (D) due to binary agglomeration are modeled using Hulburt and Katz' formulation (Hulburt and Katz, 1964). The B and D terms in Equation 1 are modeled using Equation 4 and 5, respectively.

$$B = \frac{L^2}{2} \cdot$$
$$\int_0^L \frac{\beta\left(\left(L^3 - \lambda^3\right)^{\frac{1}{3}}, \lambda, t\right) \cdot m\left(\left(L^3 - \lambda^3\right)^{\frac{1}{3}}, t\right) \cdot m(\lambda, t)}{\left(L^3 - \lambda^3\right)^{\frac{2}{3}}} \cdot$$
$$d\lambda, \quad (4)$$

$$D = m(L,t)\int_0^\infty \beta(L,\lambda)m(\lambda,t)\,d\lambda. \quad (5)$$

Here, the B term represents the particle birth of diameter L, while the D term represents the disappearance (death) of particle of diameter L, and β is the agglomeration rate (kernel) that defines the collision frequency of the two particles with diameters λ and $L - \lambda$. In this paper, the agglomeration kernel is defined using the Kapur agglomeration kernel model (Kapur, 1972) by taking $a = 2$ and $b = 1$:

$$\beta = \left(\frac{6}{\pi}\right)^{\frac{2}{3}}\frac{1}{\rho}\beta_0\beta_{jk}, \quad (6)$$

where the term $\left(\frac{6}{\pi}\right)^{\frac{2}{3}}\frac{1}{\rho}$ arises during the conversion from a number-based formulation to the mass-based formulation of PBEs, β_0 is the particle size independent part of the agglomeration kernel, and β_{jk} is the particle size dependent part of the agglomeration kernel as shown in Equation 7.

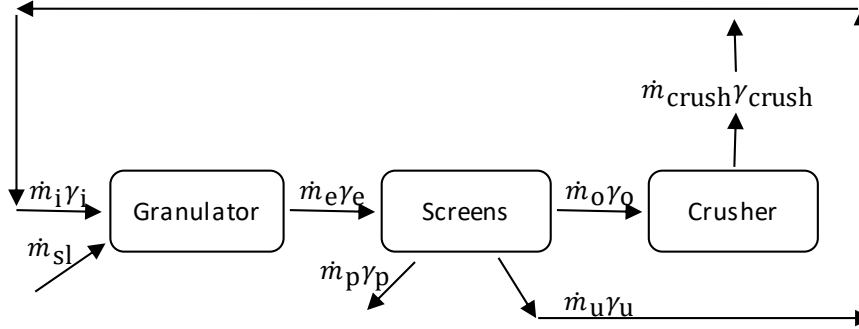$$\beta_{jk} = \frac{(L_j + L_k)^2}{L_j L_k}. \quad (7)$$

Figure 3: Simplified flow diagram of the drum granulation loop. Here,$\dot{m}_\mathrm{sl}$ is the slurry flow rate, $\dot{m}_\mathrm{i}$, $\dot{m}_\mathrm{e}$, $\dot{m}_\mathrm{o}$, $\dot{m}_\mathrm{u}$, $\dot{m}_\mathrm{p}$, $\dot{m}_\mathrm{crush}$ are the mass flow rates of influent, effluent, over-sized, under-sized, product-sized and crushed particles respectively. The corresponding distribution functions of the influent, effluent, over-sized, under-sized, product-sized and crushed particles particles are denoted with γ_i, γ_e, γ_o, γ_u, and γ_p, γ_crush, respectively.

The effluent from the granulator is calculated by assuming a 3-compartment granulator model. For this, the length of the granulator L_g is divided into 3 equally sized sections (compartments) which are numbered by $l \in \{1, 2, 3\}$, as shown in Figure 2. In each of the compartments the concept of *perfect mixing* is assumed. The influent to the granulator (recycled particles), $\dot{m}_\mathrm{i}$, enters the 1st compartment and the effluent, $\dot{m}_\mathrm{e}$, leaves the granulator from the 3rd (last) compartment. The particle velocity is assumed constant in all three compartments and is calculated as

$$\frac{dz}{dt} = \frac{L_\mathrm{g}}{\tau}, \tag{8}$$

where τ is the particle retention (residence) time in the granulator.

2.2 Model for upper and lower screen

The mass flow rates out from the screens are described using probability function P_upp and P_low from Molerus and Hoffmann (1969). If P is the probability with which particles remain lying on the screen (do not pass the screen) and $(1 - P)$ is the probability with which particles pass through the screen, then the mass flow rates from the screen are calculated as

$$\dot{m}_\mathrm{o}\gamma_\mathrm{o} = P_\mathrm{upp}\dot{m}_\mathrm{e}\gamma_\mathrm{e}, \tag{9}$$

$$\dot{m}_\mathrm{u}\gamma_\mathrm{u} = (1 - P_\mathrm{upp})(1 - P_\mathrm{low})\dot{m}_\mathrm{e}\gamma_\mathrm{e}, \tag{10}$$

$$\dot{m}_\mathrm{p}\gamma_\mathrm{p} = (1 - P_\mathrm{upp})P_\mathrm{low}\dot{m}_\mathrm{e}\gamma_\mathrm{e}. \tag{11}$$

Here, $\dot{m}_\mathrm{o}$, $\dot{m}_\mathrm{u}$, $\dot{m}_\mathrm{p}$ are the mass flow rates of over-sized, under-sized, and product-sized particles, respectively. The corresponding distribution functions of the over-sized, under-sized, and product-sized particles are denoted with γ_o, γ_u, and γ_p, respectively. The screening probability functions P_upp and P_low defined by Molerus and Hoffmann (1969) and also given in Heinrich et al. (2003) are calculated using Equation 12 and 13.

$$P_\mathrm{upp} = \frac{1}{1 + \left(\frac{L_\mathrm{m,\,upp}}{L}\right)^2 \exp\left(K_\mathrm{eff,\,upp}\left(1 - \left(\frac{L}{L_\mathrm{m,\,upp}}\right)^2\right)\right)}, \tag{12}$$

and

$$P_\mathrm{low} = \frac{1}{1 + \left(\frac{L_\mathrm{m,low}}{L}\right)^2 \exp\left(K_\mathrm{eff,low}\left(1 - \left(\frac{L}{L_\mathrm{m,low}}\right)^2\right)\right)}, \tag{13}$$

where L_m is the mesh size of the screen (sieve diameter), L is the particle diameter, and K_eff is the screen separation efficiency.

2.3 Model for crusher

A mathematical model of the crusher represents the distribution function (Equation 14) that re-distributes the total over-sized mass flow ($\dot{m}_\mathrm{o}\gamma_\mathrm{o}$) with the new distribution function γ_crush. This distribution function γ_crush reassigns the net over-sized flow rate to lower sized classes. Having a crusher gap spacing and a standard deviation as design choices, the crusher distribu-

tion function is defined as

$$\gamma_{\text{crush}} = \frac{1}{\sqrt{2\pi\sigma_{\text{crush}}^2}} \exp(-\frac{(L - L_{\text{crush}})^2}{2\sigma_{\text{crush}}^2}). \qquad (14)$$

Here, σ_{crush} is the standard deviation, and L_{crush} is the crusher diameter, which is the mean size of the crushed particle distribution such that $L_{\text{crush}} > 0$. In addition, L is bounded, $0 < L \leq L_{\text{max}}$. For proper choice of σ_{crush}, L_{crush} and L, $\gamma_{\text{crush}} \geq 0$. The total over-sized particle flow rate is then calculated as

$$\dot{m}_{\text{crush}}\gamma_{\text{crush}} = \left(\sum \dot{m}_{\text{o}}\gamma_{\text{o}}\right) \cdot \gamma_{\text{crush}}. \qquad (15)$$

The mass flow rate that is recycled back to the granulator, i.e., the mass flow of the off-spec particles, is given as

$$\dot{m}_{\text{i}}\gamma_{\text{i}} = \dot{m}_{\text{crush}}\gamma_{\text{crush}} + \dot{m}_{\text{u}}\gamma_{\text{u}}. \qquad (16)$$

The overall balance scheme for the drum granulation loop is given in Figure 3.

3 Model solution

The solution to PBEs is found by transforming the partial differential equation (PDE) into a system of ordinary differential equations (ODEs) that further can be solved using an appropriate time integrator. The PDEs for PBE are discretized in terms of the internal coordinate, i.e., particle diameter, and also in terms of the external coordinate, i.e., the length of the drum granulator. The discretization is 2-dimensional. For the internal coordinate discretization, particles are classified into N_i particle classes using a linear grid and are numbered by $i \in \{1, 2, ...N_i\}$. On the other hand, for the external coordinate discretization, the granulator length in axial direction is divided into l equally sized compartments (sections) and are numbered by $l \in \{1, 2, 3\}$.

Numerical solution for the layering term $L^3 \frac{\partial}{\partial L}\left[G\frac{m(L,z,t)}{L^3}\right]$ is found by applying a high resolution finite volume scheme. In particular, a finite volume scheme extended by a Koren flux limiter function is used to discretize the layering term in terms of its internal coordinate. The Koren flux limiter scheme is described in Koren (1993) and applied for granulation process in Vesjolaja et al. (2018).

Finding a sufficiently accurate solution for the agglomeration terms (Equation 4 and 5) is challenging. Agglomeration is a discrete event, and as shown by Equation 4 and 5, PB modeling of the agglomeration terms result in partial integro-differential equations. In this paper, approximation of the birth and death terms is performed by applying one of the sectional schemes. In particular, the cell average scheme that is introduced
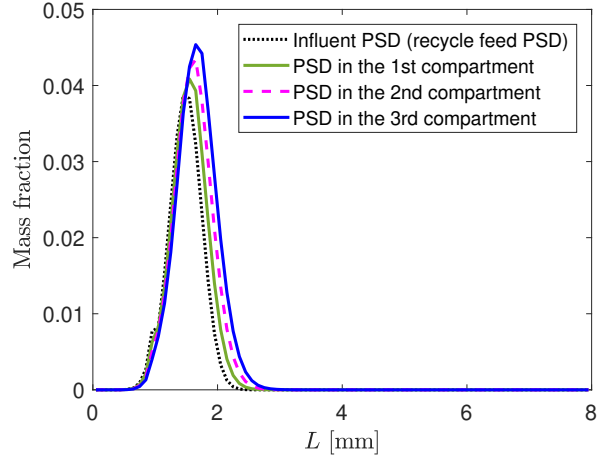
Figure 4: PSD in the 1st, 2nd and 3rd compartments of the 3-compartment granulator for $L_{\text{crush}} = 1.5$ mm.

by Kumar et al. (2006) is used to find a numerical solution. A detailed explanation of the cell average scheme is given in Kumar (2006). The cell average scheme has shown higher accuracy and faster solution compared to other frequently used sectional methods as the Hounslow scheme (Hounslow et al., 1988) and the Fixed Pivot scheme (Kumar and Ramkrishna, 1996).

In this paper, the proposed by Kumar et al. (2006) cell average scheme is re-formulated to give a numerical solution for a mass based PBE with the particle diameter as internal coordinate. To achieve this, the zeroth moment (total number of particles), and the third moment (total mass of particles) has been chosen to be conserved (compared to zeroth and first moments for volume based description, Kumar et al. (2006); Kumar (2006)). Mathematical expressions are reported in Vesjolaja et al. (2018).

Spatial discretization of the granulator length is performed by using a high resolution scheme with Koren flux limiter function (KFL). For this, the granulator is divided into N_z uniformly spaced compartments, and each compartment is assumed to be *perfectly mixed*. Integration of the particle flux term for N_z compartments gives

$$\frac{\partial}{\partial z}\left(\frac{dz}{dt}m_{i,z}\right) = w\frac{\partial}{\partial z}\left(m_{i,z}\right) = w\left[m_{i,z-\frac{1}{2}} - m_{i,z+\frac{1}{2}}\right], \qquad (17)$$

where $\frac{dz}{dt} = w$ is the particle velocity along the granulator and is assumed to be constant inside the granulator. The approximation of the terms $m_{i,z\pm\frac{1}{2}}$ is then performed using a KFL scheme (Koren, 1993). The approximation of the terms $m_{i,z\pm\frac{1}{2}}$ using the KFL scheme

is given by Equation 18 and Equation 19.

$$m_{i,z-\frac{1}{2}} \approx \frac{1}{\Delta z} \left\{ \frac{M_{i,z-1}}{L_i} + \frac{1}{2}\phi\left(\theta_{i-\frac{1}{2}}\right) \right. \\ \left. \times \left(\frac{M_{i,z-1}}{L_i^3} - \frac{M_{i,z-2}}{L_i^3}\right) \right\}, \quad (18)$$

$$m_{i,z+\frac{1}{2}} \approx \frac{1}{\Delta z} \left\{ \frac{M_{i,z}}{L_i} + \frac{1}{2}\phi\left(\theta_{i-\frac{1}{2}}\right) \right. \\ \left. \times \left(\frac{M_{i,z}}{L_i^3} - \frac{M_{i,z-1}}{L_i^3}\right) \right\}, \quad (19)$$

where, M_i is the total mass of the particle in the ith class and $\Delta z = \frac{L_g}{N_z}$ is the length of the each section in the granulator (Figure 2). The limiter function ϕ in Equation 18 and Equation 19 is defined as

$$\phi\left(\theta\right) = \max\left[0, \min\left(2\theta, \min\left(\frac{1}{3} + \frac{2\theta}{3}, 2\right)\right)\right], \quad (20)$$

and parameter θ is defined as

$$\theta_{i-\frac{1}{2}} = \frac{\frac{M_{i,z}}{L_i^3} - \frac{M_{i,z-1}}{L_i^3} + \varepsilon}{\frac{M_{i,z-1}}{L_i^3} - \frac{M_{i,z-2}}{L_i^3} + \varepsilon}, \quad \theta_{i+\frac{1}{2}} = \frac{\frac{M_{i,z+1}}{L_i^3} - \frac{M_{i,z}}{L_i^3} + \varepsilon}{\frac{M_{i,z}}{L_i^3} - \frac{M_{i,z-1}}{L_i^3} + \varepsilon}. \quad (21)$$

The constant ε is a very small number to avoid division by zero, e.g. $\varepsilon = 10^{-8}$.

Figure 5: d_{50} of the influent/effluent as a response to the step-by-step change of the crusher gap $L_{\text{crush}} = 1.5 \to 1.4 \to 1.3 \to 1.2 \to 1.1$ mm.

4 Simulation Results and Discussion

4.1 Simulation Setup

The numerical solution of PBE described by Equation 1 is found by applying the Koren flux limiter scheme and the cell average schemes as discussed in Section 3. Particles are classified into 80 size classes and the drum length is divided into 3 equally sized compartments. Thus, the PDE represented by Equation 1 is transformed into a set of 240 ODEs which are further solved using a 4-th order Runge-Kutta method with fixed time step. Dynamic simulations are performed using MATLAB and Simulink (MATLAB, 2017a). The parameters used to simulate the drum granulation loop process are listed in Table 1.

Initialization of the mass distribution function inside the granulator is performed using a Gaussian normal distribution function given by Equation 14. For comparison of simulation results, the evolution of the average size of the particles is represented by their d_{50} diameter (median diameter that corresponds to intercept for 50% of cumulative mass).

Table 1: Simulation parameters.

Parameter	Value
Range of L [mm]	0-8
Number of particle classes	80
Length of granulator [m]	10
Number of compartments	3
ρ [kg· m^{-3}]	1300
β_0 [s^{-1}]	$1.0 \cdot 10^{-13}$
τ [min]	10
$\dot{m}_{\text{sl,i}}$ [kg· h^{-1}]	100
$L_{\text{screen, upp}}$ [mm]	1.5
$L_{\text{screen, low}}$ [mm]	0.9
$K_{\text{eff, upp}}$	45
$K_{\text{eff, low}}$	45
L_{crush} [mm]	1.7-0.3
σ_{crush}	0.25
$X_{\text{sl,i}}$	0.05
Time step for RK4 [s]	20
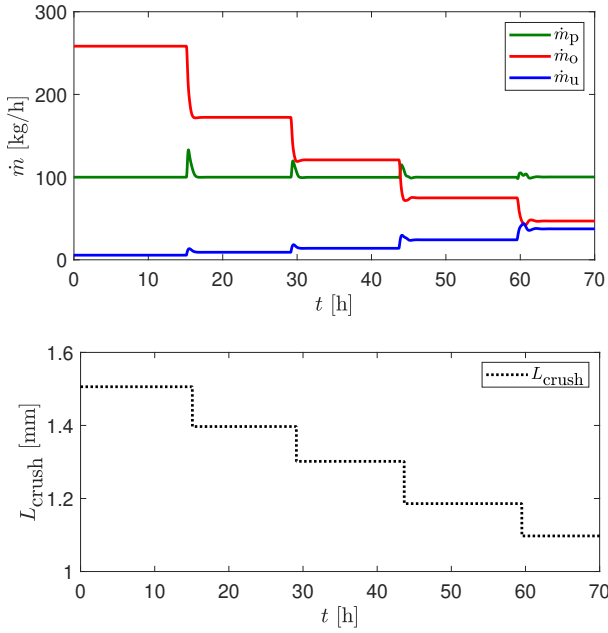
Figure 6: Mass flow rates of over-sized, product-sized and under-sized particles as a response to the step-by-step change of the crusher gap ($L_{\text{crush}} = 1.5 \rightarrow 1.4 \rightarrow 1.3 \rightarrow 1.2 \rightarrow 1.1$ mm).
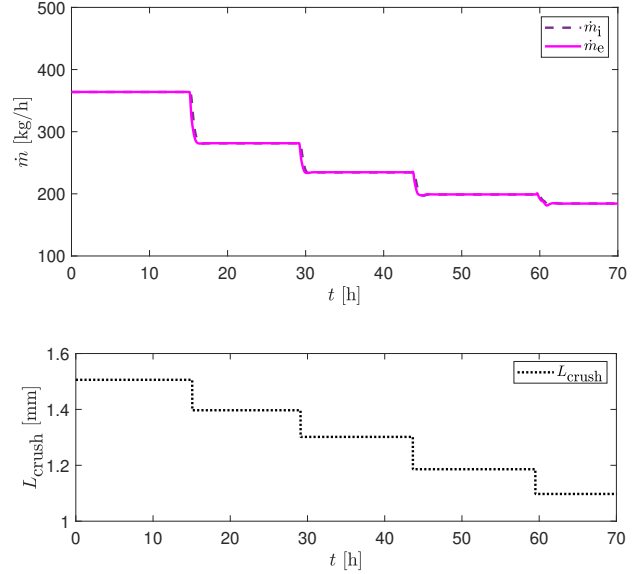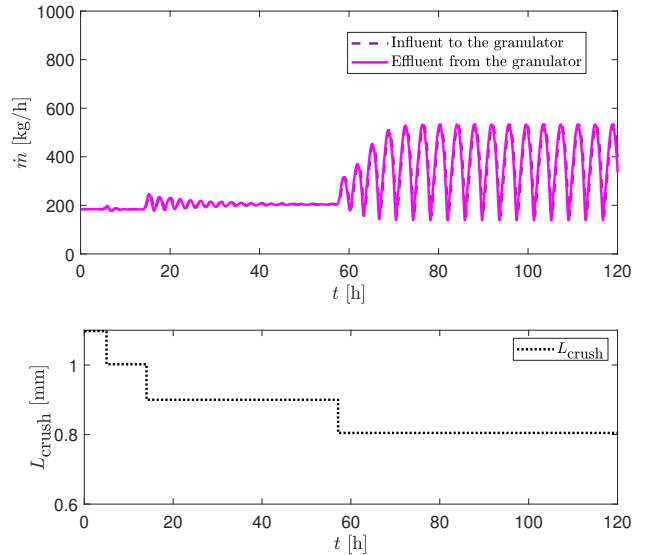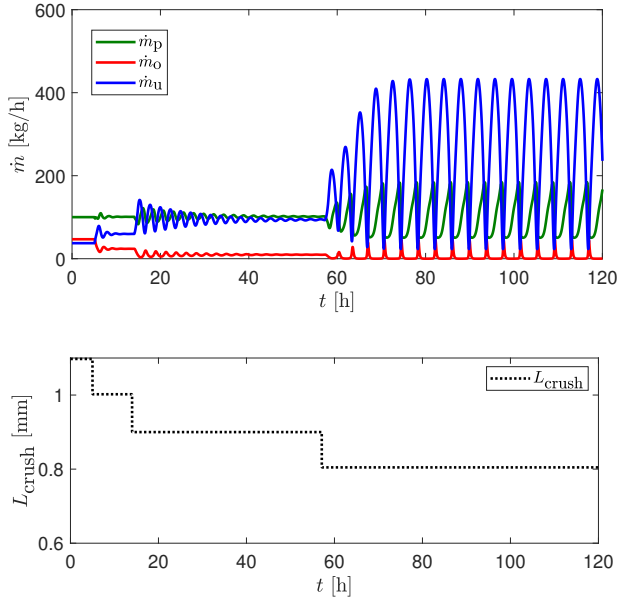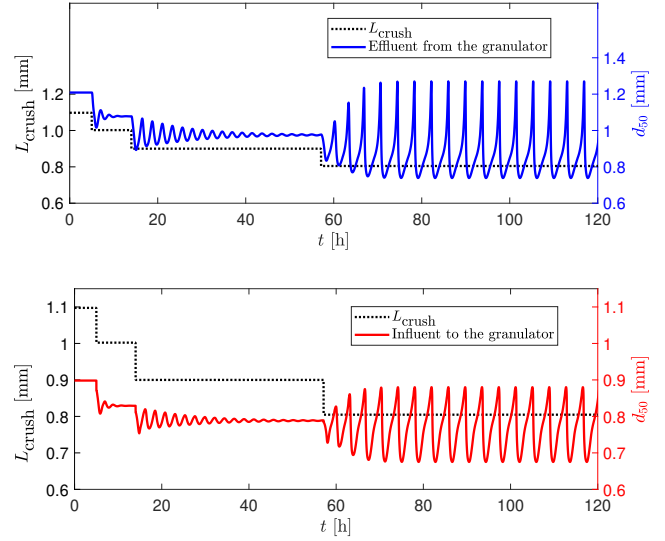

Figure 7: Total mass flow rates of the influent/effluent as a response to the step-by-step change of the crusher gap ($L_{\text{crush}} = 1.5 \rightarrow 1.4 \rightarrow 1.3 \rightarrow 1.2 \rightarrow 1.1$ mm).

4.2 Growth of particles inside the 3-compartment drum granulator

Simulations are performed by applying a 3-compartment drum granulation loop model. This is done to achieve (i) higher accuracy of the developed model, and thus to account for property inhomogeneity inside the granulator, and (ii) the developed granulation loop model will be further used in control studies where spatial discretization is significant to achieve proper system dynamics, e.g., to include some effect of time delay.

Figure 4 shows evolution of particle growth in 3 different compartments of the drum granulator. In the first compartment, particles begin to grow and to collide with each other. In the second compartment, further grow and collision of particles occur. This results in the larger amount of coarser particles in the second compartment of the drum granulator compared to the first one. As particles are transferred to the third compartment, the more time they spend in the granulator, and, thus, the more time they have to agglomerate and to grow. As a result, the third compartment contains the largest amount of coarser particles among all the 3 compartments. The PSD in the flow of the 3rd compartment corresponds to the PSD in the effluent flow from the granulator, that is further sent to screens to

Figure 8: Total mass flow rates of the influent/effluent as a response to the step-by-step change of the crusher gap ($L_{\text{crush}} = 1.1 \rightarrow 1.0 \rightarrow 0.9 \rightarrow 0.8$ mm).

71

Figure 9: Mass flow rates of over-sized, product-sized and under-sized particles as a response to the step-by-step change of the crusher gap ($L_{crush} = 1.1 \rightarrow 1.0 \rightarrow 0.9 \rightarrow 0.8$ mm).

Figure 10: d_{50} of the granulator influent/effluent as a response to a step-by-step change of the crusher gap ($L_{crush} = 1.1 \rightarrow 1.0 \rightarrow 0.9 \rightarrow 0.8$ mm).

separate the flow into the size fractions (under-sized, over-sized, and product-sized particle fractions).

4.3 Effect of crusher gap on granulation loop stability

The dynamic behavior of the granulation loop is inevitably connected with the crusher parameters. In particular, a crusher gap (also called mill grade) plays a significant role in understanding the dynamics of the granulation loop. As is shown in Figure 5, particles are growing inside the drum granulator, and as a result, the average diameter d_{50} of the particles leaving the granulator (effluent) is larger compared to the d_{50} of the particles that are sent to the granulator with the recycle feed (influent).

Stable granulation loop process is observed when a step-by-step change of $L_{crush} = 1.5 \rightarrow 1.4 \rightarrow 1.3 \rightarrow 1.2 \rightarrow 1.1$ mm are given to the system. This includes stable mass flow rates and d_{50}, for the main granulation loop units, i.e., granulator, screens, crusher (Figure 6 and 7). In particular, stable mass flow rates of both the product-sized particles, off-spec particles, as well as the total mass flow rates in and out of the drum granulator are observed.

Relatively high values of crusher gap spacings ($L_{crush} > 1.2$ mm) produce larger particles at the outlet of granulator, that therefore results in the higher
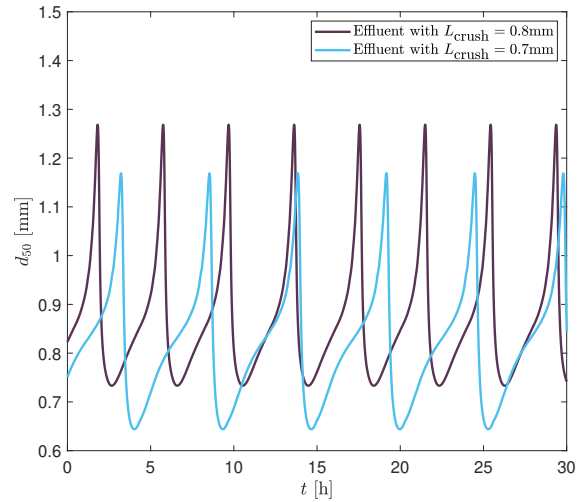
Figure 11: Sustained oscillations at $L_{crush} = 0.8$ mm versus at $L_{crush} = 0.7$ mm.
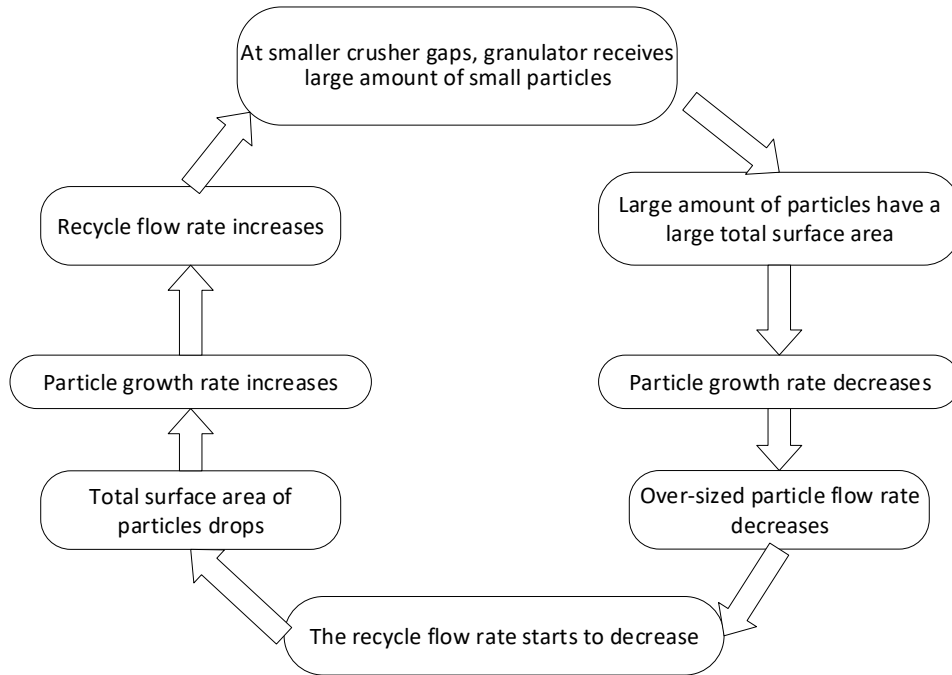
Figure 12: Explanation of the oscillations.

mass flow rate of the over-sized particles leaving the screens. As shown in Figure 6, at crusher gap spacing larger than 1.2 mm, the flow rate of over-sized particles are larger than the product-sized particles. This case is not desirable in industrial granulation plants since less of product is produced. However, over-sized particle flow contributes to the total recycle flow that acts as a seed to the granulator, and hence a larger over-sized fraction maintain the high flow rate of the influent to the drum granulator. Note that separation efficiency K_{eff} of lower and upper screens are set to $\sim 45\%$ that lead to the appearance of the under-sized particles at $L_{\text{crush}} \leq 1.2$ mm. The screen efficiency of $\sim 45\%$ is applied in simulations to achieve higher accuracy of the mathematical model with the real plant operation. In the plant, performance of the screens are *not ideal*, i.e., the under-sized-particles may remain on the upper screen with the over-sized particles and, vice versa, larger particles (e.g., product-sized) may occur in the under-sized fraction. As expected, the smaller the crusher gap is, the smaller is the recycle feed, and the flow of the effluent from the granulator (Figure 7). At smaller crusher gaps, more of the product is produced, and thus, more of particles are collected and taken out from the drum granulation loop.

A decrease in the crusher gap spacing from 1.1 mm to 1.0 mm introduces some damped oscillations in the

process (Figure 8, 9 and 10 at simulation time $t \lessapprox 10$ h). At the latter crusher gap spacing, more of fine particles are produced, as a result of which the mass flow rate of under-sized particles increases (Figure 9), and d_{50} in the recycle feed starts to fluctuate (Figure 10). Consequently, d_{50} of the effluent from the granulator also starts to fluctuate. These fluctuations are not sustained (see simulation time $t \lessapprox 10$ h) and quickly the system reaches stable steady state. As the crusher gap is reduced, more of the under-sized particles are formed, and the amplitude of fluctuations increases. Damped oscillations are observed at 0.9 mm crusher gap when the granulation loop produces similar amount of product as the under-sized particles (see simulation time $t \approx 18$ h). These damped oscillations are seen both in the mass flow rates, as well as in the d_{50} of the granulator influent and effluent. A further step change of L_{crush} to 0.8 mm gives a rise in the amplitude of the oscillations, and consequently, sustained oscillations are observed (see simulation time $t \gtrapprox 58$ h).

Interestingly, the period of oscillations changes as crusher gap is changed. In Figure 11, a close look at sustained oscillations for 0.8 mm and 0.7 mm crusher is shown. The period of the sustained oscillations is larger in the case of 0.7 mm crusher gap compared to the case of 0.8 mm crusher gap. Periodic oscillations in

73
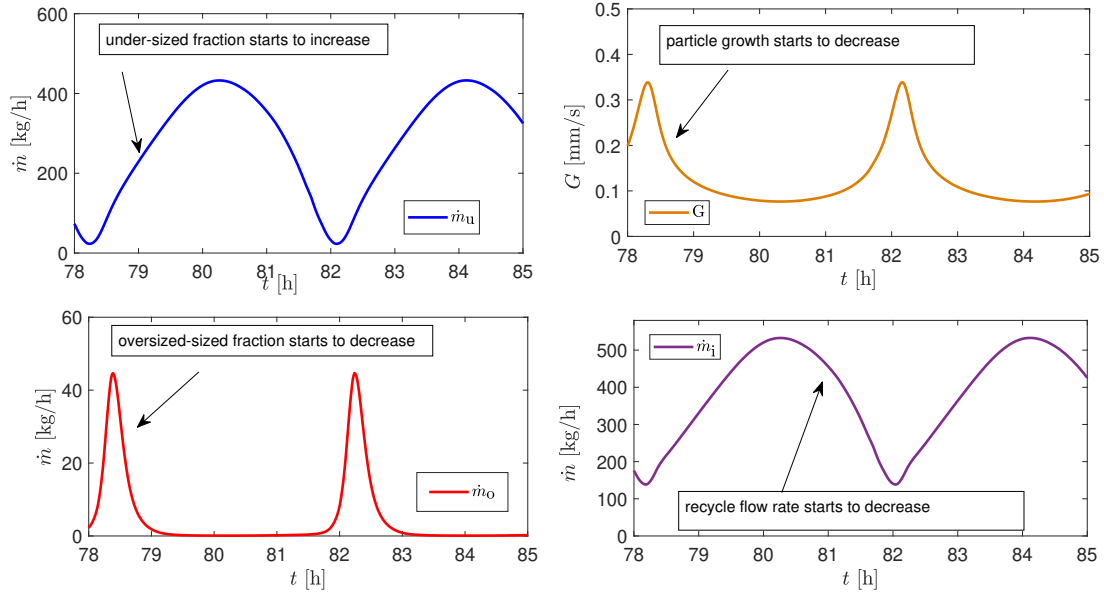
Figure 13: Zoomed oscillations in the process variables.

the granulation loop process can be explained by the recycle stream that is fed back to the granulator. Or, more precisely, with the large amount of fine (under-sized) particles that constitute to a large total surface area of particles in the granulator (Figure 12). For illustration, consider the following numerical example. Assume that there is one particle (sphere) with radius of $r_1 = 1$ mm. This particle will have a volume V_1 and a surface area A_1 as follows:

$$V_1 = \frac{4}{3}\pi r_1^3 = 4.1888e - 09 \qquad (22)$$

$$A_1 = 4\pi r_1^2 = 1.2566e - 05. \qquad (23)$$

Next, assume that this single particle is crushed into smaller particles of radius $r_2 = \frac{1}{2}r_1$. The volume V_2 and area A_2 of one such smaller particle is

$$V_2 = \frac{4}{3}\pi r_2^3 = 5.2360e - 10 = \frac{1}{8}V_1 \qquad (24)$$

$$A_2 = 4\pi r_2^2 = 3.1416e - 06 = \frac{1}{4}A_1. \qquad (25)$$

Therefore, for the same volume as the single large particle there will be 8 smaller particles. These 8 smaller particles will have the double surface area compared to the single particle, since $\frac{8}{4}A_1 = 2A_1$

When $L_{\text{crush}} \leq 0.9$ mm, the crusher produces a relatively large amount of crushed fine particles. These fine particles are then combined with the under-sized particles to form the recycle feed. Thus, the recycle feed contains a large amount of fine particles that have

a large surface area. The recycle feed containing large amount of fines is then fed back to the rotary drum. Inside the drum, for the large amount of fine particles with large surface area, the particle growth rate reduces (for a constant supply of the slurry) and the amount of over-sized particle fraction rapidly drops. On the other hand, this rapid drop in the mass flow rate of the over-sized particle fraction leads to a decrease in the total flow rate of the recycle feed (product-sized flow rate, which is not fed back, increases). Due to a lower flow rate of the recycle feed, the drum granulator receives less amount of fine particles per unit time, and consequently, the particle growth rate increases again. This increased particle growth rate results in the beginning of the new cycle of the periodic behavior. In Figure 13, a zoomed region of oscillations is shown. An increase in the under-sized mass flow rate results in a decrease in the growth rate of particles. The decrease in particle rate, in turn, results in the decrease of the over-sized mass flow rate. As a consequence the recycle feed decreases.

4.4 Effect of slurry feed on granulation loop stability

As discussed in Section 4.3, the high total surface area of large amount of fine particles limits the growth rate of particles. Consequently, particles do not grow sufficiently fast to form large particles. Thus, by increasing the slurry feed, the process might become more stable. To illustrate this, simulations are also performed with
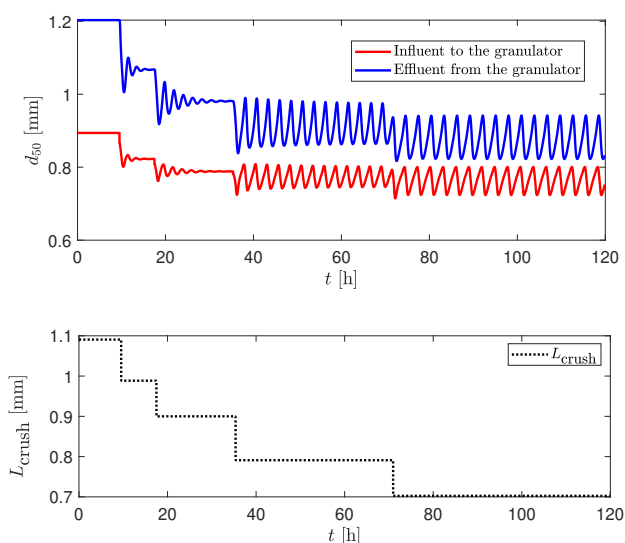
Figure 14: d_{50} as a response to the step-by step change of L_{crush} with $\dot{m}_{slurry} = 500$ kg/h.

the increased slurry flow rate.

Simulation results show that an increase in the mass flow rate of slurry improve the stability of the process (Figure 14 and 15). Periodic oscillations with the increased slurry flow rate appear at smaller crusher gap compared to the simulation results with the original value of the slurry flow rate. When the slurry feed $\dot{m}_{sl}$ is increased to 500 kg/h (Figure 14), significantly less oscillations (more damped oscillations) are observed at $L_{crush} \leq 0.8$ mm compared to the original case with $\dot{m}_{sl} = 100$kg/h (Figure 10).

Simulations with $\dot{m}_{sl} = 1000$ kg/h (Figure 15) show even more stable process having only a few fluctuations even at very small crusher gaps of 0.5 mm. Typically, for granulation plants, it is important to maintain a constant solid-to-liquid ratio. The constant solid-to-liquid ratio assures product quality requirements, e.g., moisture content, dustiness, flow-ability, etc., and thus, slurry feed is usually kept constant and is not changed during the operation. In addition, increased slurry feed may result in over-wetting of the particles, i.e., particles will not stick together and will not grow. Consequently, for stable granulation loop operation, at least the crusher gap spacing should be monitored systematically.

5 Conclusions

A dynamic model for rotary drum granulation loop is presented in this paper. For the analysis of dynamic behavior, a mass based population balance equation using particle diameter as the internal coordinate and granulator length as the external coordinate is developed. The drum granulation loop model is able to capture two granulation mechanisms: particle growth due to layering and particle size change due to binary agglomeration. Simulation results of a granulation loop having a 3-compartment rotary drum model show that the crusher gap spacing has a significant influence on the overall stability of the granulation loop. At larger crusher gap spacings, a stable granulation process is observed. However, as the crusher gap spacing is reduced, the granulation loop starts to show oscillatory behavior, and at a certain reduced crusher gap spacing, sustained periodic oscillations occur. The reason of the occurring oscillations is the off-spec particle flow that is recycled to the granulator and acts as nuclei for the new granule generation. At smaller crusher gap spacings, the granulator receives large amount of fines with the recycle feed. In the granulator, large amount of fines have a large total particle surface that slows down the particle growth. Thus, the growth rate and d_{50} of particles decreases. On the other hand, slower growth rate contributes to the rapid drop in the production of coarse (over-sized) particles, that in turn, reduce the total recycle feed to the granulator. As a result, the granulator receives smaller amount of fine particles that now have smaller particle total surface area. Thus, the growth rate and d_{50} of particles again increases and gives the start of the new cycle of periodic oscillations. To illustrate the effect of deficiency of slurry feed on the total granulation loop stability, simulations are also performed with the increased slurry feed. These simulation results show that increased slurry feed has a positive effect on overall stability of the loop. The higher the flow rate of slurry is, the less oscillations occur. However, the increased slurry feed may result in over-wetting of the particles, and as a result the particles will not stick to each other (agglomerate). Therefore, crusher gap and slurry feed influence the stability of the granulation loop, and both should be properly controlled during granulation loop operation. The developed dynamic granulation loop model in this study can be further used to develop control strategies for granulation loops applicable to different configurations of such loops.

Acknowledgments
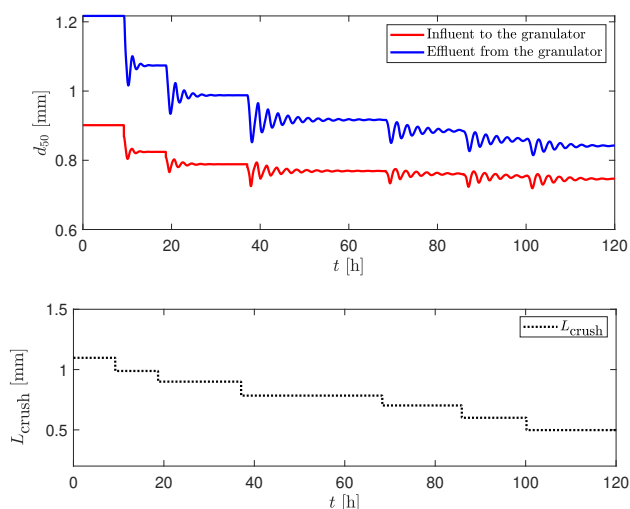
Figure 15: d_{50} as a response to the step-by step change of L_{crush} with $\dot{m}_{slurry} = 1000$ kg/h.

References

Bück, A., Dürr, R., Schmidt, M., and Tsotsas, E. Model predictive control of continuous layering granulation in fluidised beds with internal product classification. *Journal of Process Control*, 2016. 45:65–75. doi:10.1016/j.jprocont.2016.07.003.

Cameron, I., Wang, F., Immanuel, C., and Stepanek, F. Process systems modelling and applications in granulation: A review. *Chemical Engineering Science*, 2005. 60(14):3723–3750. doi:10.1016/j.ces.2005.02.004.

Drechsler, J., Peglow, M., Heinrich, S., Ihlow, M., and Mörl, L. Investigating the dynamic behaviour of fluidized bed spray granulation processes applying numerical simulation tools. *Chemical Engineering Science*, 2005. 60(14):3817–3833. doi:10.1016/j.ces.2005.02.010.

Heinrich, S., Peglow, M., Ihlow, M., and Mörl, L. Particle population modeling in fluidized bed-spray granulationanalysis of the steady state and unsteady behavior. *Powder Technology*, 2003. 130(1-3):154–161. doi:10.1016/S0032-5910(02)00259-0.

Herce, C., Gil, A., Gil, M., and Cortés, C. A capetaguchi combined method to optimize a npk fertilizer plant including population balance modeling of granulation-drying rotary drum reactor. In *Computer Aided Chemical Engineering*, volume 40, pages 49–54. Elsevier, 2017. doi:10.1016/B978-0-444-63965-3.50010-6.

Hounslow, M., Ryall, R., and Marshall, V. A discretized population balance for nucleation, growth, and aggregation. *AIChE Journal*, 1988. 34(11):1821–1832. doi:10.1002/aic.690341108.

Hulburt, H. and Katz, S. Some problems in particle technology: A statistical mechanical formulation. *Chemical Engineering Science*, 1964. 19(8):555–574.

Iveson, S., Litster, J., Hapgood, K., and Ennis, B. Nucleation, growth and breakage phenomena in agitated wet granulation processes: a review. *Powder technology*, 2001. 117(1-2):3–39. doi:10.1016/S0032-5910(01)00313-8.

Kapur, P. Kinetics of granulation by non-random coalescence mechanism. *Chemical Engineering Science*, 1972. 27(10):1863–1869. doi:10.1016/0009-2509(72)85048-6.

Koren, B. A robust upwind discretization method for advection, diffusion and source terms. In C. B. Vreugdenhil and B. Koren, editors, *Numerical Methods for Advection-Diffusion Problems, Notes on Numerical Fluid Mechanics*, pages 117–138. 1993.

Kumar, J. *Numerical approximations of population balance equations in particulate systems*. Ph.D. thesis, Otto-von-Guericke-Universität Magdeburg, Universitätsbibliothek, 2006.

Kumar, J., Peglow, M., Warnecke, G., Heinrich, S., and Mörl, L. Improved accuracy and convergence of discretized population balance for aggregation: The cell average technique. *Chemical Engineering Science*, 2006. 61(10):3327–3342. doi:10.1016/j.ces.2005.12.014.

Kumar, S. and Ramkrishna, D. On the solution of population balance equations by discretization -I. A fixed pivot technique. *Chemical Engineering Science*, 1996. 51(8):1311–1332. doi:10.1016/0009-2509(96)88489-2.

Litster, J. and Ennis, B. *The science and engineering of granulation processes*, volume 15. Springer Science & Business Media, 2004.

MATLAB. The MathWorks, Inc., Natick, Massachusetts, United States., 2017a.

Molerus, O. and Hoffmann, H. Darstellung von windsichtertrennkurven durch ein stochastisches modell. *Chemie Ingenieur Technik*, 1969. 41(5-6):340–344. doi:10.1002/cite.330410523.

Mörl, L. *Anwendungsmöglichkeiten und Berechnung von Wirbelschichtgranulationstrocknungsanlagen*. Ph.D. thesis, Technische Hochschule Magdeburg, 1981.

Mörl, L., Mittelstrab, M., and Sachse, J. Zum kugelwachstum bei der wirbelschichtrocknung von suspensionen oder losungen. *Chemical Technology*, 1977. 29(10):540–541.

Radichkov, R., Müller, T., Kienle, A., Heinrich, S., Peglow, M., and Mörl, L. A numerical bifurcation analysis of continuous fluidized bed spray granulator with external product classification. *Chemical Engineering and Processing*, 2006. 45:826–837. doi:10.1016/j.cep.2006.02.003.

Ramachandran, R. and Chaudhury, A. Model-based design and control of a continuous drum granulation process. *Chemical Engineering Research and Design*, 2012. 90(8):1063–1073. doi:10.1016/j.cherd.2011.10.022.

Ramachandran, R., Immanuel, C. D., Stepanek, F., Litster, J. D., and Doyle III, F. J. A mechanistic model for breakage in population balances of granulation: Theoretical kernel development and experimental validation. *Chemical Engineering Research and Design*, 2009. 87(4):598–614. doi:10.1016/j.cherd.2008.11.007.

Ramkrishna, D. *Population balances: Theory and applications to particulate systems in engineering.* Academic press, 2000.

Valiulis, G. and Simutis, R. Particle growth modelling and simulation in drum granulator-dryer. *Information Technology and Control*, 2009. 38(2).

Vesjolaja, L., Glemmestad, B., and Lie, B. Population balance modelling for fertilizer granulation process. *Proceedings of The 59th Conference on Simulation and Modelling (SIMS 59), 26-28 September 2018, Oslo Metropolitan University, Norway*, 2018. doi:10.3384/ecp1815395.

Wang, F., Ge, X., Balliu, N., and Cameron, I. Optimal control and operation of drum granulation processes. *Chemical Engineering Science*, 2006. 61(1):257–267. doi:10.1016/j.ces.2004.11.067.

Paper E

Double-Loop Control Structure for Rotary Drum Granulation Loop

Double-Loop Control Structure for Rotary Drum Granulation Loop

Ludmila Vesjolaja [1,*] **, Bjørn Glemmestad** [2] **and Bernt Lie** [1]

[1] Department of Electrical Engineering, IT and Cybernetics, University of South-Eastern Norway, 3918 Porsgrunn, Norway; bernt.lie@usn.no

[2] Process Modeling and Control Department, Yara Technology Center, 3936 Porsgrunn, Norway; bjorn.glemmestad@yara.com

* Correspondence: ludmila.vesjolaja@usn.no

Abstract: The operation of granulation plants on an industrial scale is challenging. Periodic instability associated with the operation of the granulation loop causes the particle size distribution of the particles flowing out from the granulator to oscillate, thus making it difficult to maintain the desired product quality. To address this problem, two control strategies are proposed in this paper, including a novel approach, where product-sized particles are recycled back to maintain a stable granulation loop process. A dynamic model of the process that is based on a population balance equation is used to represent the process dynamics. Both of the control strategies utilize a double-loop control structure that is suitable for highly oscillatory systems. The simulation results show that both control strategies, including the novel approach, are able to remove the oscillating behaviour and stabilize the granulation plant loop.

---

1. Introduction

Granulation is a particle enlargement process during which fine particles and/or atomizable liquids are converted into granules via a series of complex physical processes [1]. Granulation processes are used in a wide range of industrial applications, including the fertilizer industry. Fertilizer manufacturing using the granulation process has received considerable research interest during the last few decades, due to (i) the increasing requirements for efficient production of high quality fertilizers for increased food production in a growing global population and (ii) difficult process control and operation, e.g., among others [2–6], have focused their research on granulation processes.

This paper is focused on the last part of NPK (Nitrogen, Phosphorus, Potassium) fertilizer production. A granulation loop is used in order to produce different grades, i.e., various N:P:K ratios, of fertilizers. The NPK fertilizer is a high value type of fertilizer containing the three main elements that are essential for crop nutrition. Various NPK grades are specifically developed for different crops growing in different climates and soils [7]. The granulation loop that was studied in this paper consists of a rotary drum granulator, a granule classifier (screens), and a roll crusher. Figure 1 shows a typical schematic of a granulation process with a recycle loop. Rotary drums, as granulation units, are frequently used in fertilizer industries due to the ability of rotary drums to handle large amounts of material.

During the granulation process, a slurry of liquid ammonium nitrate and partly dissolved minerals is solidified to form granules. Granules that are too small (under-sized particles) are recycled to the granulation unit and granules that are too large (over-sized particles) are first crushed and then recycled

back to the granulator. The recycle feed is an integral part of the granulation process. The recycle feed flow rate, as well as its particle size distribution (PSD), are important for proper process operation. The recycle of off-spec (under-sized and crushed over-sized) particles is needed in order to seed the granulator. Another reason to recycle the feed is to follow the regulations: the off-spec granules cannot be considered as a waste material, and must be recycled from an environmental and economic point of view [7].
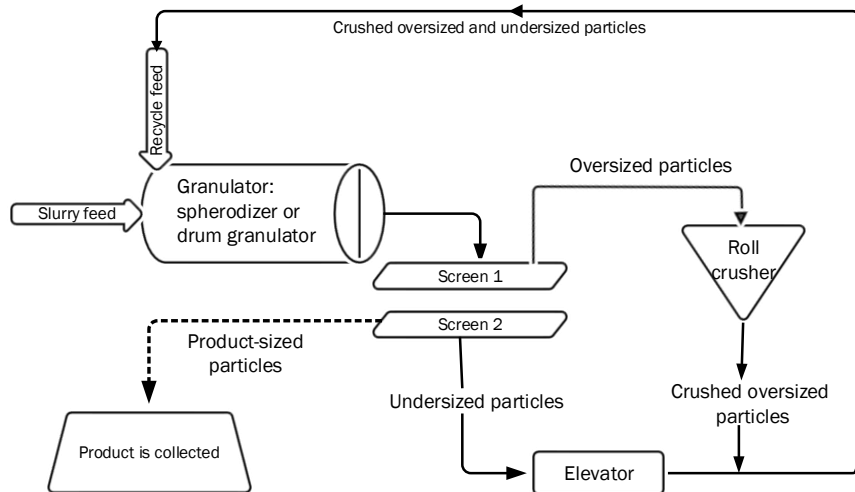
Figure 1. Schematic diagram of a rotary drum granulation loop [7].

For some granulation processes, drum processes are operated below design capacity and the amount of the recycled material is large. A typical recycle ratio in granulation plants is 4:1. This indicates a high ratio between off-spec and on-spec particles. Moreover, granulation loops may show oscillatory behavior for certain operating points. Characteristic oscillatory behavior that is faced in a granulation process industry is shown in Figure 2. In Figure 2, the PSD is represented while using the particle median diameter d_{50} (diameter that corresponds to the intercept for 50% of cumulative mass).
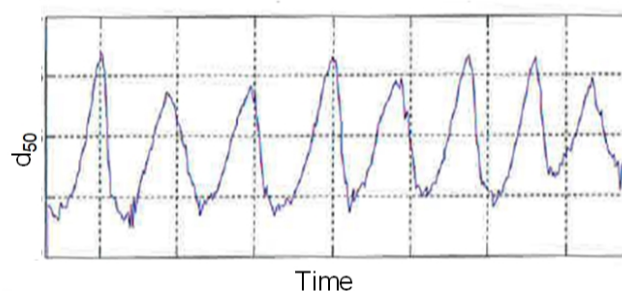
Figure 2. Oscillatory behavior of d_{50} in an industrial granulation loop plant.

The observed instability (oscillatory behavior) is linked to the entire granulation loop, since the granulator receives a fluctuating recycled stream as input. This leads to additional challenges in the fertilizer production industry. The need to guarantee that the product complies with the specifications motivates the use of process control systems in the operation of the granulation loop. Thus, it is essential to design a proper control strategy that enables the production and increase the efficiency of the granulation loop.

Granulation processes have been ubiquitous in the industry for many years with significant research being undertaken to gain further insight into designing a control strategy for improved plant

operation. Oscillatory behavior in granulation loops are reported in [8–10]; the authors have analyzed granulation loop dynamics for fluidized bed spray granulators with internal and external classification. Drum granulation processes were extensively studied at University of Queensland, Brisbane, Australia. Some of their published contributions include [5,11,12]. These works focused on the dynamics and control of the drum granulator itself, not on the entire granulation loop. The control of the granulation loop using model-based design is reported in [8,13,14], while studies on the stabilization of granulation loops using H_∞-theory and discrepancy-based control are presented in [15–17].

The main objective of this study is to design the control structure to stabilize the granulation loop process, i.e., to propose possible control structures that would reduce or remove the oscillatory behaviour and possibly make granulation loops more steady to operate. To achieve this objective, a feedback control structure using double loop PID controllers reported in [18,19] is applied. In addition, a novel approach where product-sized particles are recycled back to maintain a stable granulation loop process is presented.

The paper is organized, as follows: in Section 2, a mathematical model of a granulation loop, including models of a rotary drum, screens, and a crusher, is given. In Section 3, the system dynamics of the granulation loop process are studied. Two control strategies to suppress the oscillating behavior of the process are proposed in Section 4. In Section 5, the double-loop control structure for composition controller is discussed. Closed loop simulation results and discussions are given in Section 6, while conclusions are drawn in Section 7.

2. Granulation Loop Model

2.1. Rotary Drum

In this study, a rotary drum was modeled using population balance principles. The developed models are two-dimensional (2D) models that are discretized in terms of its internal coordinate (particle diameter) and external coordinate (axial length of the granulator). A mass based population balance equation (PBE) was used, since in an industrial application, it is relatively easier to work with mass based PBEs than number based PBEs. The general form of a mass based PBE with particle diameter (d) as the internal coordinate, spatial variation (z) as the external coordinate and time (t) is represented as

$$\frac{\partial m(d,z,t)}{\partial t} = -d^3 \frac{\partial}{\partial d}\left[G\frac{m(d,z,t)}{d^3}\right] + B(d,z,t) - D(d,z,t) - \frac{\partial}{\partial z}[v \cdot m(d,z,t)], \tag{1}$$

where $m(d,z,t)$ is the mass density function, d is the particle diameter, G is the particle growth rate, B is the particle birth rate, D is the particle death rate, and v is the velocity of the particles in the granulator [20]. The first term on the right hand side represents the particle growth due to layering, the second and third terms stand for particle birth and death, respectively, due to agglomeration, and the last term represents a continuous process and it gives the flow of particles through the granulator. In this study, the particle velocity is the same for all particle sizes (particle size classes). Equation (1) is derived by assuming that all of the particles are ideal spheres with a constant solid density.

In this study, the rotary drum model is based on the one-dimensional (1-D) model that was reported in [21]. However, in this study, a 2-D model reported in [7] is used in simulations. The extension of the 1-D model to the 2-D model is performed by including the spatial variations in property through the axial direction of the granulator. For this, the length of the granulator L_g is divided into equally sized sections (compartments). Detailed formulations for a three-compartment granulator model is given in [7].

Particle growth G due to layering was modeled while using a size-independent linear growth model reported in [22,23] and used in [7,21]. The *layering* term was then discretized using a finite volume scheme that was extended by a Koren flux limiter function [24]. Particle agglomeration (B and D) was modeled using Hulburt and Katz' formulation [25], as given in [7,21]. The discretization of the

agglomeration term was then performed by applying one of the sectional schemes—the cell average scheme reported in [26,27].

2.2. Screens

The mass flow rates out from the screens are described while using probability function Y_{upp} and Y_{low} from [28]. The mass flow rates from the screen are then calculated as

$$\dot{m}_o \gamma_o = Y_{upp} \dot{m}_e \gamma_e,$$ (2)

$$\dot{m}_u \gamma_u = \left(1 - Y_{upp}\right)\left(1 - Y_{low}\right) \dot{m}_e \gamma_e,$$ (3)

$$\dot{m}_p \gamma_p = \left(1 - Y_{upp}\right) Y_{low} \dot{m}_e \gamma_e.$$ (4)

Here, $\dot{m}_o$, $\dot{m}_u$, $\dot{m}_p$ are the mass flow rates of over-sized, under-sized, and product-sized particles, respectively. The corresponding distribution functions of the over-sized, under-sized, and product-sized particles are denoted with γ_o, γ_u, and γ_p, respectively. The screening probability functions Y_{upp} and Y_{low} defined by [28] and also given in [29] are calculated while using Equations (5) and (6)

$$Y_{upp,\,low} = \frac{1}{1 + \left(\frac{d_{screen,\,upp,\,low}}{d}\right)^2 \exp k}$$ (5)

and

$$k = \left[K_{eff,\,upp,\,low}\left(1 - \left(\frac{d}{d_{screen,\,upp,\,low}}\right)^2\right)\right],$$ (6)

where d_{screen} is the mesh size of the screen (sieve diameter), d is the particle diameter, and K_{eff} is the screen separation efficiency.

2.3. Crusher

A mathematical model of the crusher is the distribution function (Equation (7)) that re-distributes the total over-sized mass flow ($\dot{m}_o \gamma_o$). Thus, over-sized particles with γ_o distribution flowing into the crusher, leave the crusher with the γ_{crush} distribution. Having a crusher gap spacing and a standard deviation as the design choices, the crusher distribution function is defined as a Gaussian distribution, as

$$\gamma_{crush} = \frac{1}{\sqrt{2\pi\sigma_{crush}^2}} \exp\left(-\frac{(d - d_{crush})^2}{2\sigma_{crush}^2}\right).$$ (7)

Here, σ_{crush} is the standard deviation and d_{crush} is the crusher diameter, which is the mean size of the crushed particle distribution. The total over-sized particle flow rate is then calculated as

$$\dot{m}_{crush}\gamma_{crush} = \left(\sum \dot{m}_o \gamma_o\right) \cdot \gamma_{crush}.$$ (8)

The mass flow rate that is recycled back to the granulator, i.e., the mass flow of the off-spec particles, is given as

$$\dot{m}_i \gamma_i = \dot{m}_{crush}\gamma_{crush} + \dot{m}_u \gamma_u.$$ (9)

An elevator that is used to transfer under-sized particles, together with the crushed over-sized particles to the recycle belt, is modeled as a transport delay.

3. System Dynamics

3.1. Simulation Setup

For studying the system dynamics, particles are classified into 80 size classes and the drum length is divided into three equally sized compartments. The PDE given by Equation (1) is transformed into a set of 240 ODEs by applying the Koren flux limiter scheme [24] for the *layering term* discretization and the cell average scheme [26,27] for the *agglomeration term* discretization. Obtained ODEs are then solved using a fourth order Runge–Kutta method with fixed time step. The simulations are performed using MATLAB and Simulink [30]. The parameters used to simulate the granulation loop process are listed in Table 1.

Table 1. Simulation parameters.

Parameter	Value
Range of d [mm]	0–8
Number of particle classes	80
Grid type	linear
Length of granulator [m]	10
Number of compartments	3
ρ [kg·m^{-3}]	1300
β_0 [s^{-1}]	1.0×10^{-13}
$\dot{m}_{\text{sl,i}}$ [kg·h^{-1}]	1000
$d_{\text{screen, upp}}$ [mm]	3.3
$d_{\text{screen, low}}$ [mm]	1.9
$K_{\text{eff, upp}}$	45
$K_{\text{eff, low}}$	45
d_{crush} [mm]	2.0–1.3
σ_{crush}	0.25
T_R [s]	600
Transport delay [s]	600
Time step for RK4 [s]	20

The initialization of the mass distribution function inside the granulator is performed using a Gaussian normal distribution function given by Equation (7). For a comparison of simulation results, the evolution of the average size of the particles is represented by their d_{50} diameter.

3.2. Effect of Crusher Gap Parameters on Process Dynamics

During granulation, the particles are growing inside the drum granulator, and as a result, the average diameter d_{50} of the particles leaving the granulator (effluent) is larger compared to the d_{50} of the particles that are sent to the granulator with the recycle feed (influent). In Figures 3–5, a step-by-step change of the crusher gap spacing (d_{crush}) is given to the system.

At larger crusher gap spacings, a stable granulation process is observed ($d_{\text{crush}} \geq 2$ mm in Figure 3). However, as the crusher gap spacing is reduced ($d_{\text{crush}} < 2$ mm in Figures 4 and 5), the granulation loop starts to show oscillatory behavior and, at a certain reduced crusher gap spacing ($d_{\text{crush}} = 1.3$ mm), sustained periodic oscillations occur. Oscillations occur not only in the product quality, i.e., d_{50}, but also in the product-sized, off-spec, and total mass flow rates (Figures 4–6). Thus, the dynamic behavior of the granulation loop is inevitably connected with the crusher parameter, i.e., with the crusher gap spacing.

The probable reason for the occurrence of oscillations is the off-spec (over-sized and under-sized) particle flow that is recycled to the granulator and acts as nuclei for the new granule generation. At smaller crusher gap spacings, the granulator receives a large amount of fines with the recycle feed. In the granulator, a large amount of fines has a large total particle surface area that slows down the particle growth. Thus, the growth rate and d_{50} of particles decreases. On the other hand, slower growth

rate contributes to the rapid drop in the production of coarse (over-sized) particles, which, in turn, reduces the total recycle feed to the granulator. As a result, the granulator receives smaller amounts of fine particles that now have lower total surface area. Thus, the growth rate and d_{50} of particles again increases and gives the start of the new cycle of oscillations [7].
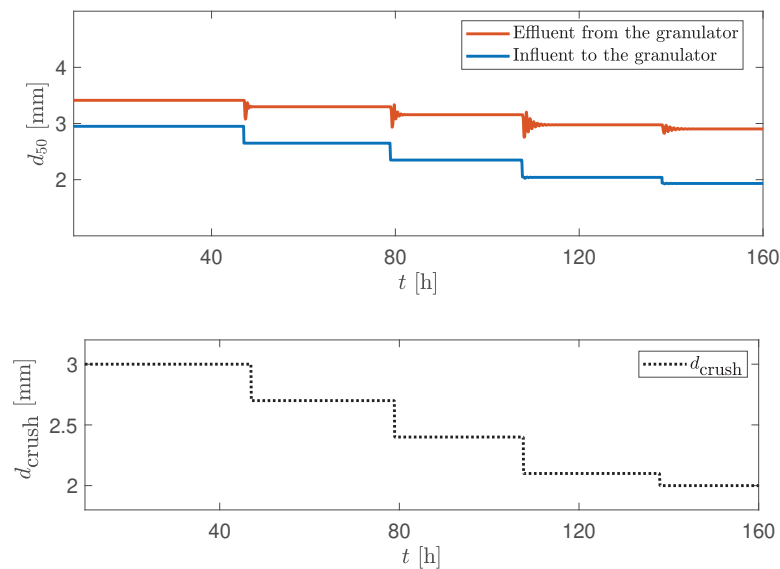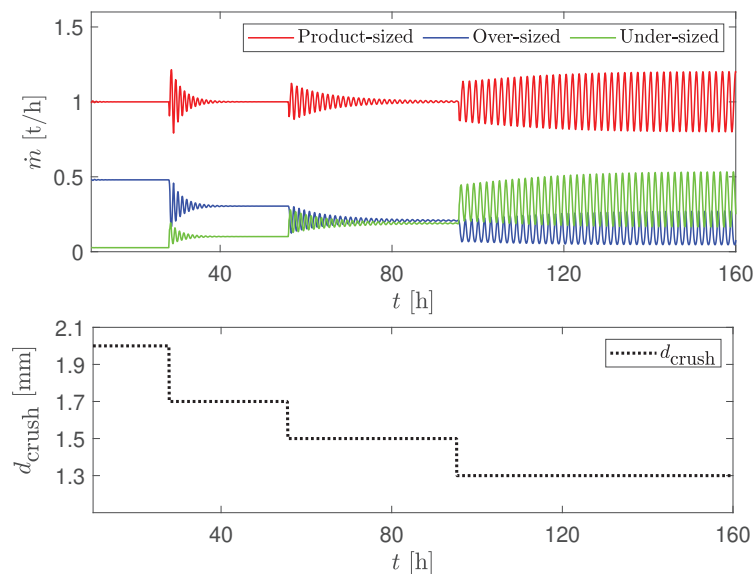

Figure 3. d_{50} of the influent/effluent as a response to the step-by-step change of the crusher gap $d_{\text{crush}} = 3.0 \rightarrow 2.7 \rightarrow 2.4 \rightarrow 2.1 \rightarrow 2.0$ mm.
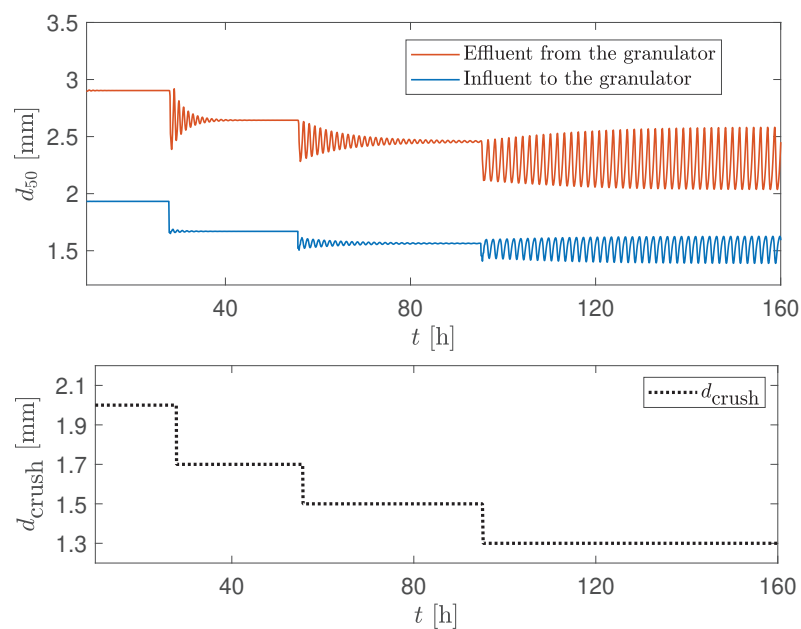
Figure 4. d_{50} of the influent/effluent as a response to the step-by-step change of the crusher gap $d_{\text{crush}} = 2.0 \rightarrow 1.7 \rightarrow 1.5 \rightarrow 1.3$ mm.
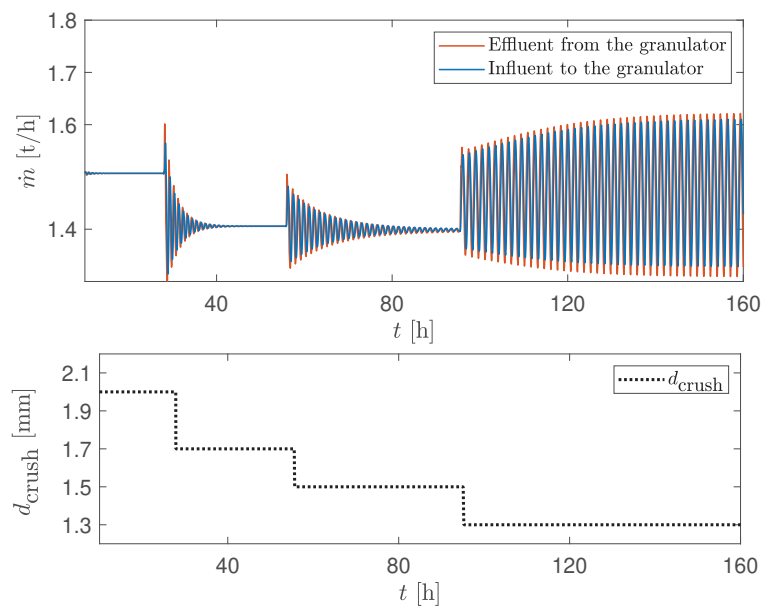
Figure 5. Total mass flow rates of the influent/effluent as a response to the step-by-step change of the crusher gap $d_{\text{crush}} = 2.0 \rightarrow 1.7 \rightarrow 1.5 \rightarrow 1.3$ mm.

Figure 6. Mass flow rates of over-sized, product-sized and under-sized particles as a response to the step-by-step change of the crusher gap $d_{\text{crush}} = 2.0 \rightarrow 1.7 \rightarrow 1.5 \rightarrow 1.3$ mm.

3.3. Recycle of Product-Sized Particles

In these open loop simulation, some of the product-sized particle flow was recycled back to the granulator. In particular, some fraction of the product-sized particle flow was sent to the recycle belt and then added to the off-spec (crushed over-sized and under-sized) particle flows.

In Figure 7, after obtaining the sustained oscillations, 20 % of the product-sized particle flow is recycled. As a result, a stable operation of the process was obtained (Figure 7). A stable operation is achieved, since the PSD distribution, measured as particle d_{50}, becomes more narrow when some fraction of product-sized particles are combined with the off-spec particles and the recycle stream

contains less (proportion wise) under-sized particles. One of the aims of the paper is to exploit this particular dynamic behaviour of the process in order to design a control structure for stabilizing the granulation plant.
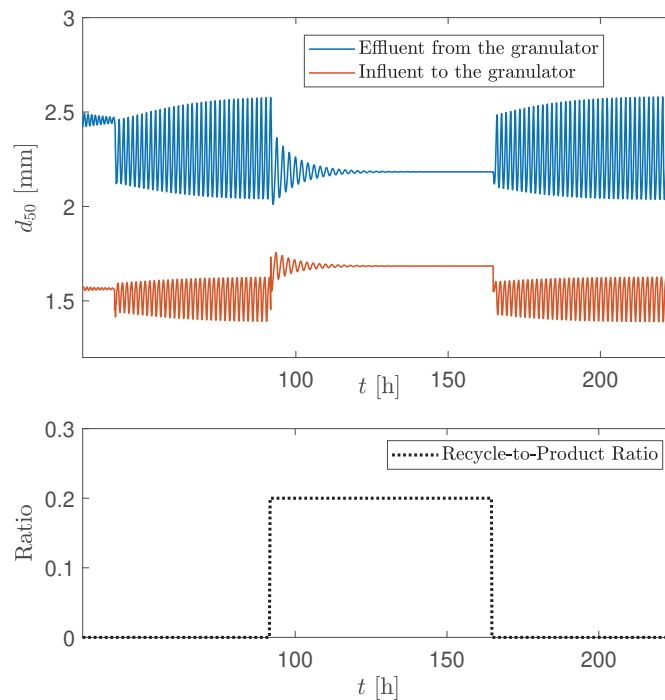
Figure 7. d_{50} of the influent/effluent as a response to the step change of the product-sized particle flow: between $92 < t < 165$ 20% of the particle-sized flow rate was recycled.

4. Control Strategies

4.1. Background

The main goal of controlling the granulation plant is to stabilize the process operation by reducing or removing the oscillatory behaviour that occurs in the product quality (PSD) and quantity (mass flow rates), as stated in Section 1. In this paper, two control strategies (CS) are designed. In both CSs, the controlled variable is the granule PSD distribution, as measured by d_{50}, coming from the rotary drum (effluent from the granulator). The choice of manipulatable variable depends on the plant configuration. In some industrial-scale rotary drum granulation loop plants, the crusher gap spacing can be easily manipulated by operators from the control room. In other rotary drum granulation loop plants, the crusher gap spacing can only be changed manually by operators on the plant itself, and, thus, the crusher gap spacing can not be chosen as manipulatable variable. A novelty of this paper is to show that product-to-recycle ratio can also be used as a manipulated variable in order to stabilize the granulation plant.

4.2. Control Strategy 1

The first control strategy (CS1) is based on the open loop simulations that are given in Section 3.2 and can be applied in the granulation plants where crusher gap spacings can be controlled by operators from the control room. In this control strategy, the controlled variable is the PSD distribution, as measured by d_{50}, of the granules coming from the rotary drum before the granules are sieved. The manipulatable variable is the crusher gap spacing. Figure 8 shows the schematic diagram of the proposed CS1.
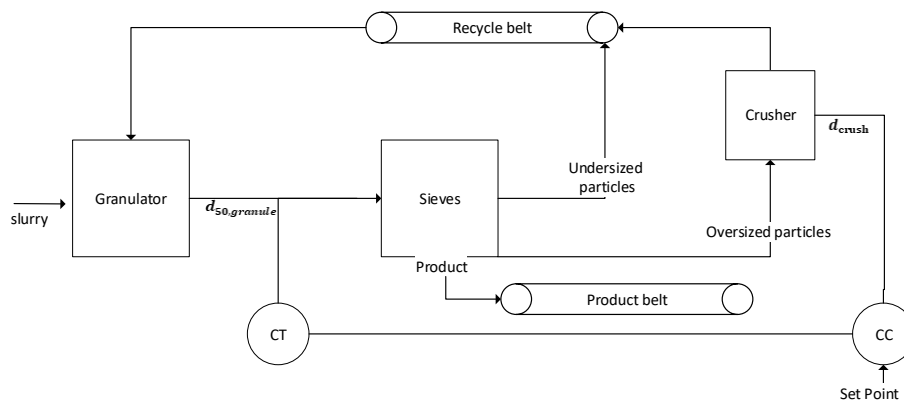
Figure 8. Schematic diagram of CS1. CT—composition (d_{50}) transmitter; CC—composition (d_{50}) controller.

4.3. Control Strategy 2

In the second control strategy (CS2), the control of the granulation loop is performed by recycling some of the product-sized granules. Figure 9 shows the schematic diagram of the proposed CS2. Similarly to CS1, the controlled variable is the granule PSD distribution, as measured by d_{50}, on the elevator coming from the rotary drum before the granules are sieved. However, here, unlike CS1, the manipulatable variable is the three-way valve opening α in Figure 9. When the valve is closed ($\alpha = 0$), none of the product-sized particles are recycled; when the valve is opened ($0 < \alpha \le 1$)—some fraction of the product-sized particle mass flow rate is added to the recycle stream, i.e., mixed with the crushed over-sized and under-sized particle mass flow rates.
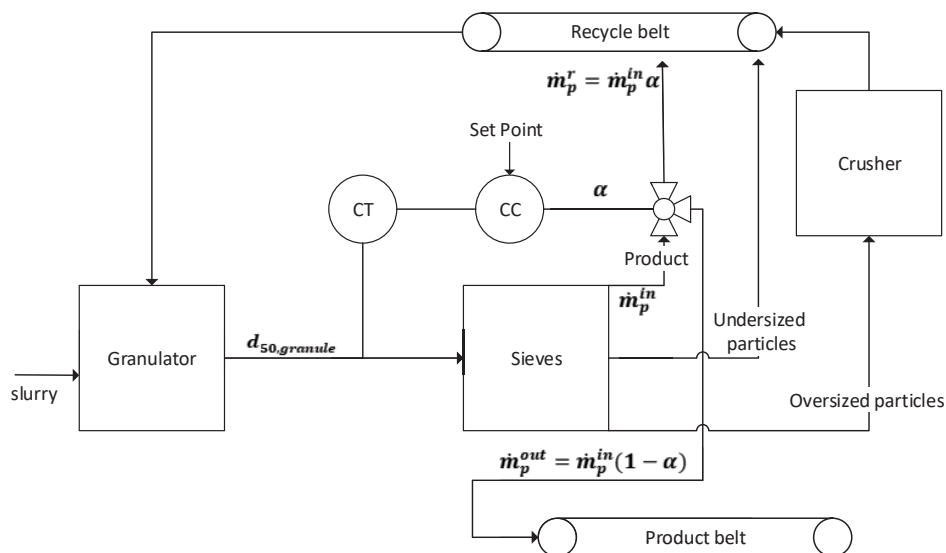
Figure 9. Schematic diagram of CS2. CT—composition (d_{50}) transmitter; CC—composition (d_{50}) controller; α—valve opening.

5. Double-Loop Control Structure for CC Controllers

The proportional-integral-derivative (PID) controller is still the most used control algorithm in the industry, due to its simple structure and easiness in operation. In this paper, the CC – composition (d_{50}) controllers for both control strategies 1 and 2 are designed as a double-loop control structure [18,19] for oscillatory systems.

The main idea of the control structure is to convert a given underdamped (oscillatory) system to an overdamped system while using a proportional controller ($P_{dc}(s)$) and then use an outer PI controller ($P_c(s)$) to this overdamped system to track the specified reference point. Figure 10 illustrates the double-loop control structure.
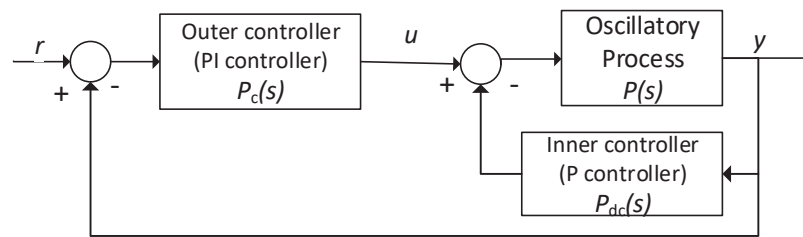
Figure 10. The proposed double-loop control algorithm. u—control signal, y—controlled variable, r—reference point [18].

The granulation plant can be represented as an oscillatory process (a 2nd order plus time delay process) having a transfer function

$$P(s) = \frac{K_p e^{-\tau s}}{1 + \frac{2\zeta s}{\omega_0} + \left(\frac{s}{\omega_0}\right)^2},$$ (10)

where $P(s)$ is the transfer function of the underdamped (oscillatory) process, K_p is the process gain, τ is the process time delay, ω_0 is the natural frequency, and ζ is the damping factor. Process parameters, K_p, τ, ζ and ω_0 were found using a simulated step-response of the granulation plant at a stable operating range.

5.1. Inner Controller

The first step in applying the double-loop control structure is to design the inner controller, which is a damping controller ($P_{dc}(s)$ in Figure 10). In our case, a P-controller to change an underdamped system to an overdamped system. The process parameters of the overdamped system can be found while using the combined transfer function from u to y in Figure 10, i.e.,

$$P_o(s) = \frac{P(s)}{1 + P(s) \cdot P_{dc}(s)},$$ (11)

where $P_o(s)$ is the transfer function of the overdamped system and $P_{dc}(s) = K_c^i$ is the damping controller.

By approximating the time delay with $\exp(-\tau s) \approx 1 - \tau s$ and specifying the inner loop damping factor $\zeta_i > 1$, the required P-controller gain K_c^i is,

$$K_c^i = 2 \cdot \frac{\left(\zeta_i^2 + \zeta\tau\omega_0\right) \pm \sqrt{\left(\zeta_i^2 + \zeta\tau\omega_0\right)^2 + \tau^2\omega_0^2\left(\zeta_i^2 - \zeta^2\right)}}{\tau^2 w_0^2 K_p}.$$ (12)

Here, ζ_i can be viewed as a design variable that should be selected appropriately. In this study, $\zeta_i = 1.5$ was used. The resulting inner loop natural frequency is

$$\omega_i = \omega_0 \sqrt{1 + K_c^i K_p}. \tag{13}$$

5.2. Outer Controller

A simple PI controller was used as the outer controller. Tuning of the PI-controller was performed while using the SIMC tuning rules for PID controllers [31]. It is possible to directly apply SIMC tuning rules for our second order system. However, it is easier to work with a first order system. Thus, in this paper, the 2nd order overdamped system $P_o(s)$ was changed to a 1st order system using Skogestad's half rule reported in [31]. According to the half rule, the 2nd order overdamped system was approximated as a 1st order system plus time delay as

$$P_o(s) \approx \frac{K_p^i(1 - \tau_{\text{eff}} s)}{(T_{\text{eff}} s + 1)}, \tag{14}$$

where the effective time delay τ_{eff} and the effective speed of the response T_{eff} were calculated while using expressions summarized in Table 2.

Table 2. Expressions used to find the controller parameters.

Parameter	Expression
τ_{eff}	$\tau + 0.5 T_2$
T_{eff}	$T_1 + 0.5 T_2$
T_1	$\frac{\zeta_i + \sqrt{\zeta_i^2 - 1}}{\omega_i}$
T_2	$\frac{\zeta_i - \sqrt{\zeta_i^2 - 1}}{\omega_i}$
K_c	$\frac{T_{\text{eff}}}{K_p^i(T_c + \tau_{\text{eff}})}$
T_i	$\min(T_{\text{eff}}, 4(T_c + \tau_{\text{eff}}))$
K_p^i	$\frac{K_p}{1 + K_c^i K_p}$
T_c	$-\tau_{\text{eff}} < T_c < \infty$

Tuning of the PI-controller, i.e., finding controller parameters K_c and T_i in Equation (15), was then performed using SIMC PI tuning rule for the 1st order plus time delay system. The PI controller equation in frequency domain is

$$P_c(s) = K_c \left(1 + \frac{1}{T_i s}\right), \tag{15}$$

where K_c is the proportional gain of the PI controller and T_i is the integral time constant of the PI controller that were calculated while using expressions summarized in Table 2.

6. Simulation Results and Discussion

6.1. Control Strategy 1

In this case, the crusher gap spacing is chosen as manipulatable variable and d_{50} of the particles leaving the granulator as the controlled variable. The double-loop controller was turned on when the sustained oscillations in the controlled variable were observed. The controller was again turned off, as the stability in the controlled variable was achieved. Figure 11 shows the simulation results when the controller was turned on at the maximum point of the cycle, while in Figure 12, the controller was turned on at the minimum point of the cycle.
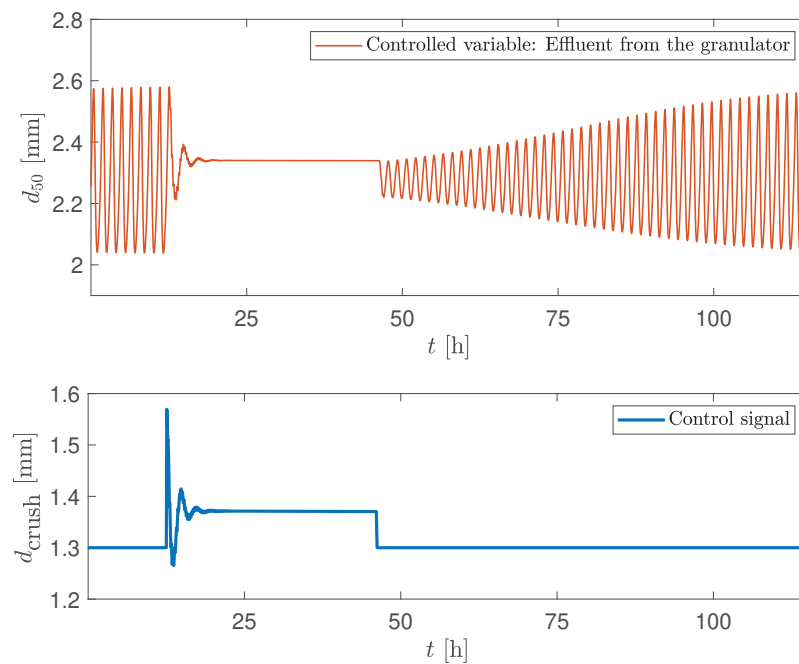
Figure 11. Simulation of CS1: manipulatable variable—crusher gap, controlled variable—d_{50} of the effluent. Controller is turned on at the maximum point of the cycle at $t = 13$ h and turned off at $t = 46$ h.
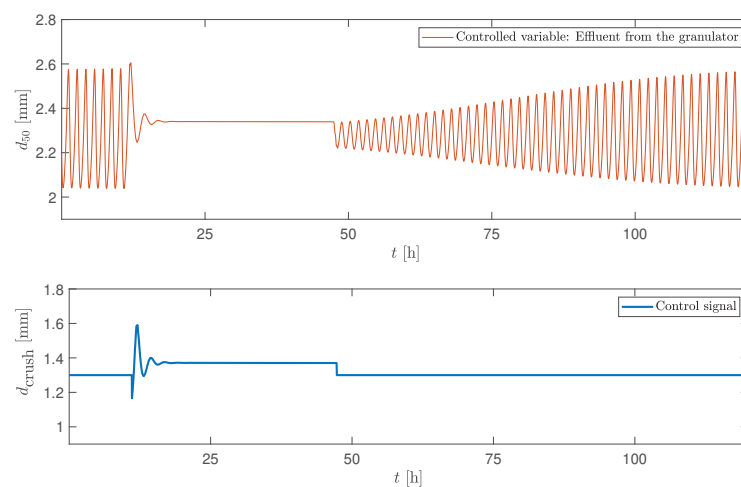
Figure 12. Simulation of CS1: manipulatable variable—crusher gap, controlled variable—d_{50} of the effluent. Controller is turned on at the minimum point of the cycle at $t = 11$ h and turned off at $t = 47$ h.

Both of the simulation scenarios showed similar results: after the controller was turned on, a steady state value (the set point) was reached after around 6 h in both simulation scenarios. For these two cases, identical controller parameters were used. The simulation results show that the control structure was able to eliminate the oscillatory behaviour. This resulted in a stable PSD, d_{50} of the effluent and mass flow rates of both the product-sized and off-spec particles. Overall, the total mass flow rates in and out of the granulator was stabilized (Figure 13).
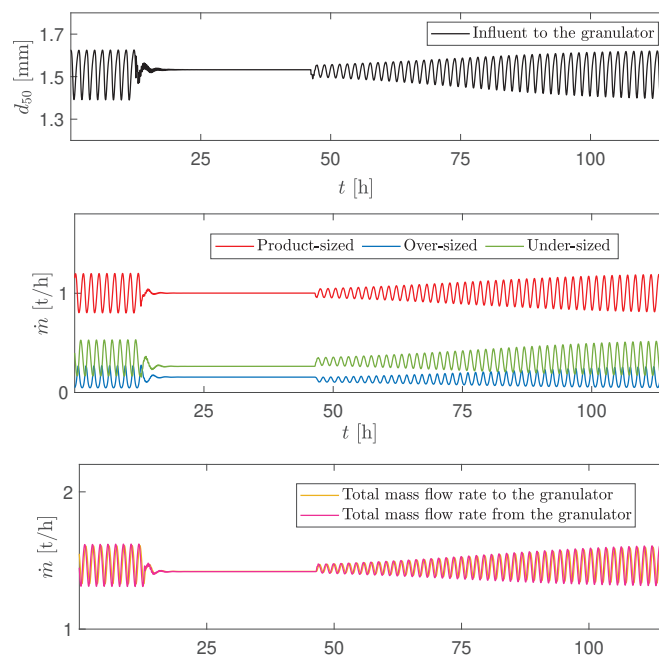
Figure 13. Simulation of CS1: stabilization of granulation loop process. Controller is turned on at the maximum point of the cycle at $t = 13$ h and turned off at $t = 46$ h.

6.2. Control Strategy 2

Here, the closed loop simulations were performed using Control Strategy 2 (CS2), as described in Section 4.3 and illustrated in Figure 9. The stabilization of the granulation loop (stabilization of the oscillatory behaviour) is achieved by controlling the PSD of particles leaving the granulator. This is achieved by recycling some of the product-size particles back to the granulator, i.e., by adding some of the product to the recycle feed by adjusting the valve opening. Thus, the controlled variable is the d_{50} of the particles leaving the granulator and the manipulatable variable is the valve opening that controls the recycled product flow.

In Figures 14 and 15 , the controller was turned on when the granulation plant exhibited sustained oscillations, i.e., at $t = 20$ h with $d_{crush} = 1.3$ mm. The oscillations were quickly damped when the controller was turned on and the controller was able to track the d_{50} to its desired set point. A stable (non-oscillating) PSD of the effluent (and hence a stable d_{50} of the effluent) was obtained (Figure 14). In addition, a stable flow rate of the product-sized, over-sized, and under-sized particles was also obtained (Figure 15). As expected, when the controller was turned off (at $t = 60$ h), the sustained oscillations reappeared. A similar stabilization of d_{50} of the effluent, and in the mass flow rates can be also obtained for the smaller crusher gap spacings, i.e., when $d_{crush} < 1.3$ mm. In the case when $d_{crush} < 1.3$ mm, the controller should be re-tuned. Thus, it is possible to stabilize the oscillatory behaviour by recycling some of the product-sized particles (control input signal in Figure 14). Even though some of the product is recycled, it is still economically favorable: unstable operation can lead to an increase in operational expenses due to occurances of peaks in recycled mass flow rates (both total and product mass flow rates). This, in turn, results in higher energy consumption, i.e., cost. In addition, unpredictable operation also increases safety concerns and may increase maintenance costs in industrial scale plants.
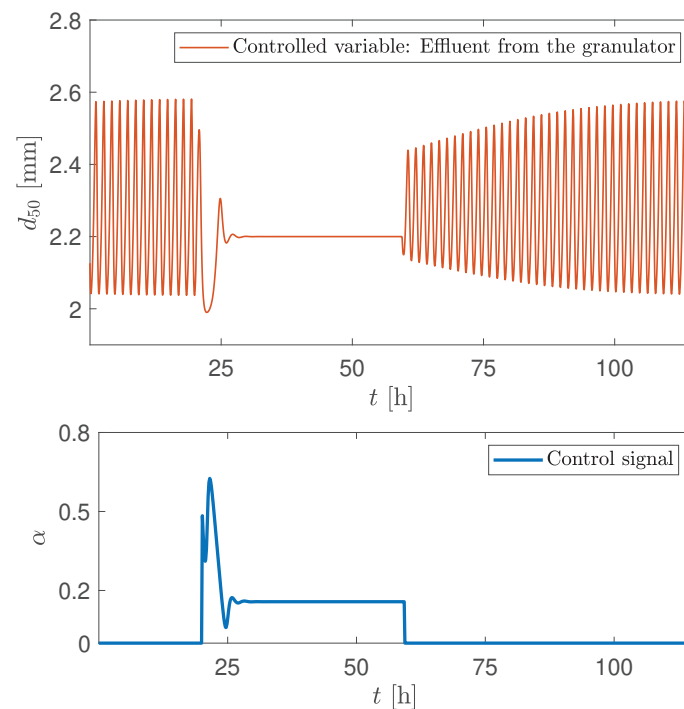
Figure 14. Simulation of CS2: manipulatable variable—valve opening, controlled variable—d_{50} of the effluent. Controller is turned on at $t = 20$ h and turned off at $t = 60$ h.
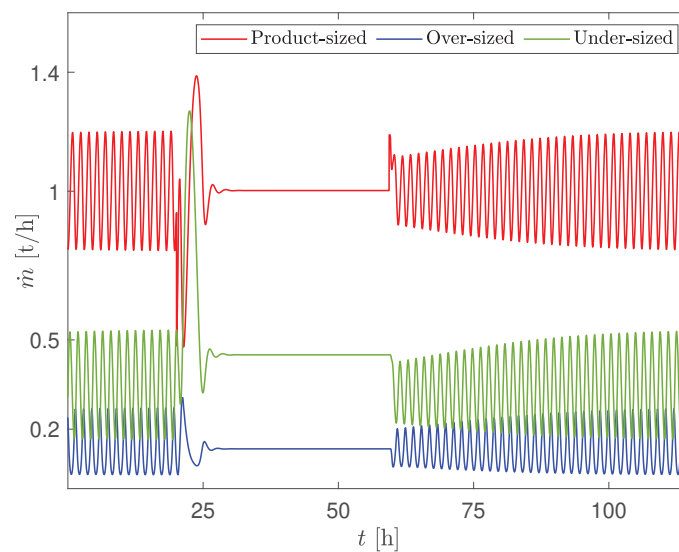
Figure 15. Simulation of CS2: mass flow rates. Controller is turned on at the minimum point of the cycle at $t = 20$ h and turned off at $t = 60$ h.

For further understanding of the controller behavior, the controller was turned on at different points of the sustained oscillating behaviour, at the minimum and the maximum points of the cycle. In Figure 14, the controller was turned on at the minimum point of the cycle, while, in Figure 16 at the maximum point of the cycle. Comparison of the controller behaviours for these two cases showed that the steady state value after the controller is turned on can be reached faster if the controller is turned on at the maximum point of the cycle. It took around 7 h to reach steady state value when the controller was turned on at the minimum point (Figure 14) of the cycle, while it took around 6 h when

the controller was turned on the maximum point of the cycle (Figure 16). In both these cases, identical controller parameters were used for fair comparison.
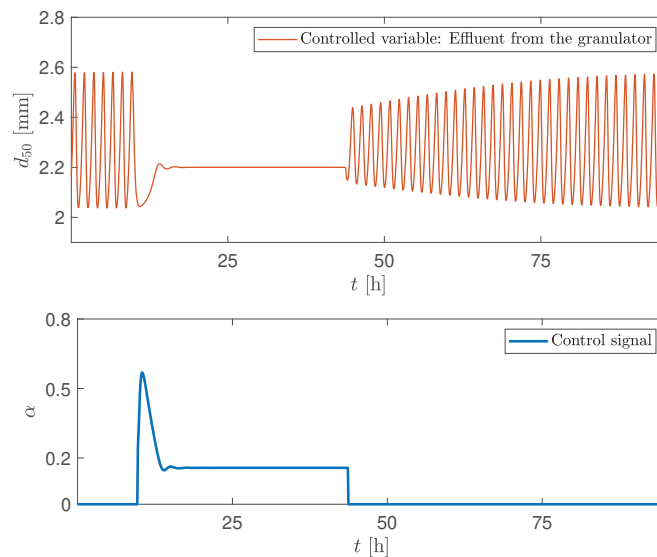
Figure 16. Simulation of CS2: Controller is turned on at the maximum point of the cycle at $t = 10$ h and turned off at $t = 44$ h.

7. Conclusions

The dynamic model that was developed for the rotary drum granulation loop used in fertilizer production is able to capture the main dynamics of the granulation process. Through dynamic simulations, the model was found to reproduce unstable operation typically seen in granulation loops. In particular, the model is able to reproduce oscillating behaviour in the particle size distribution. Two feedback control strategies are designed in order to suppress the oscillations and remove the oscillating behaviour. One possible and novel implementation is to recycle the product-sized particles in order to obtain a desired PSD distribution, as measured by d_{50}, of the granules leaving the granulator. This novel control strategy is particularly useful in these granulation plants where the crusher gap spacing cannot be directly manipulated. Another possibility is to control the PSD of the granules leaving the granulator by manipulating the crusher gap spacing. If a plant configuration allows for choosing between these two control strategies, i.e., if it is possible to manipulate the crusher gap spacing from the control room, then the CS1 seems a better choice for obtaining stability in operation, since the stability in the produced d_{50} is obtained faster with the CS1 than with CS2. Both control strategies utilize a double-loop structure consisting of P and PI controllers, which are widely accepted and used in process industries.

References

1. Litster, J.D.; Ennis, B. *The Science and Engineering of Granulation Processes*; Kluwer Academic Publishers: Dordrecht, The Netherlands, 2004; Volume 15.
2. Herce, C.; Gil, A.; Gil, M.; Cortés, C. A CAPE-Taguchi combined method to optimize a NPK fertilizer plant including population balance modeling of granulation-drying rotary drum reactor. *Comput. Aided Chem. Eng.* **2017**, *40*, 49–54.
3. Ramachandran, R.; Immanuel, C.D.; Stepanek, F.; Litster, J.D.; Doyle III, F.J. A mechanistic model for breakage in population balances of granulation: Theoretical kernel development and experimental validation. *Chem. Eng. Res. Des.* **2009**, *87*, 598–614. [CrossRef]
4. Valiulis, G.; Simutis, R. Particle growth modelling and simulation in drum granulator-dryer. *Inf. Technol. Control.* **2009**, *38*, 147–152.
5. Wang, F.Y.; Ge, X.Y.; Balliu, N.; Cameron, I.T. Optimal control and operation of drum granulation processes. *Chem. Eng. Sci.* **2006**, *61*, 257–267. [CrossRef]
6. Cameron, I.T.; Wang, F.Y.; Immanuel, C.D.; Stepanek, F. Process systems modelling and applications in granulation: A review. *Chem. Eng. Sci* **2005**, *60*, 3723–3750. [CrossRef]
7. Vesjolaja, L.; Glemmestad, B.; Lie, B. Dynamic model for simulating transient behaviour of rotary drum granulation loop. *Model. Identif. Control* **2020**, *41*, 65–77. [CrossRef]
8. Bück, A.; Palis, S.; Tsotsas, E. Model-based control of particle properties in fluidised bed spray granulation. *Powder Technol.* **2015**, *270*, 575–583. [CrossRef]
9. Drechsler, J.; Peglow, M.; Heinrich, S.; Ihlow, M.; Mörl, L. Investigating the dynamic behaviour of fluidized bed spray granulation processes applying numerical simulation tools. *Chem. Eng. Sci.* **2005**, *60*, 3817–3833. [CrossRef]
10. Radichkov, R.; Müller, T.; Kienle, A.; Heinrich, S.; Peglow, M.; Mörl, L. A numerical bifurcation analysis of continuous fluidized bed spray granulator with external product classification. *Chem. Eng. Process.* **2006**, *45*, 826–837. [CrossRef]
11. Ramachandran, R.; Chaudhury, A. Model-based design and control of a continuous drum granulation process. *Chem. Eng. Res. Des.* **2012**, *90*, 1063–10733. [CrossRef]
12. Wang, F.Y.; Cameron, I.T. A multi-form modelling approach to the dynamics and control of drum granulation processes. *Powder Technol.* **2007**, *179*, 2–11. [CrossRef]
13. Bück, A.; Dürr, R.; Schmidt, M.; Tsotsas, E. Model predictive control of continuous layering granulation in fluidised beds with internal product classification. *J. Process Control* **2016**, *45*, 65–75. [CrossRef]
14. Glaser, T.; Sanders, C.F.W.; Wang, F.Y.; Cameron, I.T.; Litster, J.D.; Poon, J.M.-H.; Ramachandran, R.; Immanuel, C.D.; Doyle, F.J., III. Model predictive control of continuous drum granulation. *J. Process Control* **2009**, *19*, 615–622. [CrossRef]
15. Palis, S.; Kienle, A. Stabilization of continuous fluidized bed spray granulation with external product classification. *Chem. Eng. Sci.* **2012**, *70*, 200–209. [CrossRef]
16. Palis, S.; Kienle, A. Discrepancy based control of continuous fluidized bed spray granulation with internal product classification. *IFAC Proc. Vol.* **2012**, *45*, 756–761. [CrossRef]
17. Palis, S.; Kienle, A. Stabilization of continuous fluidized bed spray granulation-a Lyapunov approach. *IFAC Proc. Vol.* **2010**, *43*, 1362–1367. [CrossRef]
18. Nandong, J. Double-loop control structure for oscillatory systems: Improved PID tuning via multi-scale control scheme. In Proceedings of the 10th Asian Control Conference (ASCC), Kota Kinabalu, Malaysia, 31 May–3 June 2015.
19. Park, J.H.; Sung, S.W.; Lee, I-B. An enhanced PID control strategy for unstable processes. *Automatica* **1998**, *34*, 751–756. [CrossRef]
20. Ramkrishna, D. *Population Balances: Theory and Applications to Particulate Systems in Engineering*; Academic Press: Cambridge, MA, USA; London, UK, 2000.
21. Vesjolaja, L.; Glemmestad, B; Lie, B. Population balance modelling for fertilizer granulation process. In Proceedings of the 59th Conference on Simulation and Modelling (SIMS 59), Oslo, Norway, 26–28 September 2018.
22. Mörl, L. Anwendungsmöglichkeiten und Berechnung von Wirbelschichtgranulationstrocknungsanlagen. Ph.D. Thesis, Technische Hochschule Magdeburg, Magdeburg, Germany, 1981.

23. Mörl, L.; Mittelstrab, M.; Sachse, J. Zum Kugelwachstum bei der Wirbelschichtrocknung von Suspensionen oder Losungen. *Chem. Technol.* **1977**, *29*, 95–102.

24. Koren, B. *A Robust Upwind Discretization Method for Advection, Diffusion and Source Terms*; Centrum voor Wiskunde en Informatica: Amsterdam, The Netherlands, 1993; pp. 117–138.

25. Hulburt, H.M.; Katz, S. Some problems in particle technology: A statistical mechanical formulation. *Chem. Eng. Sci.* **1964**, *19*, 555–574. [CrossRef]

26. Kumar, J.; Peglow, M.; Warnecke, G.; Heinrich, S.; Mörl, L. Improved accuracy and convergence of discretized population balance for aggregation: The cell average technique. *Chem. Eng. Sci.* **2006**, *61*, 3327–3342. [CrossRef]

27. Kumar, J. Numerical Approximations of Population Balance Equations in Particulate Systems. Ph.D. Thesis, Otto-von-Guericke-Universität Magdeburg, Universitätsbibliothek, Magdeburg, Germany, 2006.

28. Molerus, O.; Hoffmann, H. Darstellung von Windsichtertrennkurven durch ein stochastisches Modell. *Chem. Ing. Tech.* **1969**, *41*, 340–344. [CrossRef]

29. Heinrich, S.; Peglow, M.; Ihlow, M.; Mörl, L. Particle population modeling in fluidized bed-spray granulation—analysis of the steady state and unsteady behavior. *Powder Technol.* **2003**, *130*, 154–161. [CrossRef]

30. MATLAB. *MathWorks Announces Release 2019b of MATLAB and Simulink*; The MathWorks, Inc.: Natick, MA, USA, 2019.

31. Skogestad, S. Simple analytic rules for model reduction and PID controller tuning. *J. Process Control* **2003**, *13*, 291–309. [CrossRef]

136

Paper F

Comparison of feedback control strategies for operation of granulation loops

Authors L. Vesjolaja, B. Glemmestad, B. Lie

Comparison of feedback control strategies for operation of granulation loops

Ludmila Vesjolaja
Department of Electrical Engineering, IT and Cybernetics, University of South-Eastern Norway. E-mail: ludmila.vesjolaja@usn.no

Bjørn Glemmestad
Digital Production Department, Yara International ASA, Norway. E-mail:bjorn.glemmestad@yara.com

Bernt Lie
Department of Electrical Engineering, IT and Cybernetics, University of South-Eastern Norway. E-mail: bernt.lie@usn.no

Corresponding author: ludmila.vesjolaja@usn.no

Granulation is a particle enlargement process during which fine particles or atomizable liquids are converted into granules via a series of complex granulation mechanisms. In this paper, two feedback control strategies are implemented to make granulation loop processes more steady to operate, i.e., to suppress oscillatory behavior in the produced granule sizes. In the first control strategy, a classical proportional-integral (PI) controller is used, while in the second, a double-loop control strategy is used to control the median diameter of the granules leaving the granulator. The simulation results showed that using the proposed control design for the granulation loop can eliminate the oscillatory behaviour in the produced granule median diameter and make granulation loop processes more steady to operate. A comparison between the two proposed control strategies showed that it is preferable to use the double-loop control strategy.

KEYWORDS: granulation loop, oscillatory behavior, dynamic modeling, population balance, automatic control, PID controller

1 Introduction

Granulation is a particle design technique during which fine particles are converted into larger particles called granules. As a result of granulation process, granules with the desired properties are produced. The desired granule properties depend on the product quality requirements. Some of the common granule properties of interest are particle size, moisture content, porosity, compressibility and etc. Granule formation and their properties also depends on granulation mechanisms. According to Iveson et al. [8], there are three main granulation mechanisms: (i) particle nucleation that is the initial stage of particle formation, (ii) particle growth that can occur due to various mechanisms such as particle layering and and particle agglomeration, and (iii) particle breakage, e.g., particle surface attrition due to particle collision [8, 3]. This paper is focused on the granulation process used in fertilizer industry. A rotary drum granulator is used to produce particles with the desired particle properties. Here, the particle property of interest is the particle size distribution (PSD). Granule growth inside the drum granulator is assumed due to (i) particle layering, and (ii) binary particle agglomeration as shown in Figure 1. Here, particle layering is considered as a continuous process during which particle growth occurs by successive coating of the slurry onto a particle. Binary particle agglomeration is considered as a process that occurs due to successful collision of two particles, resulting in the formation of a larger, composite particle [8, 12, 31, 30].

In fertilizer industry, there are operational challenges in the granulation processes that are of interest in terms of process control view. Control of granulation processes is needed since (i) granulation processes are operated below design capacity, and (ii) oscillatory behavior may occur in the produced granule size and in the granule flow rates. This paper focuses on damping and elimination of oscillatory behavior seen on granulation loop plants.

Oscillatory behavior is observed on different, with regard to the granulator type, granulation loop plants. For example, studies on oscillatory behaviour

Figure 1
Particle growth due to particle layering and particle agglomeration inside the drum granulator [31].

seen in fluidized bed granulators are given in [17, 23]. Numerous studies are focused on control of fluidized bed granulators, including [1, 2, 4, 19, 20, 21]. The recent studies regarding stabilization of the continuous granulation loop process in the fluidized bed are reported in [17, 18]. Similarly to fluidized bed granulators, granulation loop processes using drum granulators also show oscillatory behavior of particle sizes and particle flow rates [29, 30]. Studies regarding the control of the granulation processes where the rotary drums are used as the granulators are given in [5, 24, 29, 33, 32].
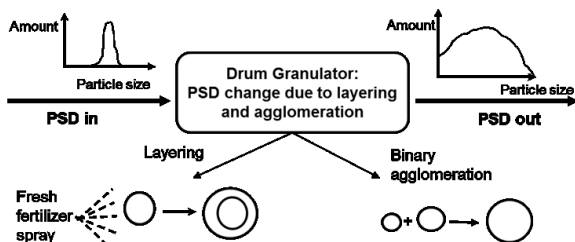
A mathematical model of the granulation process is needed to study the possibilities for eliminating the oscillatory behaviour seen on industrial scale granulation loop plants. There are several approaches to modeling granulation processes. Typically modeling approahes are divided into (i) black box models also referred as empirical models that are based on actual plant data, and (ii) grey-box models called also mechanistic models that are based on conservation principles. Mathematical modeling of the granulation processes for control studies is commonly performed using the population balance (PB) principle [26]. In [3, 18, 23, 31, 30, 7, 25, 28, 33, 32] mechanistic models using the PB principles are developed. Generic drum granulation models are presented in [24, 25, 28]. In this paper, a mechanistic model using the PB principles is used to model the granulation process.

Even though numerous research works have been performed in studying granulation processes, the control of the granulation loop process still remains a challenge. The motivation of this research is to design proper control strategies to make production of granulation loop processes more steady to operate, i.e., to eliminate the oscillatory behavior observed in the produced particle sizes.

This paper is the extension of our previous studies reported in [29]. In this paper, the authors extend the previous study [29] by comparing two feedback control strategies with the objective to eliminate the oscillatory behaviour in the the produced particle sizes. Thus, the main contribution of this paper is the comparison of the double-loop control strategy [29] with the classical PI controller. Another contribution of this paper is the analysis of the system dynamics using a bifurcation analysis.

The paper is organized as follows: In Section 2, the description and the model of the granulation loop are given. Open loop simulations of the dynamic model are performed in Section 3. The design of the control system for the granulation loop process is given in Section 4.1. In Section 4.2, a classical PI-controller is applied to the granulation loop process. A description of a double-loop control strategy is provided in Section 4.3. Simulation results and discussion are given in Section 5, while conclusions are drawn in Section 6. Descriptions of the symbols used in the paper are listed in Appendix 1.
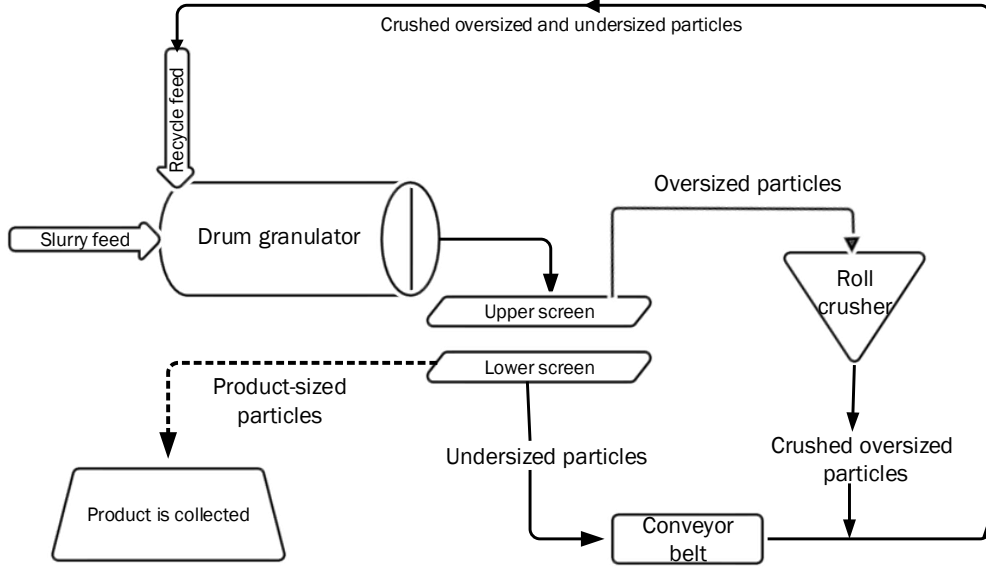
2 Granulation loop

2.1 Process description

The granulation loop with the recycling studied in this paper is shown in Figure 2. The main granulation loop units are: (i) rotary drum granulator, (ii) double-deck screen (particle classifier), and (iii) roll crusher. The rotary drum is used to produce solid particles (granules) by spraying a slurry melt on recycled particles. In the granulation drum, particles grow in their sizes due to various granulation mechanisms. In this paper, the particle growth is assumed to occur due to both the particle layering and the binary particle agglomeration [8, 12, 31, 30].

Together with the granulator, the granulation loop also consists of a product classification step (double-deck screens). Granules that remain lying on the upper screen (over-sized particles) are sent to the crusher. The crushed granules act as a seed to the granulator, and are recycled back to the granulator. Granules that pass through the upper screen but remain lying on the lower screen are the product-sized particles that are collected for further use. Granules that are too small to remain lying on the upper nor on the lower screen are the under-sized particles that are recycled back to the granulator together with the crushed over-sized particles. Thus, the recycle feed contains both the crushed over-sized particles and the under-sized particles.

2.2 Mathematical model

The overall flow scheme for the drum granulation loop is given in Figure 3 (Symbol descriptions are given in Appendix 1). A continuous granulation process in a rotary drum was modeled using a mass based population balance equation (PBE). Here, the developed models are 2-dimensional models with respect to particle size and position in the granulator. The resulting PBE is partial differential equation (PDE) that is discretized in terms of its internal coordinate (particle diameter) and external coordinate (axial position in the granulator). The mass

Figure 3
Simplified flow diagram of the drum granulation loop used for modeling the granulation loop [30].
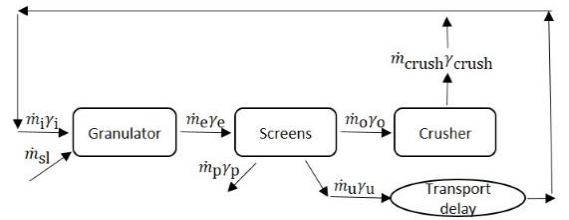
based PBE with particle diameter (d) as the internal coordinate, spatial variation (z) as the external coordinate, and time coordinate (t) is

$$\frac{\partial m(d,z,t)}{\partial t} = -d^3 \frac{\partial}{\partial d}\left[G\frac{m(d,z,t)}{d^3}\right] + B(d,z,t)$$
$$- D(d,z,t) - \frac{\partial}{\partial z}\left[v \cdot m(d,z,t)\right], \quad (1)$$

where $m(d,z,t)$ is the mass density function [29, 30, 31]. Equation (1) is formed by assuming the two granulation mechanisms, particle growth due to layering and particle agglomeration. Equation (1) is derived from a number based PBE as in [26, 31]. Derivation of Equation (1) and mathematical expres-

sions for the G, B, D terms in Equation (1) are reported in detail in [31, 30]. Mathematical models of the screens and the crusher (Figure 3) are given in Table 1.

2.3 Model solution

The solution to PBEs is found by discretizing the PDE (Equation (1)) into a system of ordinary differential equations (ODEs). The PDEs for PBE are discretized in terms of the internal coordinate, i.e., particle diameter, and also in terms of the external coordinate, i.e., the position in the drum granulator.

The two granulation mechanisms, particle layering and particle agglomeration, require different discretization algorithms. In this paper, the *layering term* in Equation (1) is discretized using a finite volume scheme extended by a Koren flux limiter function (KFL) [9, 30]. The *agglomeration term* in Equation (1) is discretized using a cell average scheme described in [10, 11], and applied to a mass-based PBE in [30, 31].

If N_c is the total number of particle size classes (cells), the discretized PBE in terms of particle size can be written as,

$$
\begin{aligned}
\frac{dM_i}{dt} = {} & d^3 \left[Gm\left(t, d_{i-\frac{1}{2}}\right) - Gm\left(t, d_{i+\frac{1}{2}}\right) \right] \\
& + d_i^3 [B_{i-1}\lambda_i^-\left(\bar{d}_{i-1}\right) H\left(\bar{d}_{i-1} - d_{i-1}\right) \\
& \quad + B_i\lambda_i^-\left(\bar{d}_i\right) H\left(d_i - \bar{d}_i\right) \\
& \quad + B_i\lambda_i^+\left(\bar{d}_i\right) H\left(\bar{d}_i - d_i\right) \\
& \quad + B_{i+1}\lambda_i^+\left(\bar{d}_{i+1}\right) H\left(d_{i+1} - \bar{d}_{i+1}\right)] \\
& - M_i \sum_{k=1}^{N_c} \beta_{ik}\frac{M_k}{d_k^3} + \frac{\partial}{\partial z}\left(v \cdot m_{i,z}\right), \quad (2)
\end{aligned}
$$

where

$$
\begin{aligned}
m\left(z, t, d_{i-\frac{1}{2}}\right) \approx {} & \frac{1}{\Delta d}\left\{ \frac{M_{i-1}}{d_{i-1}} + \frac{1}{2}\phi\left(\theta_{i-\frac{1}{2}}\right) \right. \\
& \left. \times \left(\frac{M_{i-1}}{d_{i-1}^3} - \frac{M_{i-2}}{d_{i-2}^3} \right) \right\},
\end{aligned}
\quad (3)
$$

$$
\begin{aligned}
m\left(z, t, d_{i+\frac{1}{2}}\right) \approx {} & \frac{1}{\Delta d}\left\{ \frac{M_i}{d_i} + \frac{1}{2}\phi\left(\theta_{i+\frac{1}{2}}\right) \right. \\
& \left. \times \left(\frac{M_i}{d_i^3} - \frac{M_{i-1}}{d_{i-1}^3} \right) \right\},
\end{aligned}
\quad (4)
$$

with

$$
\theta_{i-\frac{1}{2}} = \frac{\frac{M_i}{d_i^3} - \frac{M_{i-1}}{d_{i-1}^3} + \varepsilon}{\frac{M_{i-1}}{d_{i-1}^3} - \frac{M_{i-2}}{d_{i-2}^3} + \varepsilon}, \quad (5)
$$

Table 1
Model expressions for the screens and the crusher in Figure 3.

Model unit	Model expression
Screen	$\dot{m}_o\gamma_o = \Upsilon_{\text{upp}}\dot{m}_e\gamma_e$
	$\dot{m}_u\gamma_u = \left(1 - \Upsilon_{\text{upp}}\right)\left(1 - \Upsilon_{\text{low}}\right)\dot{m}_e\gamma_e$
	$\dot{m}_p\gamma_p = \left(1 - \Upsilon_{\text{upp}}\right)\Upsilon_{\text{low}}\dot{m}_e\gamma_e$
	$\Upsilon_{\text{upp, low}} = \dfrac{1}{1 + \left(\frac{d_{\text{screen, upp, low}}}{d}\right)^2 \exp(k)}$
	$k = \left[K_{\text{eff, upp, low}}\left(1 - \left(\frac{d}{d_{\text{screen, upp, low}}}\right)^2\right) \right]$
Crusher	$\gamma_{\text{crush}} = \dfrac{1}{\sqrt{2\pi\sigma_{\text{crush}}^2}} \exp\left(-\dfrac{(d - d_{\text{crush}})^2}{2\sigma_{\text{crush}}^2}\right)$
	$\dot{m}_{\text{crush}}\gamma_{\text{crush}} = \left(\sum \dot{m}_o\gamma_o\right) \cdot \gamma_{\text{crush}}$
	$\dot{m}_i\gamma_i = \dot{m}_{\text{crush}}\gamma_{\text{crush}} + \dot{m}_u\gamma_u$

and

$$\theta_{i+\frac{1}{2}} = \frac{\frac{M_{i+1}}{d_{i+1}^3} - \frac{M_i}{d_i^3} + \varepsilon}{\frac{M_i}{d_i^3} - \frac{M_{i-1}}{d_{i-1}^3} + \varepsilon}. \tag{6}$$

The birth B_i of the particles are given as

$$B_i = \frac{1}{2} \sum_{j=1}^{i} \sum_{k=1}^{i} \beta_{jk} \frac{M_j}{d_j^3} \frac{M_k}{d_k^3}, \tag{7}$$

and the average diameter of all the new-born particles in the ith class is

$$\bar{d}_i = \left[\frac{\sum_{j=1}^{i} \sum_{k=1}^{i} \beta_{jk} \frac{M_j}{d_j^3} \frac{M_k}{d_k^3} \left(d_j^3 + d_k^3 \right)}{\sum_{j=1}^{i} \sum_{k=1}^{i} \beta_{jk} \frac{M_j}{d_j^3} \frac{M_k}{d_k^3}} \right]^{\frac{1}{3}}. \tag{8}$$

Agglomeration kernels (β_{jk} and β_{ik}), the dimensionless term $\lambda_i^{\pm}(d)$ and the Heaviside step function H in Eq. 2 are defined in [30, 31].

Assuming constant particle velocity inside the granulator space, the external coordinate discretization is

$$v \frac{\partial}{\partial z} (m_{i,z}) = v \left[m_{i,z-\frac{1}{2}} - m_{i,z+\frac{1}{2}} \right]. \tag{9}$$

The approximation of the terms $m_{i,z\pm\frac{1}{2}}$ is performed using the KFL scheme similarly to the *layering term* approximation. The resulting expressions are given in detail in [30].

3 System dynamics

3.1 Simulation setup

Dynamic simulations are performed using MATLAB and Simulink [14]. Simulation setup is the same as given in [29]. Simulation parameters are listed in Table 2.
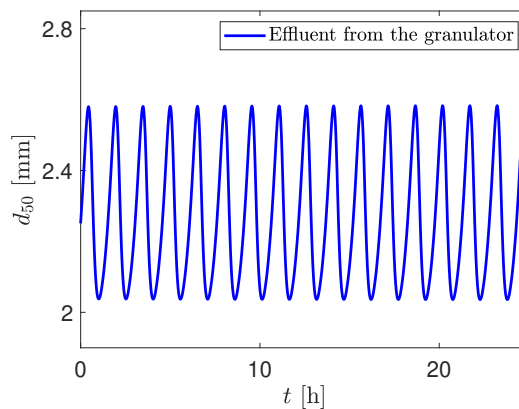
3.2 Oscillatory behavior

The dynamic model developed for the rotary drum granulation loop is able to capture the main dynamics of the granulation process. Through dynamic simulations, the model was found to reproduce the oscillatory behaviour typically seen in granulation loops. In particular, the developed model is able to reproduce oscillatory behaviour in the particle size distribution, measured as the particle size d_{50} diameter (median diameter that corresponds to the intercept for 50% of cumulative mass), Figure 4.

Similarly to the simulation results, oscillatory behaviour is also observed in the industrial-scale plants as shown in Figure 5. Oscillatory behaviour is observed not only in the granule d_{50} but also in the product quantity (mass flow rates). Illustrations showing oscillatory behavior in product quantity are given in [30] and not illustrated in this paper for the sake of brevity.

Table 2
Simulation parameters [29].

Parameter	Value
Range of d [mm]	0-8
Number of particle classes	80
Grid type	linear
Length of granulator [m]	10
Number of compartments	3
ρ [kg· m^{-3}]	1300
β_0 [s^{-1}]	$1.0 \cdot 10^{-13}$
$\dot{m}_{\text{sl,i}}$ [kg· h^{-1}]	1000
$d_{\text{screen, upp}}$ [mm]	3.3
$d_{\text{screen, low}}$ [mm]	1.9
$K_{\text{eff, upp}}$	45
$K_{\text{eff, low}}$	45
d_{crush} [mm]	2.0–1.0
σ_{crush}	0.25
T_{R} [s]	600
Transport delay [s]	600

Figure 4
Simulated PSD of the effluent from the granulator.

Figure 5
Oscillatory behavior in PSD of an industrial granulation loop process [29].
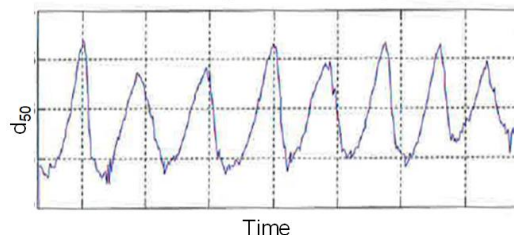
Further insight into the system dynamics of the granulation loop process is obtained from a bifurcation analysis. Here, a simple bifurcation analysis based on model simulations was performed. For this, the system was simulated until stationary conditions were reached, and the upper and the lower d_{50} value was registered when the system oscillated. In these simulations, the crusher gap spacing d_{crush} was chosen as a bifurcation parameter to analyse the change in the behaviour of the PSD, being measured as d_{50}, in the effluent from the granulator. The simulations were performed with the different values of d_{crush}, from 2 mm to 1 mm with an interval of 0.1 mm. Stable and unstable points (oscillatory behavior) of d_{crush} were determined using the obtained amplitude of stationary solutions at different d_{crush} values.

Figure 6
Bifurcation plot with the crusher gap spacing d_{crush} as bifurcation variable.
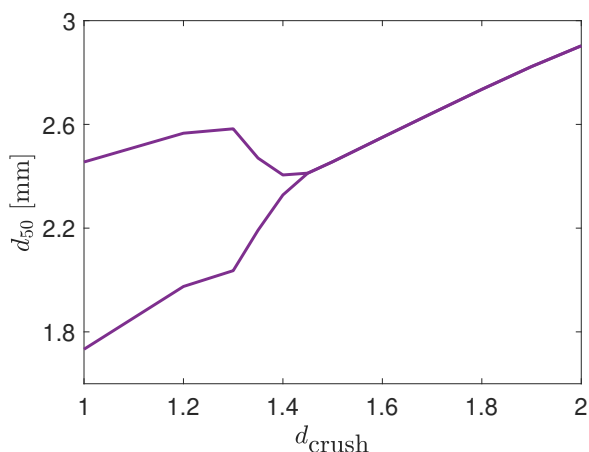
Simulation results of the bifurcation analysis are illustrated in Figure 6. In Figure 6, the minimum and the maximum d_{50} value of the oscillations at a certain d_{crush} is depicted. These simulation results showed that at larger crusher gap spacings, a stable granulation process is observed ($d_{\text{crush}} < 1.5$ mm). However, as the crusher gap spacing is reduced, the granulation loop starts to show oscillatory behavior, and at a certain crusher gap spacing ($d_{\text{crush}} < 1.4$ mm), sustained periodic oscillations occur. The probable reason of the oscillatory behavior of the granulation process is described in [30].

4 Control of the granulation loop

4.1 Design of the control system

In this paper, the stability of the d_{50} diameter is performed by implementing a controller having a 3-way valve opening α as the control input. When the valve α is opened, i.e., $0 < \alpha \le 1$, some fraction of the product-sized particle mass flow rate is added to the

recycle flow. The control output is the particle d_{50} diameter in the effluent, i.e., on the elevator coming from the granulator before the granules are sieved. Details regarding the design of the control system are given in [29].

4.2 Classical PI-controller

Here, a classical proportional-integral PI-controller was used to eliminate the oscillatory behavior of the process. The schematic diagram of the PI-controller for the granulation loop process (oscillatory process) is illustrated in Figure 7.

Figure 7
Classical PI-controller control strategy for granulation loop process. $u = \alpha$ — control signal (valve opening); y — controlled variable (d_{50} of the effluent); r — reference point.
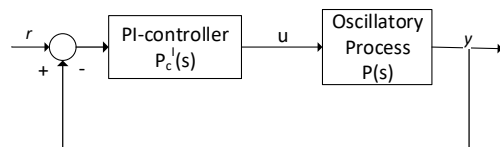
The granulation plant can be approximated as an oscillatory process having a transfer function

$$P(s) = \frac{K_{\text{p}} e^{-\tau s}}{1 + \frac{2\zeta s}{\omega_0} + \left(\frac{s}{\omega_0}\right)^2}, \qquad (10)$$

where $P(s)$ is the transfer function of the underdamped (oscillatory) process, K_{p} is the process gain, τ is the process time delay, ω_0 is the natural frequency and ζ is the damping factor.
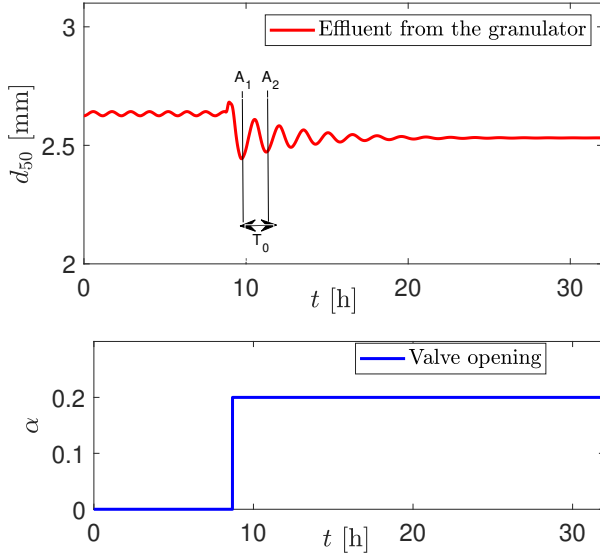
Process parameters K_{p}, τ, ζ, and ω_0 were found using a simulated step-response of the granulation process. For this, a step-change of the valve opening (ratio of the product-sized particles to be recycled) is given to the system. An example of such a step-response is shown in Figure 8. Expressions for calculating process parameters are summarized in Table 3.

Table 3
Model parameter identification.

Parameter	Expression
ζ	$\frac{1}{\sqrt{1 + (\frac{2\pi}{\sigma})^2}}$
ω_0	$\frac{2\pi}{T_0}$
σ	$\ln\left(\frac{A_1}{A_2}\right)$

Figure 8
Illustrative example of a step-response: A change in d_{50} of the effluent from the granulator as a response to a step change in the valve opening α; T_0—period of the oscillation and A_1, A_2—amplitudes of the first two overshoots of the 2nd order response.

Figure 9
Representation of the double-loop control strategy as: (a) double-loop control algorithm, (b) single-loop control algorithm [16]; $u = \alpha$ — control signal (valve opening), $y = d_{50}$ — controlled variable (d_{50} of the effluent), r — reference point.

The PI controller equation in frequency domain is written as,

$$P_\mathrm{c}^\mathrm{I}(s) = K_\mathrm{c}^\mathrm{I}\left(1 + \frac{1}{T_\mathrm{i}^\mathrm{I} s}\right), \qquad (11)$$

where K_c^I is the proportional gain of the PI controller and T_i^I is the integral time constant of the PI controller. The PI controller tuning parameters, K_c^I and T_i^I, were found using Skogestad's tuning rules for oscillatory processes [13] that are given in Table 4.

Table 4
Expressions for designing the classical PI controller $P_\mathrm{c}^\mathrm{I}(s)$.
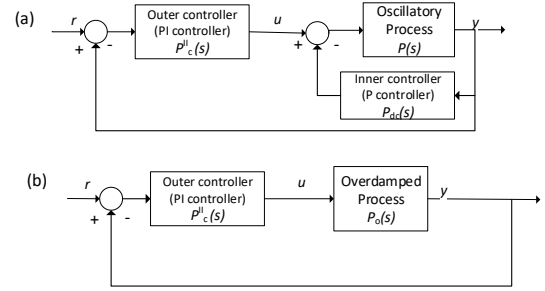
Parameter	Expression
K_c^I	$\frac{2\left(\frac{1}{\omega_0}\zeta\right)}{k\left(T_\mathrm{c}^\mathrm{I}+\tau\right)}$
T_i^I	$2\left(\frac{1}{\omega_0}\zeta\right)$
T_c^I	$-\tau < T_\mathrm{c}^\mathrm{I} < \infty$

4.3 Double-loop control strategy

In this section, a double-loop control strategy for oscillatory systems [16, 22, 29], is applied to control the d_{50} diameter in the effluent from the granulator. The double-loop control strategy consists of two controllers, an inner controller and an outer controller. The proposed double-loop control strategy is illustrated in Figure 9.

The inner controller ($P_\mathrm{dc}(s)$ in Figure 9) is used to convert the underdamped process ($P(s)$ in Figure 9) to an overdamped process ($P_\mathrm{o}(s)$ in Figure 9). The outer controller ($P_\mathrm{c}^\mathrm{II}(s)$ in Figure 9), which is the main controller, is used to achieve specified performance. The double-loop control strategy resembles the cascade control structure. However, the main differences between the double-loop control structure and the conventional cascade control structure are:

- With the double-loop control structure, the same measurement, y, is used for both the inner controller and the outer controller (Figure 9). In the conventional cascade control structure, usually the measurement used for the inner loop controller and the measurement used for the outer loop controller are different. The measurement for the outer control loop, for the conventional cascade control structure, is the controlled variable of the system that needs to be tracked to a given set (reference) point.

- With the double-loop control structure, the inner and the outer control loops are usually not categorized into slow or fast controller loops as is usually done in the conventional cascade control structure.

The combined transfer function from u to y in Figure 9 is

$$P_\mathrm{o}(s) = \frac{P(s)}{1 + P(s)\cdot P_\mathrm{dc}(s)} = \frac{P(s)}{1 + P(s)\cdot K_\mathrm{c}^\mathrm{i}}, \quad (12)$$

where $P_\mathrm{o}(s)$ is the transfer function of the overdamped system and $P_\mathrm{dc}(s)$ is the transfer function of the inner (damping) controller. Here, the damping controller is a P-controller, i.e., $P_\mathrm{dc}(s) = K_\mathrm{c}^\mathrm{i}$.

Expressions for finding process parameters of the overdamped system are summarized in Table 5. The expressions listed in Table 5 are derived by using an approximation of the time delay as $e^{-\tau s} \approx 1 - \tau s$.

7

Table 5
Expressions for designing the double-loop control strategy $P_c^{II}(s)$.

Overdamped system parameters	$K_c^i = 2 \cdot \dfrac{(\zeta_i^2 + \zeta\tau\omega_0) \pm \sqrt{(\zeta_i^2 + \zeta\tau\omega_0)^2 + \tau^2\omega_0^2(\zeta_i^2 - \zeta^2)}}{\tau^2 w_0^2 K_p}$ $\omega_i = \omega_0 \sqrt{1 + K_c^i K_p}$ $K_p^i = \dfrac{K_p}{1 + K_c^i K_p}$ $\zeta_i > 1$ $T_1 = \dfrac{\zeta_i + \sqrt{\zeta_i^2 - 1}}{\omega_i}$ $T_2 = \dfrac{\zeta_i - \sqrt{\zeta_i^2 - 1}}{\omega_i}$
Outer controller in frequency domain	$P_c^{II}(s) = K_c^{II}\left(1 + \dfrac{1}{T_i^{II} s}\right)$
Outer controller parameters	$K_c^{II} = \dfrac{T_{eff}}{K_p^i (T_c^{II} + \tau_{eff})}$ $T_i^{II} = \min(T_{eff}, 4(T_c^{II} + \tau_{eff}))$ $-\tau_{eff} < T_c^{II} < \infty$ $\tau_{eff} = \tau + 0.5 T_2$ $T_{eff} = T_1 + 0.5 T_2$

For the outer controller, the PI controller was used. The outer controller was used to track a reference point. Tuning of the outer controller was performed using SIMC PI tuning rules given in [27] and applied to the granulation control system in [29].

Expressions used to find the PI controller tuning parameters, overdamped process parameters and outer controller parameters, for the double-loop control strategy are summarized in Table 5. In overdamped systems, the damping factor is greater than 1. In this study, the value for the inner loop damping factor is set to $\zeta_i = 1.5$. Underdamped process parameters, K_p, τ , and ω_0, are calculated using expressions given in Table 3, i.e., were found using a simulated step-response of the granulation process shown in Figure 8.
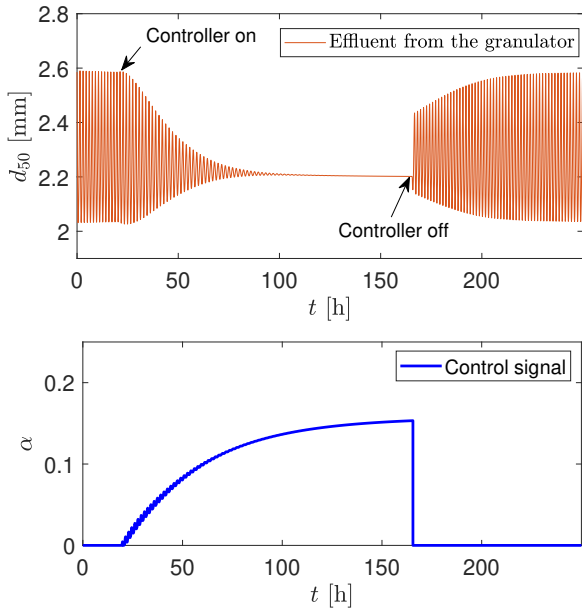
5 Simulation Results

Feedback control strategies are applied to make granulation loops more steady in operation. The closed loop simulations were performed using the design of the control system of the granulation loop process described in Section 4.1. The controller is implemented to suppress the oscillatory behavior of the process parameters as discussed in Section 3. In particular, the controller is designed to control the PSD, measured as d_{50}, of the particles leaving the granulator. Thus, the control output is the d_{50} of the particles leaving the granulator (effluent from the granulator). Stabilization of the oscillatory behavior is performed by recycling some of the product-sized particles back to the granulator. Thus, the control input is the valve opening α that controls the recycled product flow.

Two control strategies are used to control the d_{50} diameter: (i) a classical PI-controller and (ii) a double-loop control strategy. First, the closed simulations were performed using the classical PI-controller. The PI-controller was tuned using SIMC tuning rules for the oscillatory systems. Then fine tuning was done to achieve better performance of the PI-controller.

In Figure 10 and 11, the controller was turned on when the sustained oscillatory behavior in PSD distribution, measured as (d_{50}), of the particles leaving the granulator was observed. Particularly, the controller was turned on at the maximum point of the cycle, at $t = 20$ h with $d_{crush} = 1.3$ mm.

Figure 10
Control input and control output when the classical PI-controller is used: controller turned on at the maximum point of the cycle.

Figure 11
Product-sized mass flow when the classical PI-controller is used: controller turned on at the maximum point of the cycle.
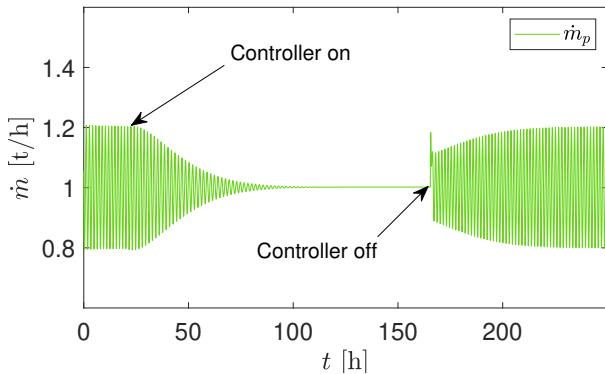

Simulation results using the classical PI-controller showed that it is possible to use a simple PI controller in order to eliminate the oscillatory behaviour in product quality (PSDs) and quantity (mass flow rate). When the PI controller was turned on, the oscillations were suppressed (damped) and the desired reference point was tracked. However, the convergence rate towards the operating point was relatively slow (it took more than 24 h of process simulation). This would limit the use of a such control strategy in a industrial-scale plant.

Simulations results when the double-loop control strategy was used are depicted in Figure 12 and 13. Similarly to simulations with the classical PI-controller, these simulations were also performed when the sustained oscillations in the granulation process were observed, i.e., at $d_{crush} = 1.3$. For a fair comparison, in Figure 12 and 13 the controller

was turned on at the same maximum point of the cycle, at $t = 20$. With the double-loop control strategy the oscillations were quickly damped when the controller was turned on - a non-oscillating particle d_{50} and mass flow rates of the effluent were obtained. It took only around 6 h to reach steady state value when the controller was turned on. Thus, with the double control strategy it is possible to reach significantly faster controller response compared to the classical PI-controller.

Figure 12
Control input and control output when the double-loop control strategy is used: controller turned on at the maximum point of the cycle [29].
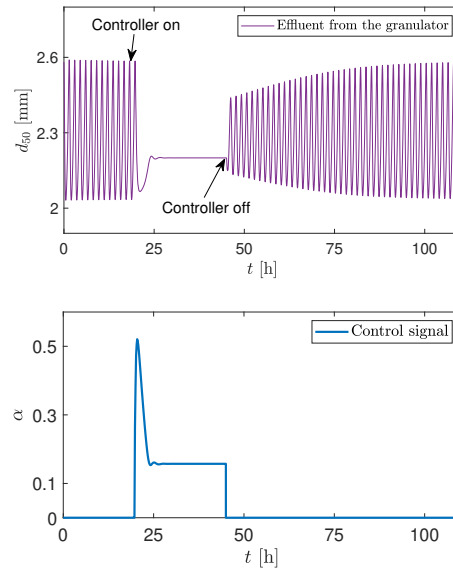

Figure 13
Product-sized mass flow when the double-loop control strategy is used: controller turned on at the maximum point of the cycle.

9
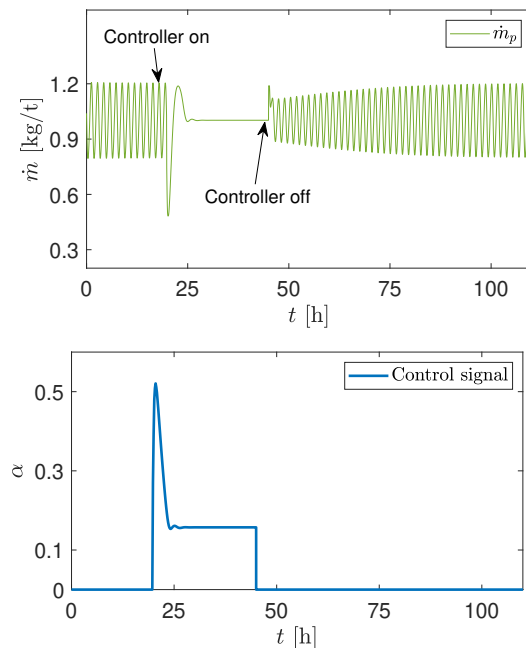
For further understanding of the controller behavior, the controller was turned on at the minimum point of the cycle (Figure 14). For fair comparison, identical controller parameters were used when controller was turned on at maximum and minimum cycle points. These simulations were performed both with the classical PI-controller and with the double-loop control strategy. In Figure 14, the response in the controlled variable for both control strategies are shown.

Figure 14
Classical PI-controller vs double-loop control strategy: controller turned on at the minimum point of the cycle.
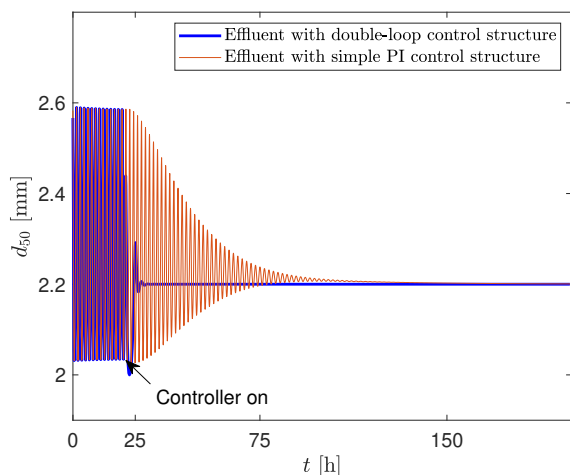

Similarly to the previous simulation results, significantly faster convergence rate towards the operating point is achieved when double-loop control strategy is used. As to the position in the cycle when the controller was turned on, no significant differences were seen for either control strategies, Figure 15 and 16. In the case of the double-loop control strategy, a slightly faster convergence rate towards the operating point is achieved when the controller is turned on at the maximum point of the cycle, 7h vs 6h with the minimum and maximum points respectively (Figure 16). To sum up, stabilization of the granulation process is achieved significantly faster with the double-loop control strategy than with the classical PI-controller.

For both control strategies, the point of the cycle at which the controller is turned on (maximum or minimum point of the cycle) does not significantly affect the closed loop response. This allows the operators to instantaneously turn on the controller without having to wait for several hours to reach either the maximum or minimum point of the cycle.

The double-loop control strategy is based on the well-established linear system theory which is already widely excepted in the process industry. This also allows for easier integration of this control strategy in the existing control system. Implementation requires to combine current on-line sensors for particle size distribution to provide an estimate of the median d_{50}. Online particle size analyzers are com-

Figure 15
Comparison of the control outputs for the classical PI-controller: controller turned on at minimum vs maximum point.
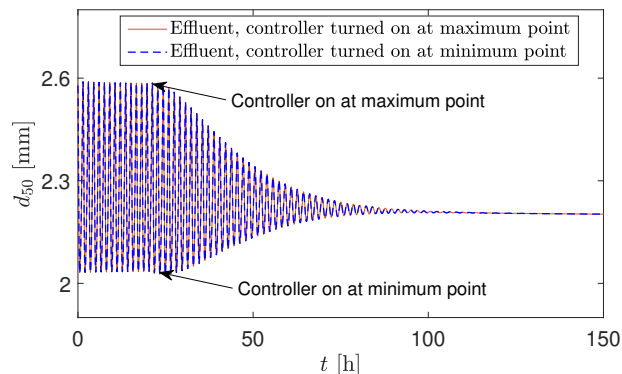
Figure 16
Comparison of the control outputs for the double-loop control strategy: controller turned on at minimum vs maximum point.
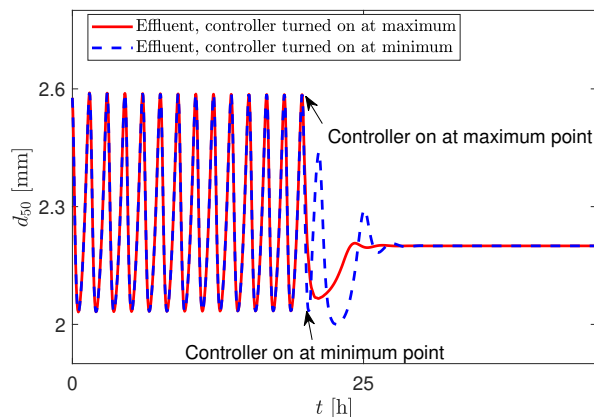
mercially available and often installed in granulation plants. Such devices can analyze several properties related to size and shape of particles, and the median d_{50} is used as a measurement to a PID controller in the Process Control System. In addition, process must allow for direct manipulation (preferably automatic) of the discussed control input, the fraction of return flow. The double-loop control strategy uses a combination of a P controller and a PI controller, and the design of the inner loop controller provides flexibility in the sense that the operator can freely choose the desired damping ratio and calculate the gain of the inner controller. The additional inner loop of the double control strategy does make the control system slightly complex compared to the classical PI controller. However, the advantage with the double-loop control strategy is that the oscillatory behaviour is suppressed significantly faster. This also means shorter transient periods in the plant and, hence, less production of the off-spec particles (over-sized and under-sized particles). Faster and tighter control of the product specification (d_{50} of the effluent from the granulator) leads

to improved operation with further means improved profit. With the double-loop control strategy the particle mass flow rates also converges towards the operating point significantly faster compared to the classical PI controller. A stable mass flow rate also eliminates overloading or under loading of various equipment in the granulation loop.

Figure 17 shows that the double-loop control strategy is able to compensate for disturbances. Here, a crusher gap spacing is used as the disturbance. First, disturbances are applied when the controller is turned on. Second, the controller is turned off using the last value of the control input that is obtained while the controller was turned on. When the controller is turned off and the disturbance is applied to the system, the oscillatory behaviour in the particle d_{50} reappears (Figure 17). Like the double-loop control strategy, the classical PI controller is able compensate for the disturbances, however, not illustrated in this paper for the sake of brevity.

6 Conclusions

The model presented in this paper was found to reproduce oscillatory behaviour of the granulation loop process seen on industrial-scale granulation plants. According to the performed bifurcation analysis, oscillatory behaviour in the particle d_{50} occurs at

crusher gap spacing $d_{\mathrm{crush}} < 1.4$ mm. Dynamic open loop simulations showed that it is possible to suppress oscillatory behavior of granulation loop process by recycling back some fraction of the product-sized particles.

Two feedback control strategies are proposed to suppress the oscillatory behavior of granulation loop process. Both control strategies utilize the most used control algorithm in the industry, namely the PI controller. In the first control strategy, a classical PI-controller is used. In the second — a double-loop control strategy with the two controllers, a P-controller and a PI-controller. Closed loop simulation results showed that both control strategies are able to suppress oscillatory behavior in PSD of the granules leaving the granulator. Different simulation scenarios are performed for understanding the controllers behaviors.

Simulation results showed that there is no significant difference in the dynamic response when the controller is turned on at the minimum point in the cycle or at the maximum point. The comparison between the two proposed control strategies shows that it is possible to achieve faster convergence rate towards the operating point when the double-loop control strategy is used. Thus, it can be advantageous to use the double-loop control strategy to make the granulation loop processes more steady to operate.

Figure 17
Disturbance rejection: Disturbances are applied at $t = 20$ h and $t = 65$ h (controller is turned on), and at $t = 142$ h (controller is turned off, $u_{\mathrm{manual}} = u_{\mathrm{auto}}$).

11
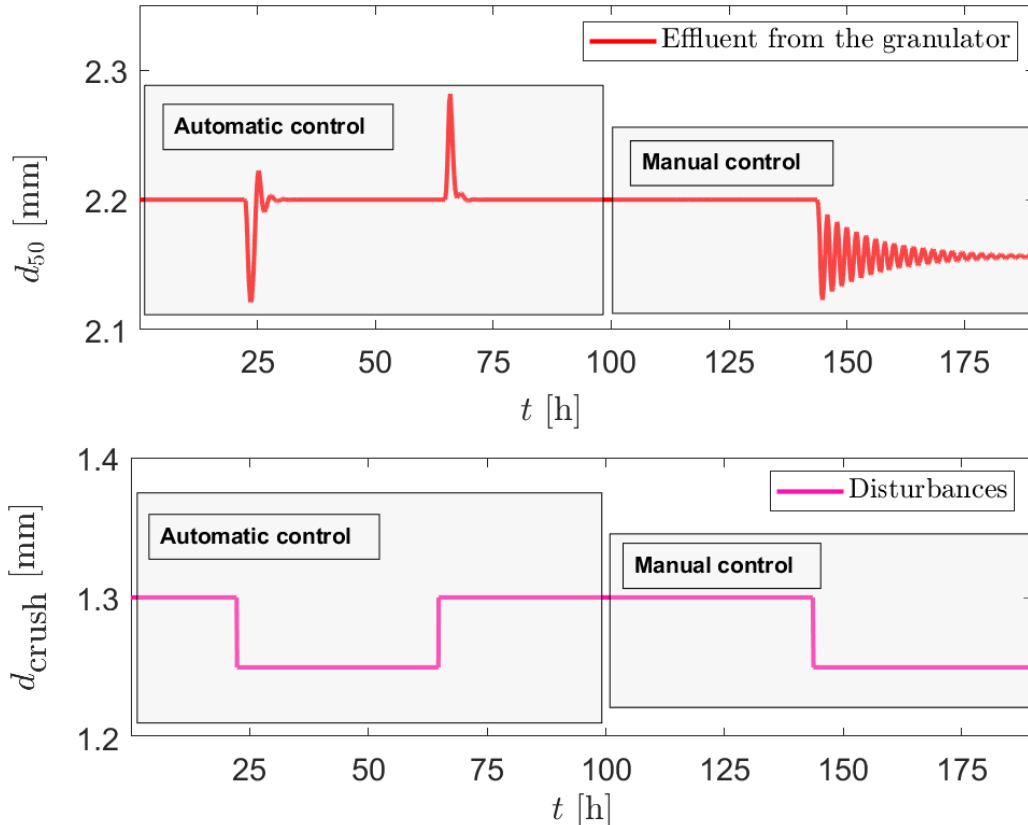
Appendix 1

Symbol	Description
B	birth rate due to particle agglomeration
D	death rate due to particle agglomeration
G	growth rate due to particle layering
H	Heaviside step function
K_{eff}	separation efficiency of the screen
K_{c}	proportional gain of the controller
T_{i}	integral time constant
K_{p}	process gain
$P(s)$	transfer function
d	particle diameter
d_{50}	particle median diameter
d_{screen}	mesh size of the screen
m	mass density function
$\dot{m}$	mass flow rate
t	time
v	velocity
u	manipulatable variable
y	controlled variable
α	valve opening
β	agglomeration rate (kernel)
γ	particle size distribution function
Υ	probability function of the screen
ρ	particle density
σ	standard deviation
τ	time delay
ζ	damping factor
λ	dimensionless term
ω	natural frequency

Subscript	Description
crush	crusher
e	effluent from the granulator
i	influent to the granulator
o	over-sized particles
p	product-sized particles
sl	slurry
u	under-sized particles
upp	upper screen
low	lower screen
i	size class
z	compartment of the granulator

Acknowledgment

References

[1] Bück, A., Dürr, R., Schmidt, M., and Tsotsas, E. Model Predictive Control of Continuous Layering Granulation in Fluidised Beds with Internal Product Classification. Journal of Process Control, 2016, 45,65-75. doi:10.1016/j.jprocont.2016.07.003.

[2] Bück, A., Palis, S., Tsotsas, E. Model-Based Control of Particle Properties in Fluidised Bed Spray Granulation. Powder Technology, 2015, 270, 575-583. doi:10.1016/j.powtec.2014.07.023.

[3] Cameron, I., Wang, F., Immanuel, C., Stepanek, F. Process Systems Modelling and Applications in Granulation: A Review. Chemical Engineering Science, 2005, 60(14),3723-3750. doi:10.1016/j.ces.2005.02.004.

[4] Drechsler, J., Peglow, M., Heinrich, S., Ihlow, M., Mörl, L. Investigating the Dynamic Behaviour of Fluidized Bed Spray Granulation Processes Applying Numerical Simulation Tools. Chemical Engineering Science, 2005, 60(14),3817-3833. doi:10.1016/j.ces.2005.02.010.

[5] Glaser, T., Sanders, C., Wang, F., Cameron, I., Litster, J., Poon, J. M.-H., Ramachandran, R., Immanuel, C., Doyle III, F. Model Predictive Control of Continuous Drum Granulation. Journal of Process Control, 2009, 19(4),615-622. doi:10.1016/j.jprocont.2008.09.001.

[6] Heinrich, S., Peglow, M., Ihlow, M., Mörl, L. Particle Population Modeling in Fluidized Bed-Spray Granulation. Analysis of the Steady State and Unsteady Behavior. Powder Technology, 2003, 130(1-3),154-161. doi:10.1016/S0032-5910(02)00259-0.

[7] Herce, C., Gil, A., Gil, M., Cortes, C. A Capetaguchi Combined Method to Optimize a NPK Fertilizer Plant Including Population Balance Modeling of Granulation-Drying Rotary Drum Reactor. In Computer Aided Chemical Engineering, 2017, 40, 49-54. doi:10.1016/B978-0-444-63965-3.50010-6.

[8] Iveson, S., Litster, J., Hapgood, K., Ennis, B. Nucleation, Growth and Breakage Phenomena in Agitated Wet Granulation Processes: A Review. Powder Technology, 2001, 117(1-2),3-39. doi:10.1016/S0032-5910(01)00313-8.

[9] Koren, B. A Robust Upwind Discretization Method for Advection, Diffusion and Source terms. In Vreugdenhil, C. B., Koren, B. Numerical Methods for Advection-Diffusion Problems, Notes on Numerical Fluid Mechanics, 1993, 117-138.

[10] Kumar, J. Numerical Approximations of Population Balance Equations in Particulate Systems. Ph.D. Thesis, Otto-von-Guericke-Universitat Magdeburg, Universitatsbibliothek, 2006.

[11] Kumar, J., Peglow, M., Warnecke, G., Heinrich, S., Mörl, L. Improved Accuracy and Convergence of Discretized Population Balance for Aggregation: The Cell Average Technique. Chemical Engineering Science, 2006, 61(10),3327-3342. doi:10.1016/j.ces.2005.12.014.

[12] Litster, J., Ennis, B. The Science and Engineering of Granulation Processes, Springer Science & Business Media, 2004.

[13] Manum, H. Extensions of Skogestad's SIMC Tuning Rules to Oscillatory and Unstable Processes. NTNU Technical Report, 2005. Viewed 17 November 2020, http://folk.ntnu.no/skoge/diplom/prosjekt05/manum/rapport.pdf

[14] MATLAB. The MathWorks, Inc., Natick, Massachusetts, United States., 2019a.

[15] Molerus, O., Hoffmann, H. Darstellung von Windsichtertrennkurven Durch ein Stochastisches Modell. Chemie Ingenieur Technik, 1969,41(5-6),340-344. doi:10.1002/cite.330410523.

[16] Nandong, J. Double-Loop Control Structure for Oscillatory Systems: Improved PID Tuning via Multiscale Control Scheme. In 10th Asian Control Conference (ASCC), IEEE, 2015, 1-6. doi:10.1109/ASCC.2015.7244476.

[17] Neugebauer, C., Bück, A., Kienle, A. Control of Particle Size and Porosity in Continuous Fluidized-Bed Layering Granulation Processes. Chemical Engineering and Technology, 2020, 43(5),813-8. doi:10.1002/ceat.201900435.

[18] Neugebauer, C., Diez, E., Bück, A., Palis, S., Heinrich, S., Kienle, A. On the Dynamics and Control of Continuous Fluidized Bed Layering Granulation with Screen-Mill-Cycle. Powder Technology, 2019, 354,765-78. doi:10.1016/j.powtec.2019.05.030

[19] Palis, S. and Kienle, A. Stabilization of Continuous Fluidized Bed Spray Granulation - a Lyapunov Approach. IFAC Proceedings Volumes, 2010, 43(14),1362-1367. doi:10.3182/20100901-3-IT-2016.00204.

[20] Palis, S., Kienle, A. Discrepancy Based Control of Continuous Fluidized Bed Spray Granulation with Internal Product Classification. IFAC Proceedings Volumes, 2012, 45(15),756-761. doi:10.3182/20120710-4-SG-2026.00136.

[21] Palis, S., Kienle, A. Stabilization of Continuous Fluidized Bed Spray Granulation with External Product Classification. Chemical Engineering Science, 2012, 70,200-209. doi:10.1016/j.ces.2011.08.026.

[22] Park, J. H., Sung, S. W., Lee, I.-B. An Enhanced PID Control Strategy for Unstable Processes. Automatica, 1998, 34(6),751-756. doi:10.1016/S0005-1098(97)00235-5.

[23] Radichkov, R., Müller, T., Kienle, A., Heinrich, S., Peglow, M., Mörl, L. A Numerical Bifurcation Analysis of Continuous Fluidized Bed Spray Granulator with External Product Classification. Chemical Engineering and Processing, 2006, 45,826-837. doi:10.1016/j.cep.2006.02.003.

[24] Ramachandran, R., Chaudhury, A. Model Based Design and Control of a Continuous Drum Granulation Process. Chemical Engineering Research and Design, 2012, 90(8),1063-1073. doi:10.1016/j.cherd.2011.10.022.

[25] Ramachandran, R., Immanuel, C. D., Stepanek, F., Litster, J. D., and Doyle III, F. J. A Mechanistic Model for Breakage in Population Balances of Granulation: Theoretical Kernel Development and Experimental Validation. Chemical Engineering Research and Design, 2009, 87(4),598-614. doi:10.1016/j.cherd.2008.11.007.

[26] Ramkrishna, D. Population balances: Theory and Applications to Particulate Systems in Engineering. Academic Press, 2000.

[27] Skogestad, S. Simple Analytic Rules for Model Reduction and PID Controller Tuning. Journal of Process Control, 2003, 13(4),291-309. doi:10.1016/S0959-1524(02)00062-8.

[28] Valiulis, G., Simutis, R. Particle Growth Modelling and Simulation in Drum Granulator-Dryer. Information Technology and Control, 2009, 38(2),147-152.

[29] Vesjolaja, L., Glemmestad, B., Lie, B. Double-Loop Control Structure for Rotary Drum Granulation Loop. Processes, 2020, 8, 1423. doi:10.3390/pr8111423

[30] Vesjolaja, L., Glemmestad, B., Lie, B. Dynamic Model for Simulating Transient Behaviour of Rotary Drum Granulation Loop. Modeling, Identification and Control, 2020,41(2),65-77. doi:10.4173/mic.2020.2.3.

[31] Vesjolaja, L., Glemmestad, B.,Lie, B. Population Balance Modelling for Fertilizer Granulation Process. Linköping Electronic Conference Proceedings, 2018,153,95-102. doi:10.3384/ecp1815395.

[32] Wang, F., Cameron, I. A Multi-Form Modelling Approach to the Dynamics and Control of Drum Granulation Processes. Powder Technology, 2007, 179(1-2),2-11. doi:doi.org/10.1016/j.powtec.2006.11.003.

[33] Wang, F., Ge, X., Balliu, N., Cameron, I. Optimal Control and Operation of Drum Granulation Processes. Chemical Engineering Science, 2006, 61(1),257-267. doi:10.1016/j.ces.2004.11.067.

Paper G

Non-linear model based predictive control for drum granulation loop process

Authors L. Vesjolaja, B. Glemmestad, B. Lie

Non-linear model based predictive control for drum granulation loop process

Ludmila Vesjolaja[a,*], Bjørn Glemmestad[b], Bernt Lie[a]

[a]*Department of Electrical Engineering, IT and Cybernetics, University of South-Eastern Norway, Norway.*
[b]*Digital Production Department, Yara International ASA, Norway.*

Abstract

Several operational challenges occur in industrial-scale granulation loop processes. One challenge is the oscillatory behaviour in the product particle size distribution. This paper is concerned with suppressing oscillatory behaviour using advanced process control. A model based predictive controller together with a previously developed mechanistic model are used to simulate and control the granulation loop process. The main objective of this paper is to eliminate oscillatory behaviour seen in granulation loop plants by manipulating either a crusher gap spacing or by recycling some fraction of the product-sized particles. The simulation results showed that with both control strategies, the oscillatory behaviour is eliminated when the non-linear model predictive controller is applied. A comparative study between the model based predictive controller and a double-loop control structure showed that higher convergence rate is achieved when the non-linear model predictive controller is used.

Keywords: granulation, automatic control, model predictive control, oscillation, population balance

---

[*]Department of Electrical Engineering, IT and Cybernetics, University of South-Eastern Norway, Kjølnes ring 56, 3918 Porsgrunn, Norway.
Email address: `ludmila.vesjolaja@usn.no` (Ludmila Vesjolaja)

1. Introduction

Granulation loop processes are frequently used in the fertilizer industry to produce granular fertilizers. During the granulation process, particle growth occurs, resulting in granule formation with the desired particle properties (particle size, moisture content, etc.). The produced granules have several advantageous over a non-granule form, such as improved product flow properties and homogeneity, ease of handling and packaging, and storage of the product (Litster and Ennis, 2004; Wang and Cameron, 2002).

Granule formation in a granulator depends on various aspects, such as type of the granulation process (e.g., batch/continuous, internal/external drying of the particles), granulator type (e.g., spherodizer, rotary drum, pan, fluidized-bed granulator), operating conditions, etc. According to Iveson et al. (2001), granulation mechanisms can be divided into three main groups: (i) particle nucleation, (ii) particle growth, and (iii) particle breakage. Particle nucleation is the first step in the granulation process. In a spraying zone, the powder interacts with the binder spray droplets, resulting in the formation of initial aggregates. However, nucleation is rarely identified and separated from other granulation mechanisms (e.g., the particle growth mechanism). As to the particle growth mechanism, particles grow inside the granulator due to two key mechanisms: particle layering and particle agglomeration. Particle layering refers to a continuous particle growth mechanism in which particle growth occurs due to coating of a slurry onto the particle. This mechanism produces compact and hard granules. Particle agglomeration is a second particle growth mechanism. Particle agglomeration is a discrete particle growth mechanism that occurs due to collision of two particles, resulting in the formation of a larger, composite particle. The third granulation mechanism, i.e, particle breakage, is important in high shear devices, especially in high impact mixer granulators. Particle breakage by fragmentation is a discrete event, that changes number of particles in the system (Iveson et al., 2001; Wang and Cameron, 2002; Litster and Ennis, 2004; Cameron et al., 2005).

2

1.1. Granulation loop

The granulation loop studied in this paper is depicted in Figure 1. The main granulation loop units are: a granulator, a screen, and a crusher.
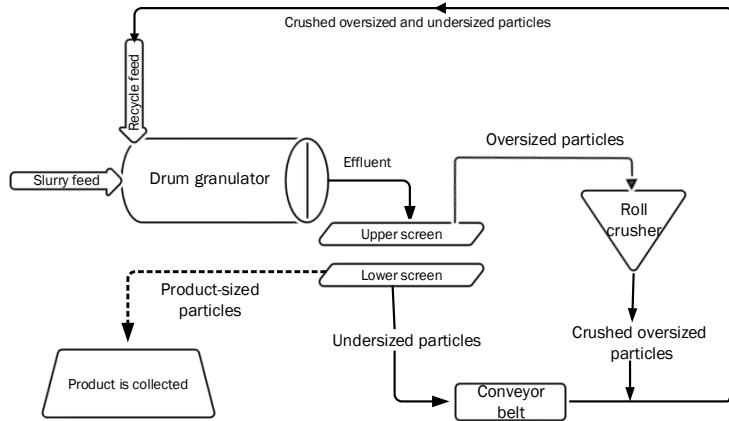

Figure 1: Process description: rotary drum granulation loop (Vesjolaja et al., 2020b).

The particle enlargement process occurs in a drum granulator. Inside the
rotary drum, a slurry melt and recycled particles are mixed together, resulting in formation of composite granules. As granules leave the granulator, they are sent to the double-deck screen. The double-deck screen is used to classify the particle flow from the granulator (effluent) into different size fractions. Particles that are too large to pass the upper screen, i.e., particles that remain lying on the upper screen, are sent to a roll crusher. Particles that are small enough to pass through the upper screen but remain lying on the lower screen, are the product-sized particles. The product-sized particles are collected for further use. The remaining particle flow that contain particles that pass through both of the screens are the under-sized particles. The under-sized and the crushed over-sized particles form the off-spec particle flow. The off-spec particles are recycled back to the rotary drum, acting as nuclei for new granule formation (Vesjolaja et al., 2020a,b).

3

From a process control view, there are several operational challenges that occur in industrial-scale granulation loop processes. Some of these are: (i) operation below the design capacity, (ii) wide particle size distribution (PSD) of the produced particles compared to the desired product PSD, and (iii) oscillatory behavior in the product quality (e.g., the produced median particle size d_{50}) and the product quantity (e.g., particle mass flow rates). This paper is concerned with the oscillatory behaviour observed in granulation loop plants.

In (Cotabarren et al., 2010; Radichkov et al., 2006; Drechsler et al., 2005), and Heinrich et al. (2003), the authors have developed dynamic models of the granulation loop process in order to study the complex dynamic behaviour of granulation. Some studies are devoted to numerical bifurcation analysis of the granulation process with the purpose to identify the reason of the oscillatory behavior. In (Radichkov et al., 2006), numerical bifurcation analysis showed that the dynamic behaviour of the fluidized bed granulation loops strongly depended on the crushed particles that are recycled back to the granulator. Since then, several studies regarding stabilization of the granulation loop processes have been published. In (Bück et al., 2016, 2015; Cotabarren et al., 2015; Palis and Kienle, 2012b,a; Bertin et al., 2011; Palis and Kienle, 2010; Neugebauer et al., 2020, 2019), the control of the fluidized bed granulation processes have been studied. In the most recent study (Neugebauer et al., 2020), the authors have eliminated oscillatory behavior in a fluidized bed granulator with external sieve mill cycle using the decentralized PI control. Oscillatory behavior in the produced particle size is also reported in granulation loop processes were rotary drums are used as a granulator unit (Vesjolaja et al., 2020a,b; Ramachandran and Chaudhury, 2012; Glaser et al., 2009; Wang et al., 2006). In Figure 2, the oscillatory behaviour in the produced particle d_{50} of an industry-scale drum granulation loop plant is shown.
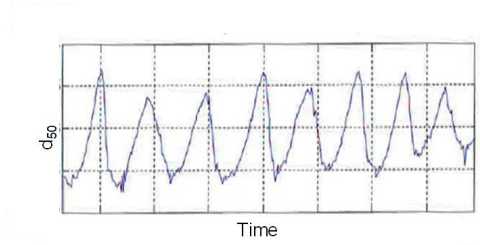
Figure 2: Oscillatory behavior in the produced median particle size (d_{50}) in an industrial granulation loop plant (Vesjolaja et al., 2020a).

1.3. Research objectives

This study is focused on controlling the rotary drum granulation loop process. The main goal is to achieve stability in operation by eliminating the oscillatory behaviour observed in the particle median size d_{50}. Our previous study (Vesjolaja et al., 2020a) showed that it is possible to eliminate the oscillatory behaviour in the produced particle d_{50}, by recycling some of the product-sized particles back to the rotary drum granulator or by manipulating the crusher gap spacing. In Vesjolaja et al. (2020a), a double-loop control structure using the PI control was used to control the produced particle d_{50} in the effluent from the granulator. Here, we want to contribute by applying a non-linear model predictive controller (MPC) in the granulation loop process. An MPC controller was chosen since MPC is known for simple handling of process constraints, and simple tuning of the controller. Potentially, the MPC controller could also show a higher convergence rate towards an operating point in the particle d_{50} than the classical PID controllers. Thus, the main goal of this paper is to apply the non-linear MPC controller to the rotary drum granulation loop process with the objective to remove oscillatory behavior in produced particle d_{50}. In addition, a comparative study of the simulation results obtained using a double loop control structure (Vesjolaja et al., 2020a) and the MPC will be performed.

The paper is organized as follows: In Section 2, the basis of the granulation loop model is given. The control strategies used to control the granulation pro-

5

cess are described in Section 3, while the implementation of a non-linear model predictive controller is given in Section 4. In Section 5, closed loop simulation results for both control strategies are provided. Discussion of the simulation results are given in Section 6, while conclusions are drawn in Section 7.

2. Process modeling

2.1. Granulation loop model

The mathematical model of a rotary drum granulation loop process used in this study is reported in Vesjolaja et al. (2020b). The developed granulation process model is a mechanistic model that is based on the population balance (PB) principles. Here, a multi-compartment granulator model is used. Thus, the resulting mass-based population balance equation over the granulator is a partial differential equation (PDE) formulated with respect to the particle size (internal coordinate) and the particle position in the granulator (external coordinate). The developed model captures both of the particle growth mechanisms, i.e., particle growth due to layering and agglomeration. Nucleation and breakage effects are neglected in the model.

Particle flow through the double-deck screens is modeled using probability functions. The model of the crusher is based on a Gaussian distribution function, having a crusher gap spacing and a standard deviation as design choices. An elevator that is used to transfer off-spec particles is modeled as a transport delay. For more details regarding mathematical modeling of the granulation loop, see Vesjolaja et al. (2020b).

2.2. Semidiscrete process model

In order to find the solution of the PB equation that represents the granulation process, the resulting PDE is transformed into a set of ordinary differential equations (ODEs). The PDE is discretized into 80 particle size classes using a linear grid, while the granulator is divided into 3 equally-sized compartments. In total 240 ODEs are obtained (80 × 3). For the internal coordinate (particle size) discretization, two different discretization schemes are applied: a high

6

resolution scheme is applied for the *layering term* discretization, while a cell average scheme for the *agglomeration term* discretization. For the external coordinate discretization, the high resolution scheme is applied. Application of the above mentioned discretization techniques to the resulting PB equation is given in detail in Vesjolaja et al. (2020b).

3. Design of the control system

Here, the main purpose of studying control of the granulation loop is to suppress and remove the oscillatory behaviour in the particle median diameter, d_{50}, in the effluent from the granulator, thus, to achieve stabilization in the particle d_{50}. By *stability* we mean a system to be stable at a steady operating point.

Similarly to Vesjolaja et al. (2020a), two control strategies, CS1 and CS2, are utilized to achieve stabilization in the produced particle d_{50}. A single-input-single-output (SISO) control system is used. In both of the control strategies, the controlled output is the produced particle d_{50} in the effluent from the granulator (particle d_{50} before the granules are sieved). The control inputs are different for the different control strategies.
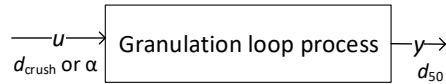

Figure 3: Control system applied to the simulated process. Control inputs u: (i) d_{crush} — crusher gap spacing, (ii) α — valve opening that defines how much of the product-sized particles is recycled; Controlled output y — the produced particle d_{50} of the effluent from the granulator, i.e., particle d_{50} before the granules are sieved.

Control Strategy 1 (CS1). As was shown in previous studies, e.g., in Radichkov et al. (2006) and Vesjolaja et al. (2020b), oscillatory behvaiour in the particle d_{50} is strongly dependent on the size of the crushed particles that are recycled back to the granulator. Thus, in CS1 the crusher gap spacing, d_{crush}, is being utilized

7

as the control input (Figure 3). The CS1 strategy assumes that the granulation plant configuration allows operators to easily manipulate the crusher gap spacing from the control room.

Control Strategy 2 (CS2). Our previous simulation results (Vesjolaja et al., 2020a) showed that it is possible to eliminate the oscillatory behvaiour in the d_{50} of the effluent from the granulator by recycling some of the product-sized particles back to the granulator. The control input is a 3-way valve opening α (Figure 3). If the valve is closed, $\alpha = 0$ and none of the product-sized particles are recycled back to the granulator. If the valve is opened, $0 < \alpha \leq 1$, and some fraction of the product-sized particles are recycled back to the granulator. Product-sized particles are recycled by adding the product-sized mass flow rate to the recycle stream that includes the flow of crushed over-sized particles and the under-sized particles (Vesjolaja et al., 2020a). We refer to Vesjolaja et al. (2020a) for details regarding the control strategies CS1 and CS2.

4. Implementation of non-linear MPC

A model predictive controller is applied to the rotary drum granulation loop process in order to eliminate the oscillatory behaviour seen in the particle d_{50} in the effluent from the granulator. The non-linear dynamic model of the granulation loop process is described in Section 2. Potentially, both linear and non-linear MPC could be applied. In the case of linear MPC, the model of the granulation loop should be linearized in order to use it as the prediction model. In this paper, a non-linear MPC is implemented. Thus, the nonlinear model of the process is directly utilized to formulate the nonlinear optimization problem. A simplified schematic of the implemented MPC to the simulated granulation process is given in Figure 4. The controller design consists of: (i) process model, (ii) non-linear estimator, (iii) non-linear MPC controller.

In this simulation study, the process block Figure 4 is represented by the non-linear model described in Section 2. The same non-linear model is also used as the prediction model in the MPC block (Figure 4).
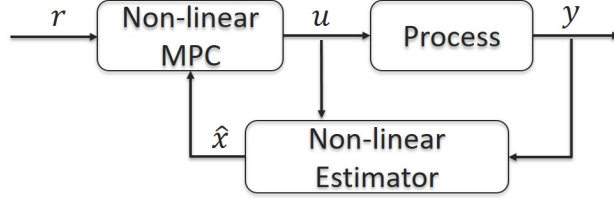
Figure 4: Simplified schematic diagram of the implementation of non-linear MPC; u — control input (α in CS1 or d_{crush} in CS2); y — controlled output (the produced particle d_{50} of the effluent from the granulator); r — reference point; $\hat{x}$ — states of the prediction model used in the MPC.

4.1. State estimator

In order to predict the future values of the states and output throughout the prediction horizon, the prediction model needs to know the initial values of the states at the current time step. Thus, the non-linear MPC block in Figure 4 needs to be supplied with the current values of the states. As was mentioned in Section 2, the process model is represented by 240 ODEs, i.e., the model has 240 states. In real granulation plants, it is unrealistic to assume a sensor to measure mass for each particle size class and at different locations inside the drum granulator. Therefore, in reality the model states are not measured or known. Thus, for a practical implementation of MPC, a state estimator is required to estimate the states that are needed in the non-linear MPC block in Figure 4. The state estimator is also used to filter out the noisy measurements, and to calculate the estimated process output. In this study, an unscented Kalman filter (UKF) for nonlinear estimation is implemented, for details see Simon (2006).

Figure 5 shows application of the UKF filter: the simulated states using the process model (with added measurement noise) and the estimated states using the UKF filter. For the sake of brevity, only 3 arbitrary chosen (out of 240) process states in 3 different granulator compartments are plotted in Figure 5. According to Figure 5, the implemented UKF filter converges to the true value (estimated values the same as the simulated values). The zoomed-in
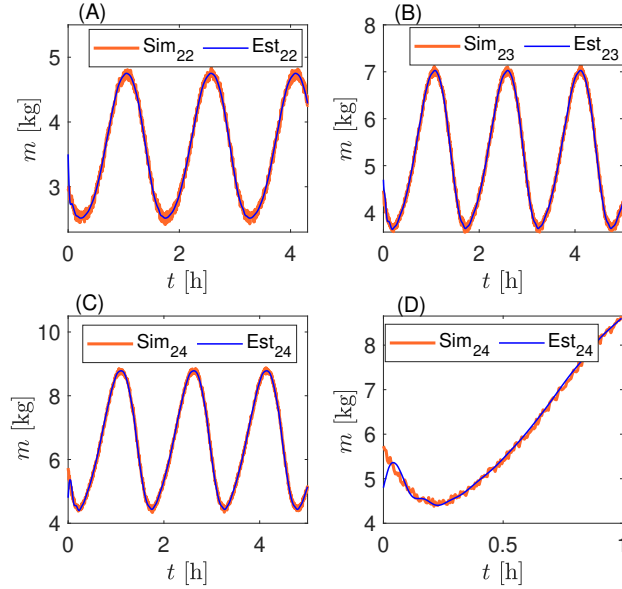
9

Figure 5: Simulated process model (with measurement noise) vs estimated states using the UKF filter. Simulation results showing mass in: (A) first compartment for the particle size class 22 ($d = 2.15$mm); (B) second compartment for the particle size class 23 ($d = 2.25$mm); (C) third compartment for the particle size class 24 ($d = 2.35$mm); (D) Zoomed in results for the particle size class 24 in the third compartment ($d = 2.35$mm).

plot, Figure 5 (D), also shows that the UKF estimator converges to the true simulated values relatively fast.

4.2. Objective function for MPC

The main idea of MPC is to find the optimum value of the control input by solving a dynamic optimization problem and using a so called receding horizon strategy. Here, the MPC objective is to regulate the output to its desired set point. This is achieved by minimizing the sum of the squares of the errors between the future output and the set point through the prediction horizon. In doing so, the rate of change of control inputs (Δu_k) are considered to be the decision variables. Thus, we have a minimization problem with the following

constrained nonlinear optimization problem:

$$\min_{\Delta u_k} \quad J = \frac{1}{2} \sum_{k=1}^{N} \left(r_k - y_k\right)^T Q_e \left(r_k - y_k\right) + \Delta u_{k-1}^T P_{\Delta u} \Delta u_{k-1} + u_{k-1}^T P_u u_{k-1}$$

$$\text{(1a)}$$

$$\text{s.t.} \quad x_{k+1} = \mathcal{F}\left(x_k, u_k, \sigma_k, t_k\right), \tag{1b}$$

$$\Delta u_{\text{LB}} \leq \Delta u_k < \Delta u_{\text{UB}}, \tag{1c}$$

$$u_{\text{LB}} \leq u_k < u_{\text{UB}} \tag{1d}$$

where J is the objective function, u is the control input (d_{crush} in CS1 and α in CS2); y is the controlled output (d_{50} of the effluent from the granulator); r is the reference point (set point); N is the prediction horizon; Q_e, $P_{\Delta u}$ and P_u are weighting matrices.

Equation 1b is the non-linear model of the process in discrete time. This is the prediction model for the non-linear MPC which is used to predict the future behaviour of the states and eventually the output in order to make the non-linear optimization problem given by Equations 1a- 1d. Equation 1b is a complex model obtained by solving a PB model for the drum granulator using appropriate discretization schemes. The model used in this study is discussed in Section 2. The details for this model is not presented in this paper for brevity; see Vesjolaja et al. (2020b) and Vesjolaja et al. (2020a) for details.

Equation 1c is the constraint on the rate of change of control inputs, which says that the control inputs (crusher gap spacing d_{crush} or 3-way valve opening α) can only be increased or decreased by 0.01 at each time step (Δu_{LB} and Δu_{UB} in Table 1). This constraint is extremely important in practice where the actuators always have some physical restriction/limit as to how fast they can be increased or decreased.

Equation 1d is the bounds on the control inputs with the LB and UB representing the lower and the upper bound respectively. For CS1, u_{LB} and u_{UB} are 0 and 3 respectively. This means the crusher gap gap opening can not be lower that 0 mm and higher than 3 mm. For CS2, u_{LB} and u_{LB} are 0 and 1 respectively. This means that the 3-way valve can be anywhere between fully

11

closed, $\alpha = 0$, and fully open, $\alpha = 1$.

The MPC controller for the granulation loop process is implemented in Simulink and MATLAB (MATLAB, 2019b). The prediction horizon is the same as the control horizon ($N = 100$). To reduce the computational time for solving the optimization problem, the control inputs are grouped into 4 unequal length groups. With this, the number of variables to optimize is 4 with grouping, instead of 100 without grouping. The non-linear optimization problem is solved using the *fmincon* solver in MATLAB (MATLAB, 2019b), with the Sequential Quadratic Programming (SQP) optimization algorithm.

5. Simulation results

5.1. Simulation setup

Simulations of the applied non-linear MPC are performed using Simulink (MATLAB, 2019b). Both the semi-discrete process model representing the granulation plant and the prediction model used in the MPC are solved using a built-in ODE integrator in Simulink, namely the 4-th order Runge-Kutta (RK-4) integrator with fixed time step. The non-linear optimization problem is solved using the *fmincon* optimizer in MATLAB with the SQP optimization algorithm. The controller parameters used in the simulations are summarized in Table 1. The model parameters are the same as used in Vesjolaja et al. (2020a) when the double-loop control structure was used to eliminate the oscillatory behaviour in the produced particle d_{50}. In simulations, the non-linear MPC (NMPC) controller was turned on where the sustained oscillations in the particle d_{50} of the effluent from the granulator were observed. Similarly to Vesjolaja et al. (2020a), the simulations were initiated at crusher gap spacing $d_{crush} = 1.3$ mm for the model parameter set given in Vesjolaja et al. (2020a). Figure 6 shows the sustained oscillations (without a controller) in the particle d_{50} of the effluent from the granulator at $d_{crush} = 1.3$ mm.

Table 1: Controller parameters.

Parameter	CS1	CS2
N	100	100
Q_e	200	200
P_{du}	0.02	0.01
P_u	75	50
u_{LB}	0	0
u_{UB}	3	1
Δu_{LB}	0.01	0.01
Δu_{UB}	0.01	0.01
Optimizer	*fmincon*	*fmincon*
Optimization algorithm	SQP	SQP
Integrator	RK4	RK4
Time step for RK4 [s]	20	20
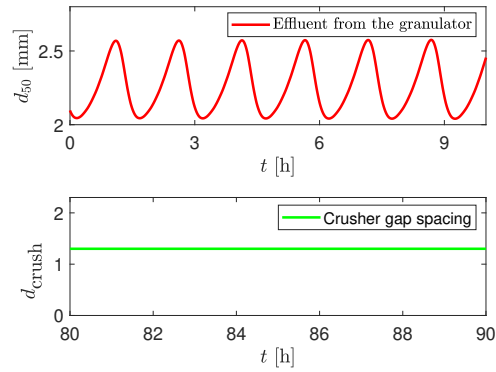
Figure 6: Simulated sustained oscillations in the particle d_{50} of the effluent from the granulator at $d_{\mathrm{crush}} = 1.3mm$.

250 *5.2. Simulation results for CS1*

First, simulations were performed with the CS1 strategy in which the control input is the crusher gap spacing, while the controlled output is the produced particle median size d_{50} in the effluent from the granulator. Our previous studies

13
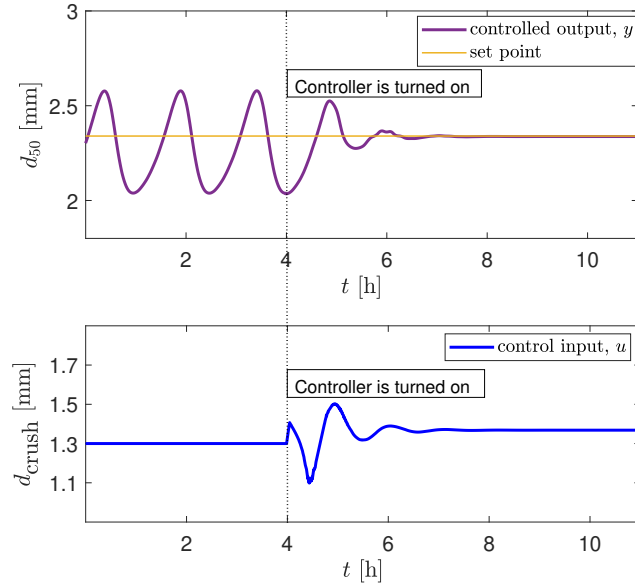
Figure 7: NMPC using CS1: Simulation results showing the controlled output and the control input when the controller in turned on. NMPC controller is turned on at $t = 4$ h.

(Vesjolaja et al., 2020a) showed that the point of the cycle at which the controller is turned on, maximum or minimum point of the cycle, does not affect the closed loop response. In this paper, the non-linear MPC controller was turned on at the minimum point of the cycle, at $t = 4$ h.

Simulation results with the controlled output and the control input are shown in Figure 7. After 3.5 h of transients, the controlled output converged towards the reference point and the oscillatory behaviour in the particle d_{50} was eliminated. The crusher gap spacing was at 1.4 mm when the oscillatory behaviour in the particle d_{50} was eliminated. The controller ability to compensate for disturbances is shown in Figure 8. Here, a slurry feed is assumed as the process disturbance. Disturbances were applied to the process when the controller was turned on, and when the controller was turned off (keeping the same control signal) . Figure 8 shows that the designed controller is able to compensate for disturbances. However, when the disturbance is applied while the controller is
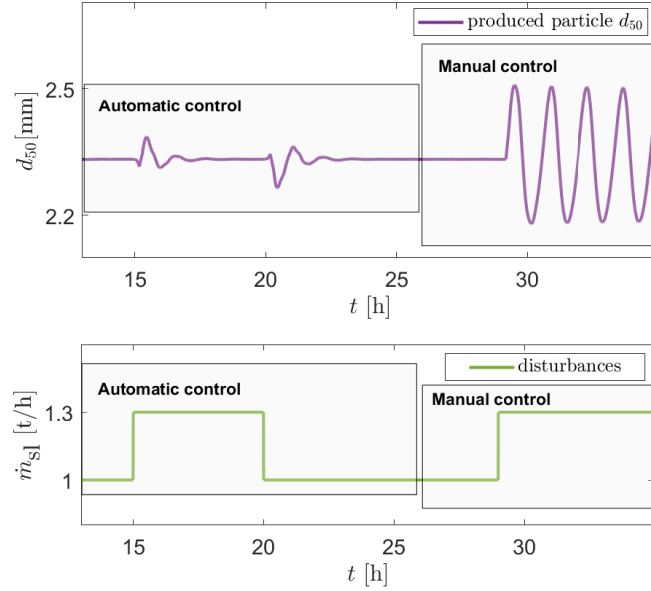
14

turned off, the oscillatory behaviour reappears.

Figure 8: Disturbance rejection using NMPC for the CS1 strategy: Simulation results showing the produced particle d_50 and the introduced disturbances (slurry feed). The NMP controller is turned off at $t = 26$ h keeping the same control signal ($u_{\mathrm{manual}} = u_{\mathrm{auto}}$).

5.3. Simulation results for CS2

Here, the non-linear MPC controller was implemented using the CS2 control strategy. Thus, the control input is the valve opening α that reflects how much of the product-sized particles is recycled to the granulator, and, the controlled output is the produced particle d_{50} in the effluent from the granulator.

In Figure 9, simulation results for the controlled output and the control input are shown. The non-linear MPC controller was turned on at $t = 3.6$ h when the simulated granulation plant showed sustained oscillations at $d_{\mathrm{crush}} = 1.3$ mm. Figure 9 shows the control input reached its maximum peak of 25% during the transients ($\alpha = 0.25$). However, at steady state, only 16% of the product-sized particles are recycled back to the granulator to achieve stability in the produced
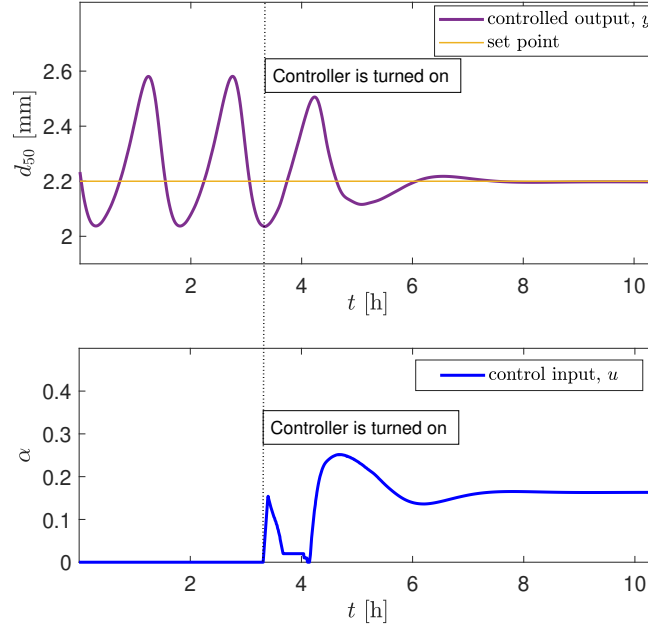
15

Figure 9: NMPC using CS2: Simulation results showing the dynamic behaviour in controlled output and the control input when the controller is turned on; NMPC controller is turned on at $t = 3.6$h.

particle d_{50}. The oscillatory behaviour in the particle d_{50} was eliminated after around 4.4 h since the controller was turned on. In Figure 10, disturbances were introduced. Here, the disturbance is the crusher gap spacing. Similarly to CS1, the disturbance was introduced when the controller was turned on, and turned off (with the same control input value). According to Figure 10, the controller is able to maintain the non-oscillatory behaviour in the controlled output even when the disturbance is introduced. The controlled output showed a small off-set from the reference point (0.08 mm). Such an off-set is obtained since the designed NMPC controller does not include integral action. In this work, the integral action is not included since the paper is focused on eliminating the oscillatory behaviour rather than tracking the reference point. The size of the produced product-sized particles in the industry is not a fixed value, rather classified in a given size range (the interest is to produce consistent size of the
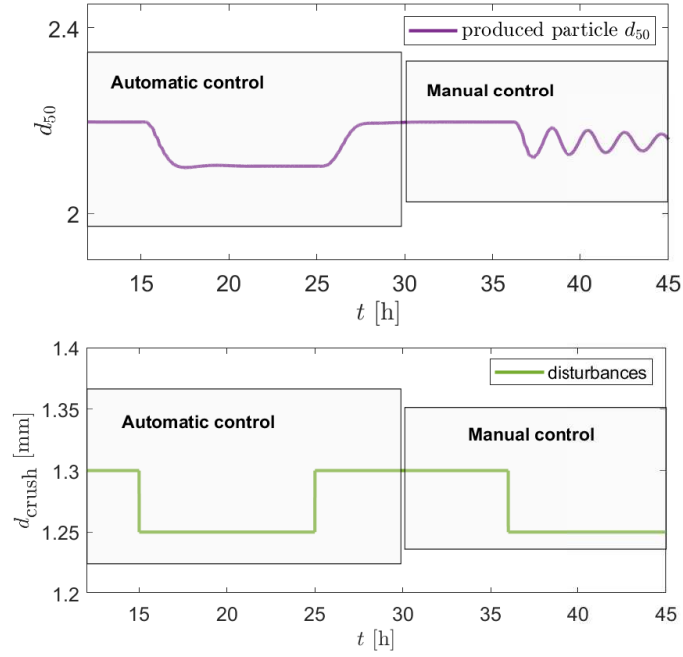
16

Figure 10: Disturbance rejection using NMPC for the CS2 strategy: Simulation results showing the produced particle d_50 when disturbances (crusher gap spacing) are applied. The NMP controller is turned off at $t = 30$ h keeping the same control signal ($u_{\mathrm{manual}} = u_{\mathrm{auto}}$).

particles within a certain range but not necessarily to a specific size value), and hence, integral action is not included.

6. Discussion

The simulation results shows that it is possible to eliminate the oscillatory behavior in the produced particle d_{50} when a non-linear MPC controller is used. System is stable and converges towards the operating point either by manipulating the crusher gap spacing (CS1) or by recycling some of the product-sized particles back to the granulator (CS2). The CS2 strategy can be economically favorable since the occurrence of oscillatory behaviour (peaks) in product quality and product quantity can lead to increased operational expenses and energy
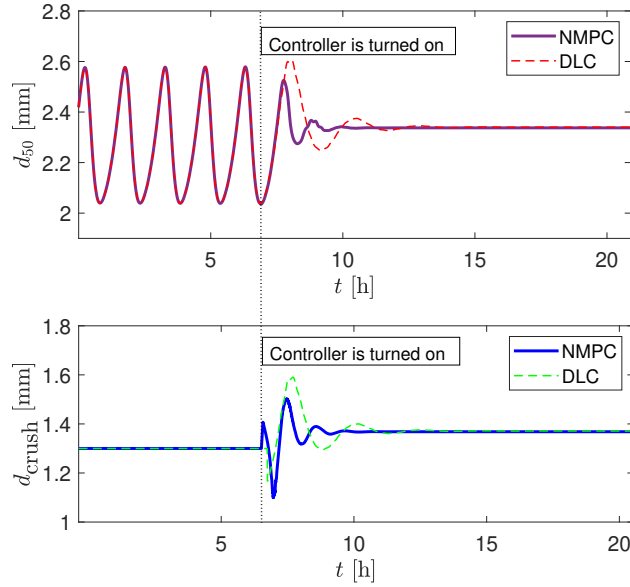
17

Figure 11: Simulation results with the CS1 strategy: NMPC vs DLC; the controllers are turned on at $t = 7$ h.

consumption, as well as lower the risks of the unforeseen plant shut-downs. As to the CS1 strategy, this strategy represents a 'direct' control that manipulates the size of the particles that are recycled back to the granulator. Another potential benefit of using the CS1 strategy over the CS2 strategy is a higher convergence rate: the system is stable and converges towards the operating point faster when the CS1 strategy is utilized. It takes 4.4 h (Figure 9) to eliminate the oscillatory behaviour in the produced particle d_{50} when CS2 strategy is applied, while it takes only 3.5 h with the CS1 strategy (Figure 7). However, the CS1 strategy assumes that the crusher gap spacing can be easily manipulated by operators or by an automatic controller from the control room. Such crushers are not typically seen in the granulation loop plants. Instead, the crusher gap spacing should be manually changed on the plant directly by operators. This indicates the importance of having a crusher whose gap spacing can be changed on-line from the control room.
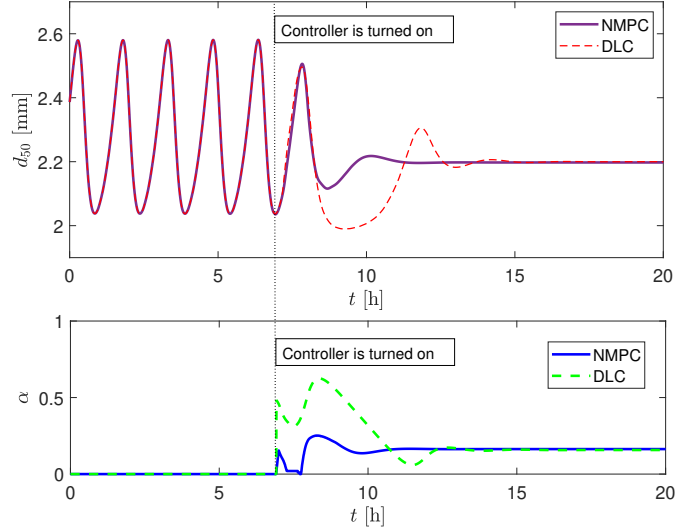
18

Figure 12: Simulation results with the CS2 strategy: NMPC vs DLC; the controllers are turned on at $t = 6.9h$ (NMPC—non-linear model predictive control, DLC—double loop control structure).

Higher convergence rate using the CS1 strategy is observed both when the NMPC controller and the double-loop control structure is used. In the double loop control structure (DLC), the PI controller is used to control the product d_{50}.

320   We refer to Vesjolaja et al. (2020a) regarding the DLC applied to the granulation loop process. In Figure 11 and 12, the simulation results obtained with the NMPC controller and our previously reported results (Vesjolaja et al., 2020a) using the double-loop control structure (DLC) are shown. For fair comparison, both controllers, NMPC and DLC, are turned on at exactly the same time. The

325   best achieved results, i.e., with the controller tuning parameters that gives the highest convergence rate around the operating point, are compared. In the case of the DMC structure, the PI controller tuning parameters were found, first, by applying Skogestad's tunings rules (Skogestad, 2003), and then fine tuning was applied to achieve better controller performance (higher convergence rate).

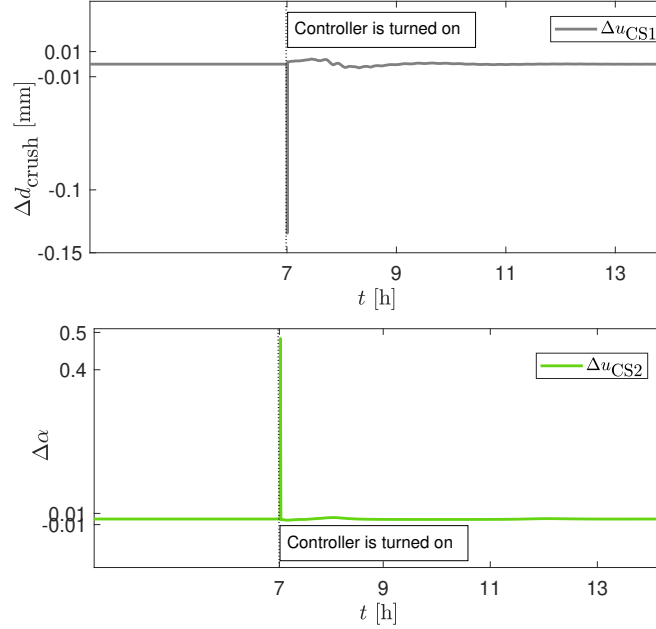330   Details regarding the DLC structure are given in Vesjolaja et al. (2020a).

19

Figure 13: The change in the control input using the DLC: CS1 and CS2 strategies ($\Delta u_{\mathrm{CS1}} = d_{\mathrm{crush}}$; $\Delta u_{\mathrm{CS2}} = \alpha$).

A comparison between the NMPC and the DLC (Figure 11 and 12) shows that it is possible to achieve higher convergence rate in the produced particle d_{50} when the MPC controller is used. In the case of CS1 strategy, the oscillatory behaviour is eliminated after around 6.5 h with the DLC controller, while after 3.5 h with the NMPC controller (Figure 11). A similar advantage of MPC over DLC is obtained for the CS2 strategy. Higher convergence rate of the produced particle d_{50} is obtained with the MPC controller, 4.4 h vs 7 h for the NMPC and DLC, respectively (Figure 12).

A more important advantage of MPC over the DLC is the handling of constraints. In real plants, there are always physical constraints on the equipment that need to be addressed. Constraints that determine the way that the control inputs (i.e., the actuators in a real plant) can be manipulated can be easily implemented in the MPC: MPC by virtue of its design, is an optimization prob-
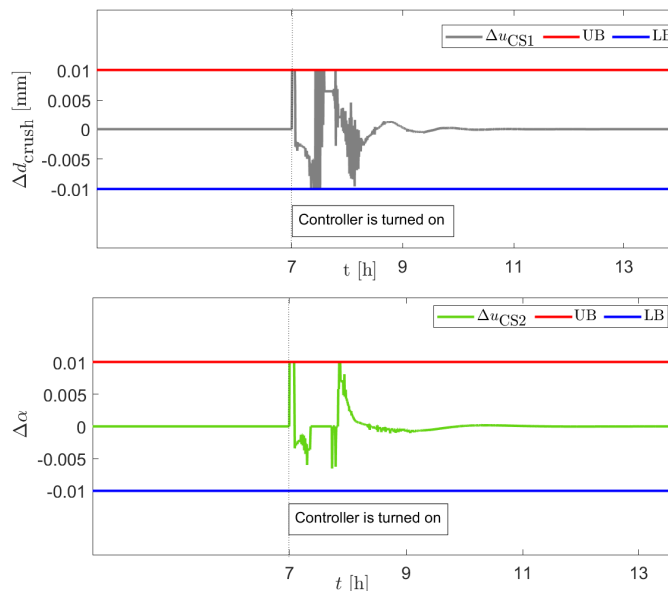
20

Figure 14: The change in the control input using the NMPC: CS1 and CS2 strategies ($\Delta u_{CS1} = d_{crush}$; $\Delta u_{CS2} = \alpha$; LB — lower bound; UB —upper bound).

lem and generates optimal values for control inputs while still satisfying the
constraints. In the case of the DLC structure where a PI controller is used, it is also possible to put limits on the control input but it results in a simple ad-hoc management of input constraints, and it does not necessarily generate control inputs which are optimal in nature since no optimization problem is solved. With the MPC, process constraints are already a part of the optimal control problem and are therefore handled systematically. If the constraints are specified in the optimal control problem formulation, the control input will not change abruptly like it does with the DLC structure where the PI controller is used. For comparison, in Figure 13, it can be clearly seen that with the DLC, the value of α is changed rapidly from 0 to 0.48 at $t = 7$ h when the controller is turned on. In fact, this rapid change of α (by a value of 0.48) occurs during one time step (20 s). However, due to the presence of operational constraint, it has been considered that the value of α cannot be changed by more than 3 %

21

in a minute ($-0.01 \leq \Delta u_k < 0.01$). This means that the double loop control structure may not always satisfy the operational constraints.

360   The plot of the rate of change of the control input α with the double loop control structure clearly shows that the constraints are violated, as shown in Figure 14. On the other hand, with the MPC for both CS1 and CS2, the constraints on the rate of change of control inputs are properly satisfied as shown in Figure 14: the change in the control inputs do not exceed 1 % per

365 time step. Specifying the constraints is also important for safety reasons.

7. Conclusions

In this paper, a non-linear model based predictive controller is applied for a granulation loop model with the purpose to eliminate the oscillatory behavior seen in the produced median particle size d_{50}. The simulation results show that

370 it is possible to eliminate the oscillatory behaviour in the produced particle d_{50} using the NMPC controller.

The oscillatory behaviour in the particle d_{50} is eliminated either by manipulating the crusher gap spacing, or by recycling some of the product-sized particles back to the granulator. Among the simulated control strategies, the

375 control strategy where the crusher gap spacing is selected as control input, is favorable: by manipulating the crusher gap spacing, the convergence in the produced particle d_{50} was higher than by recycling some of the product-sized particles back to the granulator.

A comparative study between the model predictive controller design and the

380 double-loop control structure showed that it is possible to achieve faster closed loop response when the NMPC controller is used. With the non-linear model based predictive controller, the convergence rate towards a operating point in the produced particle d_{50} was achieved almost two times faster compared to the simulation results obtained with the double-loop control structure. Higher

385 convergence rate using the model predictive controller was obtained for both control strategies. In addition, the advantage of specifying the constraints in

22

the model based design, makes the model predictive controller favorable over the double-loop control structure.

Acknowledgment

References

Bertin, D.E., Cotabarren, I.M., Bucalá, V., Piña, J., 2011. Analysis of the product granulometry, temperature and mass flow of an industrial multichamber fluidized bed urea granulator. Powder Technol. 206, 122–31.

Bück, A., Dürr, R., Schmidt, M., Tsotsas, E., 2016. Model predictive control of continuous layering granulation in fluidised beds with internal product classification. J Process Control 45, 65–75.

Bück, A., Palis, S., Tsotsas, E., 2015. Model-based control of particle properties in fluidised bed spray granulation. Powder Technol. 270, 575–83.

Cameron, I., Wang, F., Immanuel, C., Stepanek, F., 2005. Process systems modelling and applications in granulation: A review. Chem. Eng. Sci. 60, 3723–50.

Cotabarren, I., Bertín, D., Romagnoli, J., Bucalá, V., Piña, J., 2010. Dynamic simulation and optimization of a urea granulation circuit. Ind. Eng. Chem. Res. 49, 6630–40.

Cotabarren, I.M., Bertín, D.E., Bucalá, V., Piña, J., 2015. Feedback control strategies for a continuous industrial fluidized-bed granulation process. Powder Technol. 283, 415–32.

Drechsler, J., Peglow, M., Heinrich, S., Ihlow, M., Mörl, L., 2005. Investigating the dynamic behaviour of fluidized bed spray granulation processes applying numerical simulation tools. Chem. Eng. Sci. 60, 3817–33.

Glaser, T., Sanders, C., Wang, F., Cameron, I., Litster, J., Poon, J.M.H., Ramachandran, R., Immanuel, C., Doyle III, F., 2009. Model predictive control of continuous drum granulation. J Process Control 19, 615–22.

Heinrich, S., Peglow, M., Ihlow, M., M´orl, 2003. Particle population modeling in fluidized bed-spary granulaiton - analysis of the steady state and unsteady behavior. Powder Technol. 130, 154–61. doi:10.1016/S0032-5910(02)00259-0.

Iveson, S., Litster, J., Hapgood, K., Ennis, B., 2001. Nucleation, growth and breakage phenomena in agitated wet granulation processes: a review. Powder Technol. 117, 3–39.

Litster, J., Ennis, B., 2004. The science and engineering of granulation processes. volume 15. Springer Science & Business Media.

MATLAB, 2019b. The MathWorks, Inc., Natick, Massachusetts, United States.

Neugebauer, C., Bück, A., Kienle, A., 2020. Control of particle size and porosity in continuous fluidized-bed layering granulation processes. Chem Eng Technol 43, 813–8.

Neugebauer, C., Diez, E., Bück, A., Palis, S., Heinrich, S., Kienle, A., 2019. On the dynamics and control of continuous fluidized bed layering granulation with screen-mill-cycle. Powder Technol. 354, 765–78.

Palis, S., Kienle, A., 2010. Stabilization of continuous fluidized bed spray granulation-a lyapunov approach. IFAC Proceedings Volumes 43, 1362–7.

Palis, S., Kienle, A., 2012a. Discrepancy based control of continuous fluidized bed spray granulation with internal product classification. IFAC Proceedings Volumes 45, 756–61.

Palis, S., Kienle, A., 2012b. Stabilization of continuous fluidized bed spray granulation with external product classification. Chem. Eng. Sci. 70, 200–9.

Radichkov, R., Müller, T., Kienle, A., Heinrich, S., Peglow, M., Mörl, L., 2006. A numerical bifurcation analysis of continuous fluidized bed spray granulator with external product classification. Chem Eng Process 45, 826–37. doi:`10.1016/j.cep.2006.02.003`.

Ramachandran, R., Chaudhury, A., 2012. Model-based design and control of a continuous drum granulation process. Chem Eng Res Des 90, 1063–73.

Simon, D., 2006. Optimal state estimation: Kalman, h∞, and nonlinear approaches. John Wiley & Sons, Inc 10, 0470045345.

Skogestad, S., 2003. Simple analytic rules for model reduction and pid controller tuning. J Process Control 13, 291–309.

Vesjolaja, L., Glemmestad, B., Lie, B., 2020a. Double-loop control structure for rotary drum granulation loop. Processes 8, 1423.

Vesjolaja, L., Glemmestad, B., Lie, B., 2020b. Dynamic model for simulating transient behaviour of rotary drum granulation loop. Model. Identif. Control doi:`10.1016/j.jprocont.2016.07.003`.

Wang, F., Cameron, I., 2002. Review and future directions in the modelling and control of continuous drum granulation. Powder Technol. 124, 238–53.

Wang, F., Ge, X., Balliu, N., Cameron, I., 2006. Optimal control and operation of drum granulation processes. Chem. Eng. Sci. 61, 257–67.

—

usn.no